





Dipl.-Ing. Michael Haas, BSc

## **Cyclic Silenes and Germanes**

### **PhD THESIS**

zur Erlangung des akademischen Grades

Doktor der technischen Wissenschaften

eingereicht an der

**Technischen Universität Graz**

Betreuer

Ao. Univ. Prof. Dipl.-Ing. Dr. techn. Harald Stüger

Institut für Anorganische Chemie

Fakultät für Technische Chemie, Verfahrenstechnik und Biotechnologie

Graz, November 2015

### **Eidesstattliche Erklärung**

Ich erkläre an Eides statt, dass ich die vorliegende Arbeit selbstständig verfasst, andere als die angegebenen Quellen/Hilfsmittel nicht benutzt, und die den benutzten Quellen wörtlich und inhaltlich entnommenen Stellen als solche kenntlich gemacht habe. Das in TUGRAZonline hochgeladene Textdokument ist mit der vorliegenden Dissertation identisch.

### **Affidativ**

I declare that I have authored this thesis independently, that I have not used other than the declared sources/resources, and that I have explicitly indicated all material which has been quoted either literally or by content from the sources used. The text document uploaded to TUGRAZonline is identical to the present doctoral thesis.

---

Datum/ Date

---

Unterschrift/ Signature

Für meine Eltern und Steffi

„Die Wissenschaft fängt eigentlich erst da an, interessant zu werden, wo sie aufhört.“

Justus von Liebig

## Danksagung:

Allen voran gilt mein besonderer Dank meinem Betreuer, Herrn Professor Harald Stüger, für die interessante Aufgabenstellung, die zahlreichen Anregungen und hervorragende Betreuung während meiner Zeit am Institut.

Meinen zahlreichen Bachelorstudenten möchte ich hiermit für ihre Mithilfe und ihr Engagement danken. Christoph, Dominik, Janine, Lukas, Manfred, Patrick, Thomas und Viktor ihr habt dafür gesorgt, dass ich immer gerne an meine Zeit am Institut zurückdenken werde.

Der gesamten Arbeitsgruppe (Andrea, Bernd, Birgit, Christoph, Hansi, Judith, Martin, Nicki, Thomas, und Uwe) danke ich für das gute Arbeitsklima und für die fachliche Hilfe, außerdem auch für die amüsanten Stunden nach der Arbeit.

Für die Aufklärung der Kristallstrukturen möchte ich Frau Dr. Ana Torvisco Gomez und Herrn Professor Roland Fischer danken. Prof. Robert Saf möchte ich für die zahlreichen HRMS Messungen danken.

Ganz besonders danke ich meinen Eltern und meiner Freundin Steffi für die Liebe und Unterstützung in schwierigen Zeiten. Ohne euch wäre diese Arbeit nicht möglich gewesen!

Natürlich nicht unerwähnt sollten alle meine Freunde bleiben, die immer genau über meine Fortschritte und diversen Rückschritte informiert wurden. (Ob sie wollten oder nicht) Ich danke euch für euer Zuhören!

# CONTENTS

ABSTRACT.....	1
KURZFASSUNG .....	2
INTRODUCTION .....	3
1. LITERATURE OVERVIEW.....	4
1.1    SILENES .....	4
1.1.1    Introduction.....	4
1.1.2    Reactivity of Silenes .....	6
1.1.3    Spectroscopic and Structural Properties of Silenes.....	8
1.1.4    Preparation of Silenes .....	9
1.2    GERMENES .....	19
1.2.1    Introduction.....	19
1.2.2    Reactivity of Germenes.....	20
1.2.3    Spectroscopic and Structural Properties of Germenes.....	23
1.2.4    Preparation of Germenes.....	23
1.3    REFERENCES .....	29
2. PUBLICATIONS .....	33
2.1    SYNTHESIS AND CHARACTERIZATION OF CYCLIC ACYLSILANES .....	33
2.1.1    Abstract .....	33
2.1.2    Introduction.....	34
2.1.3    Results and Discussion .....	34
2.1.4    References .....	38
2.2    PHOTOINDUCED BROOK-TYPE REARRANGEMENT OF ACYLCYCLOPOLYSILANES .....	39
2.2.1    Abstract .....	39
2.2.2    Introduction.....	40
2.2.3    Results and Discussion .....	42
2.2.4    Conclusion .....	51
2.2.5    Experimental Section .....	52
2.2.6    References .....	56
2.3    PHOTOINDUCED REARRANGEMENT OF ARYL-SUBSTITUTED ACYLCYCLOHEXASILANES.....	58
2.3.1    Abstract .....	58
2.3.2    Introduction.....	59
2.3.3    Results and Discussion .....	61
2.3.4    X-ray Crystallography .....	65
2.3.5    Conclusion .....	68
2.3.6    Experimental Section .....	69
2.3.7    References .....	73

2.4	STABLE SILENOLATES AND BROOK-TYPE SILENES WITH EXOCYCLIC STRUCTURES .....	75
2.4.1	Abstract .....	75
2.4.2	Introduction .....	76
2.4.3	Conclusion .....	82
2.4.4	Experimental Section .....	82
2.4.5	References .....	87
2.5	STABLE GERMENOLATES AND GERMENES WITH EXOCYCLIC STRUCTURES .....	90
2.5.1	Abstract .....	90
2.5.2	Introduction .....	91
2.5.3	Results and Discussion .....	92
2.5.4	Conclusion .....	99
2.5.5	Experimental Section .....	100
2.5.6	References .....	104
2.6	SYNTHESIS AND CHARACTERIZATION OF THE FIRST RELATIVELY STABLE DIANIONIC GERMENOLATES .....	106
2.6.1	Abstract .....	106
2.6.2	Introduction .....	107
2.6.3	Results and Discussion .....	107
2.6.4	References .....	111
2.7	PHOTOCHEMICAL REACTIVITY OF CYCLIC ACYLGERMANES .....	112
2.7.1	Abstract .....	112
2.7.2	Introduction .....	113
2.7.3	Results and Discussion .....	113
2.7.4	References .....	118
3.	CONCLUSION AND OUTLOOK .....	119
4.	LEBENS LAUF: .....	123

## Abstract

Silenes and germenes are trivalent compounds containing a Si=C double bond or a Ge=C double bond respectively. Unlike the alkenes, silenes and germenes have to be kept under inert atmosphere (argon or nitrogen) and ambient conditions, otherwise they dimerize intermolecularly or they simply decompose. The high reactivity of these derivatives prevented their isolation for a long time. Meanwhile, however, a number of different silenes and germenes with kinetically and/or electronically stabilized double bonds have been isolated and characterized.

This thesis reports on the synthesis and characterization of such cyclic silenes and germenes. Most silenes and germenes are acyclic molecules. As a consequence of the fact that Graz is a historic center for cyclic polysilane synthesis, we synthesized cyclopolysilanes containing endo- or exocyclic M=C (M = Si, Ge) double bonds. In the literature it is well known that oligo- and polysilanes exhibit interesting photophysical and electrochemical properties caused by delocalized  $\sigma$ -electrons along the silicon backbone. In this work we investigated the interaction between our exo- or endocyclic double bonds with delocalized  $\sigma$ -electrons of the cyclopolysilane rings.

Therefore, the previously unknown cyclic acylsilanes and germanes have been synthesized according to standard procedures for polysilane synthesis.

For the synthesis of silenes, two synthetic protocols have been applied. The first was the photochemical synthesis of silenes. In this method, the cyclic acylsilane precursors were photolyzed with  $\lambda > 300$  nm radiation and depending on the substituent at the carbonyl moiety either endo or exocyclic silenes were obtained. The second synthetic approach was the reaction of our cyclic acylsilanes with KO<sup>t</sup>Bu to yield silenolates. Subsequently silenolates with aryl substituents attached to the carbonyl C atom reacted with chlorosilanes to form exocyclic silenes.

For the synthesis of germenes the photochemical route was not successful. Instead we observed the formation of germyl radicals, which undergo germanium-germanium bond formation. The first examples of exocyclic germenes which could be isolated and fully characterized as in the case of silenes, however, were obtained by the reaction of our cyclic acylgermanes with KO<sup>t</sup>Bu and subsequently with chlorosilanes.

According to spectroscopical data and time-dependent DFT calculations, our cyclic silenes and germenes show minor conjugation between the delocalized  $\sigma$ -electrons along the silicon backbone and the  $\pi$ -electrons of the exo- and endocyclic double bonds.

**Keywords:** cyclic acylsilanes, exo- or endocyclic silenes, silenolates, cyclic acylgermanes, exocyclic germenes, germenolates



## Kurzfassung

Silene und Germene sind trivalente Verbindungen, die eine Si=C Doppelbindung oder eine Ge=C Doppelbindung aufweisen. Im Gegensatz zu Alkenen müssen Silene und Germene unter inerten Bedingungen (Argon oder Stickstoff) und bei niedrigen Temperaturen gelagert werden, da sonst intermolekulare Dimerisierung oder Zersetzung beobachtet wird. Mittlerweile wurde jedoch eine Reihe von Silenen und Germanen durch kinetische und/oder elektronische Stabilisierung der Doppelbindung isoliert und vollständig charakterisiert.

Die meisten Silene und Germene sind acyclische Moleküle. In der vorliegenden Arbeit wird nun erstmals über die Synthese und Charakterisierung von Cyclopolysilanen mit exo- oder endocyclischen M=C (M = Si, Ge) Doppelbindungen berichtet. In der Literatur ist bekannt, dass Oligo- und Polysilane interessante photophysikalische und elektrochemische Eigenschaften aufweisen, welche auf die delokalisierten  $\sigma$ -Elektronen entlang des Siliziumgrundgerüsts zurückzuführen sind. Die mögliche Interaktion der exo- oder endocyclischen Doppelbindung mit den delokalisierten  $\sigma$ -Elektronen des Cyclopolysilanrings sollte untersucht werden.

Für die Darstellung der Silene wurden zwei Synthesemethoden angewandt. Die erste Methode stellt die photochemisch induzierte Silensynthese dar. Dafür wurden die cyclischen Acylsilane mit  $\lambda > 300$  nm bestrahlt und abhängig vom Substituenten an der Carbonylgruppe exo- oder endocyclische Silene beobachtet. Die Silensynthese via Silenolatintermediat war die zweite Darstellungsmethode. Die dabei gebildeten Silenolate wurden im nächsten Reaktionsschritt mit Chlorsilanen umgesetzt. Im Falle von aromatischen Substituenten an der Carbonylgruppe konnten die gewünschten exocyclischen Silene isoliert werden.

Die photochemisch induzierte Germensynthese war mit den Acylgermanen nicht möglich. Stattdessen bildeten sich Germylradikale, welche eine Germanium-Germanium Bindungsknüpfung ausbilden. Nur bei der Germensynthese via Germanolatintermediat und nachfolgender Reaktion mit Chlorsilanen konnte eine Germanbildung nachgewiesen werden. Wie im Falle der Silene wurden auch die Germene vollständig isoliert und charakterisiert.

Die erhaltenen spektroskopischen Daten und auch die dichtefunktional (DFT) Berechnungen zeigen jedoch nur eine geringe Interaktion der exo- oder endocyclischen M=C (M = Si, Ge) Doppelbindungen mit den delokalisierten  $\sigma$ -Elektronen entlang des Silizium-Grundgerüsts.

**Schlagwörter:** cyclische Acylsilane, exo- endo-cyclische Silene, Silenolate, cyclische Acylgermane, exocyclische Germene, Germanolate

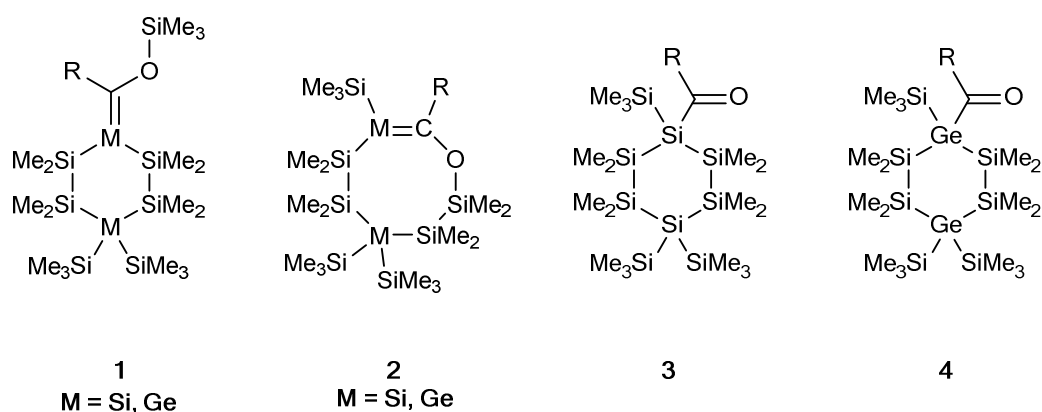
## Introduction

Oligo- and polysilanes exhibit interesting photophysical and electrochemical properties caused by delocalized  $\sigma$ -electrons along the silicon backbone. The so-called  $\sigma$ -delocalization gives rise to surprising bathochromic shifted light absorption bands of oligo- and polysilanes. The absorption maxima are found in the near UV and in some cases at the edge of the visible region.<sup>1</sup>

West *et al.* showed that  $\sigma$ -delocalization is not only apparent in linear systems, but also in cyclic polysilanes of the type  $(\text{Me}_2\text{Si})_n$ .<sup>2</sup> In many respects, furthermore, these cyclic derivatives behave like aromatic compounds such as benzene and toluene.

In contrast to polysilanes silenes and germenenes contain  $\pi$ -electrons. Stable derivatives of these substance classes are known since the mid-eighties. Most silenes and germenenes, however, are acyclic molecules while stable species with Si=C or Ge=C double bonds with the unsaturated silicon or germanium atom incorporated into cyclic polysilane structures are not known.

As a consequence of the fact that Graz is a historic center for cyclic polysilanes, it was obvious for us to attempt the synthesis of cyclopolysilanes containing either endo- or exocyclic M=C (M = Si, Ge) double bonds. Thus, the major target of this thesis was to elaborate suitable synthetic approaches towards the doubly bonded species **1** and **2** depicted in Scheme 1 and to characterize the products with a variety of spectroscopic methods. Further attention should be given to the interaction of the exo- and endocyclic double bonds with the delocalized  $\sigma$ -electrons of the cyclopolysilane rings. For the synthesis of **1** and **2**, finally, it was necessary to develop synthetic pathways to previously unknown starting materials, namely the cyclic acylsilanes and -germanes **3** and **4**.



**Scheme 1:** Target molecules and used starting materials

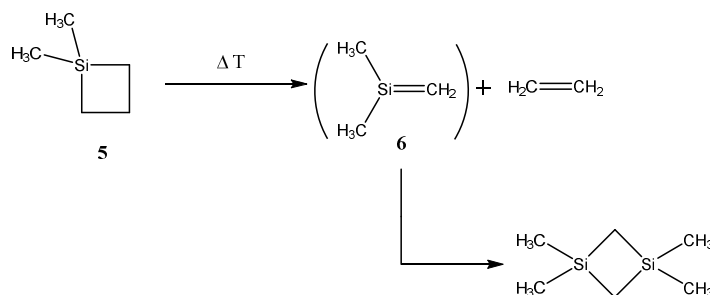
In the first part of this thesis a literature overview on the chemistry of silenes and germenenes is given. Part two consists of the articles published in peer reviewed journals, which were submitted during this thesis.

# 1. Literature Overview

## 1.1 Silenes

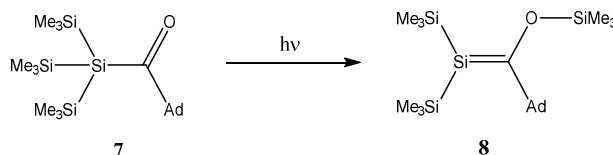
### 1.1.1 Introduction

After a series of unsuccessful attempts to synthesize a silicon carbon double bond, Frederick Stanley Kipping, one of the fathers of organosilicon chemistry, stated that a silicon and a carbon atom could never be united with a double bond. His observation and the findings of other working groups who attempted to synthesize multiply-bonded compounds of elements outside the first row of the periodic table led to the development of the double binding rule. This rule states that elements with a principal quantum number greater than two do not form multiple bonds with themselves or with other elements.<sup>3</sup> Double binding rule was shattered in 1967, when Gusel'nikov and Flowers reported the first evidence for the existence of a silene obtained by a thermolysis reaction (1,1-dimethylsilene **6**, Scheme 2).<sup>4</sup>



**Scheme 2:** Thermolysis of 1,1-dimethyl-1-silacyclobutane **1**

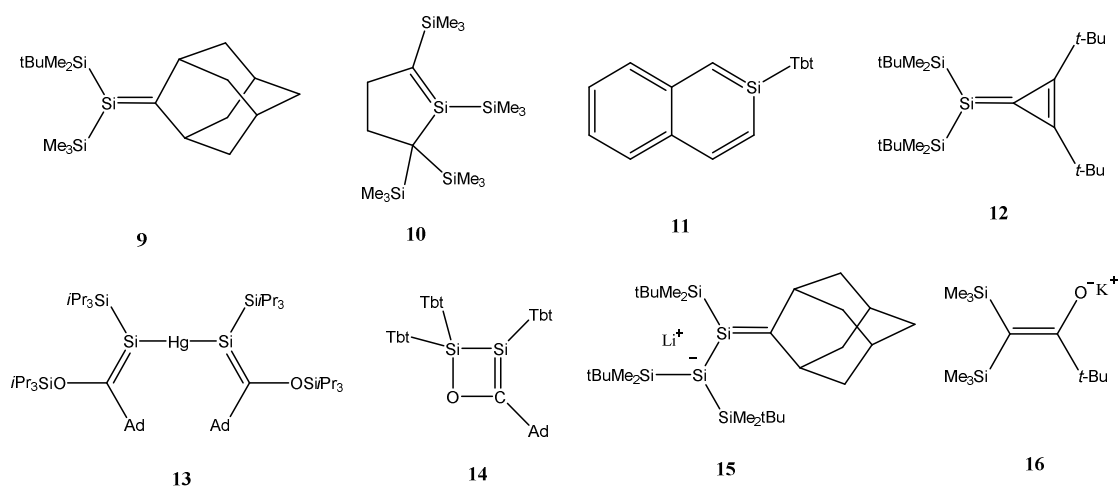
This result inspired chemists all over the world to investigate these species. An outstanding breakthrough was accomplished by Adrian Brook in 1981, who reported the preparation of the first relatively stable silene (Scheme 3). The X-ray crystal structure of **8** revealed a Si=C double bond length of 1.764 Å, somewhat longer than the calculated value of ~1.700 Å. This significant lengthening arises from the ylidic electron donation from the oxygen atom into the double bond.<sup>5</sup>



**Scheme 3:** Synthesis of the Brook silene

Only three years later, the first donor free silene was isolated by Wiberg and his group.<sup>6</sup> The so-called Wiberg-Silene was obtained by a route involving intramolecular LiF elimination and showed a normal Si=C double bond length of 1.702 Å. The chemistry of silenes has evolved remarkably in the last 30 years. New synthetic methods were applied to synthesize a variety of new silenes. Worth mentioning

are the syntheses of the stable silene **9** by Apeloig and co-workers *via* a Sila-Peterson type reaction, and of the first endocyclic silene **10**, which was obtained by the rearrangement of a silylene.<sup>7,8</sup> Tokitoh *et al.* published a series of papers on stable sila-aromatic compounds such as the 2-silanaphthalene **11** and Kira *et al.* isolated and structurally characterized the 4-silatriafulvene **12**.<sup>9,10</sup> In 2008, Apeloig and Bravo-Zhivotovskii isolated the first example of a stable metal-substituted bissilene **13**.<sup>11</sup> Recently, Scheschkewitz and Sekiguchi *et al.* reported on the formation of the cyclic Brook type silene **14**.<sup>12</sup> The first charged silenes were described by Sekiguchi *et al.*, who synthesized the silyl-anion-substituted silene **15**.<sup>13</sup> In addition, Ottosson *et al.* isolated the first stable 2-silenolate **16**.<sup>14</sup>



**Scheme 4:** Selected silenes

### 1.1.2 Reactivity of Silenes

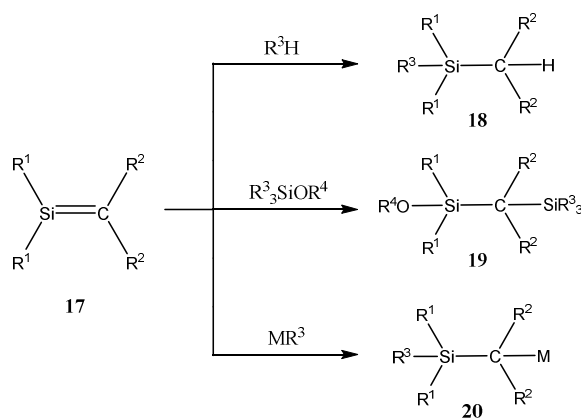
Properties and synthesis of silenes have been summarized in several recent reviews.<sup>15</sup> Thus, in the following only a brief account on silene chemistry will be given which is mainly based on this comprehensive material already available.

Starting from the simplest silene  $\text{H}_2\text{Si}=\text{CH}_2$ , which has a transient existence, a huge variety of different silenes have been synthesized. Stable silenes can be directly characterized under ambient temperature and inert atmosphere (nitrogen, argon). The stability of silenes is strongly influenced by the size and the electronic nature of the substituents. By increasing the size of the substituents the stability of the silene is enhanced. The  $\text{Si}=\text{C}$  double bond is a polarized double bond. One can distinguish between naturally polarized silenes, that display a  $\text{Si}^{\delta+}=\text{C}^{\delta-}$  bond polarity and those that display reversed  $\text{Si}^{\delta-}=\text{C}^{\delta+}$  bond polarity (Scheme 5).



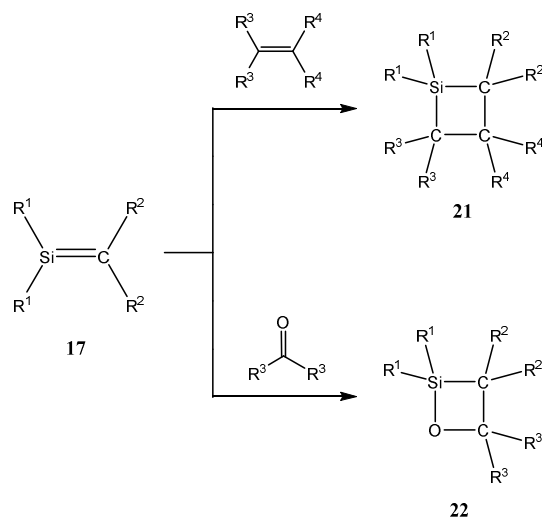
**Scheme 5:** Polarity of the  $\text{Si}=\text{C}$  double bond

As a consequence of their high reactivity, silenes are valuable starting materials for further synthesis. Silenes **17** react regioselectively with reagents of the type  $\text{RH}$  ( $\text{R} = \text{OH}, \text{OR}, \text{NR}_2$  etc.) to give silanes **18**. The addition of alkoxy silanes to the  $\text{Si}=\text{C}$  double bond gave rise to new alkoxy silanes **19**. Carbanions **20** were formed by the reaction of silenes with organometallic reagents (Scheme 6).<sup>16-17,18</sup>



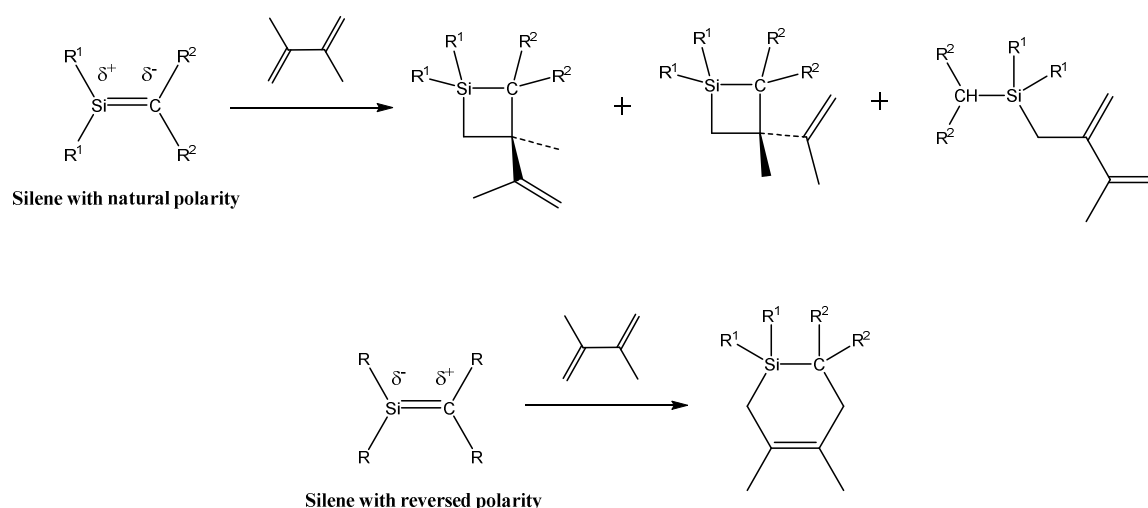
**Scheme 6:** Reactivity of silenes with standard trapping reagents

The reaction between silenes and other double bonds (such as alkenes, ketones, alkynes, dienes etc.) were also thoroughly investigated. The product distribution is strongly influenced by the polarization of the silene and by the organic reagent. Thus, alkenes react with silenes not only by [2+2] cycloaddition to give **21**, but also under the formation of ene-addition products, if the alkene has  $\alpha$ -hydrogens. Ketones on the other hand react regioselectively with silenes under the formation of the oxasiletane **22** (Scheme 7).<sup>17,18,19</sup>



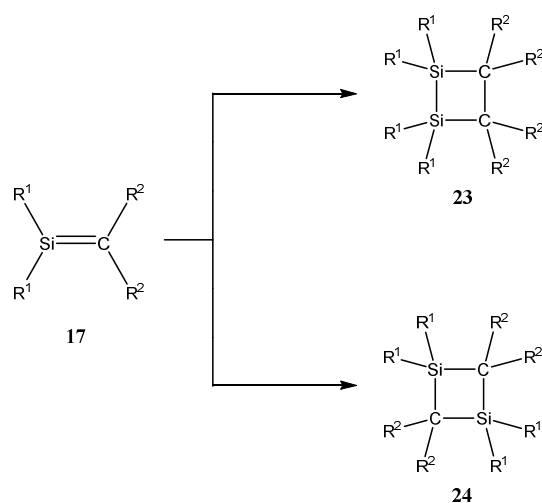
**Scheme 7:** Reactivity of silenes with other double bonds

Dienes and naturally polarized silenes afford mixtures of [4+2]-, [2+2]- cycloadducts and ene-adducts in the presence of  $\alpha$ -hydrogens. On the other hand, reversed polarized silenes and dienes primarily give the [4+2] cycloadducts (Scheme 8).<sup>19,20</sup>



**Scheme 8:** Reactivity of silenes with dienes

In the absence of a trapping reagent transient silenes react intermolecularly. The manner of dimerization, head to head **23** or head to tail **24**, is strongly influenced by the substitution pattern and by the polarity of the silicon-carbon double bond.<sup>17</sup>



**Scheme 9:** Reactivity of transient silenes in the absence of trapping reagents

### 1.1.3 Spectroscopic and Structural Properties of Silenes

Selected important spectroscopic and physical data are depicted in Table 1. All values are strongly influenced by the substitution pattern of the Si=C double bond.

**Table 1:** Spectroscopic and physical properties of the Si=C double bond<sup>21-22-23-24</sup>

Spectroscopic and Physical properties	values
Si=C bond length	1.702-1764 Å
$\pi$ -bond strength	~160 kJ·mol <sup>-1</sup>
<sup>29</sup> Si-NMR shifts	41-144 ppm
Characteristic absorption ( $\pi$ - $\pi^*$ transition)	320-340 nm
Si=C stretching band	1003-1135 cm <sup>-1</sup>

## 1.1.4 Preparation of Silenes

Since the first evidence for the formation of silenes in 1967, a number of general synthetic pathways towards silenes have been developed. The most common synthetic strategies are summarized below.

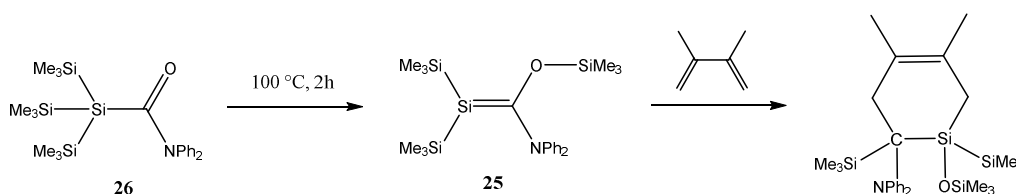
### 1.1.4.1 Thermolysis Reactions

This synthetic method was used in order to synthesize the first transient silenes by Gusev and Flowers (Scheme 2).<sup>2</sup> Generally the strong ring strain in silacyclobutanes was used to obtain transient silenes under very mild conditions.<sup>25</sup> With this building block, most of the fundamental work in silene chemistry has been conducted. For more complete information, the reader is referred to the review by Raabe and Michl.<sup>26</sup>

In the last twenty years thermolysis reactions led to the formation of transient silenes with one amino group attached to the carbon atom forming the Si=C double bond (Variation 1). Further developments have been implemented by the group of Y. Apeloig, who isolated the first stable bisilene via the thermolysis of mercury-bis(acylsilanes) (Variation 2). Both variations used a thermal [1,3]-silyl shift to obtain the corresponding silenes.

#### 1.1.4.1.1 Variation 1: Thermolysis of Carbamoylpolysilanes

Ottosson *et al.* exploited the thermal [1,3]-trimethylsilyl shift in order to synthesize the 2-amino-2-siloxysilene **25**. The thermolysis of the carbamoylpolysilane **26** was performed at 65-180°C. Due to the reversed polarization of the Si=C fragment, **25** reacted exclusively with dienes to give [4+2] cycloadducts (Scheme 9). Interestingly, this cycloaddition is followed by a Me<sub>3</sub>SiO-Me<sub>3</sub>Si-[1,2]-transposition.<sup>27</sup>

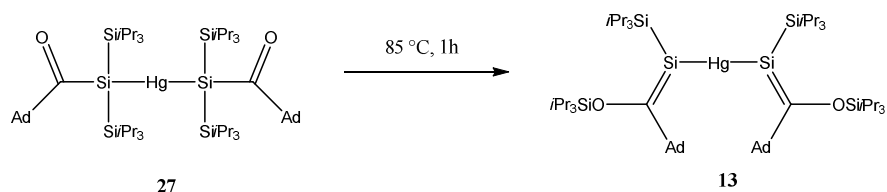


**Scheme 10:** Thermolysis of carbamoylpolysilanes



#### 1.1.4.1.2 Variation 2: Thermolysis of Mercury-(II)-bis(acylsilanes)

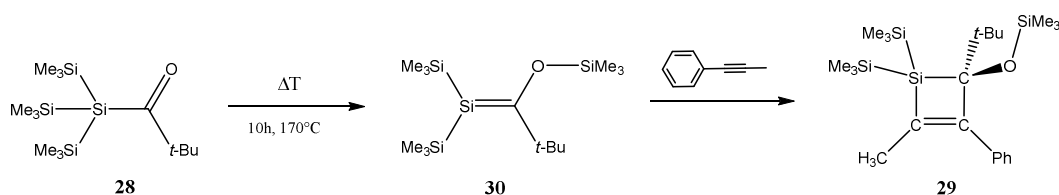
The thermal [1,3]-silyl rearrangement from mercury-(II)-bis(acylsilane) **27** to mercury-(II)-bis(2-siloxysilene) **13** was found by Apeloig *et al.*<sup>28</sup> Silene formation was possible only with two sterically demanding triisopropylsilyl-groups at the two central silicon atoms. Compound **13** is the first literature known representative of a bissilene (Scheme 11).



**Scheme 11:** Synthesis of the first bissilene

#### 1.1.4.1.3 Variation 3: Thermolysis of tris(trimethylsilyl)acylsilanes

It is also possible to induce a thermal “Brook-rearrangement”. The thermolysis of neat acylpolysilanes gives rise to a mixture of different compounds, but with the addition of standard trapping agents, the reaction proceeds much cleaner. Brook *et al.* showed that the thermolysis of pivaloyltris(trimethylsilyl)silane **28** in the presence of 1-phenylpropyne yields the 2-silacyclobutene **29**, which indicates the thermolytic formation of the silene **30** (Scheme 12).<sup>29</sup>

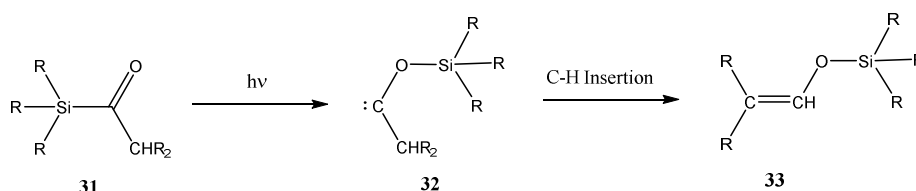


**Scheme 12:** Thermolysis of tris(trimethylsilyl)acylsilanes

### 1.1.4.2 Photochemical Synthesis

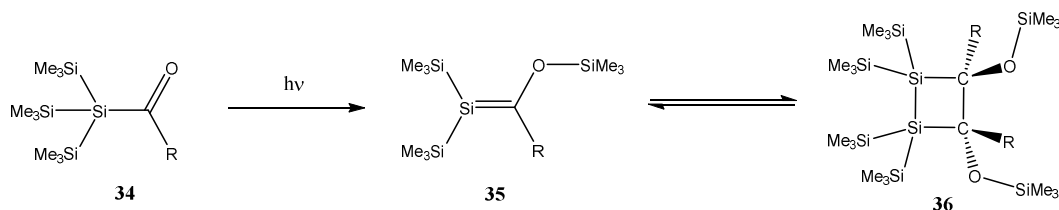
#### 1.1.4.2.1 Variation 1: Photolysis of Acylpolysilanes

The photochemical silene synthesis is inextricably connected to Adrian Brook and his so-called “Brook-Rearrangement”. He and his group worked on a series of acylsilanes **31**, which underwent a photochemically induced 1,3-trimethylsilyl migration to form the intermediate siloxycarbenes **32**. After C-H insertion, the siloxyalkenes **33** were formed (Scheme 13).<sup>30</sup>



**Scheme 13:** Photolysis of acylpolysilanes

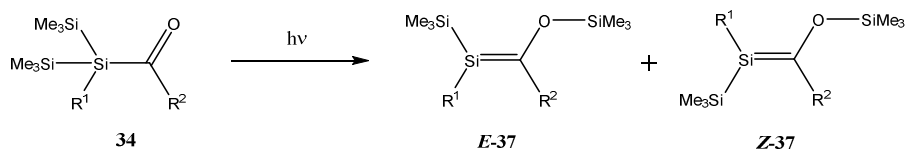
In a related manner the tris(trimethylsilyl)acylsilanes **34** afforded the corresponding silenes **35** when photolyzed with UV light of  $\lambda > 300$  nm (Scheme 14).<sup>31,32</sup>



**Scheme 14:** Photolysis of tris(trimethylsilyl)acylsilanes

The stability of these silenes is strongly influenced by the substituents at the carbonyl moiety. In the case of the phenyl substituted derivative, complete dimerization occurs to yield the 1,2-disilacyclobutanes **36**. At room temperature the *t*-butyl substituted silene forms a dynamic monomer-dimer equilibrium in solution. The synthesis of the 1-adamantyl substituted acylsilanes, finally, brought the historic breakthrough. The highly sterically demanding 1-adamantyl group suppresses dimer formation, which enabled Brook and his co-workers to isolate and fully characterize the first room temperature stable silene **35** (R = 1-adamantyl).<sup>33</sup>

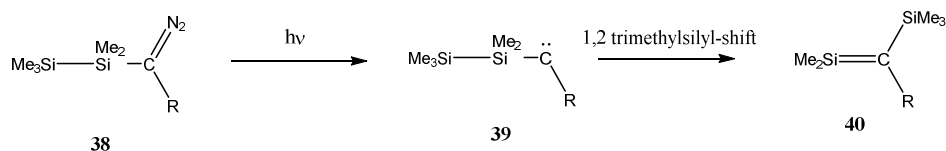
This methodology was further exploited by Brook and many other siloxysilenes **37** with a variety of different substituents were prepared. Nearly all of these silenes were characterized by NMR spectroscopy and isolated as their trapping or dimerization product. Furthermore, photolysis of these acylsilanes **34** afforded mixtures of the *E*-**37** and *Z*-**37** isomers (Scheme 15).<sup>34,35</sup>



**Scheme 15:** Photolysis of bis(trimethylsilyl)acylsilanes

#### 1.1.4.2.2 Variation 2: Photolysis of Silyldiazoalkanes

The photolysis of silyldiazoalkanes **38**, leads to the formation of transient disilylcarbenes **39**. This intermediate carbene undergoes a 1,2-silyl migration yielding silene **40**.<sup>36,37,38,39</sup>



**Scheme 16:** Photolysis of silyldiazoalkanes

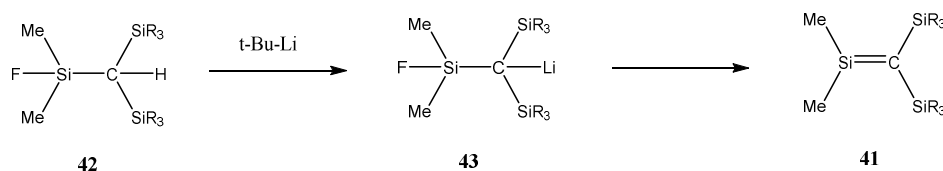
Although none of these silenes were isolated, many silenes isolated later such as the Wiberg silene, were observed by NMR spectroscopy in the course of this reaction in solution.

#### 1.1.4.3 Salt Elimination reactions

The salt elimination reaction is one of the most important synthetic tools in inorganic chemistry. Also in the chemistry of silenes, this synthetic approach led to very important breakthroughs, such as the synthesis of the first donor-free silene by Wiberg and his group.<sup>7</sup> Other important salt elimination reactions, which are still widely used, are the Sila-Peterson alkenation and the silene synthesis *via* a silenolate intermediate.

### 1.1.4.3.1 Variation 1: Intramolecular Salt Elimination

Wiberg *et al.* exploited the intramolecular salt metathesis reaction in order to synthesize various donor-free "Wiberg type" silenes **41**.<sup>40</sup> For this purpose the halotrisilylmethane **42** was metalated at the carbon position to yield compound **43** followed by thermal 1,2-LiF elimination (Scheme 17).

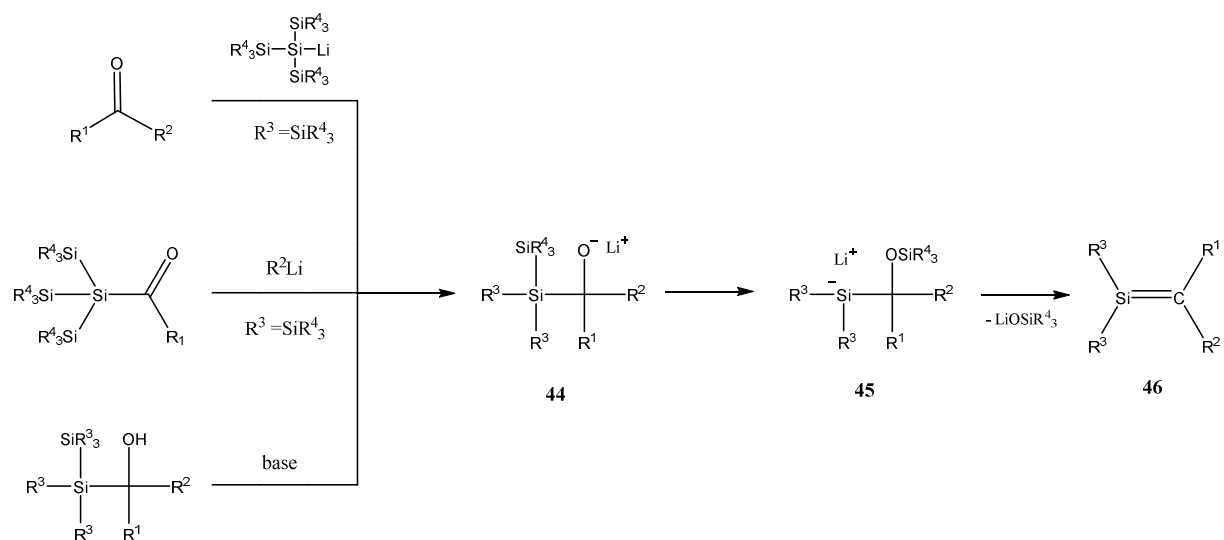


**Scheme 17:** Synthesis of the Wiberg silene

The temperature and the used solvent are very important parameters in order to observe an intramolecular salt metathesis reaction and the formation of the desired silene. Among many other silenes prepared by Wiberg *et al.*,  $\text{Me}_2\text{Si}=\text{C}(\text{SiMe}_3)(\text{SiMe}(t\text{-Bu})_2)$  is of particular importance, because it turned out to be stable enough to obtain its crystal structure.<sup>41</sup>

### 1.1.4.3.2 Variation 2: Sila-Peterson Alkenation

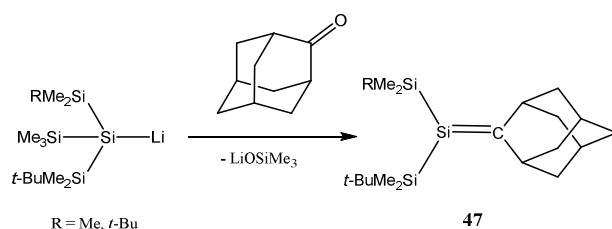
This method was simultaneously introduced by Oehme, Apeloig and Ishikawa.<sup>42-43-44-45-46-47-48-49-50</sup> It involves the reaction of an organo- or silyllithium reagent with carbonyl compounds or the reaction of  $\beta$ -silyl alcohols with bases to lithium salts of type **44** which undergo spontaneous rearrangement to form **45** and subsequently after elimination of lithiumsilenolate the silene **46**.



**Scheme 18:** Sila-Peterson alkenation reactions

The introduction of Sila-Peterson alkenation displaced the intramolecular salt metathesis reaction due to two improvements. The starting materials are easier to synthesize and the reaction has a higher

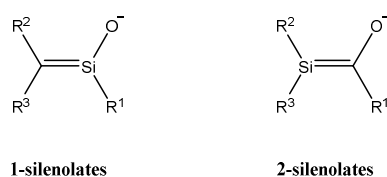
tolerance to functional groups as compared to the Wiberg method. Many of the ‘Apeloig-Ishikawa-Oehme’ type silenes are only transient species. They can be trapped by standard trapping reagents or dimerize in a head to head fashion. Room temperature stable silenes like **47** were successfully synthesized by Apeloig and Bravo-Zhivotovskii by the reaction of very bulky polysilyl anions with 2-adamantone.



**Scheme 19:** Silenesynthesis via Sila-Peterson alkenation

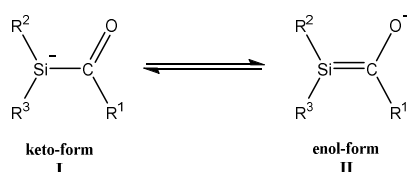
#### 1.1.4.3.3 Variation 3: Silene Synthesis via a Silenolate Intermediate

Two different types of silenolates are possible, the 1-silenolates and the 2-silenolates. However, only the 2-silenolates have been observed thus far.



**Scheme 20:** Types of silenolates

As in the case of enolates, two tautomeric structures of silenolates can be drawn: the keto form with the negative charge residing predominantly on the silicon atom (I), while in the enol form (II) the negative charge is located primarily on the oxygen atom (Scheme 21).<sup>51</sup>

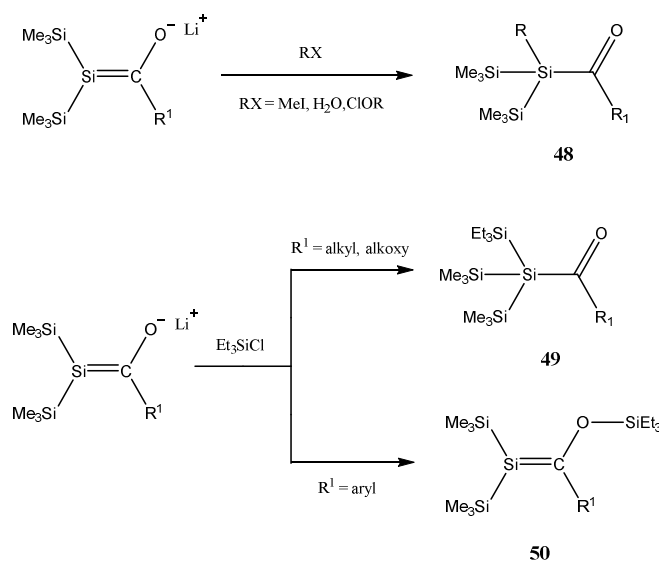


**Scheme 21:** Tautomeric structures of silenolates

For metal enolates, the dominant structure is the enol form, which is preferably formed in the solid state as well as in solution.<sup>52</sup> Silenolates on the other hand show a significant different tautomeric equilibrium. The position of the equilibrium is strongly influenced by the used alkali metal, the solvent and the substituent of the carbonyl moiety.<sup>52</sup>

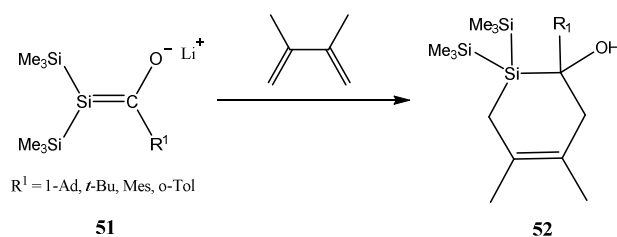
The first synthesized silenolates were the lithium silenolates in the early 1990's. Four scientists made valuable contributions to this field of research, namely Bravo-Zhivotovskii<sup>53</sup>, Apeloig<sup>54</sup>, Ishikawa and

Ohshita<sup>52a-e</sup>. However, the low thermal stability of these Li-silenolates prevented their general use as reagents for further derivatization. In Scheme 22, the reactivity of Li-silenolates with various electrophiles is summarized. Li-silenolates react with MeI, BzI, PhI and acid chlorides to give the alkylated acylpolysilane **48**. Interestingly, lithium silenolates with alkyl and aryl groups attached to the carbonyl moiety exhibit different reactivity patterns versus chlorosilanes. With alkyl- or alkoxy groups, the corresponding acylpolysilanes **49** are isolated, while aryl substituents give rise to oxygen carbon bond formation yielding the silenes **50**. Although none of the silenes were isolated as pure compounds, this method will gain particular importance in the course of this thesis.



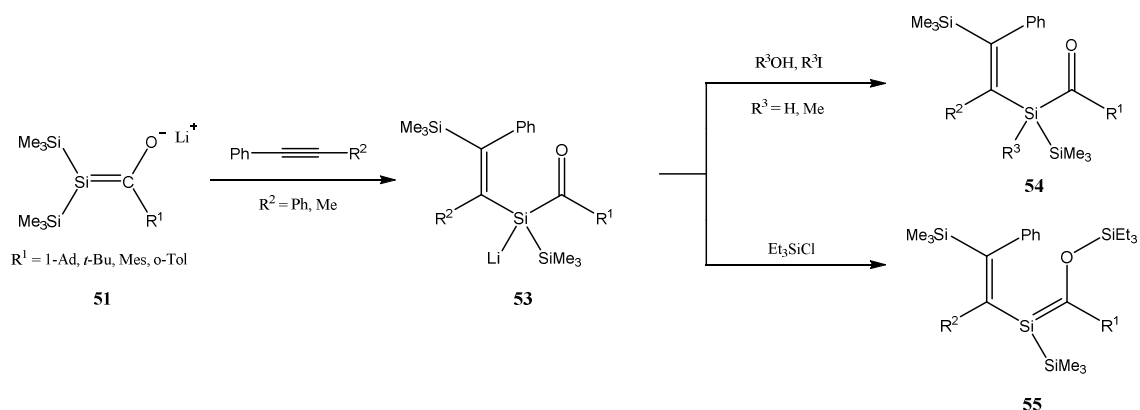
**Scheme 22:** Reactivity of silenolates towards electrophiles

Li-silenolates were also trapped with dienes and alkynes. Ohshita *et al.* found that the Li-silenolates **51** react with 2,3-dimethylbutadiene exclusively under formation of the [4+2] cycloadduct **52**.<sup>52b</sup>



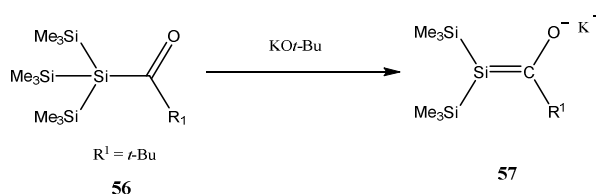
**Scheme 23:** Reactivity of silenolates towards dienes

The reaction of **51** with phenyl-substituted acetylenes,  $\text{PhC}\equiv\text{CR}^2$  ( $\text{R}^2 = \text{Ph}, \text{Me}$ ), cleanly afford the lithium ethenylsilenolates **53**, which reacts with  $\text{H}_2\text{O}$  or  $\text{MeI}$  to give the corresponding silicon substituted products **54**. In contrast, the same silanides reacts with chlorosilanes to the O-silylated products **55**.<sup>52f</sup>



**Scheme 24:** Reactivity of silenolates towards alkynes

Significant improvements were made by the replacement of lithium by potassium as the counter-ion in silenolates reported by Ottosson and coworkers,<sup>52g</sup> who abstracted one of the three trimethylsilyl groups in **56** with  $\text{KO}t\text{Bu}$  (Scheme 25). The cleavage of a  $\text{Me}_3\text{Si}$ -polysilanyl bond with  $\text{KO}t\text{Bu}$  is widespread in polysilane chemistry and was first introduced by Marschner *et al.*<sup>55,56</sup>



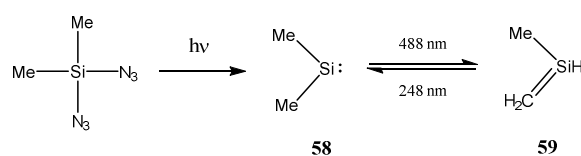
**Scheme 25:** Synthesis of potassium silenolates

These potassium silenolates **57** could be kept under inert atmosphere and ambient temperature for three months without any notable decomposition. Due to the enhanced stability in comparison to the Li-silenolates, Ottosson *et al.* were able to obtain the molecular structure of **57**, which adopts the keto-type resonance structure with a strongly pyramidal central silicon atom and unusually long Si-C single bond.<sup>52g</sup>

The reactivity of these K-silenolates closely resembles the reactivity observed for the Li-silenolates **53**. Thus, trapping of **57** with  $\text{MeI}$  yields the silicon methylated product **48**, the reaction of **57** with 2,3-dimethylbutadiene also proceeds identically under formation of the [4+2] cycloaddition product **52**.

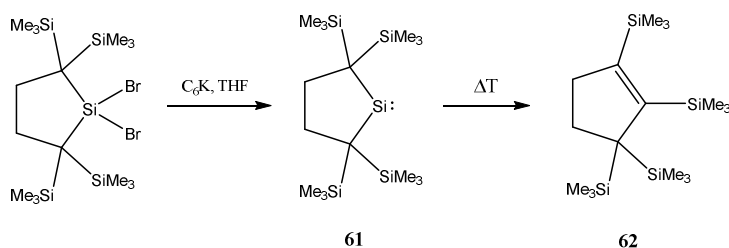
#### 1.1.4.4 Silylene-Silene Carbene-Silene Isomerization

Silylenes and carbenes can undergo [1,2]-hydrogen- or [1,2]-silyl-migration reactions to yield silenes. Many working groups investigated this isomerization and found a dynamic equilibrium between silylenes, carbenes and the corresponding silenes.<sup>57</sup> As ideal starting materials,  $\alpha$ -diazidosilanes or diazomethanes were used. Maier *et al.* showed that by the irradiation of diazomethane at the appropriate wavelength, silylene **58** was formed. Upon prolonged photolysis at  $\lambda = 488$  nm a [1,2]-hydrogen shift occurs and silene **59** was obtained. Photolysis of **59** at  $\lambda = 248$  nm caused a reversed [1,2]-hydrogen shift under back-formation of the silylene **58**.<sup>58</sup>



**Scheme 26:** Silylene-Silene Carben-Silene Isomerization

Only in the case of compound **61** an irreversible silylene-silene isomerization occurred. Upon moderate heating of the silylene, which is incorporated into a ring system, the stable silene **62** was formed. This silene generated by [1,2]-silyl migration was also the first isolated endocyclic silene.<sup>59</sup>

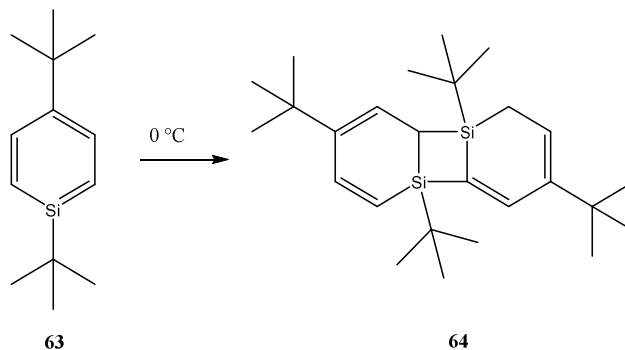


**Scheme 27:** First isolated endocyclic silene



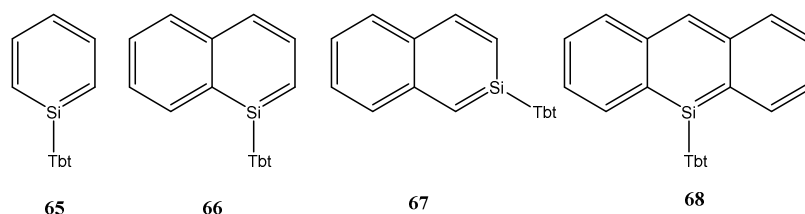
### 1.1.4.5 Silaaromatic Compounds

Silaaromatic compounds are far more reactive as compared to related species with nonconjugated Si-C double bonds. For instance, it has been reported by Märkl *et al.* that even 1,4-di-*t*-butyl-1-silabenzene **63** readily dimerizes at 0°C to give the corresponding [2+2] dimer **64**.<sup>60</sup>



**Scheme 28:** Reactivity of 1,4-di-*t*-butyl-1-silabenzene **63**

The decisive breakthrough was achieved by Tokitoh *et al.* who used the extremely bulky and effective protection group Tbt (2,4,6-tris[bis(trimethylsilyl)methyl]phenyl) to synthesize and to isolate a series of stable silaaromatic compounds, such as silabenzene **65**<sup>61</sup>, 1- and 2-silannaphthalenes (**66**<sup>62</sup> and **67**<sup>63</sup>) and 9-silanthracene **68**<sup>64</sup>.



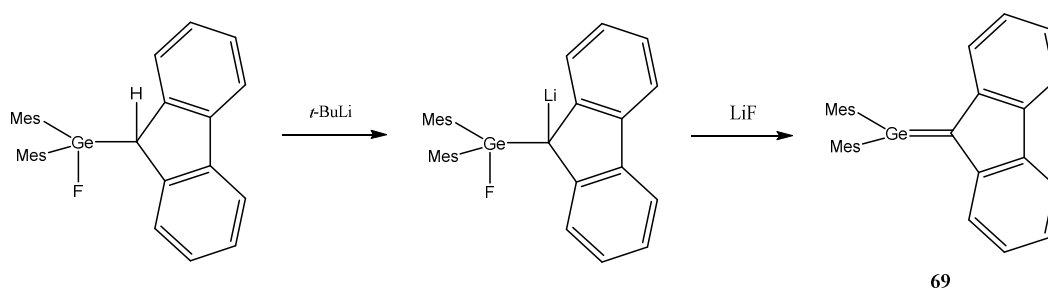
**Scheme 29:** Isolated silaaromatic compounds

The high planarity and other structural features of **65-68** indicate a delocalized  $\pi$ -system. Tokitoh *et al.* also examined the similarities and differences between silaaromatic compounds and the parent aromatic hydrocarbons by measuring the UV-Vis and Raman spectra of **65-68**. They were able to show that the replacement of one of the ring carbons by a silicon atom has minor influence on  $\pi$ -conjugation within the aromatic ring.

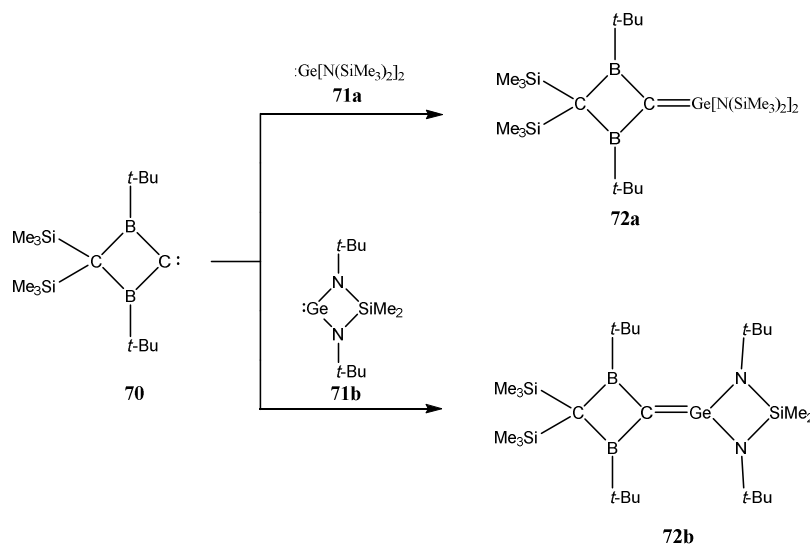
## 1.2 Germanes

### 1.2.1 Introduction

The outstanding breakthroughs in silene chemistry encouraged scientists in the field of organo-germanium chemistry to synthesize the corresponding low-valent germanium compounds. The first stable germanes were reported nearly simultaneously by two working groups in 1987. Escudié *et al.* synthesized dimesityl(fluorenylidene)germene **69** by a route involving intramolecular lithium fluoride elimination (Scheme 30),<sup>65</sup> while Berndt *et al.* employed the coupling of the cryptocarbene **70** with the stable germylenes **71a,b** to prepare the stable germanes **72a,b** (Scheme 31).<sup>66</sup>

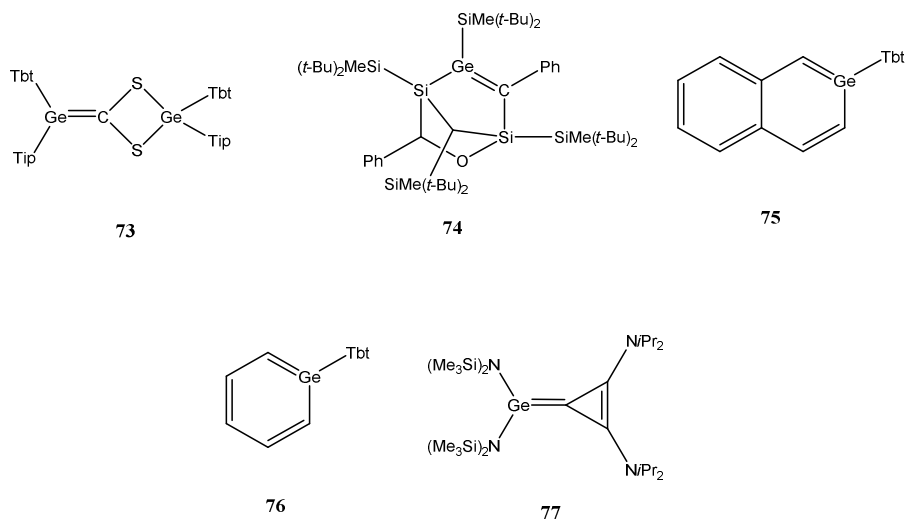


**Scheme 30:** Synthesis of germene **69** via intramolecular salt metathesis



**Scheme 31:** Synthesis of germanes via coupling reactions between a germylene and a carbene

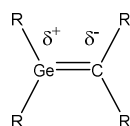
Since then new synthetic methods were applied to synthesize a variety of new germenes. Worth mentioning are the synthesis of the stable germene **73** by Tokitoh and co-workers *via* the reaction of a germylene with CS<sub>2</sub>, and the synthesis of the first endocyclic germene **74** by Sekiguchi's group.<sup>67-68</sup> Tokitoh *et al.* published a series of papers on stable germaaromatic compounds such as the 2-germanaphthalene **75** and germabenzene **76**.<sup>69,70</sup> In addition, Schumann *et al.* isolated and structurally characterized the 4-germatrifalvene **77**.<sup>71</sup>



**Scheme 32:** Selected germenes

### 1.2.2 Reactivity of Germenes

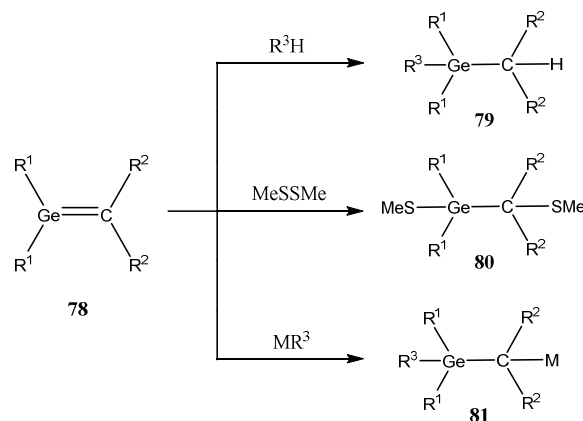
Starting from the simplest germene H<sub>2</sub>Ge=CH<sub>2</sub>, which has a transient existence, a huge variety of different germenes have been synthesized. Stable germenes can be directly detected under ambient temperature and inert atmosphere (nitrogen, argon). The stability of germenes, like for the silenes, is strongly influenced by the size and the electronic nature of the substituents. By increasing the size of the substituents the stability of the germenes increases. The Ge=C double bond is a polarized double bond. The positive charge is located at the germanium atom while the carbon atom carries the negative charge (Scheme 33).<sup>72</sup> Reverse-polarized germenes are unknown so far.



Germene with natural polarity

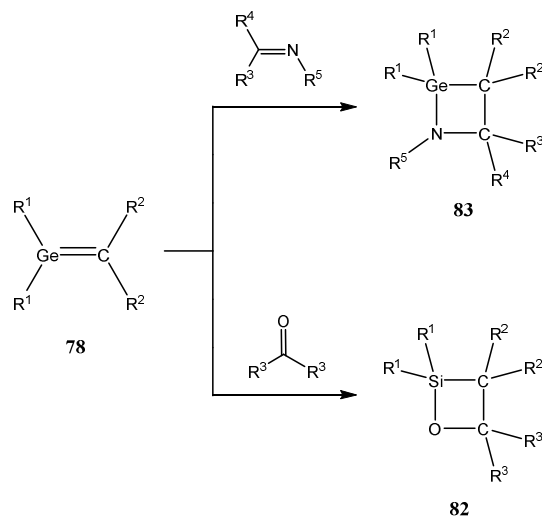
**Scheme 33:** Polarity of the Ge=C double bond

As a consequence of their high reactivity, germenes are valuable starting materials for synthesis. Germenes **78** react regioselectively with reagents of the type RH (R= OH, OR, HCl, HF, etc.) to give the germanes **79**. Disulfides add to the double bond to form the sulfur compound **80**. Carbanions **81** are formed during the reaction of silenes with organometallic reagents (Scheme 34).<sup>73</sup>



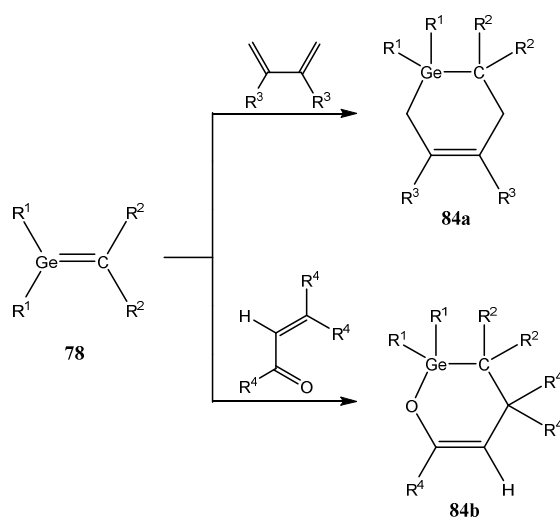
**Scheme 34:** Reactivity of germenes with standard trapping reagents

The reaction between germenes and other double bonds (such as alkenes, ketones, alkynes, dienes etc.) were most intensively investigated. Ketones and aldehydes react nearly regioselectively with germenes under the formation of the oxagermetanes **82** (Scheme 35) while nitrosobenzene reacts with germenes by [2+2] cycloaddition to give **83**.<sup>74</sup>



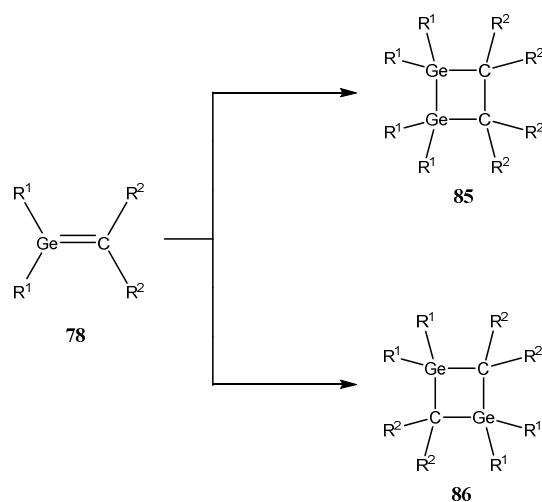
**Scheme 35:** Reactivity of germenes with other double bonds

Dienes,  $\alpha$ -ethylenic aldehydes and germenes afford the [4+2]-cycloadducts **84a,b**. In the literature no evidence exists for the formation of the [2+2]-cycloadducts, which are often found in the reaction of dienes with silenes (Scheme 36).<sup>74</sup>



**Scheme 36:** Reactivity of germenes with dienes

In the absence of a trapping reagent transient germenes react intermolecularly. The manner of dimerization, head to head **85** or head to tail **86**, is strongly influenced by the substitution pattern and by the polarity of the germanium-carbon double bond.<sup>74,75</sup>



**Scheme 37:** Reactivity of transient germenes in the absence of trapping reagents

### 1.2.3 Spectroscopic and Structural Properties of Germenes

Selected important spectroscopic and physical data are depicted in Table 2. Again all values are strongly influenced by the substitution pattern of the Ge=C double bond.

**Table 2:** Spectroscopic and physical properties of the Ge=C double bond<sup>76</sup>

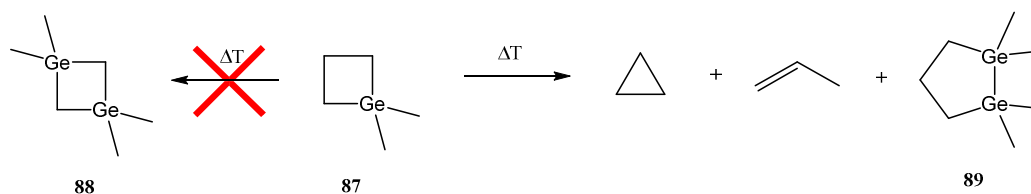
Spectroscopic and Physical properties	values
Ge=C bond length	1.771-1827 Å
$\pi$ -bond strength	~134 kJ·mol <sup>-1</sup>
<sup>13</sup> C-NMR shifts	79-115 ppm
Characteristic absorption ( $\pi$ - $\pi^*$ transition)	262-396 nm
Ge=C stretching band	988-1018 cm <sup>-1</sup>

### 1.2.4 Preparation of Germenes

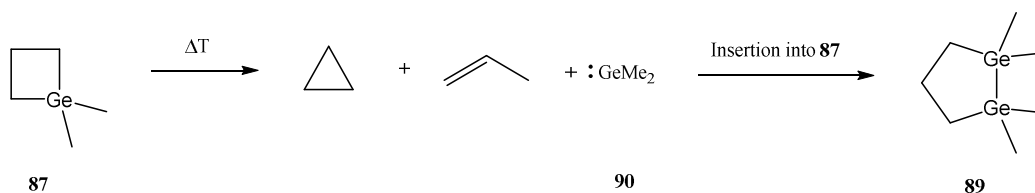
The first evidence for the formation of germenes was provided in the 1960s and 1970s by the isolation of their corresponding trapping products. Since that time, a number of general synthetic pathways toward germenes have been developed. The most common synthetic strategies are summarized below.

#### 1.2.4.1 Thermolysis reactions

In 1970s, Gusel'nikov and Flowers reported that the thermal fragmentation of 1,1-dimethylgermetane **87** in the gas phase significantly differs from the pyrolysis of the corresponding silicon and carbon analogues.<sup>77</sup> They expected 1,3-digermacyclobutane **88** as a product. Instead, they found considerable quantities of cyclopropane, propene and 1,2-digermacyclopentane **89** and postulated a reaction mechanism including the initial formation of propene, cyclopropane and dimethylgermylene **90**, which subsequently inserts into the germanium-carbon bond of the starting material **87** to give the 1,2-digerma-cyclopentane **89**.

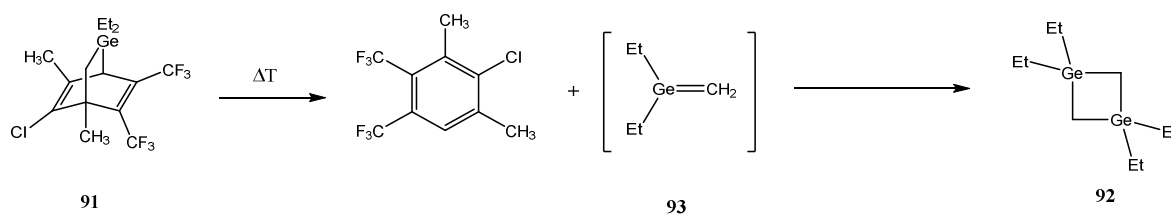


**Scheme 38:** Thermal fragmentation of 1,1-dimethylgermetane



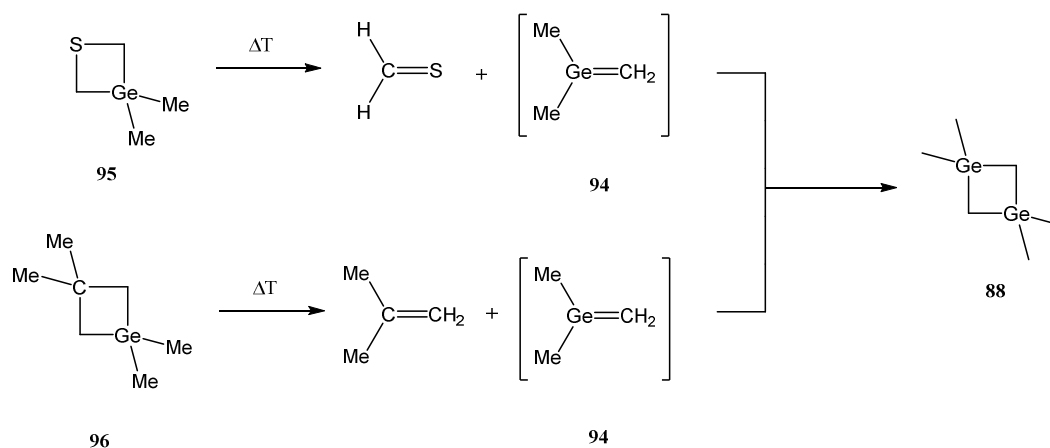
**Scheme 39:** Postulated mechanism of the thermal fragmentation of 1,1-dimethylgermetane

Only three years later, Barton *et al.* demonstrated that the thermolysis of the bicyclic structure **91** leads to the formation of 1,1,3,3-tetraethyl-1,3-digermacyclobutane **92**. As an intermediate of this reaction they postulated the transient germene **93**.<sup>78</sup>



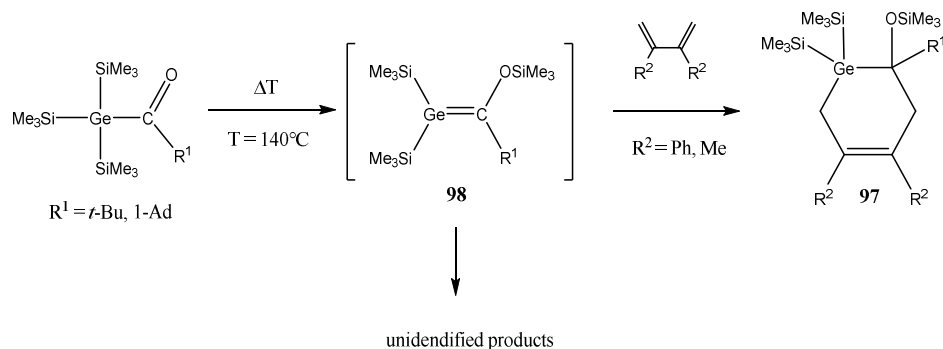
**Scheme 40:** Thermolysis of the bicyclic structure **91**

Khabashesku *et al.* performed the spectroscopic characterization of the transient 1,1-dimethyl-1-germene **94** in a rigid matrix. **94** has been obtained by the pyrolysis of 1,1-dimethyl-1-germa-3-thietane **95** or 1,1,3,3-tetramethyl-1-germacyclobutane **96**. In contrast to the work of Gusel'nikov and Flowers no evidence was found for the formation of dimethylgermylene **90**. Instead they observed clean formation of the transient germene and isolated its intermolecular trapping product **88**.<sup>79</sup>



**Scheme 41:** Spectroscopic characterization of the transient 1,1-dimethyl-1-germene **94**

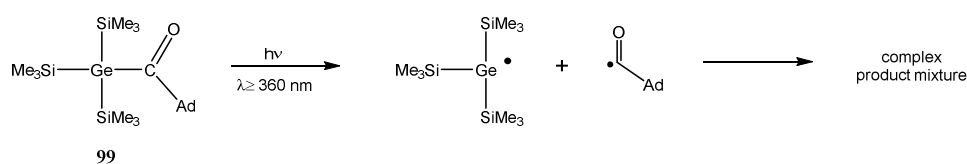
The thermolysis reactions of a series of acylgermanes were investigated by Ishikawa *et al.*<sup>80-81</sup> In the presence of trapping reagents, such as butadiene's, they observed the clean formation of the respective cycloadducts **97**. Interestingly, in the absence of trapping reagents, thermolysis afforded large amounts of nonvolatile and smaller amounts of volatile unidentified products. Therefore, they stated that the formed germenes **98** are unstable under these conditions and decompose in the absence of a trapping reagent to uncharacterized products.



**Scheme 42:** Thermolysis of acylgermanes

#### 1.2.4.2 Photochemical Synthesis

Although the photochemical silene synthesis is a very important synthetic strategy to isolate stable silenes, no light induced germene formation reactions are apparent in the literature. This arises from the fact that acylgermanes do not undergo photochemical Brook-type rearrangement reactions.<sup>82</sup> Instead, acylgermanes react under irradiation by the homolytic cleavage of the Ge-C bond *via* a Norrish type I reaction.<sup>83</sup> In line with this picture Brook *et al.* showed that the photolysis of the tris(trimethylsilyl)acylgermane **99** gives a complex product mixture due to extensive follow-up reactions of the initially formed germyl radicals.<sup>84</sup>



**Scheme 43:** Photolysis of tris(trimethylsilyl)acylgermanes

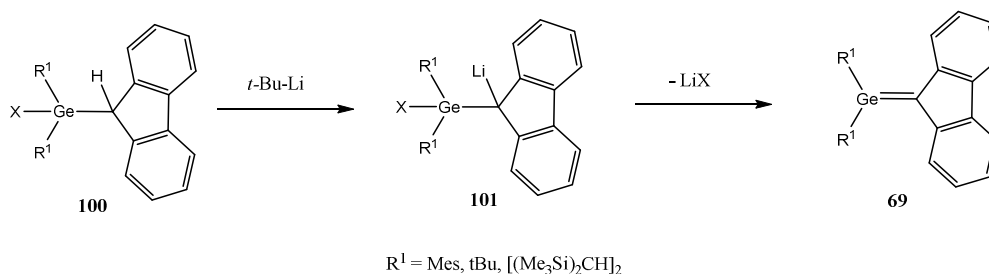


### 1.2.4.3 Salt Elimination reactions

As mentioned previously for silenes, the salt elimination reaction is one of the most important synthetic methods in inorganic chemistry. Also in the chemistry of germenes this synthetic approach led to very important breakthroughs, such as the synthesis of the first stable germene by Escudié and his group.

#### 1.2.4.3.1 Variation 1: Intramolecular Salt Metathesis

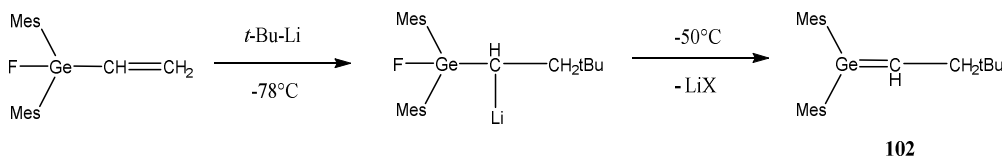
Escudié *et al.* exploited the intramolecular salt metathesis reaction in order to synthesize different germenes of the type **69**.<sup>85,86,87</sup> Therefore, chloro- or fluorogermanes **100** were metalated at the carbon position to yield compound **101**. The best results were generally obtained with fluorogermanes. After a subsequent thermal 1,2-LiX-elimination step germene **69** was formed. The use of a bulky lithio compound is necessary to prevent direct alkylation of the germanium atom.



**Scheme 44:** Synthesis of germene **69** via intramolecular salt metathesis reaction

#### 1.2.4.3.2 Variation 2: Addition-Elimination Reactions

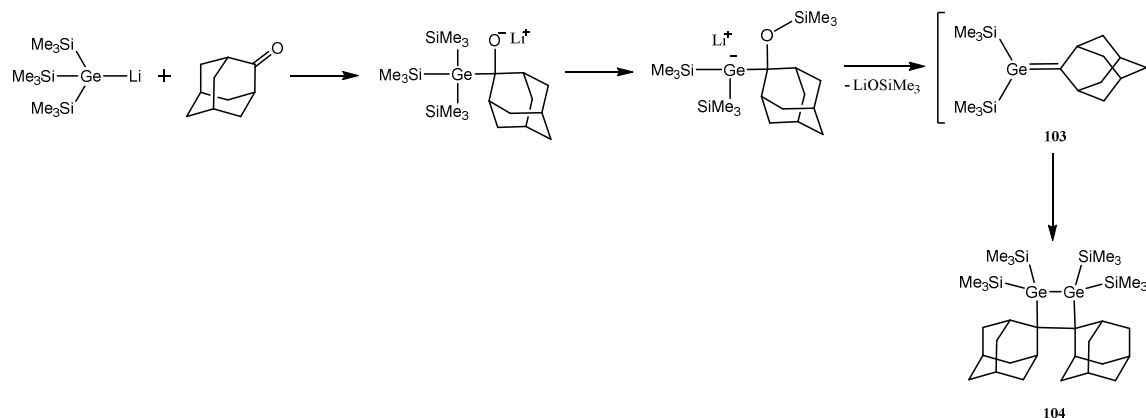
This synthetic strategy was first published by Jones and adopted by Auner for the synthesis of silenes.<sup>88,89</sup> By the use of the bulky mesityl group, Couret *et al.* were able to isolate and to characterize the stable dimesitylneopentylgermene **102**. **102** represent the first example of a germene bearing a prochiral carbon center.



**Scheme 45:** Synthesis of germene **102** bearing a prochiral carbon center

### 1.2.4.3.3 Variation 3: Germa-Peterson Alkenation

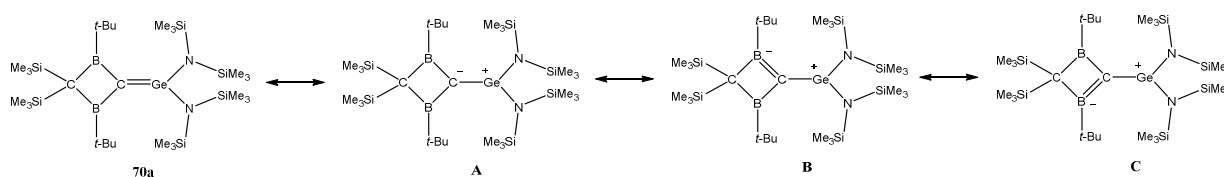
This method was introduced by Apeloig and Bravo-Zhivotovskii (compare Scheme 46). Like Sila-Peterson alkenation, it involves the reaction of a germyllithium derivative with a carbonyl compound. After rearrangement and elimination of lithiumsilenolate the transient germene **103** is formed. This germene, however, is not stable and gives the corresponding head-to-head dimer **104** in the absence of trapping reagents.<sup>90</sup>



**Scheme 46:** Germa-Peterson alkenation reaction

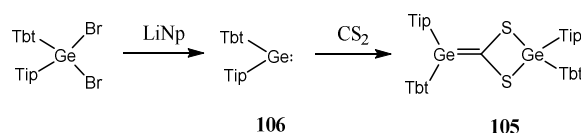
### 1.2.4.4 Coupling between a Germylene and a Carbene

Germylenes and carbenes can undergo coupling reactions to yield germenes. Berndt *et al.* introduced this synthetic approach in order to synthesize the germenes **70a,b** (see Scheme 31), which are stable at room temperature and in solution. The presence of a germanium-carbon double bond was confirmed by X-ray diffraction analysis of **70a**.<sup>91</sup> The significantly elongated Ge=C double bond (1.827(4) Å), the short distance between the tricoordinated carbon and the boron atoms (152.3 (6) Å to 153.4 (7) Å) and the higher shielding of the boron atoms in <sup>11</sup>B-NMR compared to the starting material indicates considerable ylid character. In Scheme 47, all three possible ylid resonance structures are depicted.



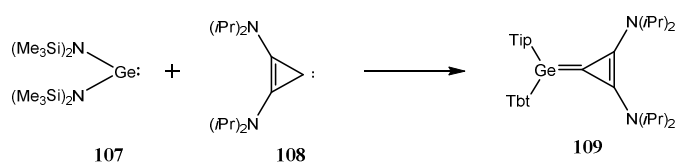
**Scheme 47:** Three possible ylid resonance structures of **70a**

The synthesis of the germene **105** by the reaction of the sterically protected diarylgermylene **106** with CS<sub>2</sub> was reported by Tokitoh *et al.* The planar germanium-carbon double bond in **105** exhibits a bond length of 1.771 (16) Å, which is the shortest double bond length among all structurally characterized germenes. Due to the very bulky Tip and Tbt groups, **105** is surprisingly inert. Even in refluxing benzene, no reaction with methanol was found.<sup>92</sup>



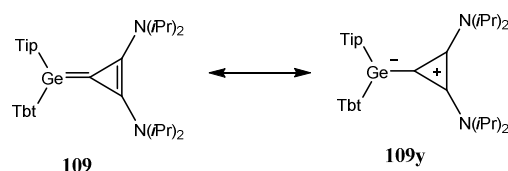
**Scheme 48:** Synthesis of germene **105**

Another germene forming an ylid structure was published by Schumann *et al.*, who reacted the stable bis(amino)germylene **107** with the transient cyclic carbene **108**, to give the germene **109**.<sup>93</sup>



**Scheme 49:** Synthesis of germene **109**

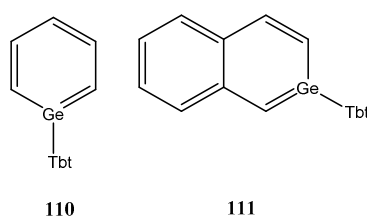
As mentioned above **109** exhibit properties of the ylid structure **109y**. This is apparent from the long Ge-C bond length of 2.085 (3) Å, which is even longer than a normal Ge-C single bond, and the high pyramidalization angle of the germanium atom. Furthermore, the <sup>13</sup>C-NMR resonances of the carbon atoms forming the three-membered ring are characteristic for a cyclopropenylium compound.



**Scheme 50:** Resonance structures of compound **109**

### 1.2.4.5 Germaaromatic Compounds

As in the case of silaaromatic compounds Tokitoh and his coworkers made valuable contributions to this field with the synthesis and the characterization of the first stable germabenzene **110** and 2-germanaphthalene **111**.<sup>94,95</sup> The high planarity and other structural features indicate a delocalized  $\pi$ -system. Tokitoh *et al.* also examined the similarities and differences between germaaromatic compounds and the parent aromatic hydrocarbons by measuring the UV-Vis and Raman spectra of **110** and **111** and observed only minor impact of the endocyclic heteroatom on the aromatic  $\pi$ -system in close analogy to the silicon case.



**Scheme 51:** Isolated germaaromatic compounds

## 1.3 References

- <sup>1</sup> a) H. Gilman, W. H. Atwell, G. L. Schwebke, *Chem Ind.* (1964) 1063; b) H. Gilman, W. H. Atwell, G. L. Schwebke, *J. Organomet. Chem.* 2 (1964) 369; c) M. Kumada, K. Tamao, *Adv. Organomet. Chem.* 6 (1969) 19; d) R. D. Miller, D. Hofer, J. F. Rabolt, G. N. Fickes, *J. Am. Chem. Soc.* 107 (1985) 2172; e) J. Michl, *Acc. Chem. Res.* 23 (1990) 127; f) D. W. Rooklin, T. Schepers, M. K. Raymond-Johansson, J. Michl, *Photochem. Photobiol. Sci.* 2 (2003) 511
- <sup>2</sup> R. West, *Pure Appl. Chem.* 54 (1982) 1041
- <sup>3</sup> P. Jutzi, *Angew. Chem., Int. Ed. Engl.* 14 (1975) 232
- <sup>4</sup> L. E. Gusel'nikov, M. C. Flowers, *J. Chem. Soc. Chem. Commun.* (1967) 864
- <sup>5</sup> S. C. Nyburg; A. G. Brook, F. Abdesaken, G. Gutekunst, W. Wong-Ng, *Acta Cryst.* C41 (1985) 1632
- <sup>6</sup> N. Wiberg, G. Wagner, G. Müller, J. Reids; *Angew. Chem., Int. Ed. Engl.* 22 (1984) 381
- <sup>7</sup> Y. Apeloig, M. Bendikov, M. Yuzefovich, M. Nakash, D. Bravo-Zhivotovskii, D. Blaser, R. Boese, *J. Am. Chem. Soc.* 118 (1996) 12228
- <sup>8</sup> M. Kira, S. Ishida, T. Iwamoto, C. Kabuto, *J. Am. Chem. Soc.* 121 (1999) 9722
- <sup>9</sup> a) N. Tokitoh, A. Shinohara, T. Matsumoto, T. Sasamori, N. Takeda, Y. Furukawa, *Organometallics* 26 (2007) 4048; b) N. Takeda, A. Shinohara, N. Tokitoh, *Organometallics* 21 (2002) 256; c) N. Takeda, A. Shinohara, N. Tokitoh, *Organometallics* 21 (2002) 4024; d) K. Wakita, N. Tokitoh, R. Okazaki, S. Nagase, *Angew. Chem., Int. Ed.* 39 (2000) 634; e) K. Wakita, N. Tokitoh, R. Okazaki, S. Nagase, P. von Schleyer, H. Jiao, *J. Am. Chem. Soc.* 121 (1999) 11336; f) N. Tokitoh, K. Wakita, R. Okazaki, S. Nagase, P. von Schleyer, H. Jiao, *J. Am. Chem. Soc.* 119 (1997) 6951
- <sup>10</sup> K. Sakamoto, J. Ogasawara, Y. Kon, T. Sunagawa, C. Kabuto, M. Kira, *Angew. Chem. Int. Ed.* 41 (2002) 1402

11 D. Bravo-Zhivotovskii, R. Dobrovetsky, D. Nemirovsky, V. Molev, M. Bendikov, G. Molev, M.  
Botoshansky, Y. Apeloig, *Angew. Chem., Int. Ed.* 47 (2008) 4343

12 I. Bejan, D. Güclü, S. Inoue, M. Ichinohe, A. Sekiguchi, D. Scheschkewitz, *Angew. Chem., Int.  
Ed.* 46 (2007) 3349

13 S. Inoue, M. Ichinohe, A. Sekiguchi, *Angew. Chem., Int. Ed.* 46 (2007) 3346

14 T. Guliashvili, I. El-Sayed, A. Fischer, H. Ottosson, *Angew. Chem., Int. Ed.* 42 (2003) 1640

15 A. Brook, *Adv. Organomet. Chem.* 39 (1996) 71; R. West, *J. Organomet. Chem.* 21 (2001) 467;  
c) L. E. Gusel'nikov, *Coord. Chem Rev.* 244 (2003) 149; H. Ottosson, A. M. Eklöf, *Coord. Chem  
Rev.* 252 (2008) 1287

16 K. Baines, M. S. Samuel, *Science of Synthesis* 4 (2002) 125

17 G. Raabe, J. Michl, In *The Chemistry of Organic Silicon Compounds*, S. Patai, Z. Rappoport,  
Eds.; Wiley: New York, Chapter 17 (1989) 1015

18 T. Müller, W. Ziche, N. Auner, In *The Chemistry of Organic Silicon Compounds*, Z. Rappoport,  
Y. Apeloig, Eds.; Wiley: New York, Chapter 16 (1998) 857

19 H. Ottosson, A. M. Eklöf, *Coord. Chem. Rev.* 252 (2008) 1287

20 K. Sakamoto, J. Ogasawara, H. Sakurai, M. Kira, *J. Am. Chem. Soc.* 119 (1997) 3405

21 a) S. Bailleux, M. Bogey, J. Breidung, H. Burger, R. Fajgar, Y. Liu, J. Pola, M. Senzlober, W.  
Thiel, *Angew. Chem. Int. Ed. Engl.* 35 (1996) 2513; b) S. Bailleux, M. Bogey, J. Demaison, H.  
Burger, M. Senzlober, J. Breidung, W. Thiel, R. Fajgar, J. Pola, *J. Chem. Phys.* 106 (1997) 10016

22 C. Liang, L. C. Allen, *J. Am. Chem. Soc.* 112 (1990) 1039

23 M. W. Schmidt, M. S. Gordon, M. Dupuis, *J. Am. Chem. Soc.* 107 (1985) 2585

24 J. M. Galbraith, E. Blank, S. Shaik, P. C. Hiberty, *Chem. Eur. J.* 6 (2000) 2425

25 A. G. Brook, J. W. Harris, J. Lennon, M. El Sheikh, *J. Am. Chem. Soc.* 101 (1979) 83

26 J. Michl, G. Raabe, *Chem. Rev.* 85 (1985) 125

27 I. El-Sayed, T. Guliashvili, R. Hazell, A. Gogoll, H. Ottosson, *Org. Lett.* 4 (2002) 1915

28 D. Bravo-Zhivotovskii, R. Dobrovetsky, D. Nemirovsky, V. Molev, M. Bendikov, G. Molev, M.  
Botoshansky, Y. Apeloig, *Angew. Chem., Int. Ed.* 47 (2008) 4343

29 A. G. Brook, J. W. Harris, J. Lennon, M. El. Sheikh, *J. Am. Chem. Soc.* 101 1979 83

30 J. M. Duff, A. G. Brook, *Can. J. Chem.* 51 (1973) 2869

31 A. G. Brook, J. W. Harris, J. Lennon, M. El Sheikh, *J. Am. Chem. Soc.* 101 (1979) 83

32 A. G. Brook, F. Abdesaken, B. Gutekunst, G. Gutekunst, M. R. Kallury, *J. Chem. Soc. Chem.  
Commun.* (1981) 191

33 A. G. Brook, S. C. Nyberg, F. Abdesaken, B. Gutekunst, G. Gutekunst, R. Krishna, M. R.  
Kallury, Y. C. Poon, Y. Chang, W. Wong-Ng, *J. Am. Chem. Soc.* 104 (1982) 5667

34 P. Lassacher, A. G. Brook, A. J. Lough, *Organometallics* 14 (1995) 4359

35 A. G. Brook, A. Baumegger, A. J. Lough, *Organometallics* 11 (1992) 3088

36 A. Sekiguchi, W. Ando, K. Honda, *Tetrahedron Lett.* 26 (1985) 2237

37 A. Sekiguchi, W. Ando, *Chem. Lett.* (1986) 2025

38 A. Sekiguchi, W. Ando, *Organometallics* 6 (1987) 1857

39 G. Maas, M. Alt, K. Schneider, W. Ando, *Chem. Commun.* (1988) 72

40 N. Wiberg, G. Preiner, O. Schieda, *Chem. Ber.* 114 (1981) 2087

41 N. Wiberg, G. Wagner, G. Müller; *Angew. Chem. Int. Ed. Engl.* 24 (1985) 229

42 H. Oehme, R. Wustrack, *Z. Anorg. Allg. Chem.* 215 (1987) 552

43 R. Wustrack, H. Oehme, *J. Organomet. Chem.* 95 (1988) 352

44 H. Oehme, R. Wustrack, A. Heine, G. M. Sheldrick, D. Starke, *J. Organomet. Chem.* 33 (1993)  
452

- 45 D. Bravo-Zhivotosvskii, V. Braude, A. Stanger, M. Kapon, Y. Apeloig, *Organometallics* 11 (1992) 2326
- 46 Y. Apeloig, M. Bendikov, M. Yuzefovich, N. Moshe, D. Bravo-Zhivotosvskii, *J. Am. Chem. Soc.* 118 (1996) 12228
- 47 J. Ohshita, Y. Masaoka, M. Ishikawa, *Organometallics* 10 (1991) 3775
- 48 J. Ohshita, Y. Masaoka, M. Ishikawa, T. Takeuchi, *Organometallics* 12 (1993) 876
- 49 C. Krempner, H. Oehme, *J. Organomet. Chem.* C7 (1994) 464
- 50 C. Krempner, H. Reinke, H. Oehme, *Angew. Chem.* 106 (1994) 1709
- 51 For general reviews about enolates, see e. g.: a) D. Stolz, U. Kazmaier in *The Chemistry of Metal Enolates*, Part 1 (Eds.: Z. Rappoport, J. Zabicky), Wiley, Hoboken, (2009), pp. 355-411; b) D. Seebach, *Angew. Chem.* 100 (1988) 1685; *Angew. Chem. Int. Ed. Engl.* 27 (1988) 1624; c) P. Veya, C. Floriani, A. Chiessi Villa, C. Rizzoli, *Organometallics* 13 (1994) 214
- 52 a) J. Ohshita, Y. Masaoka, S. Masaoka, M. Ishikawa, A. Tachibana, T. Yano, T. Yamabe, *J. Organomet. Chem.* 473 (1994) 15; b) J. Ohshita, S. Masaoka, Y. Masaoka, H. Hasebe, M. Ishikawa, A. Tachibana, T. Yano, T. Yamabe, *Organometallics* 15 (1996) 3136; c) J. Ohshita, S. Masaoka, Y. Morimoto, M. Sano, M. Ishikawa, *Organometallics* 16 (1997) 1123; d) J. Ohshita, H. Sakurai, Y. Tokunaga, A. Kunai, *Organometallics* 18 (1999) 4545; e) J. Ohshita, H. Sakurai, S. Masaoka, M. Tamai, A. Kunai, M. Ishikawa, *J. Organomet. Chem.* 633 (2001) 131; f) J. Ohshita, M. Tamai, H. Sakurai, A. Kunai, *Organometallics* 20 (2001) 1065; g) T. Guliashevili, I. El-Syed, A. Fischer, H. Ottosson, *Angew. Chem. Int. Ed.* 42 (2003) 1640; h) R. Dobrovetsky, L. Zborovsky, D. Sheberla, M. Botoshansky, D. Bravo-Zhivotosvskii, Y. Apeloig, *Angew. Chem. Int. Ed.* 49 (2010) 4084; i) M. Haas, R. Fischer, M. Flock, S. Mueller, M. Rausch, S. Saf, A. Torvisco, H. Stueger, *Organometallics* 33 (2014) 5956
- 53 I. S. Biltueva, D. A. Bravo-Zhivotosvskii, I. D. Kalikhman, V. Yu. Vitkovskii, S. G. Shevchenko, N. S. Vyazankin, M. G. Voronkov, *J. Organomet. Chem.* 368 (1989) 163
- 54 D. A. Bravo-Zhivotosvskii, Y. Apeloig, Y. Ovchinnikov, V. Igonin, Y. T. Struchkov, *J. Organomet. Chem.* 123 (1993) 446
- 55 C. Marschner, *Eur. J. Inorg. Chem.* (1998) 221
- 56 C. Kayser, R. Fischer, J. Baumgartner, C. Marschner, *Organometallics* 21 (2002) 1023
- 57 For example: a) C. Chang, J. Kolc, M. E. Jung, J. A. Lowe, O. L. Chapman, *J. Am. Chem. Soc.* 98 (1976) 7846; b) V. N. Khabashesku, V. Balaji, S. E. Boganov, O. M. Nefedov, J. Michl, *J. Am. Chem. Soc.* 116 (1994) 320; c) P. P. Gaspar, R. J. Hwang, W. C. Eckelman, *J. Chem. Soc.* 7 (1974) 242
- 58 H. P. Reisenauer, G. Mihm, G. Maier, *Angew. Chem. Int. Ed. Engl.* 21 (1982) 854
- 59 M. Kira, S. Ishida, T. Iwamoto, C. Kabuto, *J. Am. Chem. Soc.* 121 (1999) 9722
- 60 G. Märkl, P. Hofmeister, *Angew. Chem. Int. Ed. Engl.* 18 (1979) 789
- 61 K. Wakita, N. Tokitoh, R. Okazaki, S. Nagase, *Angew. Chem., Int. Ed.* 39 (2000) 634
- 62 N. Takeda, A. Shinohara, N. Tokitoh, *Organometallics* 21 (2002) 4024
- 63 N. Tokitoh, K. Wakita, R. Okazaki, S. Nagase, P. v. R. Schleyer, H. Jiao, *J. Am. Chem. Soc.* 119 (1997) 6951
- 64 N. Takeda, A. Shinohara, N. Tokitoh, *Organometallics* 21 (2002) 256
- 65 C. Couret, J. Escudié, J. Satgé, M. Lazraq, *J. Am. Chem. Soc.* 109 (1987) 4411
- 66 H. Meyer, G. Baum, W. Massa, A. Berndt, *Angew. Chem. Int. Ed. Engl.* 21 (1987) 221
- 67 N. Tokitoh, K. Kishikawa, R. Okazaki, *J. Chem. Soc., Chem. Commun.* (1995) 1425
- 68 V. Ya. Lee, M. Ichinohe, A. Sekiguchi, *J. Am. Chem. Soc.* 124 (2002) 9962
- 69 N. Nakata, N. Takeda, N. Tokitoh, *Organometallics* 22 (2003) 481

70 N. Nakata, N. Takeda, N. Tokitoh, *J. Am. Chem. Soc.* 124 (2002) 6914  
71 H. Schumann, M. Glanz, F. Girgsdies, F. E. Hahn, M. Tamm, A. Grzegorzewski, *Angew. Chem. Int. Ed. Engl.* 20 (1997) 36  
72 K. N. Kudin, J. L. Margrave, V. N. Khabashesku, *J. Phys. Chem. A* 102 (1998) 744  
73 N. Takeda, N. Tokitoh, R. Okazaki, *Science of Synthesis*, 5 (2003) 47  
74 N. P. Toltl, W. J. Leigh, *J. Am. Chem. Soc.* 120 (1998) 1172  
75 D. Bravo-Zhivotovskii, I. Zharov, M. Kapon, Y. Apeloig, *J. Chem., Chem. Commun.* (1995) 1625  
76 J. Escudié, C. Couret, H. Ranaivonjatovo, J. Satgé, *Coordination Chemistry Reviews* 130 (1994) 427  
77 N. S. Nametkiu, L. E. Gwl'nikov, R. L. Uehakova, V. Yu. Orlov, O. V. Kuz'min, *Dokl. Akad. Nauk SSSR* 194 (1970) 741  
78 T. J. Barton, E. A. Kline, P. M. Garvey, *J. Am. Chem. Soc.* 9 (1973) 95  
79 V. N. Khabashesku, K. N. Kudin, J. Tama's, S. i E. Boganov, J. L. Margrave, O. M. Nefedov, *J. Am. Chem. Soc.* 120 (1998) 5005  
80 A. Naka, S. Ueda, M. Ishikawa, *J. Organomet. Chem.* 692 (2007) 2357  
81 A. Naka, S. Ueda, H. Fujimoto, T. Miura, H. Kobayashi, M. Ishikawa, *J. Organomet. Chem.* 695 (2010) 1663  
82 A. G. Brook, *Acc. Chem. Res.* 7 (1974) 77  
83 a) K. Mochida, K. Ichikawa, S. Okui, Y. Sakaguchi, H. Hayashi, *Chem. Lett.* (1985) 1433; b) M. B. Taraban, V. I. Maryasova, T. V. Leshina, L. I. Rybin, D. V. Gendin, N. S. Vyazankin, *J. Organomet. Chem.* 326 (1987) 347; c) S. Kiyooka, M. Hamada, H. Matsue, M. Hamada, R. Fujiyama, *J. Org. Chem.* 55 (1990) 5562  
84 A. G. Brook, F. Abdesaken H. Söllradl, *J. Organomet. Chem.* 299 (1986) 9-13  
85 C. Couret, J. Escudié, J. Satgé, M. Lazraq, *J. Organomet. Chem.* 190 (1987) 4411  
86 G. Anselme, J. Escudié, C. Couret, J. Satgé, *J. Organomet. Chem.* 403 (1991) 93  
87 M. Lazraq, C. Couret, J. Escudié, J. Satgé, M. Soufiaoui, *Polyhedron* 10 (1991) 1153  
88 P. R. Jones, T. F. O. Lim, *J. Am. Chem. Soc.* 99 (1977) 8447  
89 a) N. Auner, *J. Organomet. Chem.* 336 (1987) 59; 353 (1988) 275; 377 (1989) 175; b) N. Auner, *Z. Anorg. Allg. Chem.* 558 (1988) 87; c) N. Auner, J. Grobe, T. Schtier, B. Krebs, M. Dartmann, *J. Organomet. Chem.* 363 (1988) 7; d) J. Grobe, H. Schröder and N. Auner, *Z. Naturforsch.* 45b (1990) 785; e) N. Auner, C. Seidenschwarz, N. Sewald, *Organometallics* 11 (1992) 1137; W. Ziche, N. Auner, J. Behm, *Organometallics* 11 (1992) 3805.  
90 D. Bravo-Zhivotovskii, I. Zharov, M. Kapon, Y. Apeloig, *J. Chem. Soc., Chem. Commun.* (1995) 1625  
91 A. Berndt, H. Meyer, G. Baum, W. Massa, S. Berger, *Pure Appl. Chem.* 59 (1987) 1011  
92 N. Tokitoh, K. Kishikawa, R. Okazaki, *J. Chem. Soc., Chem. Commun.* (1995) 1425  
93 H. Schumann, M. Glanz, F. Girgsdies, F. Ekkehardt Hahn, M. Tamm, A. Grzegorzewski, *Angew. Chem., Int. Ed.* 36 (1997) 2232  
94 N. Nakata, N. Takeda, N. Tokitoh, *J. Am. Chem. Soc.* 124 (2002) 6914  
95 N. Nakata, N. Takeda, N. Tokitoh, *Organometallics* 22 (2003) 481

## 2. Publications

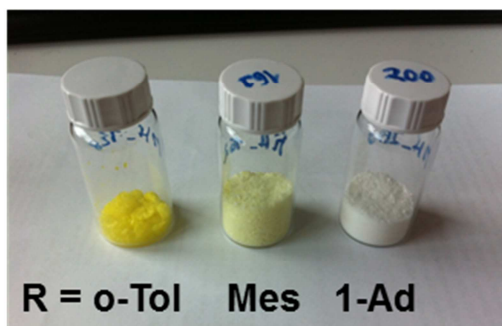
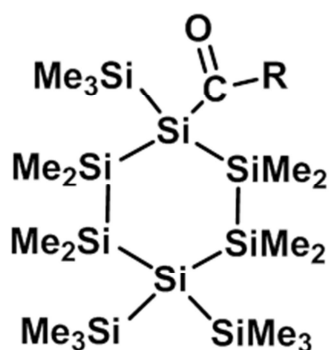
### 2.1 Synthesis and Characterization of Cyclic Acylsilanes

Michael Haas,<sup>[a]</sup> Lukas Schuh,<sup>[a]</sup> Ana Torvisco<sup>[a]</sup> and Harald Stueger,<sup>\*[a]</sup> and Christa Grogger<sup>[a]</sup>

<sup>[a]</sup> Institute of Inorganic Chemistry, Graz University of Technology, Stremayrgasse 9, A-8010 Graz, Austria

submitted to *Phosphorus, Sulfur Silicon Relat. Elem.*

graphical abstract:



#### 2.1.1 Abstract

Acylcyclohexasilanes are interesting starting materials for the formation of cyclic silenes. Employing standard cyclopolysilane synthetic procedures 9 previously unknown acylcyclohexasilanes were synthesized and characterized by NMR- and UV-Vis spectroscopy and by X-ray crystallography in order to elucidate substituent influences of the R-group attached to the carbonyl C-atom.



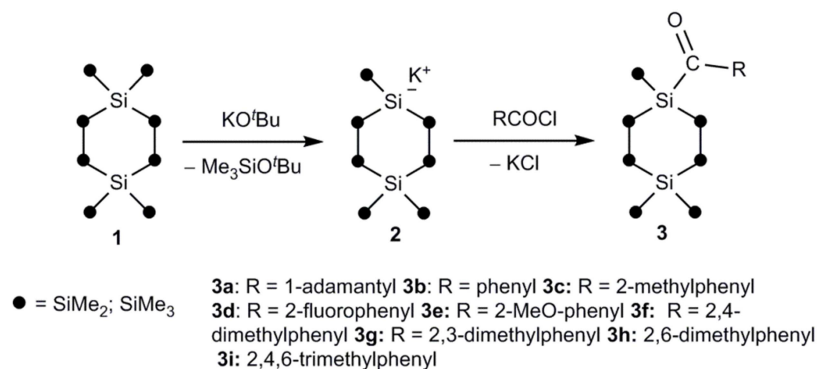
## 2.1.2 Introduction

Acylsilanes have attracted considerable attention since their discovery in 1957<sup>1</sup> because of their unique spectroscopic properties and synthetic utility in organic chemistry.<sup>2</sup> The spectral data of acylsilanes are well described in several reviews.<sup>3</sup> Acylsilanes exhibit significantly longer wavelength IR and UV absorption and downfield shifted <sup>13</sup>C NMR resonances of the carbonyl-carbon as compared with simple ketones and aldehydes. Furthermore, X-ray structure analysis studies revealed that acylsilanes possess abnormally long Si-CO bonds relative to the analogous bond length in C-CO compounds. These properties have been ascribed to considerable inductive effects of the silicon atom on the properties of the carbonyl group. The resulting large bathochromic shift of n-π\* transitions gives simple acylsilanes a green or yellow-green color while conjugated species such as aroylsilanes and α,β-unsaturated acylsilanes are bright yellow and very sensitive to light. Very recent studies performed in our laboratories showed the possibility to synthesize Brook-type cyclic silenes by the use of acylcyclohexasilanes as starting materials.<sup>4</sup> Because the previously unknown cyclic acylsilanes themselves turned out to have interesting properties, we decided to investigate in detail their structural and spectroscopic features. Herein we would like to report the initial results of the corresponding studies using NMR- and UV-Vis spectroscopy and X-ray crystallography.

## 2.1.3 Results and Discussion

### 2.1.3.1 Synthesis

The acylcyclohexasilanes **3a-i** were synthesized in order to study the influence of various substituent groups R attached to the carbonyl function on selected structural and spectroscopic properties. The target compounds were straightforwardly prepared employing standard procedures for cyclopolysilane synthesis.<sup>5,6</sup> In the first reaction step a -SiMe<sub>3</sub> group was removed from 1,1,4,4-tetrakis(trimethylsilyl)cyclohexasilane **1** with KO<sup>t</sup>Bu to give the potassium silanide **2** which subsequently was reacted with equimolar amounts of acid chlorides ClCOR in diethyl ether solution at -80 °C to the air-stable and crystalline compounds **3a-i** in yields > 60% (cf. Scheme 1). Analytical data obtained for **3a-i** were fully consistent with the proposed structures.



**Scheme 1** Synthesis of acylsilanes **3a-i**

**Table 1**  $^{13}\text{C}$ - and  $^{29}\text{Si}$  NMR chemical shifts of the Si-C=O group and UV absorption data of **3a-i**

	<b>3a</b>	<b>3b</b>	<b>3c</b>	<b>3d</b>	<b>3e</b>
<b>R</b>	1-Ad	Ph	2-MePh	2-FPh	2-MeOPh
$\delta^{13}\text{C}^{\text{a}}$	248.22	236.21	239.77	234.45	238.92
$\delta^{29}\text{Si}^{\text{a}}$	-72.14	-64.28	-66.79	-61.74	-66.03
$\lambda_{\text{max}} (\epsilon)^{\text{b}}$	371 (270)	424 (205)	414 (240)	404 (180)	385 (220)
	<b>3f</b>	<b>3g</b>	<b>3h</b>	<b>3i</b>	
<b>R</b>	2,4-Me <sub>2</sub> Ph	2,3-Me <sub>2</sub> Ph	2,6-Me <sub>2</sub> Ph	2,4,6-Me <sub>3</sub> Ph	
$\delta^{13}\text{C}^{\text{a}}$	240.46	241.27	245.95	246.17	
$\delta^{29}\text{Si}^{\text{a}}$	-66.71	-67.24	-71.23	-71.14	
$\lambda_{\text{max}} (\epsilon)^{\text{b}}$	416 (220)	410 (230)	393 (200)	394 (230)	

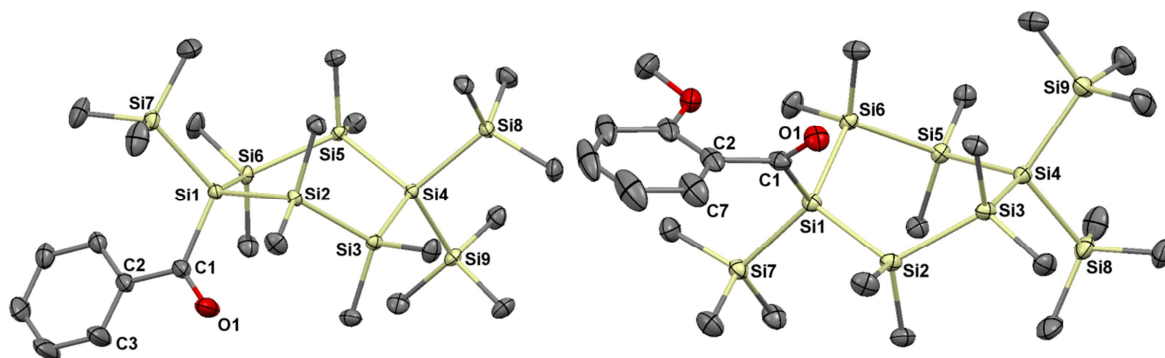
<sup>a</sup>measured in C<sub>6</sub>D<sub>6</sub> solution at 22 °C;  $\delta$  values in ppm relative to ext. TMS; <sup>b</sup>measured in hexane solution,  $c = 5 \cdot 10^{-5} \text{ mol} \cdot \text{L}^{-1}$ ;  $\lambda_{\text{max}}$  values in nm,  $\epsilon$  values in  $\text{L} \cdot \text{mol}^{-1} \cdot \text{cm}^{-1}$

Table 1 lists the characteristic  $^{13}\text{C}$ - and  $^{29}\text{Si}$ -NMR chemical shifts of the Si-C=O moiety in **3a-i**. Consistent with literature data obtained for acyclic acylsilanes R<sub>3</sub>SiC(O)R **3a-i** exhibit markedly downfield shifted  $^{13}\text{C}$  resonances as compared to simple ketones (*e. g.* Me<sub>3</sub>CCO'Bu:  $\delta^{13}\text{C} = 215$  ppm; Me<sub>3</sub>SiCO'Bu:  $\delta^{13}\text{C} = 249$  ppm)<sup>3,7</sup>. This is usually explained by the enhanced electron releasing nature of silicon which favors resonance structures with a positively charged and less shielded carbonyl C atom resulting in more positive  $\delta^{13}\text{C}$  values. Apparently this effect is considerably weakened by aromatic substituents at the C=O group by reducing the amount of positive charge on the carbonyl carbon atom thus shifting the carbonyl resonances considerably upfield relative to the aliphatic analogues (*e. g.* Me<sub>3</sub>SiCOPh:  $\delta^{13}\text{C} = 233.6$  ppm<sup>3</sup> or **3a** and **3b** in Table 1).

Our data, furthermore, show that the carbonyl  $^{13}\text{C}$  resonances exhibit a slight downfield shift in the order **3d** → **3b** → **3e** → **3c** which correlates with the electron withdrawing or releasing power of the substituent attached to the aromatic ring and corroborates the picture drawn above. Additionally the  $\delta^{13}\text{C}$  values depend on the number and the position of the substituent groups (compare the data for **3f** – **3i**). Interestingly the  $^{29}\text{Si}$  resonances are shifted downfield in the reversed order with the less shielded Si atom in the fluoro derivative **3d**.

### 2.1.3.2 X-ray Structure Analysis

Despite all attempts, only **3a-c**, **3e** and **3i** afforded crystals of sufficient quality for single crystal X-ray crystallography. The structures of **3a**, **3c** and **3i** were already reported in previous publications.<sup>6</sup> Figure 1 shows ORTEP diagrams for compounds **3b** and **3e**, selected structural data for all compounds are summarized in Table 2.



**Figure 1** ORTEP diagrams for compounds **3b** (left) and **3e** (right). Thermal ellipsoids are depicted at the 50 % probability level. Hydrogen atoms are omitted for clarity.

The cyclohexasilane ring adopts the expected *chair* conformation in **3i** and *twisted boat* conformations in **3a-c** and **3e**. Si-Si bond lengths between 2.34 and 2.37 Å agree well with typical Si-Si single bond distances in cyclopolysilanes.<sup>8</sup> The observed C=O distances are close to the ones found in simple organic ketones, carboxylic acids and ethers.<sup>9</sup> The silicon carbonyl group bond lengths at 1.942 – 1.974 Å are considerably elongated just as observed earlier for other acylsilanes. Usually, silicon carbon single bonds fall in the range 1.85 - 1.90 Å.<sup>3</sup> For steric reasons **3b** and **3c** exhibit significantly smaller dihedral angles  $\gamma$  between the C=O group and the aromatic ring plane as compared to **3e** and **3i** which allows increased conjugational type interactions between the C=O and the aromatic  $\pi$ -systems in **3b** and **3c**.

**Table 2** Selected crystallographic data for compounds **3a-c**, **3e** and **3i**

	<b>3a</b> <sup>a</sup>	<b>3b</b>	<b>3c</b> <sup>b</sup>	<b>3e</b>	<b>3i</b> <sup>b</sup>
<b>R</b>	1-Ad	Ph	2-MePh	2-MeOPh	2,4,6-Me <sub>3</sub> Ph
<b>d C(1)-O(1)</b>	1.226	1.222	1.223	1.225	1.221
<b>d C(1)-Si(1)</b>	1.962	1.963	1.942	1.974	1.967
<b>γ O(1)-C(1)-C(ph)- C(ph)</b>	-	9.03	25.65	-59.98	66.89

<sup>a</sup> data taken from ref. 4a. <sup>b</sup> data taken from ref. 4b

### 2.1.3.3 UV-Vis Spectroscopy

The experimental UV-Vis absorption spectra of **3a-i** are depicted in Figure 2, the longest wavelength absorption maxima  $\lambda_{\max}$  are presented in Table 1 together with the extinction coefficients  $\epsilon$ . All spectra exhibit long-wavelength, low-intensity absorption bands between 360 and 420 nm due to  $n-\pi^*$  type excitations of the C=O fragment. The exact position of the  $n-\pi^*$  absorption band is nearly independent of the substituents attached to the  $\alpha$ -silicon atom. Thus, for instance, quasi identical  $\lambda_{\max}$  values are observed for **3b** (424 nm) and Me<sub>3</sub>SiCOPh (425 nm) or Ph<sub>3</sub>SiCOPh (424 nm).<sup>3c</sup> Considerable substituent effects on the absorption properties, however, are apparent upon variation of the organic group R at the C=O moiety. In line with literature data it can be clearly seen from Table 1 and Figure 1 (left) that aromatic substituents produce a bathochromic shift of the  $n-\pi^*$  band as compared to aliphatic side groups caused by  $\pi-\pi$  conjugation of the carbonyl group with the aromatic ring. The first absorption maximum of the adamantyl derivative **3a** at  $\lambda_{\max} = 371$  nm, therefore, is shifted by 53 nm to the red in the phenyl substituted compound **3b**. Furthermore, the hypsochromic shift observed in the order **3b**  $\rightarrow$  **3c**  $\rightarrow$  **3i**  $\sim$  **3e** roughly correlates with the torsion angle  $\gamma$  between the plane of the phenyl ring and the C=O moiety which increases from 9.03° (**3b**) to 25.65° (**3c**), 59.95° (**3e**) and 66.89° (**3i**). This correlation is conclusive, because smaller values of  $\gamma$  enhance phenyl/C=O  $\pi-\pi$  conjugation thus reducing the HOMO-LUMO gap and shifting the corresponding UV maximum to the red. This picture is supported further by the observation that both species with two ortho methyl groups attached to the phenyl ring (**3h** and **3i**) which are also likely to have similar and large torsional angles  $\gamma$  for steric reasons exhibit nearly identical and relatively small  $\lambda_{\max}$  values. **3c**, **3f** and **3g** with no or only one ortho methyl group and presumably small  $\gamma$  values, on the contrary, absorb at significantly longer and also similar wavelengths. Finally, the nature of groups attached to the phenyl ring also affects the  $\lambda_{\max}$  values (compare the absorption data of **3b** – **e**), although it is difficult to see any reliable pattern at the present stage of the investigation without any further theoretical and experimental studies.

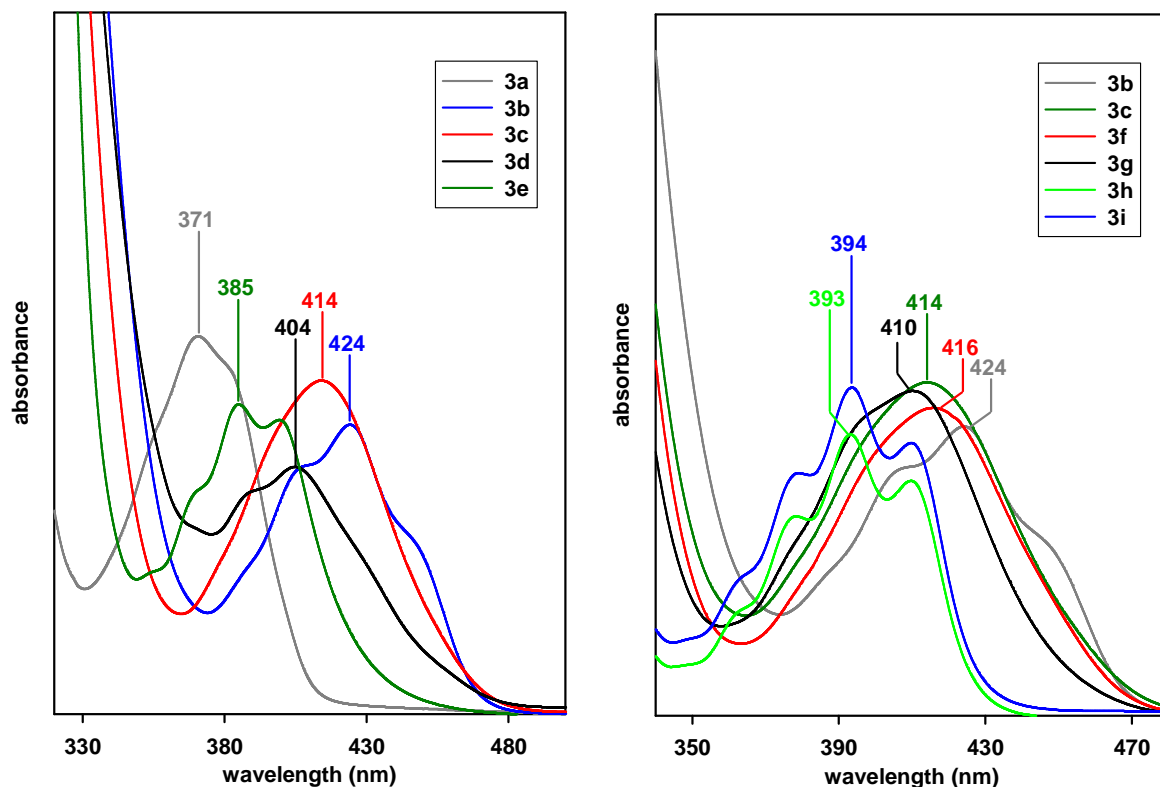


**Figure 2** UV-Vis absorption spectra of **3a-i** (n-hexane solution,  $c = 1 \cdot 10^{-3} \text{M}$ ). Left: First UV absorption band of acylcyclohexasilanes with aliphatic (**3a**) and aromatic (**3b,c,d,e**) substituents at the C=O group. Right: First UV absorption band of acylcyclohexasilanes with small (**3b,c,f,g**) and large (**3h, i**) torsion angle  $\gamma$  between the plane of the phenyl ring and the C=O moiety

## 2.1.4 References

- <sup>1</sup> A. G. Brook, *J. Am. Chem. Soc.* **79** (1957) 4373
- <sup>2</sup> a) H. Zhang, D. L. Prieppenow, C. Bolm, *Chem. Soc. Rev.* **42** (2013) 8540; b) A. F. Patrocínio, P. J. S. Moran, *J. Braz. Chem. Soc.* **12** (2001) 7
- <sup>3</sup> a) P. C. Bulman Page, M. J. McKenzie, S. S. Klair, S. Rosenthal, In *The Chemistry of Organic Silicon Compounds*, Vol. 2; Z. Rappoport, Y. Apeloig, Eds.; Wiley: Chichester, (1998); pp. 1599-1665. b) P. C. Bulman Page, S. S. Klair, S. Rosenthal, *Chem. Soc. Rev.* **19** (1990) 147; c) A. G. Brook, In *Adv. Organomet. Chem.*, F. G. A. Stone, R. West, Eds.; Academic. Press, N.Y., (1968), **7**, p 95-155
- <sup>4</sup> (a) H. Stueger, B. Hasken, M. Haas, M. Rausch, R. Fischer, A. Torvisco, *Organometallics* **33** (2014) 231
- <sup>5</sup> R. Fischer, T. Konopa, S. Ully, J. Baumgartner, C. Marschner, *J. Organomet. Chem.* **685** (2003) 79
- <sup>6</sup> The synthesis of **3a**, **3c** and **3f-i** has been reported earlier: a) M. Haas, R. Fischer, L. Schuh, R. Saf, A. Torvisco, H. Stueger, *Eur. J. Inorg. Chem.* (2015) 997; b) ref 4
- <sup>7</sup> F. Bernardi, L. Lunazzi, A. Ricci, G. Seconi, G. Tonachini, *Tetrahedron*, **42** (1986) 3607
- <sup>8</sup> M. Kaftory, M. Kapon, M. Botoshansky, In *The Chemistry of Organic Silicon Compounds*, Vol. 2; Z. Rappoport, Y. Apeloig, , Eds.; Wiley: Chichester, (1998); p 197f
- <sup>9</sup> a) R. J. Berry, R. J. Waltman, J. Pacansky, A. T. Hagler, *J. Phys. Chem.* **99** (1995) 10511; b) J. A. Kanters, J. Kroon, A. F. Peerdeman, J. C. Schoone, *Tetrahedron* **23** (1967) 4027

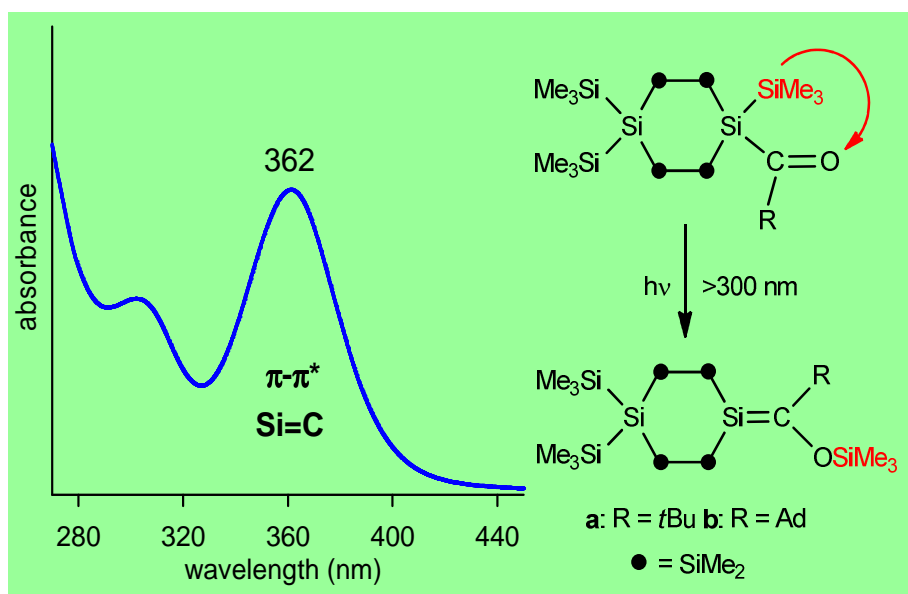
## 2.2 Photoinduced Brook-type Rearrangement of Acylcyclopolysilanes

Harald Stueger\*, Bernd Hasken, Michael Haas, Martin Rausch, Roland Fischer, Ana Torvisco

Institute of Inorganic Chemistry, Graz University of Technology, Stremayrgasse 9, A-8010 Graz,  
Austria

published in *Organometallics*, 33 (2014) 231

graphical abstract:



### 2.2.1 Abstract

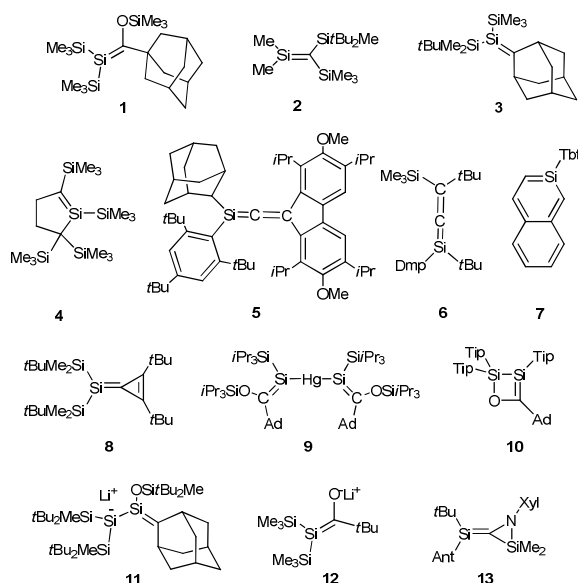
Previously unknown 1,1,4-tris(trimethylsilyl)-4-acyldodecamethylcyclohexasilanes (Me<sub>3</sub>Si)<sub>2</sub>Si<sub>6</sub>Me<sub>12</sub> (Me<sub>3</sub>Si)COR (**16a**: R = *t*-butyl, **16b**: R = 1-adamantyl) have been synthesized by the reaction of the potassium silanides (Me<sub>3</sub>Si)<sub>2</sub>Si<sub>6</sub>Me<sub>12</sub>(Me<sub>3</sub>Si)K with acid chlorides ClCOR and their photochemical rearrangement reactions have been studied. The molecular structures of **16a,b** as determined by single-crystal X-ray diffraction analysis exhibit an unusual twist boat conformation of the cyclohexasilane ring. When **16a,b** were photolyzed with  $\lambda > 300$  nm radiation, they underwent Brook type 1,3-Si→O migration reactions to generate the cyclohexasilanes **17a,b** with exocyclic Si=C bonds along with smaller amounts of the ring enlarged species **19a,b** with endocyclic Si=C double bonds. While **17a,b** were stable enough to allow characterization by NMR and UV absorption spectroscopy, the less stable products **19a,b** could only be observed in form of their methanol adducts.

## 2.2.2 Introduction

Silenes with various structures have been isolated and characterized since Brook and subsequently Wiberg about 30 years ago reported on the first stable species which contain Si=C double bonds (compare Chart 1).<sup>1</sup> Brook utilized a photochemical 1,3-Si→O shift of a SiMe<sub>3</sub> group of the acylpolysilane (Me<sub>3</sub>Si)<sub>3</sub>SiCOAd (Ad = 1-adamantyl) to generate the silene **1**<sup>2</sup> while Wiberg obtained the donor free species **2** by a route involving intramolecular lithium fluoride elimination.<sup>3</sup> Further advances in Si=C double bond chemistry include the synthesis of the stable silene **3** by Apeloig and coworkers *via* a sila-Peterson type reaction,<sup>4</sup> and the synthesis of the endocyclic silene **4**, obtained by rearrangement of a silylene.<sup>5</sup> In addition, stable 1-silaallenes **5** and **6** have been reported by the groups of West and Pietschnig<sup>6</sup> while Okazaki and Tokitoh published a series of papers on stable sila-aromatic compounds such as 2-silanaphthalene **7**.<sup>7</sup>

Only a few years ago, Kira *et al.* isolated and structurally characterized the 4-silatriafulvene **8**.<sup>8</sup> Even more recently, the first example of the stable metal-substituted silene **9** was synthesized by Bravo-Zhivotovskii and Apeloig *et al.*<sup>9</sup> while Scheschkewitz and Sekiguchi *et al.* reported on the formation of the cyclic Brook-type silene **10** from the disilenide Tip<sub>2</sub>Si=SiTip<sub>2</sub>Li (Tip = 2,4,6-*i*Pr<sub>3</sub>C<sub>6</sub>H<sub>2</sub>) and AdCOCl.<sup>10</sup> Charged silenes have been described by Sekiguchi *et al.* who synthesized the silyl anion substituted silene **11**<sup>11</sup> and by Ottosson *et al.* who succeeded in the isolation of the first stable 2-silenolate **12**.<sup>12</sup> In the most recent paper, finally, Iwamoto *et al.* reported on the synthesis of the exocyclic silene **13** showing a distinct intramolecular charge transfer transition from the π orbital of the Si=C double bond to the π\* orbital of the anthryl moiety.<sup>13</sup>

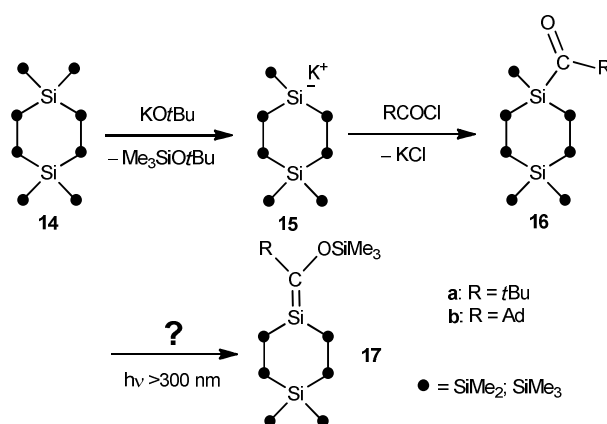
**Chart 1:** Selected stable silenes (Tip = 2,4,6-*i*Pr<sub>3</sub>C<sub>6</sub>H<sub>2</sub>; Tbt = 2,4,6-bis(trimethylsilyl)phenyl; Dmp = 2,6-dimesitylphenyl; Ad = 1-adamantyl); Ant = 9-anthryl)



Data on substituted silenes clearly demonstrate that the stability of silenes is strongly influenced by the choice of the substituents attached to the Si=C moiety.<sup>14</sup> As already has been realized by Brook the steric bulk of the substituents on the carbon atom is certainly a key factor in the kinetic stabilization of silenes with regard to dimerization. Additional stability is gained in silenes influenced by reversed ( $\text{Si}^{\delta-}=\text{C}^{\delta+}$ ) bond polarization effected by  $\pi$ -donor substituents on the carbon atom.<sup>15</sup> Reverse-polarized silenes such as Brook-type silenes **1**, the silatriafulvene **8** are less reactive towards moisture and alcohols than naturally polarized silenes ( $\text{Si}^{\delta+}=\text{C}^{\delta-}$ ), and addition of alcohol often proceeds by C-O instead of Si-O bond formation. In contrast to the naturally polarized silenes, which give [2+2] and -ene adducts as well, the reverse-polarized silenes react selectively with dienes to yield only [4+2] adducts.

Most silenes are acyclic molecules. To the best of our knowledge, in addition to the silaaromatics 1- and 2-silanaphthalene, 9-silanthracene and 9-silaphenantrene, **4** and **10** are the only stable silenes with the unsaturated silicon atom incorporated into cyclic structures which have been isolated and structurally fully characterized so far. According to DFT calculations on small model compounds the slight pyramidalization of the tricoordinate Si atom in **10** is due to reverse ( $\text{Si}^{\delta-}=\text{C}^{\delta+}$ ) bond polarization rather than steric congestion around the Si=C double bond. In line with reverse polarization **10** turned out to be remarkably stable. In contrast to Brook's silene **1** it reacts only slowly with air and moisture and does not react with MeOH at any appreciable rate.<sup>10</sup>

Larger cyclopolysilanes containing either endo- or exocyclic Si=C double bonds have not been described in the literature before. Because we are interested in substituent effects on polysilane frameworks in general,<sup>16</sup> we now want to report on the outcome of our attempts to synthesize the previously unknown Brook-type cyclic silenes **17a,b** by the photolysis of the acylcyclohexasilanes **16a,b** which we prepared successfully for the first time employing standard procedures for cyclopolysilane synthesis (Scheme 1).<sup>17</sup>



**Scheme 1:** Synthetic approach towards exocyclic silenes



## 2.2.3 Results and Discussion

### 2.2.3.1 Synthesis of Acylcyclohexasilanes

According to Scheme 1, the potassium silanide **15** cleanly reacts with equimolar amounts of acid chlorides CICOR (R = *t*-Bu, Ad) in diethyl ether solution at  $-80\text{ }^{\circ}\text{C}$  to give the air-stable and crystalline acylcyclohexasilanes **16a,b** in yields of  $>60\%$ . Analytical data obtained for **16a,b** (see the Experimental Section) are consistent with the proposed structures. Substitution of one  $\text{SiMe}_3$  group in **14** produces four magnetically nonequivalent endocyclic silicon atoms. Thus, the  $^{29}\text{Si}$  NMR spectra of **16a,b** exhibit two resonance lines near  $-38\text{ ppm}$  for the endocyclic  $\text{SiMe}_2$  groups, one signal for the Si atom bearing the acyl group near  $-70\text{ ppm}$  and one signal for the tertiary Si atom around  $-130\text{ ppm}$ .<sup>18</sup> The methyl and  $\text{SiMe}_3$  substituents, furthermore, can be attached either *cis* or *trans* relative to the acyl group which leads to five non equivalent methyl and three non equivalent  $\text{SiMe}_3$  groups. The resulting number of resonance lines actually appears in the experimental NMR spectra, although some  $^1\text{H}$  signals are too close to each other to be completely resolved.

Single crystals suitable for X-ray structure analysis could be grown from compounds **16a,b**. The obtained molecular structures are depicted in Figures 1 and 2 together with selected bond distances, bond angles, and dihedral angles. **16a,b** crystallize in the monoclinic space group  $\text{P}2_1/\text{n}$  and in the triclinic space group  $\text{P}-1$ , respectively. In both structures the cyclohexasilane ring adopts a twist boat conformation, which is rather unusual, because most cyclohexasilanes studied so far feature a chair conformation of the cyclopolysilane cycle.<sup>19</sup> The geometry around the endocyclic silicon atoms is approximately tetrahedral with Si-Si-Si bond angles close to the respective angles found in other cyclohexasilane structures<sup>18-20</sup> although Si(1) exhibits some distortion due to the steric bulk of the attached *t*-Bu or Ad group.

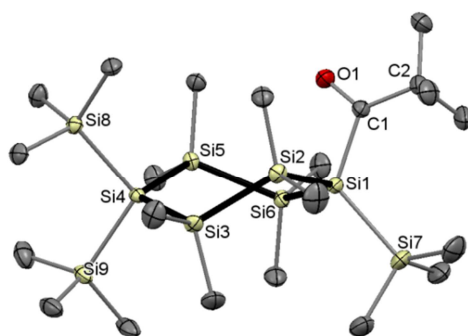


**Figure 1.** ORTEP diagram for compound **16a**. Thermal ellipsoids are depicted at the 50 % probability level. Hydrogen atoms are omitted for clarity. Selected bond lengths [Å] and bond and torsional angles [deg] with estimated standard deviations: Si-Si (mean) 2.356, C(1)-O(1) 1.213(2), Si(1)-C(1) 1.970(1), Si-C<sub>methyl</sub> (mean) 1.880, Si(6)-Si(1)-Si(2) 111.73(2), Si(3)-Si(2)-Si(1) 111.88(2), Si(4)-Si(3)-Si(2) 113.50(3), Si(5)-Si(4)-Si(3) 112.03(2), Si(4)-Si(5)-Si(6) 113.04(2), Si(5)-Si(6)-Si(1) 114.46(2), O(1)-C(1)-C(2) 120.2(1), O(1)-C(1)-Si(1) 113.9(1), C(2)-C(1)-Si(1) 125.9(1), C(1)-Si(1)-Si(7) 120.8(5), C(1)-Si(1)-Si(6) 99.1(5), C(1)-Si(1)-Si(2) 101.2(5), C-Si-C (mean) 107.6, O(1)-C(1)-C(2)-Si(1) 177.2(2).

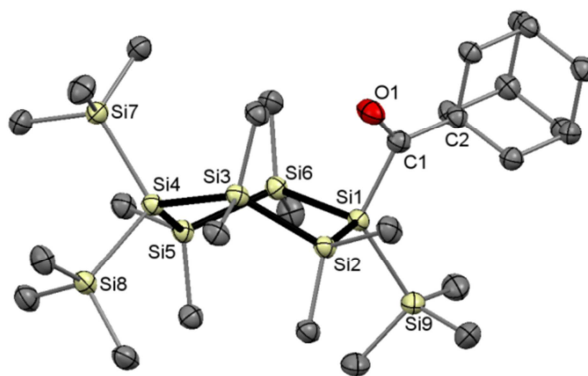


**Figure 2.** ORTEP diagram for compound **16b**. Thermal ellipsoids are depicted at the 50 % probability level. Hydrogen atoms are omitted for clarity. Selected bond lengths [Å] and bond and torsional angles [deg] with estimated standard deviations: Si-Si (mean) 2.358, C(1)-O(1) 1.226(3), Si(1)-C(1) 1.962(2), Si-C<sub>methyl</sub> (mean) 1.883, Si(6)-Si(1)-Si(2) 111.73(3), Si(3)-Si(2)-Si(1) 115.54(3), Si(4)-Si(3)-Si(2) 113.61(3), Si(5)-Si(4)-Si(3) 111.67(3), Si(4)-Si(5)-Si(6) 114.40(3), Si(5)-Si(6)-Si(1) 112.18(3), O(1)-C(1)-C(2) 119.9(2), O(1)-C(1)-Si(1) 113.2(2), C(2)-C(1)-Si(1) 126.9(2), C(1)-Si(1)-Si(9) 121.78(7), C(1)-Si(1)-Si(6) 102.07(7), C(1)-Si(1)-Si(2) 99.12(7), C-Si-C (mean) 107.6, O(1)-C(1)-C(2)-Si(1) -176.9(3).

Si-Si bond lengths between 2.34 – 2.37 Å were observed, the average Si-Si bond distance of 2.36 Å is typical for Si-Si single bonds in cyclopolysilanes<sup>21</sup> and agrees well with the Si-Si covalent bond length of 2.34 Å. The sum of the bond angles around the carbonyl C atom in **16a,b** is close to 360° and reflects the trigonal planar geometry within the SiRC=O moiety. Unexceptional carbonyl C=O bond lengths of 1.21 and 1.23 Å were measured,<sup>22</sup> while the silicon carbonyl group bond distances at 1.97 and 1.96 Å are considerably elongated relative to the length of an average Si-C(sp<sup>3</sup>) bond,<sup>23</sup> as observed earlier for other acyl silanes.<sup>24</sup> In order to minimize steric congestion the bulky *t*-Bu or Ad groups are oriented towards the outside of the molecules which brings the carbonyl oxygen atoms in **16a,b** in rather close contact to the endocyclic Si-Si bond system with non-bonding distances to the plane defined by Si(1), Si(2) and Si(6) of only 2.66 and 2.65 Å, respectively. This structural feature will gain importance because it can be used to rationalize the unprecedented course of the photolysis experiments described in the next section of this paper.

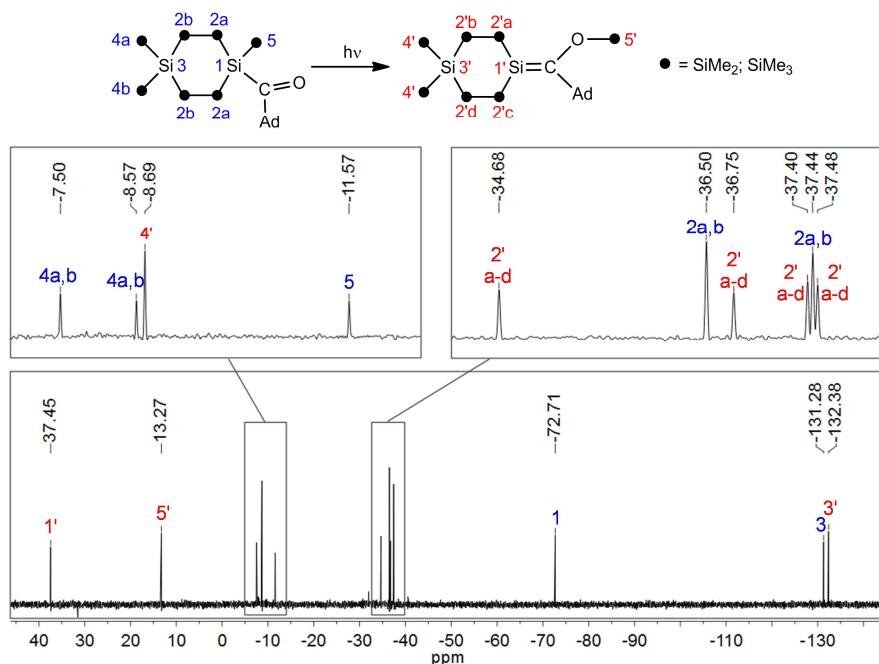


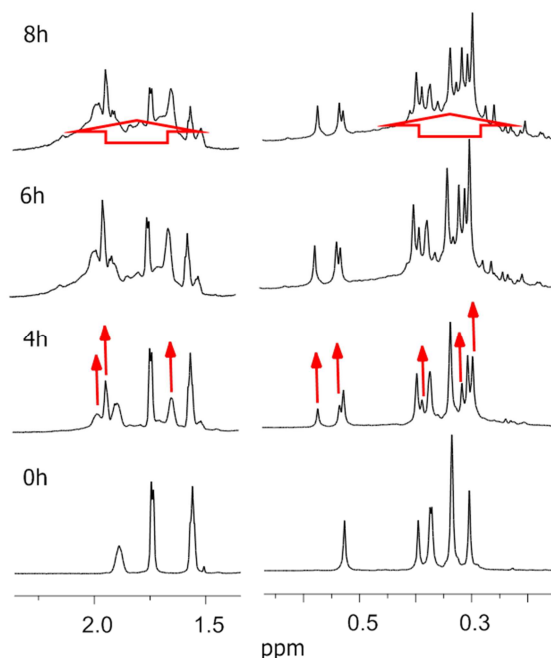
**Figure 3.**  $^{29}\text{Si}$  NMR spectrum after photolysis of **16b** in  $\text{C}_6\text{D}_6$  solution with a 150 W mercury lamp through Pyrex glass for 4h at room temperature including assignment of the resonance lines.

### 2.2.3.2 Photolysis of Acylcyclohexasilanes

When the acylsilanes **16a,b** in  $d_6$ -benzene solution ( $c \sim 0.07 \text{ M}$ ) in the absence of any other reactant were photolyzed with  $\lambda > 300 \text{ nm}$  radiation, yellow solutions were obtained. NMR analysis performed after an irradiation time of four hours showed the formation of the exocyclic silenes **17a,b** along with unreacted starting material. Figure 3 presents the  $^{29}\text{Si}$  NMR spectrum of the photolysis product derived from **16b** including the assignment of the observed resonance lines. The remaining spectra can be found in the Supporting Information.  $^{29}\text{Si}$  and  $^{13}\text{C}$  NMR chemical shift data of **17a,b** are summarized in Table 1.  $^{13}\text{C}$  and  $^{29}\text{Si}$  NMR signals characteristic of  $\text{Si}=\text{C}$  were observed near 215 and 37 ppm, respectively, while the  $^{29}\text{Si}$  signal near 13 ppm is easily assigned to the  $\text{OSiMe}_3$  moiety formed by the photochemical 1,3-trimethylsilyl shift. These values compare reasonably well with those measured for the acyclic Brook-type silenes  $(\text{Me}_3\text{Si})_2\text{Si}=\text{C}(\text{OSiMe}_3)\text{R}$  ( $\text{R} = t\text{-Bu, Ad}$ ).<sup>2</sup> The  $^1\text{H}$  NMR spectrum of the photolysis product of **16a** contains, in addition to poorly resolved signals between  $\delta 0.2$  and  $0.6 \text{ ppm}$  for the  $\text{SiMe}_3$  and  $\text{SiMe}_2$  groups, absorptions at  $\delta 1.26$  and  $0.96 \text{ ppm}$  for the  $\text{C}(\text{CH}_3)_3$  substituents in **16a** and **17a**, respectively. By integration of these signals a silene/acylsilane ratio of approximately 40:60 could be estimated.

**Table 1.**  $^{13}\text{C}$  and  $^{29}\text{Si}$  chemical shift data of silenes **17a** and **17b** ( $\text{C}_6\text{D}_6$  solution, vs. ext. TMS, ppm).

		R = <i>t</i> -Bu ( <b>17a</b> )	R = 1-Ad ( <b>17b</b> )
$^{13}\text{C}$	Si=C	214.39	215.93
	-R	42.70, 30.49	45.04, 42.15 36.78, 29.03
	-SiMe <sub>3</sub>	3.27, 1.17	3.29, 1.43
	-SiMe <sub>2</sub> -	-0.60, -1.49 -1.66, -2.54	-0.32, -1.43 -1.62, -2.47
$^{29}\text{Si}$	Si=C	37.00	37.45
	-OSiMe <sub>3</sub>	13.16	13.27
	-SiMe <sub>3</sub>	-8.79	-8.69
	-SiMe <sub>2</sub> -	-34.41, -36.81 -37.44, -37.58	-34.68, -36.75 -37.40, -37.48
	<i>SiSi</i> <sub>4</sub>	-132.43	-132.38

**Figure 4.**  $^1\text{H}$  NMR spectrum after photolysis of **16b** with a 150 W mercury lamp through Pyrex glass for 0, 4, 6 and 8 h at room temperature.

The interesting observation that it is possible to generate **17a,b** photochemically with two competing chromophores in the acylcyclopolysilane, the cyclohexasilane moiety and the acyl group, can be rationalized on the basis of the UV spectra of **13** and **15**. While **14** does not absorb above 300 nm<sup>25</sup> **16a,b** exhibit weak absorption bands near 370 nm ( $\epsilon \approx 200 \text{ l}\cdot\text{mol}^{-1}\cdot\text{cm}^{-1}$ ) which are easily assigned to the  $n\text{-}\pi^*$  transition of the C=O group in accordance with the literature.<sup>2</sup> Thus, the acyl group in **16** is selectively excited upon irradiation with 360 nm light while the endocyclic  $\sigma(\text{SiSi})$  electron system is not affected which leads to the observed Brook type reaction course. Further irradiation afforded increasing amounts of unidentified polymeric decomposition products at the expense of **17a,b**

illustrated by the appearance of broad signal groups typical for polymers containing (SiMe)<sub>n</sub> ( $\delta$  0 to 0.6 ppm) and *t*-Bu (Ad) ( $\delta$  1.0 to 2.0 ppm) groups in the <sup>1</sup>H NMR spectra of the resulting photolysis solutions (compare Figure 4). Apparently **17a,b** are less stable under photolytic conditions than Brook's open chained compounds presumably as a consequence of the presence of the cyclohexasilane cycle. Cyclohexasilanes like Si<sub>6</sub>Me<sub>12</sub> have been shown earlier to undergo silylene extrusion and ring contraction reactions when photolyzed with 254 nm light.<sup>26</sup> Although experimental evidence is missing,<sup>27</sup> it is not unlikely that **16a,b** exhibit similar reactivity upon irradiation at 360 nm because the wavelength for the onset of the photoinduced silylene extrusion might be considerably red-shifted due to conjugation of the exocyclic  $\pi$ (Si=C) chromophore with the endocyclic  $\sigma$ (SiSi) system. Thus, Si<sub>6</sub>Me<sub>12</sub> does not absorb light of wavelengths > 270 nm, while the UV absorption spectra of **17a,b** show absorption bands at 362 and 302 nm of considerable intensity (Figure 5). It is also interesting to note that there is no evidence for the presence of head-to-head dimers arising from 2+2 cycloaddition reactions of **17a,b** which are the decomposition products of most Brook-type silenes such as (Me<sub>3</sub>Si)<sub>2</sub>Si=C(OSiMe<sub>3</sub>)*t*-Bu.<sup>28</sup> This is conclusive because the formation of head-to-head dimers of **17a,b** would cause severe steric strain due to the cyclic structure of the polysilane backbone which apparently totally inhibits dimerization. Since no dimers were present in the photolysis mixtures, attempts were made to crystallize **17a,b** from the photolysis mixtures obtained after an irradiation time of four hours. Removal of solvent in vacuo, however, gave viscous yellow oils which contained mainly polymeric material of undefined composition along with unreacted **16a,b**.

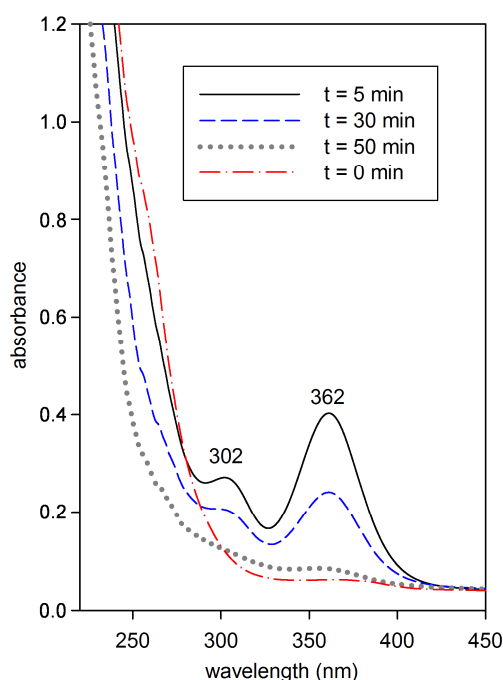
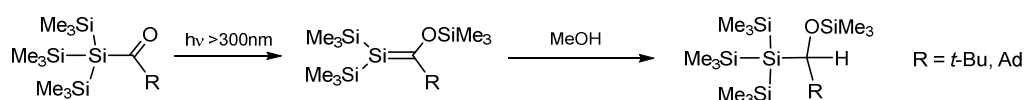


**Figure 5.** UV absorption spectra recorded after irradiation of a solution of **16b** in C<sub>6</sub>H<sub>12</sub> with a 4W 366 nm lamp ( $c = 5 \cdot 10^{-5} \text{ mol} \cdot \text{L}^{-1}$ ;  $t = 0, 5, 30, 50 \text{ min}$ ).

As mentioned earlier, solutions of the silenes **17a,b** are yellow. UV absorption spectra recorded after irradiation of a diluted hydrocarbon solution of **16b** with  $\lambda = 366$  nm radiation in a quartz cuvette are presented in Figure 5. The *quasi*-identical spectra obtained for **16a** may be found in the Supporting Information. After an irradiation time of 5 min two absorption bands appear centered at  $\lambda_{\text{max}} \sim 300$  nm and  $\lambda_{\text{max}} \sim 360$  nm which were not present prior to photolysis. The latter band tailing into the visible region is easily assigned to a  $\pi\text{-}\pi^*$  transition within the Si=C fragment. Quite remarkably it is shifted to the red by 20 nm with respect to the related acyclic silenes  $(\text{Me}_3\text{Si})_2\text{Si}=\text{C}(\text{OSiMe}_3)\text{R}$  ( $\text{R} = t\text{-Bu, Ad}$ ) which have  $\pi\text{-}\pi^*$  absorptions around 340 nm.<sup>2</sup> The bathochromic shift of the  $\pi\text{-}\pi^*$  absorption band observed for **17a,b** very likely might be explained by enhanced conjugation between the endocyclic  $\sigma(\text{Si-Si})$  bond system with the exocyclic Si=C double bond. The data presented in Figure 5, furthermore, also reflect the instability of **17a,b** under photolytic conditions. Upon prolonged irradiation the intensity of the 300 and the 360 nm absorption bands decreases until nearly complete photo bleaching occurs after about 20 min and 50 min for **17a** and **17b**, respectively. **17b**, therefore, seems to be slightly more stable which is also evident from the relative intensities of the signals in the NMR spectra of the obtained photolysis solutions.

### 2.2.3.3 Trapping Experiments

Alcohols are known to be very effective trapping agents for Brook-type silenes.<sup>1</sup> Thus, photolysis of acyltris(trimethylsilyl)silanes in the presence of MeOH to which a trace of weak base such as pyridine or  $\text{Et}_3\text{N}$  has been added usually affords the 1,2-addition product across the Si=C double bond with the RO- group attached to silicon and the alcoholic H attached to carbon (Scheme 2). Earlier work on the photolysis of acylsilanes has shown that in the absence of base subsequent acid-catalyzed C-O or Si-O bond cleavage reactions of the initially formed trapping products occur which leads to the formation of complex mixtures of "solvolysis" products.<sup>29</sup> The acid catalysts appeared to be byproducts of the photolysis reaction. In contrast to the behavior described in Scheme 2 photolysis of the cyclic acyl silanes **16a,b** in  $\text{C}_6\text{D}_6/\text{MeOH}$  2.5 : 1 gave only about 80 % of the adducts **18a,b** expected from trapping of the silenes **17a,b** which already have been observed in the absence of trapping reagents. Rather surprisingly, about 20 % of the cyclosiloxanes **20a,b** were also obtained which are the trapping products of the silenes **19a,b**.

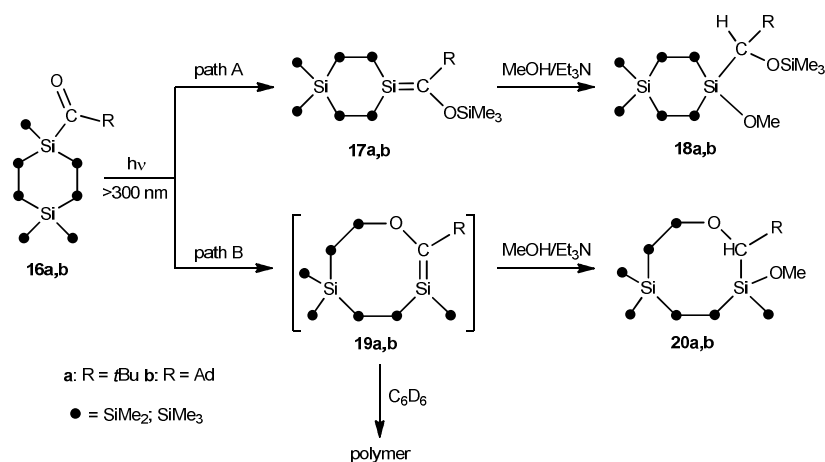


**Scheme 2:** Photolysis of acyltris(trimethylsilyl)silanes in the presence of methanol

These results are presented in Scheme 3 and clearly indicate that photochemical rearrangement of acylcyclohexasilanes to species containing Si=C double bonds can occur in two different ways. In addition to the "normal" Brook-type rearrangement including a 1,3-Si→O trimethylsilyl shift to give

silenes **17a,b** with exocyclic Si=C bonds (reaction path A) an unprecedented rearrangement takes place including ring scission and a 1,3-Si→O dimethylsilyl shift under formation of the ring enlarged silenes **19a,b** with endocyclic Si=C double bonds (reaction path B). Likely the formation of **19a,b** can be interpreted as arising from the molecular structure of the acyl silanes **16a,b**, because reaction path B might become a favorable process, due to last but not least due the close proximity of the carbonyl oxygen atom to the adjacent endocyclic Si-Si bonds already mentioned above (compare Figures 1 and 2). Furthermore, it is obvious that **19a,b** are not stable under photolytic conditions in the absence of trapping reagents because they were not detected if the photolysis was carried out in pure hydrocarbon solvents.

Pure **18a** and **20a** could be isolated from the crude photolysis solution by column chromatography over silica gel with heptane as an eluant followed by crystallization from acetone. Pure **18b** was obtained as the less soluble product from the mixture with **20b** by repeated crystallization from acetone. Slightly impure crystals of **20b** were isolated in low yield from the combined mother liquors after concentration and repeated crystallization from acetone at  $-30\text{ }^{\circ}\text{C}$ . Nevertheless, the identity of the individual adducts **18a,b** and **20a,b** was established by NMR and high resolution mass spectroscopy. Analytical data are summarized in the Experimental Section, and experimental  $^1\text{H}$  NMR spectra can be found in the Supporting Information. All adducts showed nine  $^{29}\text{Si}$  resonances, in line with the presence of nine magnetically inequivalent silicon atoms. For the six membered cycles **18a,b** four signals for the endocyclic  $\text{SiMe}_2$  groups between  $-32$  and  $-41$  ppm, two  $\text{SiMe}_3$  resonances near  $-6$  and  $-9$  ppm and one signal for the  $\text{OSiMe}_3$  group near  $+15$  ppm were detected. The isomers **20a,b** by contrast had three  $\text{SiMe}_2$  signals between  $-32$  and  $-44$  ppm and one signal for the  $\text{OSiMe}_2$  group at significantly lower field ( $\sim+19$  ppm.) while three  $\text{SiMe}_3$  signals appeared near  $-8.5$  (2 signals) and  $-19$  ppm. In  $^{13}\text{C}$  NMR eight lines appear at the high field end of the spectra for the magnetically nonequivalent methyl groups attached to the endocyclic silicon atoms.



**Scheme 3:** Photolysis of acylcyclohexasilanes **16a,b** in the presence of methanol/ $\text{Et}_3\text{N}$

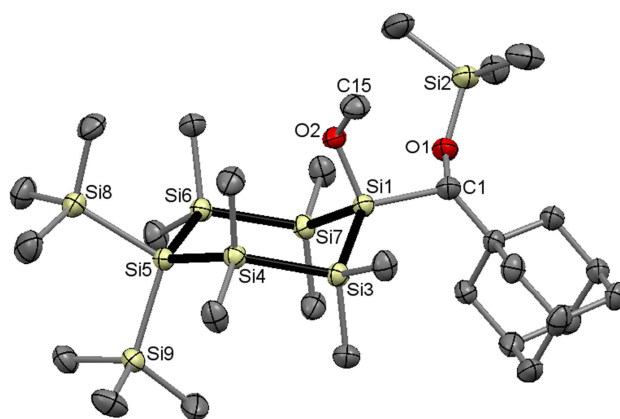


**Figure 6.** ORTEP diagram for compound **18b**. Thermal ellipsoids are depicted at the 50 % probability level. Hydrogen atoms are omitted for clarity. Selected bond lengths [Å] and bond and torsional angles [deg] with estimated standard deviations: Si-Si (mean) 2.362, C(1)-O(1) 1.434(3), Si(1)-O(2) 1.679(2), Si(2)-O(1) 1.651(2), Si(1)-C(1) 1.930(3), Si-C<sub>methyl</sub> (mean) 1.877, Si(7)-Si(1)-Si(3) 110.14(3), Si(1)-Si(3)-Si(4) 107.90(3), Si(3)-Si(4)-Si(5) 115.20(4), Si(4)-Si(5)-Si(6) 112.25(3), Si(5)-Si(6)-Si(7) 117.05(3), Si(6)-Si(7)-Si(1) 107.56(3), Si(1)-O(2)-C(15) 121.7(2), C(1)-O(1)-Si(2) 128.4(2), C-Si-C (mean) 107.8.

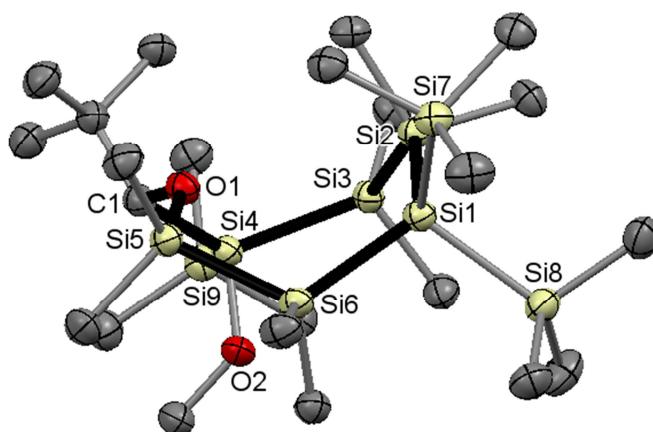


**Figure 7.** ORTEP diagram for compound **20a**. Thermal ellipsoids are depicted at the 50 % probability level. Hydrogen atoms are omitted for clarity. Selected bond lengths [Å] and bond and torsional angles [deg] with estimated standard deviations: Si-Si (mean) 2.359, C(1)-O(1) 1.448(3), Si(4)-O(2) 1.672(2), Si(5)-O(1) 1.657(2), Si(4)-C(1) 1.929(2), Si-C<sub>methyl</sub> (mean) 1.879, Si(6)-Si(1)-Si(2) 112.35(3), Si(1)-Si(2)-Si(3) 119.26(3), Si(2)-Si(3)-Si(4) 122.98(3), Si(5)-Si(6)-Si(1) 115.00(3), Si(4)-O(2)-C(23) 124.0(2), C(1)-O(1)-Si(5) 128.4(2), C-Si-C (mean) 107.4, Si(1)-Si(6)-Si(5)-O(1) -41.4(1), Si(3)-Si(4)-C(1)-O(1) 38.0(1).



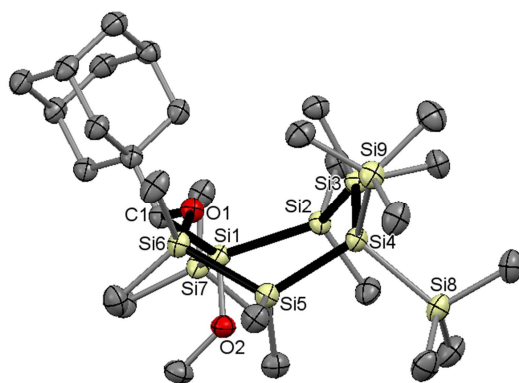


**Figure 8.** ORTEP diagram for compound **20b**. Thermal ellipsoids are depicted at the 50 % probability level. Hydrogen atoms are omitted for clarity. Selected bond lengths [Å] and bond and torsional angles [deg] with estimated standard deviations: Si-Si (mean) 2.361, C(1)-O(1) 1.458(3), Si(1)-O(2) 1.673(2), Si(6)-O(1) 1.654(2), Si(1)-C(1) 1.925(3), Si-C<sub>methyl</sub> (mean) 1.883, Si(1)-Si(2)-Si(3) 123.28(4), Si(2)-Si(3)-Si(4) 120.49(4), Si(3)-Si(4)-Si(5) 111.26(4), Si(4)-Si(5)-Si(6) 114.57(4), Si(1)-O(2)-C(20) 124.6(2), C(1)-O(1)-Si(6) 128.5(2), C-Si-C (mean) 107.6, Si(4)-Si(5)-Si(6)-O(1) 44.2(1), Si(2)-Si(1)-C(1)-O(1) -37.9(2).

The molecular structures of **18b**, **20a,b** in the solid state as determined by single-crystal X-ray diffraction are presented in Figures 6 – 8 together with selected bond distances, bond angles, and dihedral angles. **18b** crystallizes in the monoclinic space group  $P2_1/c$  with the cyclohexasilane ring in a slightly distorted chair conformation and unexceptional bond lengths and angles. **20a,b** crystallize in the triclinic space group  $P-1$ . The eight membered heterocycle adopts a boatlike conformation. The most prominent feature of the molecular structures of **20a,b** is the position of the endocyclic oxygen atom, which is oriented towards the center of the ring in order to allow an exocyclic arrangement with minimum steric congestion for the bulky R group at C(1). **20a,b** contain two chiral centers. In both cases one molecule of the *S,S* and one molecule of the *R,R* enantiomer are present in the unit cell, which are related by an inversion center (compare Figure 9). Obviously the diastomeric species with *R,S* and *S,R* configuration were not formed, because otherwise a second set of NMR signals should have been observed.

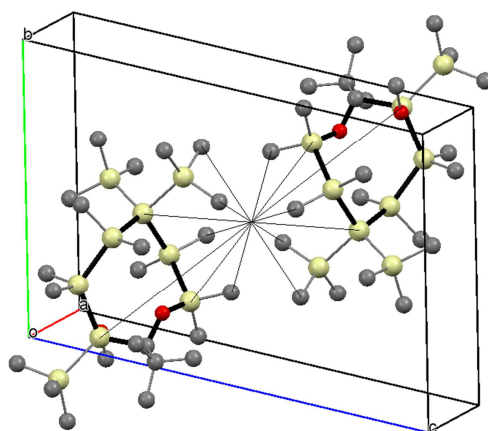
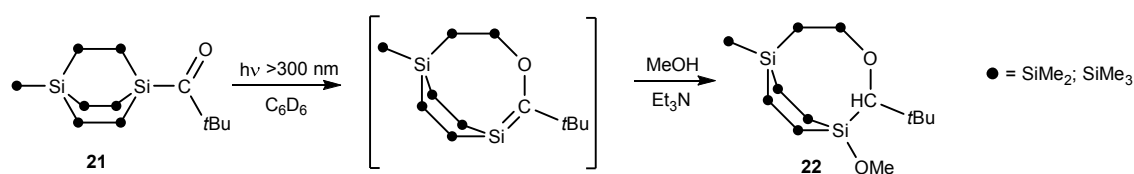


**Figure 9.** Unit cell of compound **20a** containing one *S,S*- and *R,R* enantiomeric pair which can be interconverted through an inversion centre between the molecules.

### 2.2.3.4 Photolysis of Acylbicyclo[2.2.2]octasilanes

In contrast to the behavior described above for the acylcyclohexasilanes **16a,b** the photolysis of the 1-trimethylacyl-4-(trimethylsilyl)dodecamethyl-bicyclo[2.2.2]octasilane cage **21** in a MeOH/C<sub>6</sub>D<sub>6</sub> mixture gave rise to the formation of the silene-methanol adduct **22** along with polymeric material of unknown structure, with no evidence for the presence of products derived from photochemically induced Me<sub>3</sub>Si migration (Scheme 4). When it was photolyzed in pure C<sub>6</sub>D<sub>6</sub>, **21** reacted very slowly to give unidentified polymeric decomposition products. This finding is not surprising, because **21** does not contain a Me<sub>3</sub>Si group in  $\alpha$  position to the acyl functionality. The Brook-type 1,3-SiMe<sub>3</sub> shift under formation of an exocyclic silene, thus, is simply not possible.



**Scheme 4:** Photolysis of acylbicyclo[2.2.2]octasilane **21** in the presence of methanol/Et<sub>3</sub>N

Although pure **22** could not be isolated so far from the obtained crude product mixture its structure is established by NMR and GC-MS analysis. Analytical data are summarized in the Experimental Section. GC-MS showed only one volatile product with a signal corresponding to the molecular ion at  $m/e$  594. Due to the presence of nine inequivalent silicon atoms nine <sup>29</sup>Si resonances were found at -130.5 (SiSi<sub>4</sub>), -43.7, -43.5, -40.5, -37.4 and -36.7 (SiMe<sub>2</sub>), -5.6 (SiMe<sub>3</sub>), +8.6 (SiOMe) and +18.3 ppm (SiMe<sub>2</sub>)O. Consistent with the proposed structure <sup>1</sup>H NMR showed a one proton singlet at  $\delta$  3.68 ppm (HCOMe), a three proton singlet at  $\delta$  3.47 ppm (OCH<sub>3</sub>), a nine proton singlet at  $\delta$  0.99 ppm (C(CH<sub>3</sub>)<sub>3</sub>) and a poorly resolved signal group at  $\delta$  0.18 – 0.32 ppm (SiCH<sub>3</sub>) besides some minor impurities and some polymeric background.

### 2.2.4 Conclusion

In summary, we have demonstrated that acylcyclohexasilanes which contain a Me<sub>3</sub>Si group in  $\alpha$  position to the acyl substituent upon photolysis undergo Brook-type rearrangement reactions to give products with Si=C double bonds. In contrast to the behavior of branched open-chain substrates as studied extensively by Brook *et al.* in the past, however, we observed the formation of two products: a cyclohexasilane with an exocyclic Si=C double bond arising from 1,3-Si→O shift of a SiMe<sub>3</sub> group and a ring enlarged silene with an endocyclic Si=C double bond arising from an unprecedented rearrangement including ring scission and insertion of the Si=C-O fragment into the cyclohexasilane ring. The exocyclic product was stable enough to allow detection by NMR and UV absorption spectroscopy while the less stable endocyclic product could only be observed in form of its methanol adduct. Photolysis experiments involving acylbicyclo[2.2.2]octasilane cages, furthermore, indicated

that in the absence of  $\alpha$ -SiMe<sub>3</sub> groups exclusively the endocyclic product is obtained. Further studies with the primary aim to isolate related species with enhanced stability are currently underway.

## 2.2.5 Experimental Section

### 2.2.5.1 General Considerations

All experiments were performed under a nitrogen atmosphere using standard Schlenk techniques. Solvents were dried using a column solvent purification system.<sup>30</sup> Commercial KO $t$ Bu (97 %), ClCO $t$ -Bu (99 %), ClCOAd (98 %) were used as purchased, Et<sub>3</sub>N (99 %) was dried by distillation from solid KOH, commercial anhydrous MeOH was dried with 3Å molecular sieve. **14** and **15** were synthesized as previously reported.<sup>18</sup> <sup>1</sup>H (299.95 MHz), <sup>13</sup>C (75.43 MHz) and <sup>29</sup>Si (59.59 MHz) NMR spectra were recorded on a Varian INOVA 300 spectrometer in C<sub>6</sub>D<sub>6</sub> or CDCl<sub>3</sub> solution and referenced versus TMS using the internal <sup>2</sup>H-lock signal of the solvent. Mass spectra were run either on a HP 5971/A/5890-II GC/MS coupling (HP 1 capillary column, length 25 m, diameter 0.2 mm, 0.33  $\mu$ m polydimethylsiloxane) or on a Kratos Profile mass spectrometer equipped with a solid probe inlet. Infrared spectra were obtained on a Bruker Alpha-P Diamond ATR Spectrometer from the solid sample. Melting points were determined using a Buechi 535 apparatus and are uncorrected. Elemental analyses were carried out on a Hanau Vario Elementar EL apparatus. Photolyses were performed by using a 150 W medium pressure mercury lamp (Heraeus TQ 150). Sample solutions were photolyzed under an atmosphere of nitrogen in Pyrex Schlenk or NMR tubes immersed in cold water to ensure ambient sample temperature and to prevent irradiation with light of wavelengths  $\lambda < 300$  nm. UV absorption spectra of **17a,b** were recorded on a Perkin Elmer Lambda 5 spectrometer after irradiation of diluted cyclohexane solutions of **16a,b** ( $c = 5 \cdot 10^{-5}$  mol·L<sup>-1</sup>) with a 4 W 366 nm lamp at room temperature in quartz cuvettes.

### Synthesis of 1-Trimethylacycloctamethyl-1,4,4-tris(tri-methylsilyl)cyclohexasilane (**16a**)

A solution of **15** in 20 mL of DME was freshly prepared from 1.74 g (3.0 mmol) of **14** and 0.37 g (3.3 mmol) of KO $t$ Bu and slowly added to a solution of 0.40 g (3.3 mmol) of ClCO $t$ -Bu in 50 mL of diethyl ether at -80 °C. Subsequently the mixture was stirred for another 30 min at -80 °C, allowed to warm to room temperature and finally stirred for additional 60 minutes. After aqueous work up with 100 mL of 3 % sulfuric acid the organic layer was separated, dried over Na<sub>2</sub>SO<sub>4</sub> and the solvents were stripped off with a rotary evaporator. Drying in vacuo (0.02 mbar) and crystallization from acetone solution by slow evaporation of the solvent at room temperature afforded 1.37 g (77 %) of analytically pure **16a** as colorless crystals.

mp: 159 - 161 °C. Anal. Found: C, 44.15; H, 9.82 %. Calc. for C<sub>22</sub>H<sub>60</sub>OSi<sub>9</sub>: C, 45.52; H, 10.19 %. <sup>29</sup>Si-NMR (C<sub>6</sub>D<sub>6</sub>, TMS, ppm): -7.77, -8.62, -11.55 (*Si*Me<sub>3</sub>); -37.04, -38.02 (*Si*Me<sub>2</sub>); -71.86 (*Si*CO $t$ Bu); -131.46 (*Si*(SiMe<sub>3</sub>)<sub>2</sub>). <sup>13</sup>C-NMR (C<sub>6</sub>D<sub>6</sub>, TMS, ppm): 245.41 (*Si*C=O); 48.77 (*C*(CH<sub>3</sub>)<sub>3</sub>); 24.75 (*C*(CH<sub>3</sub>)<sub>3</sub>); 3.75, 3.70, 2.55 (*Si*(CH<sub>3</sub>)<sub>3</sub>); -0.74, -0.87, -2.20, -2.26 (*Si*(CH<sub>3</sub>)<sub>2</sub>). <sup>1</sup>H-NMR (C<sub>6</sub>D<sub>6</sub>,

TMS, ppm, rel. Int.): 0.96 (9H, s, C(CH<sub>3</sub>)<sub>3</sub>); 0.50, 0.36, 0.35, (6H each, s, Si(CH<sub>3</sub>)<sub>2</sub>); 0.32 (15H, s, Si(CH<sub>3</sub>)<sub>2</sub> + Si(CH<sub>3</sub>)<sub>3</sub>); 0.29, 0.28 (9H each, s, Si(CH<sub>3</sub>)<sub>3</sub>). IR (neat):  $\nu(\text{C}=\text{O}) = 1623$  (m) cm<sup>-1</sup>. UV absorption (hexane solution):  $\lambda_1$  367 nm ( $\epsilon_1 = 190 \cdot \text{mol}^{-1} \cdot \text{cm}^{-1}$ ), absorption shoulder at 255 nm ( $\epsilon_2 = 11000 \cdot \text{mol}^{-1} \cdot \text{cm}^{-1}$ ). HRMS: calc. for [C<sub>22</sub>H<sub>60</sub>OSi<sub>9</sub>]<sup>+</sup> (M<sup>+</sup>): 592.2568; found: 592.2603.

### Synthesis of 1-Adamantylcarbonyloctamethyl-1,4,4-tris(trimethylsilyl)cyclohexasilane (16b)

The procedure followed was that used for **16a** with 2.91 g (5.0 mmol) of **14**, 0.62 g (5.5 mmol) of KO<sup>t</sup>Bu and 0.99 g (5.0 mmol) of ClCOAd. Yield: 2.02 g (60 %) of analytically pure **16b** as colorless crystals.

mp: 148 - 151 °C. Anal. Found: C, 49.91; H, 9.72 %. Calc. for C<sub>28</sub>H<sub>66</sub>OSi<sub>9</sub>: C, 50.07; H, 9.91 %. <sup>29</sup>Si-NMR (CDCl<sub>3</sub>, TMS, ppm): -7.60, -8.30, -10.90 (SiMe<sub>3</sub>); -36.80, -37.96 (SiMe<sub>2</sub>); -72.06 (SiCOAd); -131.32 (Si(SiMe<sub>3</sub>)<sub>2</sub>). <sup>13</sup>C-NMR (CDCl<sub>3</sub>, TMS, ppm): 248.22 (SiC=O); 51.50 (AdCCO); 36.99, 36.69 (Ad-CH<sub>2</sub>); 28.03 (Ad-CH); 3.86, 3.83, 2.83 (Si(CH<sub>3</sub>)<sub>3</sub>); -0.69, -0.92, -1.68, -2.01 (Si(CH<sub>3</sub>)<sub>2</sub>). <sup>1</sup>H-NMR (CDCl<sub>3</sub>, TMS, ppm, rel. Int.): 2.06 (3H, b, Ad-CH); 1.72, 1.67 (6H each, b, Ad-CH<sub>2</sub>), 0.35, 0.30 (6H each, s, Si(CH<sub>3</sub>)<sub>2</sub>); 0.28, 0.25 (15H each, s, Si(CH<sub>3</sub>)<sub>3</sub> + Si(CH<sub>3</sub>)<sub>2</sub>); 0.23 (9H, s, Si(CH<sub>3</sub>)<sub>3</sub>). IR (neat):  $\nu(\text{C}=\text{O}) = 1621$  (m) cm<sup>-1</sup>. UV absorption (hexane solution):  $\lambda_1$  371 nm ( $\epsilon_1 = 200 \cdot \text{mol}^{-1} \cdot \text{cm}^{-1}$ ), absorption shoulder at 250 nm ( $\epsilon_2 = 12000 \cdot \text{mol}^{-1} \cdot \text{cm}^{-1}$ ). HRMS: calc. for [C<sub>28</sub>H<sub>66</sub>OSi<sub>9</sub>]<sup>+</sup> (M<sup>+</sup>): 670.3037; found: 670.3065.

### Photolysis of 16a,b in hydrocarbon solution

A solution of 0.05 mmol of the acylsilanes **16a** or **16b** in 0.7 mL of d<sub>6</sub>-benzene in an NMR tube was photolyzed with a 150 W mercury lamp at 25 °C for 4 h. At this time <sup>1</sup>H- and <sup>29</sup>Si-NMR analysis showed the formation of the silenes **17a** or **17b**, respectively, along with unreacted starting material. For **16a/17a** a silene:acylsilane ratio of approximately 40:60 in the resulting yellow solution was estimated by integration of the C(CH<sub>3</sub>)<sub>3</sub> signals in the <sup>1</sup>H NMR spectra. Further irradiation afforded increasing amounts of polymeric decomposition products at the expense of **17a,b**. Attempted removal of the solvent in vacuo after an irradiation time of 4 hours also gave rise to extensive product decomposition.

**17a:** <sup>29</sup>Si-NMR (C<sub>6</sub>D<sub>6</sub>, TMS, ppm): 37.00 (Si=C), 13.16 (OSiMe<sub>3</sub>), -8.79 (Si(SiMe<sub>3</sub>)<sub>2</sub>), -34.41, -36.81, -37.44, -37.58 (SiMe<sub>2</sub>), -132.43 (Si(SiMe<sub>3</sub>)<sub>2</sub>). <sup>13</sup>C-NMR (C<sub>6</sub>D<sub>6</sub>, TMS, ppm): 214.39 (Si=C), 42.70 (C(CH<sub>3</sub>)<sub>3</sub>), 30.49 (C(CH<sub>3</sub>)<sub>3</sub>), 3.27 (Si(Si(CH<sub>3</sub>)<sub>3</sub>)<sub>2</sub>), 1.17 (OSi(CH<sub>3</sub>)<sub>3</sub>), -0.60, -1.49, -1.66, -2.54 (Si(CH<sub>3</sub>)<sub>2</sub>). <sup>1</sup>H-NMR (C<sub>6</sub>D<sub>6</sub>, TMS, ppm, rel. Int.): 1.26 (s, C(CH<sub>3</sub>)<sub>3</sub>); 0.55 - 0.28, (several overlapping signals, Si(CH<sub>3</sub>)).

**17b:** <sup>29</sup>Si-NMR (C<sub>6</sub>D<sub>6</sub>, TMS, ppm): 37.45 (Si=C), 13.27 (OSiMe<sub>3</sub>), -8.69 (Si(SiMe<sub>3</sub>)<sub>2</sub>), -34.68, -36.75, -37.40, -37.48 (SiMe<sub>2</sub>), -132.38 (Si(SiMe<sub>3</sub>)<sub>2</sub>). <sup>13</sup>C-NMR (C<sub>6</sub>D<sub>6</sub>, TMS, ppm): 215.93 (Si=C), 45.04, 42.15, 36.78, 29.03 (Ad-C), 3.29 (Si(Si(CH<sub>3</sub>)<sub>3</sub>)<sub>3</sub>), 1.43 (OSi(CH<sub>3</sub>)<sub>2</sub>), -0.32, -1.43, -1.62, -2.47 (Si(CH<sub>3</sub>)<sub>2</sub>). <sup>1</sup>H-NMR (C<sub>6</sub>D<sub>6</sub>, TMS, ppm, rel. Int.): 1.98 (b, Ad-CH); 1.89, 1.65 (b, Ad-CH<sub>2</sub>); 0.57 - 0.29 (several overlapping signals, Si(CH<sub>3</sub>)).

### Photolysis of 16a/Methanol

A solution of 0.50 g (0.84 mmol) of **16a** and 3 drops of anhydrous Et<sub>3</sub>N in 5 mL of benzene and 2 mL of methanol was photolyzed with a 150 W mercury lamp at 25 °C over 10 h. At this time NMR analysis showed that the starting material had been completely consumed. After removal of the volatile components on a rotary evaporator 20 mL of pentane were added and the resulting solution was filtered over silica gel. Evaporation of pentane afforded 0.46 g of a semi solid residue containing approximately 80 % of **18a** and 20 % of **20a**. Pure and colorless crystals of **18a** and **20a** could be isolated from the crude product by column chromatography (heptane, silica gel) followed by crystallization of the individual components from acetone at -30 °C.

**18a**: Yield: 0.1 g (20 %). mp: 124 - 127 °C. <sup>29</sup>Si-NMR (C<sub>6</sub>D<sub>6</sub>, TMS, ppm): 16.13, 14.95 (*SiOMe*, *OSiMe<sub>3</sub>*); -6.49, -9.23 (*Si(SiMe<sub>3</sub>)<sub>2</sub>*); -33.06, -33.23, -39.57, -41.02 (*SiMe<sub>2</sub>*); -132.22 (*Si(SiMe<sub>3</sub>)<sub>2</sub>*). <sup>13</sup>C-NMR (C<sub>6</sub>D<sub>6</sub>, TMS, ppm): 80.12 (*CH(t-Bu)OSi*); 53.40 (*OCH<sub>3</sub>*); 35.07 (*CCH<sub>3</sub>)<sub>3</sub>*); 28.33 (*C(CH<sub>3</sub>)<sub>3</sub>*); 3.96, 3.92, 0.85 (*Si(CH<sub>3</sub>)<sub>3</sub>*); -0.25, -0.54, -1.34, -1.54, -3.02, -3.15, -3.23, -3.81 (*Si(CH<sub>3</sub>)<sub>2</sub>*). <sup>1</sup>H-NMR (C<sub>6</sub>D<sub>6</sub>, TMS, ppm, rel. Int.): 3.55 (1H, s, *CH(t-Bu)OSi*); 3.28 (3H, s, *OCH<sub>3</sub>*); 0.93 (s, 9H, *C(CH<sub>3</sub>)<sub>3</sub>*); 0.55, 0.47, 0.41, 0.405, 0.37, 0.31, 0.30, 0.28 (3H each, s, *Si(CH<sub>3</sub>)<sub>2</sub>*); 0.35, 0.345, 0.252 (9H each, s, *Si(CH<sub>3</sub>)<sub>3</sub>*). HRMS: calc. for [C<sub>23</sub>H<sub>64</sub>O<sub>2</sub>Si<sub>9</sub>]<sup>+</sup> (M<sup>+</sup>): 624.2830; found: 624.2814.

**20a**: Yield: 0.05g (10 %). mp: 136 - 138 °C. <sup>29</sup>Si-NMR (C<sub>6</sub>D<sub>6</sub>, TMS, ppm): 19.61, 16.78 (*OSiMe<sub>2</sub>*, *SiOMe*); -8.41, -8.45 (*Si(SiMe<sub>3</sub>)<sub>2</sub>*); -19.67 (*MeOSiSiMe<sub>3</sub>*); -32.25, -41.54, -43.11 (*SiMe<sub>2</sub>*); -130.64 (*Si(SiMe<sub>3</sub>)<sub>2</sub>*). <sup>13</sup>C-NMR (C<sub>6</sub>D<sub>6</sub>, TMS, ppm): 80.96 (*OCHSi(t-Bu)*); 53.39 (*OCH<sub>3</sub>*); 34.61 (*CCH<sub>3</sub>)<sub>3</sub>*); 28.92 (*CCH<sub>3</sub>)<sub>3</sub>*); 3.72, 3.54, 1.48 (*Si(CH<sub>3</sub>)<sub>3</sub>*); 3.22, -0.10, -1.105, -1.11, -1.50, -2.10, -2.78, -4.11 (*Si(CH<sub>3</sub>)<sub>2</sub>*). <sup>1</sup>H-NMR (C<sub>6</sub>D<sub>6</sub>, TMS, ppm, rel. Int.): 3.55 (1H, s, *OCHSi(t-Bu)*); 3.28 (3H, s, *OCH<sub>3</sub>*); 0.93 (s, 9H, *C(CH<sub>3</sub>)<sub>3</sub>*); 0.55, 0.47, 0.41, 0.405, 0.37, 0.31, 0.30, 0.28 (3H each, s, *Si(CH<sub>3</sub>)<sub>2</sub>*); 0.35, 0.345, 0.25 (9H each, s, *Si(CH<sub>3</sub>)<sub>3</sub>*). HRMS: calc. for [C<sub>23</sub>H<sub>64</sub>O<sub>2</sub>Si<sub>9</sub>]<sup>+</sup> (M<sup>+</sup>): 624.2830; found: 624.2855.

### Photolysis of 16b/Methanol

A solution of 0.40 g (0.60 mmol) of **16b** and 3 drops of anhydrous Et<sub>3</sub>N in 5 mL of benzene and 2 mL of methanol was photolyzed at 25 °C with a 150 W mercury lamp over 10 h. At this time NMR analysis showed that the starting material had been completely consumed. After removal of the volatile components on a rotary evaporator 20 mL of pentane were added and the resulting solution was filtered over silica gel. Evaporation of pentane afforded 0.38 g of a semi solid residue containing approximately 80 % of **18b** and 20 % of **20b**. Small amounts of pure and colorless crystals of **18b** could be isolated as the less soluble product after repeated recrystallization from acetone solution. White crystals of slightly impure **20b** were isolated in low yield from the combined mother liquors after concentration and repeated crystallization from acetone at -30 °C.

**18b**: mp: 186 - 188 °C. <sup>29</sup>Si-NMR (CDCl<sub>3</sub>, TMS, ppm): 16.26, 14.82 (*SiOMe*, *OSiMe<sub>3</sub>*); -6.06, -9.08 (*Si(SiMe<sub>3</sub>)<sub>2</sub>*); -32.55, -32.74, -39.23, -40.66 (*SiMe<sub>2</sub>*); -131.93 (*Si(SiMe<sub>3</sub>)<sub>2</sub>*). <sup>13</sup>C-NMR (CDCl<sub>3</sub>, TMS, ppm): 81.45 (*CH(Ad)OSi*), 53.50 (*OCH<sub>3</sub>*); 40.87, 37.15, 37.10, 28.66 (*Ad*); 4.10, 4.07, 1.06 (*Si(CH<sub>3</sub>)<sub>3</sub>*); -0.13, -0.57, -1.38, -1.53, -2.82, -2.93, -3.29, -3.94 (*Si(CH<sub>3</sub>)<sub>2</sub>*). <sup>1</sup>H-NMR (CDCl<sub>3</sub>, TMS, ppm, rel. Int.): 3.74 (1H, s, *CH(Ad)OSi*); 3.37 (3H, s, *OCH<sub>3</sub>*); 1.99 (3H, b, *Ad-CH*), 1.7- 1.5 (12H, b, *Ad-CH<sub>2</sub>*); 0.35 (3H, s, *Si(CH<sub>3</sub>)<sub>2</sub>*), 0.30 (6H, b, *Si(CH<sub>3</sub>)<sub>2</sub>*); 0.27, 0.25 (3H each, s, *Si(CH<sub>3</sub>)<sub>2</sub>*);

0.26 (15H, s, Si(CH<sub>3</sub>)<sub>3</sub> + Si(CH<sub>3</sub>)<sub>2</sub>); 0.22 (12H, s, Si(CH<sub>3</sub>)<sub>3</sub> + Si(CH<sub>3</sub>)<sub>2</sub>); 0.125 (9H, s, Si(CH<sub>3</sub>)<sub>3</sub>). HRMS: calc. for [C<sub>29</sub>H<sub>70</sub>O<sub>2</sub>Si<sub>9</sub>]<sup>+</sup> (M<sup>+</sup>): 702.3300; found: 702.3335.

**20b**: <sup>29</sup>Si-NMR (CDCl<sub>3</sub>, TMS, ppm): 19.30, 16.69 (OSiMe<sub>2</sub>, SiOMe); -8.37, -8.45 (Si(SiMe<sub>3</sub>)<sub>2</sub>); -19.74 (MeOSiSiMe<sub>3</sub>); -32.23, -41.36, -42.93 (SiMe<sub>2</sub>); -130.52 (Si(SiMe<sub>3</sub>)<sub>2</sub>). <sup>13</sup>C-NMR (CDCl<sub>3</sub>, TMS, ppm): 81.85 (SiCH(Ad)OSi); 53.66 (OCH<sub>3</sub>); 41.30, 37.00, 36.72, 28.63 (Ad); 3.83, 3.62, 1.81 (Si(CH<sub>3</sub>)<sub>3</sub>); 3.62, -0.02, -1.05, -1.14, -1.38, -2.15, -2.88, -3.94 (Si(CH<sub>3</sub>)<sub>2</sub>). <sup>1</sup>H-NMR (CDCl<sub>3</sub>, TMS, ppm, rel. Int.): 3.47 (1H, s, CH(O)Ad); 3.41 (3H, s, OCH<sub>3</sub>); 1.97 (3H, b, Ad-CH); 1.7 – 1.4 (12H, b, Ad-CH<sub>2</sub>); 0.38, 0.31, 0.27, 0.20, 0.17 (3H each, s, Si(CH<sub>3</sub>)<sub>2</sub>); 0.25 (6H, b, Si(CH<sub>3</sub>)<sub>2</sub>); 0.28, 0.26 (9H each, s, Si(CH<sub>3</sub>)<sub>3</sub>), 0.24 (12H, s, Si(CH<sub>3</sub>) + Si(CH<sub>3</sub>)<sub>3</sub>). HRMS: calc. for [C<sub>29</sub>H<sub>70</sub>O<sub>2</sub>Si<sub>9</sub>]<sup>+</sup> (M<sup>+</sup>): 702.3300; found: 702.3348.

### Photolysis of 1-Trimethylacyl-4-(trimethylsilyl)dodeca-methylbicyclo[2.2.2]octasilane (**21**) in Methanol

A solution of 40 mg (0.071 mmol) of **21** and 3 drops of anhydrous Et<sub>3</sub>N in 0.3 mL of benzene and 0.3 mL of methanol in an NMR tube was photolyzed with a 150 W mercury lamp at 25 °C for 10 h. At this time NMR and GC-MS analysis showed the formation of methanol adduct **22**. Attempted purification by crystallization of the oily crude product obtained after evaporation of the solvents failed to yield a crystalline solid.

<sup>29</sup>Si-NMR (CDCl<sub>3</sub>, TMS, ppm): 18.35 (OSiMe<sub>2</sub>), 8.63 (SiOMe), -5.65 (SiMe<sub>3</sub>); -36.71, -37.38, -40.48, -43.54, -43.75 (SiMe<sub>2</sub>); -130.53 (SiSi<sub>4</sub>). <sup>13</sup>C-NMR (CDCl<sub>3</sub>, TMS, ppm): 76.31 (CH(O)*t*-Bu); 54.53 (OCH<sub>3</sub>); 35.50 (C(CH<sub>3</sub>)<sub>3</sub>); 28.17 (C(CH<sub>3</sub>)<sub>3</sub>), 3.82 (Si(CH<sub>3</sub>)<sub>3</sub>), 3.75, -0.05, -0.25, -0.36, -0.66, -1.08, -1.48, -1.68, -2.23, -3.32, -3.85, -4.07 (Si(CH<sub>3</sub>)<sub>2</sub>). <sup>1</sup>H-NMR (CDCl<sub>3</sub>, TMS, ppm, rel. Int.): 3.68 (1H, s, CH(O)*t*Bu); 3.47 (3H, s, OCH<sub>3</sub>); 0.99 (9H, s, C(CH<sub>3</sub>)<sub>3</sub>); 0.32, 0.30, 0.29, 0.27, 0.24, 0.18 (3H each, s, Si(CH<sub>3</sub>)<sub>2</sub>); 0.31 (6H, s, Si(CH<sub>3</sub>)<sub>3</sub> + Si(CH<sub>3</sub>)<sub>2</sub>), 0.28 (9H, s, Si(CH<sub>3</sub>)<sub>3</sub> + Si(CH<sub>3</sub>)<sub>2</sub>), 0.26 (12H, s, Si(CH<sub>3</sub>)<sub>3</sub> + Si(CH<sub>3</sub>)<sub>2</sub>). MS (m/e (relative intensity)): 594 (0.7 %, M<sup>+</sup>).

#### 2.2.5.2 X-ray Crystallography:

For X-ray structure analysis suitable crystals were mounted onto the tip of glass fibres using mineral oil. Data collection was performed on a Bruker Kappa Apex II CCD diffractometer at 100 K using graphite-monochromated Mo K $\alpha$  ( $\lambda = 0.71073\text{\AA}$ ) radiation. Details of the crystal data and structure refinement are provided as Supporting Information. The SHELX version 6.1 program package was used for the structure solution and refinement.<sup>31</sup> Absorption corrections were applied using the SADABS program.<sup>32</sup> All non-hydrogen atoms were refined with anisotropic displacement parameters. Hydrogen atoms were included in the refinement at calculated positions using a riding model as implemented in the SHELXTL program. Crystallographic data (excluding structure factors) have been deposited with the Cambridge Crystallographic Data Centre as supplementary publications CCDC-964365 (**16a**), CCDC-964366 (**16b**), CCDC-964367 (**18b**), CCDC-964368 (**20a**) and CCDC-964369 (**20b**). Copies of the data can be obtained free of charge on application to The Director, CCDC, 12 Union Road, Cambridge CB2 1EZ, UK (fax (internat.) +44-1223/336-033; e-mail [deposit@ccdc.cam.ac.uk](mailto:deposit@ccdc.cam.ac.uk)).

## 2.2.6 References

- <sup>1</sup> For general reviews about silenes, see e.g.: a) H. Ottosson, A. M. Eklöf, *Coord. Chem. Rev.* 252 (2008) 1287; b) H. Ottosson, P. G. Steel, *Chem. Eur. J.* 12 (2006) 1576; c) L. E. Gusel'nikov, *Coord. Chem. Rev.* 244 (2003) 149; d) R. West, *J. Organomet. Chem.* 21 (2001) 467. e) T. L. Morkin, W. J. Leigh, *Acc. Chem. Res.* 34 (2001) 129; f) T. Müller, W. Ziche, N. Auner, in: Rappoport, Z.; Y. Apeloig, (Eds.), *The Chemistry of Organic Silicon Compounds, Vol. 2*, JohnWiley&Sons Ltd., New York, (1998), pp. 1233–1310; g) A. G. Brook, M. A. Brook, *Adv. Organomet. Chem.* 39 (1996) 71
- <sup>2</sup> A. G. Brook, S. C. Nyburg, F. Abdesaken, B. Gutekunst, G. Gutekunst, R. K. Kallury, Y. C. Poon, Y. M. Chang, W. Wong-Ng, *J. Am. Chem. Soc.* 104 (1982) 5667
- <sup>3</sup> N. Wiberg, G. Wagner, G. Müller, J. Reids, *Angew. Chem., Int. Ed. Engl.* 22 (1984) 381
- <sup>4</sup> Y. Apeloig, M. Bendikov, M. Yuzefovich, M. Nakash, D. Bravo-Zhivotovskii, D. Blaser, R. Boese, *J. Am. Chem. Soc.* 118 (1996) 12228
- <sup>5</sup> M. Kira, S. Ishida, T. Iwamoto, C. Kabuto, *J. Am. Chem. Soc.* 121 (1999) 9722
- <sup>6</sup> a) S. Spirk, F. Belaj, J. H. Albering, R. Pietschnig, *Organometallics* 29 (2010) 2981; b) G. E. Miracle, J. L. Ball, D. R. Powell, R. West, *J. Am. Chem. Soc.* 115 (1993) 11598
- <sup>7</sup> a) N. Tokitoh, A. Shinohara, T. Matsumoto, T. Sasamori, N. Takeda, Y. Furukawa, *Organometallics* 26 (2007) 4048; b) N. Takeda, A. Shinohara, N. Tokitoh, *Organometallics* 21 (2002) 256; c) N. Takeda, A. Shinohara, N. Tokitoh, *Organometallics* 21 (2002) 4024; d) K. Wakita, N. Tokitoh, R. Okazaki, S. Nagase, *Angew. Chem., Int. Ed.* 39 (2000) 634; e) K. Wakita, N. Tokitoh, R. Okazaki, S. Nagase, P. von Schleyer, H. Jiao, *J. Am. Chem. Soc.* 121 (1999) 11336; f) N. Tokitoh, K. Wakita, R. Okazaki, S. Nagase, P. von Schleyer, H. Jiao, *J. Am. Chem. Soc.* 119 (1997) 6951
- <sup>8</sup> K. Sakamoto, J. Ogasawara, Y. Kon, T. Sunagawa, C. Kabuto, M. Kira, *Angew. Chem. Int. Ed.* 41 (2002) 1402
- <sup>9</sup> D. Bravo-Zhivotovskii, R. Dobrovetsky, D. Nemirovsky, V. Molev, M. Bendikov, G. Molev, M. Botoshansky, Y. Apeloig, *Angew. Chem. Int. Ed.* 47 (2008) 4343
- <sup>10</sup> I. Bejan, D. Güclü, S. Inoue, M. Ichinohe, A. Sekiguchi, D. Scheschkewitz, *Angew. Chem. Int. Ed.* 46 (2007) 3349
- <sup>11</sup> S. Inoue, M. Ichinohe, A. Sekiguchi, *Angew. Chem. Int. Ed.* 46 (2007) 3346
- <sup>12</sup> T. Guliashvili, I. El-Sayed, A. Fischer, H. Ottosson, *Angew. Chem. Int. Ed.* 42 (2003) 1640
- <sup>13</sup> T. Iwamoto, N. Ohnishi, N. Akasaka, K. Ohno, S. Ishida, *J. Am. Chem. Soc.* 135 (2013) 10606
- <sup>14</sup> the topic is discussed in detail including bibliography in ref 1a,e
- <sup>15</sup> Y. Apeloig, M. Karni, *J. Am. Chem. Soc.* 106 (1984) 6676
- <sup>16</sup> a) H. Stueger, G. Fuerpass, J. Baumgartner, T. Mitterfellner, M. Flock, *Z. Naturforsch.* 64b (2009) 1598; b) P. Hamon, F. Justaud, O. Cador, P. Hapiot, S. Rigaut, L. Toupet, L. Ouahab, H. Stueger, J. R. Hamon, C. Lapinte, *J. Am. Chem. Soc.* 130 (2008) 17372; c) J. A. Shaw-Taberlet, J. R. Hamon, T. Roisnel, C. Lapinte, M. Flock, T. Mitterfellner, H. Stueger, *J. Organomet. Chem.* 692 (2007) 2046; d) H. Stüger, G. Fürpass, K. Renger, *Organometallics* 24 (2005) 6374
- <sup>17</sup> R. Fischer, T. Konopa, S. Ully, J. Baumgartner, C. Marschner, *J. Organomet. Chem.* 685 (2003) 79
- <sup>18</sup> Compare the values measured for the central silicon atom in (Me<sub>3</sub>Si)<sub>3</sub>SiCOt-Bu ( $\delta^{29}\text{Si} = -78.1$  ppm) and (Me<sub>3</sub>Si)<sub>4</sub>Si ( $\delta^{29}\text{Si} = -135.6$  ppm): ref. 2; C. Marschner, *Eur. J. Inorg. Chem.* (1998) 221
- <sup>19</sup> Selected cyclohexasilanes with bulky substituents in *cis*-1,4-, 1,1,4,4- or 1,1,3,3-positions were recently reported to exhibit *boat*-, *twisted boat* or *twist* conformations: a) C. Marschner, J. Baumgartner, A. Wallner, *Dalton Trans.* (2006) 5667. b) A. Wallner, M. Hölbling, J.

- Baumgartner, C. Marschner, *Silicon Chemistry* 3 (2005) 175 c) V. E. M. Kaats-Richters, T. J. Cleij, L. W. Jenneskens, M. Lutz, A. L. Spek, C. A. van Walree, *Organometallics* 22 (2003) 2249
- 20 a) H. Rautz, H. Stueger, G. Kickelbick, C. Pietzsch, *J. Organomet. Chem.* 627 (2001) 167; b) P. D. Lickiss, *Adv. Inorg. Chem.* 42 (1995) 147. c) K. Kumar, M. H. Litt, R. K. Chada, J. E. Drake, *Can. J. Chem.* 65 (1987) 437
- 21 M. Kaftory, M. Kapon, M. Botoshansky, In *The Chemistry of Organic Silicon Compounds*, Vol. 2; Z. Rappoport, Y. Apeloig, Eds.; Wiley: Chichester, (1998); p 197f
- 22 The observed C=O distances are close to the ones found in simple organic ketones, carboxylic acids and esters: a) R. J. Berry, R. J. Waltman, J. Pacansky, A. T. Hagler, *J. Phys. Chem.* 99 (1995) 10511. b) J. A. Kanters, J. Kroon, A. F. Peerdeman, J. C. Schoone, *Tetrahedron* 23 (1967) 4027
- 23 The average Si-C(sp<sup>3</sup>) bond length was calculated from 19169 individual XRD experimental values to be 1.860 Å: M. Kaftory, M. Kapon, M. Botoshansky, In *The Chemistry of Organic Silicon Compounds*, Vol. 2; Z. Rappoport, Y. Apeloig, Eds., Wiley: Chichester, (1998); p. 192
- 24 P. C. Bulman Page, M. J. McKenzie, S. S. Klair, S. Rosenthal, In *The Chemistry of Organic Silicon Compounds*, Vol. 2; Z. Rappoport, Y. Apeloig, Eds., Wiley: Chichester, (1998); p 1605
- 25 A. Wallner, M. Hölbling, J. Baumgartner, C. Marschner, *Silicon Chemistry* 3 (2005) 175
- 26 T. J. Drahnak, J. Michl, R. West, *J. Am. Chem. Soc.* 101 (1979) 5427. b) M. Ishikawa, M. Kumada, *J. Organomet. Chem.* 42 (1972) 325
- 27 Trapping experiments with Et<sub>3</sub>SiH were not successful maybe because :SiMe<sub>2</sub> eventually formed in the course of the photolysis of **16a,b** immediately reacts with the Si=C double bond and, thus, ends up in the polymeric residue. Addition of silylenes to silenes has been observed earlier: M. Ishikawa, S. Matsuzawa, *J. Chem. Soc., Chem. Comm.* (1985) 588
- 28 A. G. Brook, J. W. Harris, J. Lennon, M. El Sheikh, *J. Am. Chem. Soc.* 101 (1979) 83
- 29 J. M. Duff, A. G. Brook, *Can. J. Chem.* 51 (1973) 2869
- 30 A. B. Pangborn, M. A. Giardello, R. H. Grubbs, R. K. Rosen, F. J. Timmers, *Organometallics* 15 (1996) 1518
- 31 SHELX and SHELXL PC: VERSION 5.03, Bruker AXS, Inc., Madison, WI, (1994)
- 32 SADABS: Area-detection Absorption Correction: Bruker AXS Inc., Madison, WI, (1995)



## 2.3 Photoinduced Rearrangement of Aryl-substituted Acylcyclohexasilanes

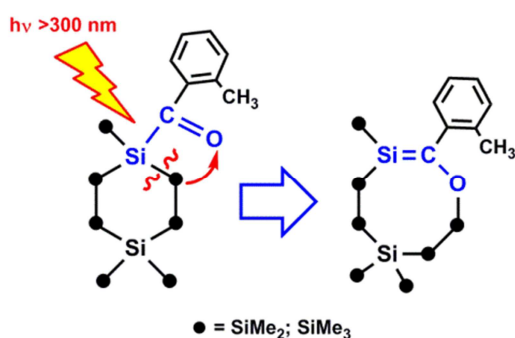
Michael Haas,<sup>[a]</sup> Roland Fischer,<sup>[a]</sup> Lukas Schuh,<sup>[a]</sup> Robert Saf,<sup>[b]</sup> Ana Torvisco<sup>[a]</sup> and Harald Stueger<sup>\*[a]</sup>

<sup>[a]</sup> Institute of Inorganic Chemistry, Graz University of Technology, Stremayrgasse 9, A-8010 Graz, Austria

<sup>[b]</sup> Institute for Chemistry and Technology of Materials, Graz University of Technology, Stremayrgasse 9, A-8010 Graz, Austria

published in *European Journal of Inorganic Chemistry*, 6 (2015) 997

Graphical abstract:



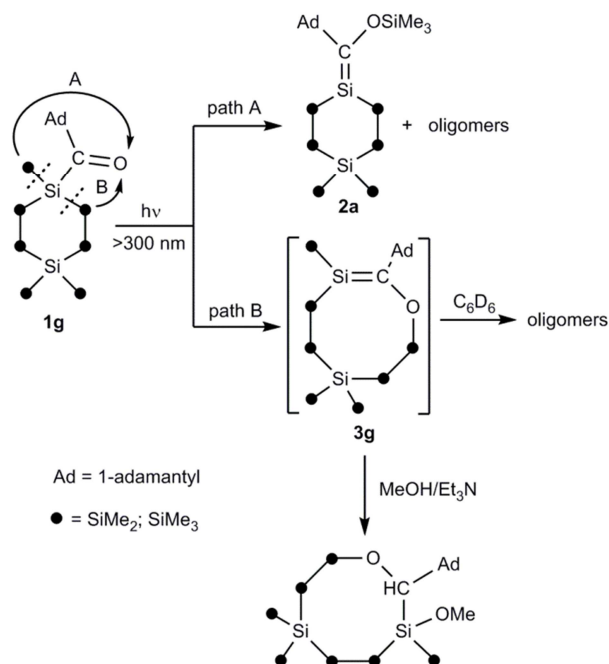
### 2.3.1 Abstract

In the present study we have examined photochemical transformations of acylcyclohexasilanes (Me<sub>3</sub>Si)<sub>2</sub>Si<sub>6</sub>Me<sub>12</sub>(Me<sub>3</sub>Si)COR (**1**) with aromatic substituents attached to the carbonyl C atom. When photolyzed at wavelengths above 300 nm in hydrocarbon solvents, **1a-c** (**a**: R = *o*-Tol; **b**: 2,3-Me<sub>2</sub>C<sub>6</sub>H<sub>3</sub>; **c**: 2,4-Me<sub>2</sub>C<sub>6</sub>H<sub>3</sub>) afforded the previously unknown eight-membered heterocyclopolysilanes **3a-c** which feature endocyclic Si=C double bonds with remarkable selectivity. If two ortho-alkyl groups are present at the aromatic ring the primary products of type **3** (**d**: R = Mes; **e**: 1,6-Me<sub>2</sub>C<sub>6</sub>H<sub>3</sub>; **f**: 2,4,6-*i*Pr<sub>3</sub>C<sub>6</sub>H<sub>2</sub>) are photochemically unstable and undergo intramolecular C-H bond addition reactions of a *ortho*-CH<sub>3</sub> group to the Si=C double, which leads to the formation of spirobenzocyclobutenes. When photolysis was performed in the presence of methanol, the expected 1,2-addition products (compound **4**) of the Si=C double bond were obtained quantitatively in all cases. **4a** (R = *o*-Tol) and **4b** (R = Mes) were isolated by crystallization from acetone and fully characterized spectroscopically and by single-crystal X-ray crystallography. Interestingly **4b** was obtained as an isomeric mixture arising from *syn* and *anti* addition of methanol to the endocyclic Si=C bond while exclusively *syn* addition was observed in the case of **4a**.

### 2.3.2 Introduction

Silenes with double bonds between one silicon and one carbon atom were considered unstable and only existent in reactive intermediates until Brook reported on the isolation of the first stable silene in 1981.<sup>1</sup> Brook photolyzed acylpolysilanes  $(\text{Me}_3\text{Si})_3\text{SiC}(\text{R})=\text{O}$  ( $\text{R} = \text{alkyl}$ ) and observed the formation of silicon-carbon unsaturated species  $(\text{Me}_3\text{Si})_2\text{Si}=\text{C}(\text{OSiMe}_3)\text{R}$ , which were stable at room temperature if bulky groups such as 1-adamantyl substituents were attached to the carbonyl C atom. Alternative approaches to stable silenes published since then include intramolecular salt elimination of  $\alpha$ -lithiofluorosilanes,<sup>2</sup> the Sila-Peterson reaction of ketones with alkali metal silanides<sup>3</sup> and the reaction of lithium silenolates with chlorosilanes  $\text{R}_3\text{SiCl}$ .<sup>4</sup> In addition, more specialized methods have been used for the synthesis of complex molecules such as stable 1-silaallenes,<sup>5</sup> silaaromatics,<sup>6</sup> metal-substituted or charged silenes<sup>7</sup> or heteroatom substituted silene species.<sup>8</sup> Nowadays the literature contains numerous experimental and theoretical studies focused on the topic, hence, extensive knowledge exists on the synthesis and reactivity of stable silenes and also on the nature of the Si=C double bond itself.<sup>9</sup>

So far, only selected examples of stable Si=C-bonded species that feature Si-Si bonds and the unsaturated silicon atom incorporated into cyclic structures have been synthesized and fully characterized.<sup>10</sup> In our laboratories we currently investigate cyclohexasilanes that contain multiply bonded silicon atoms. In the course of these studies, we discovered that the photochemical rearrangement of acylcyclohexasilanes with bulky alkyl groups, such as 1-adamantyl substituents, attached to the carbonyl C atom leads to the formation of species containing Si=C double bonds and follows two competing pathways (compare Scheme 1). Besides a "normal" Brook-type rearrangement including a 1,3-Si $\rightarrow$ O trimethylsilyl shift that gives the methylenecyclohexasilane **2** (reaction path A) the ring enlarged species **3** was generated by photochemically induced ring scission and subsequent 1,3-Si $\rightarrow$ O migration of the resulting terminal SiMe<sub>2</sub> group (reaction path B). However, **2** and **3** were not stable under the applied photolytical conditions. Whereas **2** could be detected directly by NMR and UV/Vis spectroscopy in a mixture with unreacted starting material and polymeric by-products, **3g** was only observed in form of its methanol adduct.<sup>11</sup>



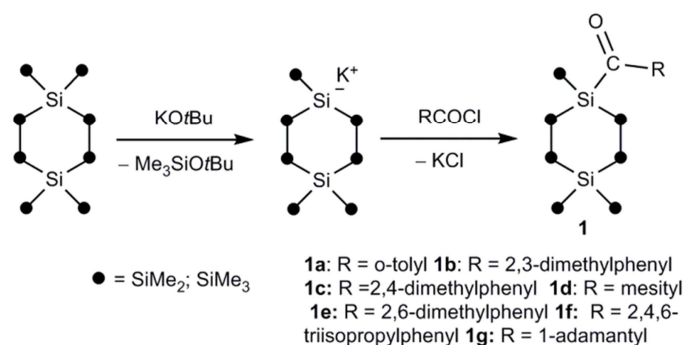
**Scheme 1.** Photolysis of alkyl substituted acylcyclohexasilanes.

More recently we reported on the synthesis and the isolation of the first stable methylenecyclohexasilane **2b**, which is stabilized by a mesityl group at the  $sp^2$  C atom, using a different approach.<sup>12</sup> In the present study we have examined photochemical transformations of various aryl-substituted acylcyclohexasilanes, which showed surprisingly different reactivity patterns. A Proper choice of the substituents attached to the aromatic ring, thus, enabled the selective synthesis of stable endocyclic silenes of type **3** which represent, to the best of our knowledge, the first directly observed examples for cyclopolysilanes with endocyclic Si=C double bonds.

## 2.3.3 Results and Discussion

### 2.3.3.1 Synthesis of Acylcyclohexasilanes

The acylcyclohexasilanes **1a-f**, which have different substitution patterns of the aromatic ring, were synthesized easily according to Scheme 2 by using standard procedures that had previously been applied for the successful preparation of the alkyl derivative **1g**.<sup>11</sup>

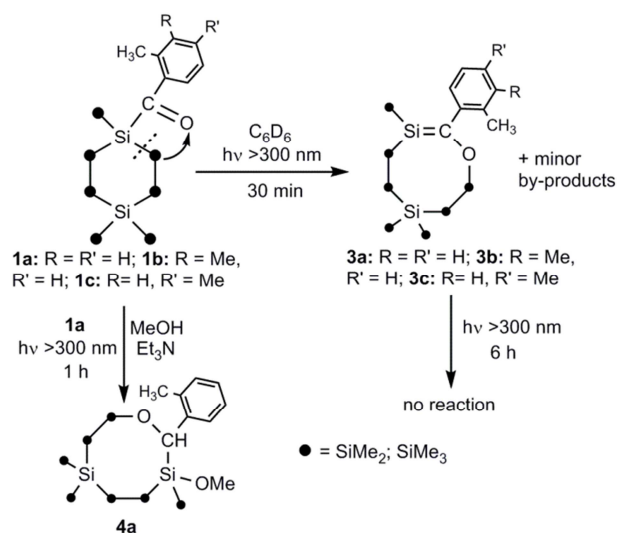


**Scheme 2.** Synthesis of acylcyclohexasilanes.

The air-stable target compounds were isolated in moderate to good yields after crystallization from acetone solution as slightly yellow crystals. In all cases, the analytical and spectroscopic data (for details consult the Experimental Section) are consistent with the proposed structures and with literature data of related compounds.<sup>11</sup>

### 2.3.3.2 Photolysis of **1a-c**

The photolysis of **1a-c** in hydrocarbon solution afforded the endocyclic rearrangement products **3a-c** with remarkable selectivity (Scheme 3). After irradiation of approximately 0.2 M solutions of **1a-c** in C<sub>6</sub>D<sub>6</sub> at wavelengths > 300 nm radiation for 30 min the starting materials had been consumed completely. <sup>13</sup>C- and <sup>29</sup>Si NMR spectra of the resulting deeply yellow solutions showed signals characteristic of Si=C bonds near 200 and 49 ppm, respectively, whereas the signals of the SiC=O moiety near 240 and -67 ppm have vanished. The molecular structures of **3a-c** were unambiguously assigned by <sup>1</sup>H-, <sup>13</sup>C- and <sup>29</sup>Si-NMR spectroscopy (see Experimental Section). As an example, Figure 1 presents the <sup>29</sup>Si NMR spectrum of the photolysis product of **1a**, including the assignment of the observed resonance lines. Residual NMR spectra are included in the Supporting Information. Furthermore, **3a-c** showed extraordinary photochemical stability and literally unchanged NMR spectra, even after prolonged photolysis times.



**Scheme 3.** Photolysis of **1a-c**.

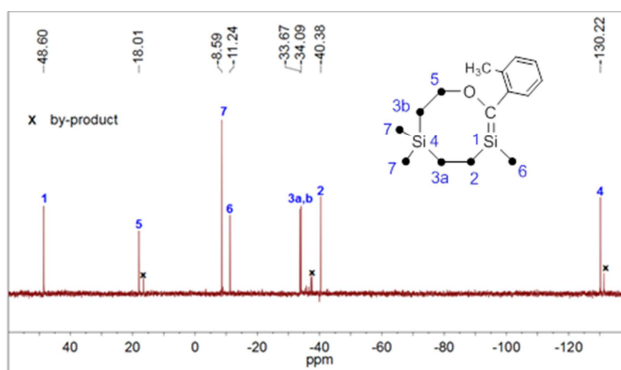


**Figure 1.** <sup>29</sup>Si NMR spectrum recorded after photolysis of **1a** (C<sub>6</sub>D<sub>6</sub> solution, c = 0.2 mol·l<sup>-1</sup>, T = 25 °C) with a 600 W mercury lamp through Pyrex glass for 30 min including assignment of the resonance lines.

Compounds **3a-c** were obtained along with small amounts of a structurally closely related by-product of unknown constitution, as indicated by the appearance of additional NMR signals. Unfortunately, pure **3a-c** could not be isolated from these mixtures, because of their reluctance to crystallize. For **3a**, integration of the <sup>1</sup>H spectra recorded in [D<sub>8</sub>]-toluene (with the residual solvent peak at δ = 2.08 ppm as an internal standard) exhibited a constant intensity ratio of standard and product peaks before and after photolysis. However, attempts to estimate the yield of **3a** from the <sup>1</sup>H-NMR spectra were unsuccessful, because significant signal overlap prevented the assignment of individual signals to the product or by-product especially in the Si-Me region.

The mechanism of the photolysis reaction proposed in Scheme 3 was supported further by trapping experiments. For instance, when **1a** dissolved in C<sub>6</sub>D<sub>6</sub> was photolyzed for 60 min in the presence of MeOH, to which a trace amount of weak base such as pyridine or Et<sub>3</sub>N had been added,<sup>13</sup> the expected 1,2-addition product of the Si=C double bond **4a** was obtained quantitatively. Pure **4a** could be isolated by crystallization from acetone and fully characterized spectroscopically and by single crystal

X-ray crystallography. The analytical and structural data are unexceptional and compare excellently with the ones measured earlier for the corresponding adamantyl derivative.<sup>11</sup>

As mentioned earlier, solutions of the silenes **3a-c** are yellow. **3a** showed an intense UV absorption band at  $\lambda_{max} = 360$  nm ( $\epsilon = 12200$ ). It is considerably red-shifted relative to the corresponding bands in the spectra of the acyclic silene  $(\text{Me}_3\text{Si})_2\text{Si}=\text{C}(\text{OSiMe}_3)\text{Ad}$  ( $\lambda_{max} = 340$  nm,  $\epsilon = 7400$ )<sup>1</sup> and of the endocyclic silene  $[-\text{Tip}_2\text{Si}-\text{TipSi}=\text{C}(\text{Ad})-\text{O}-]$  ( $\lambda_{max} = 354$  nm).<sup>10b</sup> Furthermore, **3a** an absorption band with nearly identical wavelength and intensity as the longest wavelength absorption band observed in the UV/Vis spectrum of the methylenecyclohexasilane **2b** ( $\lambda_{max} = 364$  nm,  $\epsilon = 16500$ ).<sup>11</sup> On the Basis of time-dependent DFT calculations performed earlier for **2b**, the great similarity of the absorption data of both compounds suggest an identical assignment of the low energy absorption band to a  $\pi_{\text{Si}=\text{C}} \rightarrow \pi^*_{\text{aryl}}$  transition.

Although pure **3a-c** could not be isolated, because they did not crystallize, the fact that they are formed with surprising selectivity is certainly of interest, because it contrasts with the outcome of our previous photolysis experiments involving alkyl substituted acylcyclohexasilanes such as **1g**, which afforded mixtures of the *exo*- and the *endo*-cyclic rearrangement products under the same conditions. The presence of aromatic substituents at the carbonyl C atom apparently favors reaction path B over reaction path A to a large extent (compare Scheme 1) which very likely can be attributed to the electronic impact of the aromatic  $\pi$ -system.

### 2.3.3.3 Photolysis of 1d-f

As depicted in Scheme 4, acylcyclohexasilanes with two *ortho*-alkyl groups at the aromatic ring exhibit a photochemical significantly different photochemical reactivity relative to **1a-c**. Irradiation of hydrocarbon solutions of **1d,e** for 30 min afforded mixtures of the silenes **3d,e** with unreacted starting material in an approximate molar ratio of 1:3, as evidenced by the growth of the appropriate sets of new NMR signals (in particular a <sup>13</sup>C signal near 245 ppm and a <sup>29</sup>Si signal near 42 ppm) characteristic of the sp<sup>2</sup>-hybridized carbon and silicon atoms. During prolonged irradiation of the resulting solutions, additional products of unknown composition were detected, which is illustrated by the increased complexity of the NMR spectra. Figure 2 shows the <sup>29</sup>Si NMR spectrum of **1d** after 0,30, and 70 min of irradiation. Whereas after 30 min only the resonances characteristic of **1d** and **3d** were detected (Figure 2B) the spectrum recorded after 70min (Figure 2C) showed several additional signals of unknown origin. **1e** behaved similarly (see Supporting Information).

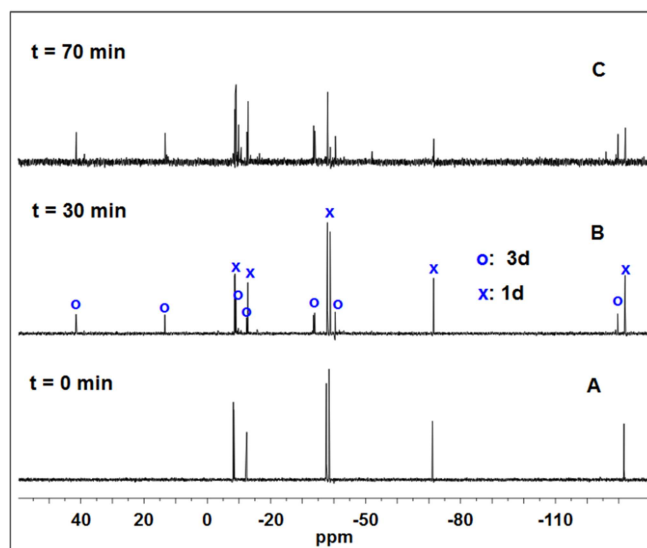
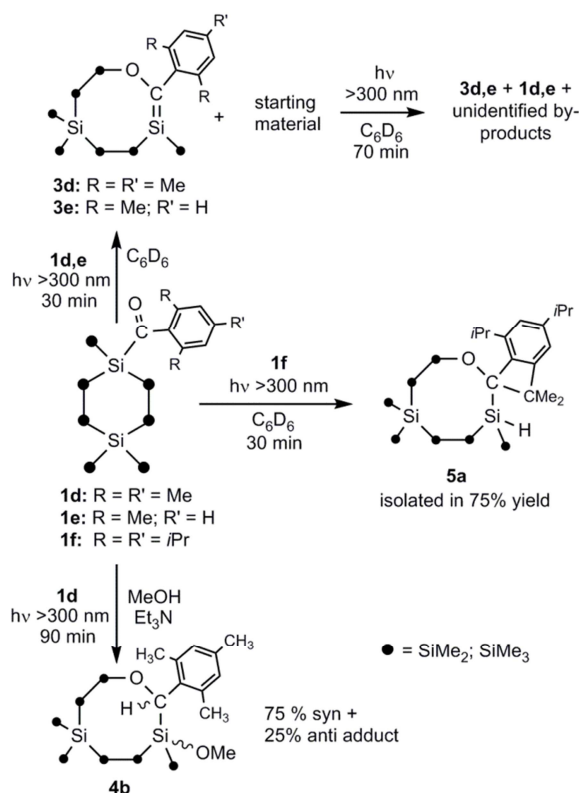


**Figure 2.**  $^{29}\text{Si}$  NMR spectrum recorded after photolysis of **1d** ( $\text{C}_6\text{D}_6$  solution,  $c = 0.2 \text{ mol}\cdot\text{l}^{-1}$ ,  $T = 25 \text{ }^\circ\text{C}$ ) with a 600 W mercury lamp through Pyrex glass for (A) 0 min, (B) 30 min and (C) 70 min.



**Scheme 4.** Photolysis of **1d,e**.

In previous studies, acyclic mesityl-substituted Brook-type silenes were found to undergo photochemically induced addition reactions of a C-H bond of a mesityl ortho- $\text{CH}_3$  group to the  $\text{Si}=\text{C}$  double bond under formation of substituted benzocyclobutenes.<sup>14</sup> Based on the observation that NMR signals typical for Si-H groups ( $\delta^1\text{H} = \sim 3.8 \text{ ppm}$ ;  $\delta^{29}\text{Si} = \sim -55 \text{ ppm}$ ) appear upon the extended photolysis of **1d,e** a similar mechanism may be operative in this case as well (compare Scheme 4). The

initially formed silenes **3d,e** are photolytically unstable and react further to give complex mixtures of photolysis products possibly including spirobenzocyclobutenes which cannot be isolated. This assumption is perfectly in line with the outcome of photolysis experiments involving the sterically more encumbered acylcyclohexasilane **1f** as the starting material. In this case the photolysis reaction proceeded much smoother and after an irradiation time of 30 min the spirobenzocyclobutene **5a** was obtained with high selectivity and could be isolated by crystallization from acetone and characterized by the usual analytical methods (for data and assignment consult the Experimental Section). From this point of view the higher photochemical stability of **3a-c** is also conclusive, because it seems likely that the molecules adopt structures with a remote position of the *ortho*-CH<sub>3</sub> group relative to the Si=C moiety in order to minimize steric congestion. Because severely restricted rotation around the C<sub>sp<sup>2</sup></sub>-C<sub>aryl</sub> bond can be assumed also in solution C-H addition is not possible in **3a-c** for steric reasons. In **3d-f**, on the contrary, one of the two *ortho*-alkyl groups is placed adjacent to the Si=C bond which apparently favors the formation of the spirobenzocyclobutene photolysis product. Nevertheless **3d** could be trapped effectively with MeOH/Et<sub>3</sub>N. Photolysis of **1d** in C<sub>6</sub>D<sub>6</sub>/MeOH/Et<sub>3</sub>N for 90 min exclusively afforded the expected addition product **4b** without any indication for the formation of **5a**. Thus, methanol O-H addition to the Si=C bond occurs much faster than the intramolecular addition of a methyl C-H bond which already had been observed earlier for acyclic mesitylsilenes R<sub>2</sub>Si=C(OSiMe<sub>3</sub>)Mes.<sup>14a</sup>

It is interesting to note that **4b** is obtained as an isomeric mixture arising from *syn*- and *anti*-addition of methanol to the endocyclic Si=C bond while exclusively *syn*-addition was observed, when **1a** was photolyzed under identical conditions. The <sup>1</sup>H NMR spectrum of the crude photolysis product derived from **1d** contains, in addition to the signals for the Me<sub>3</sub>Si-, Me<sub>2</sub>Si- and mesityl groups, absorptions at δ 5.25 and 3.46 ppm and at 4.90 and 3.28 ppm for the H and OMe substituents attached to the 8-membered ring in *Z*- and *E*-**4b**, respectively. By integration of these signals a ratio of *syn:anti*-addition of approximately 3:1 was estimated. Both isomers could be separated by preparative TLC and completely characterized including single crystal X-ray crystallography.<sup>15</sup> To the best of our knowledge this is the first example for the successful separation of cyclopolysilane *Z/E* geometrical isomers.

### 2.3.4 X-ray Crystallography

Crystals suitable for single crystal X-ray structure determination could be obtained for **4a**, *Z*- and *E*-**4b** and **5a**. The obtained molecular structures are depicted in Figures 3 – 6, selected bond lengths, bond angles and dihedral angles of **4a** and **4b** are summarized in Table 1.



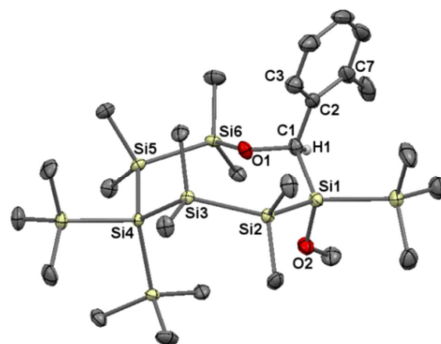


**Figure 3.** ORTEP diagram for compound **4a** (R,R-isomer). Thermal ellipsoids are depicted at the 50 % probability level. Hydrogen atoms are omitted for clarity.

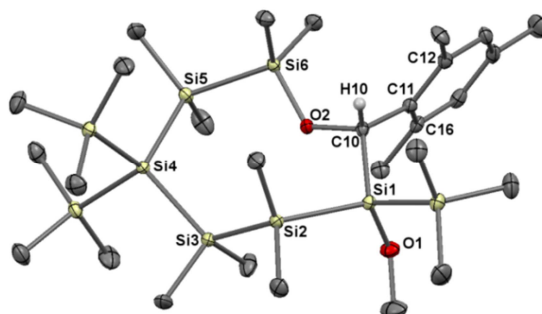


**Figure 4.** ORTEP diagram for compound **E-4b** (R,S-isomer). Thermal ellipsoids are depicted at the 50 % probability level. Hydrogen atoms are omitted for clarity.

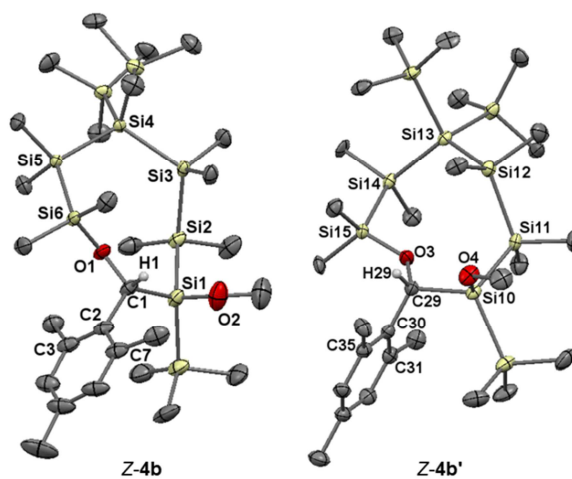


**Figure 5.** ORTEP diagram for compound **Z-4b** (R,R-isomer). The crystals contain two independent molecules (**Z-4b**, **Z-4b'**) in the asymmetric unit.<sup>16</sup> Thermal ellipsoids are depicted at the 50 % probability level. Hydrogen atoms are omitted for clarity.

**Table 1.** Endocyclic bond lengths  $d$  (Å), bond angles  $\alpha$  (deg) and selected torsional angles  $\theta$  (deg) for compounds **4a,b**

	<b>4a</b>	<b>E-4b</b>	<b>Z-4b</b>	<b>Z-4b'</b>
$d(\text{SiSi})$	2.345-2.363 (2.36 mean)	2.339-2.363 (2.35 mean)	2.340-2.373 (2.36 mean)	2.313-2.355 (2.34 mean)
$d(\text{CO})$	1.449(4)	1,458(3)	1.440(3)	1.448(3)
$d(\text{SiO})$	1.651(2)	1,666(1)	1.670(2)	1.638(4)
$d(\text{SiC})$	1.910(3)	1,918(2)	1.921(2)	1.928(2)
$\alpha(\text{SiSiSi})$	111.0-123.7 (117 mean)	112.4-119.5 (114 mean)	111.4-119.1 (115 mean)	110.7-120.1 (115 mean)
$\alpha(\text{SiSiO})$	104.6(1)	103.8(1)	101.8(1)	103.5(2)
$\alpha(\text{SiOC})$	121.9(2)	123.7(1)	123.6(1)	128.7(2)
$\alpha(\text{OCSi})$	104.6(2)	107.6(1)	109.0(1)	109.5(1)
$\alpha(\text{CSiSi})$	112.0(1)	104.0(2)	109.2(3)	109.6(4)
$\theta(\text{Si-C-C}_{\text{ar}}\text{-C}_{\text{ar}})$	-70.6(4)	77.3(2)	-84.6(3)	-83.2(2)
$\theta(\text{Si-C-C}_{\text{ar}}\text{-C}_{\text{ar}'})$	107.6(3)	-107.7(2)	92.4(2)	94.4(2)

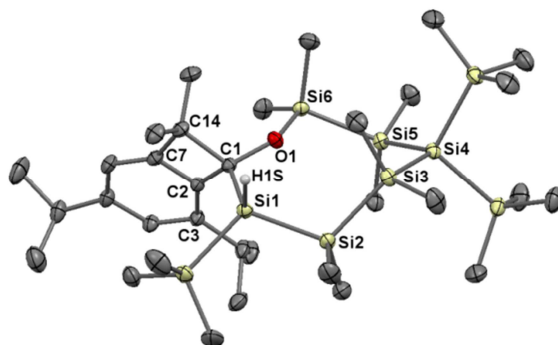


**Figure 6.** ORTEP diagram for compound **5a** (R,S-isomer). Thermal ellipsoids are depicted at the 50 % probability level. Hydrogen atoms are omitted for clarity. Selected bond lengths (Å) and bond and torsional angles (deg) with estimated standard deviations: Si-Si (mean) 2.357, Si(1)-C(1) 1.936(1), C(1)-O(1) 1.437(2), Si(6)-O(1) 1.658(1), C(1)-C(14) 1.635(2), C(14)-C(7) 1.516(2), C(7)-C(2) 1.382(1), C(2)-C(1) 1.526(2), Si(1)-Si(2)-Si(3) 113.35(2), Si(2)-Si(3)-Si(4) 120.31(2), Si(3)-Si(4)-Si(5) 111.80(2), Si(4)-Si(5)-Si(6) 114.10(2), Si(5)-Si(6)-O(1) 110.58(4), Si(6)-O(1)-C(1) 138.13(8), O(1)-C(1)-Si(1) 105.08(7), C(1)-Si(1)-Si(2) 116.89(4), C(14)-C(1)-C(2) 84.92(8), C(1)-C(2)-C(7) 94.50(9), C(2)-C(7)-C(14) 94.8(1), C(7)-C(14)-C(1) 85.36(9), Si(1)-C(1)-C(2)-C(3) -65.3(2), Si(1)-C(1)-C(2)-C(7) 108.95(9), C(1)-C(2)-C(7)-C(14) 5.5(1).

**4a**, **5a** and **E-4b** crystallize in the monoclinic space groups  $P2_1/n$  and  $Cc$ , respectively. **Z-4b** crystallizes in the orthorhombic space groups  $Pca2_1$  with two independent molecules in the asymmetric unit which comprise insignificantly different structural parameters. The eight membered heterocycles adopt puckered conformations with unexceptional Si-Si distances between 2.32 and 2.38 Å and slightly enlarged endocyclic Si-Si-Si angles of 110.7 – 123.7°. The Si-O distances measured between 1.64 – 1.67 Å are close to the average Si-O bond length of 1.63 Å in compounds containing a tetracoordinate Si bound to a dicoordinate O atom.<sup>[17]</sup> The geometry around the endocyclic Si atoms is approximately tetrahedral. In all structures the endocyclic oxygen atom is oriented towards the center of the ring in order to minimize steric congestion. In the structures of **Z-** and **E-4b** the bulky mesityl group at the endocyclic C atom occupies an equatorial position while the structure of **4a** exhibits the sterically less demanding o-tolyl substituent in an axial position. Also for steric reasons the plane of the aromatic rings are arranged roughly perpendicular with respect to the adjacent endocyclic Si-C bonds with torsion angles  $C_{aryl}-C_{aryl}-C-Si$  of 71 - 85°. A similar arrangement was observed for the benzocyclobutene moiety in **5a** ( $Si(1)-C(1)-C(2)-C(3) = -65.3^\circ$ ) which is approximately planar and contains a slightly distorted cyclobutene ring with a significantly elongated C(1)-C(14) bond of 1.63 Å. Two chiral centers are present in the 8-membered heterocycles **4a,b** and **5a**. In all structures the unit cells contain two enantiomeric pairs (*S,S*; *R,R* for **4a** and **Z-4b** and *R,S*; *S,R* for **E-4b** and **5a**). Interestingly the corresponding diastomeric species were not formed as indicated by the lack of a second set of NMR signals.

### 2.3.5 Conclusion

In conclusion, it has been found that the course of photochemically induced Brook type rearrangement reactions of acylcyclohexasilanes is significantly influenced by the nature of the substituent group attached to the carbonyl C atom. It has been demonstrated before, that alkyl substituted substrates, when irradiated with  $\lambda > 300$  nm radiation, afford photolytically labile mixtures of six- and eight membered cyclopolysilanes with exo- and endocyclic Si=C double bonds formed by two competing reaction mechanisms. In this study we were able to show, that bulky aryl substituted acylcyclohexasilanes, under the same conditions, exclusively undergo ring scission adjacent to the Si-C=O group followed by 1,3-Si→O migration of the resulting terminal SiMe<sub>2</sub> group to give the ring enlarged product with an endocyclic Si=C bond. Although the resulting endocyclic silenes could be isolated just in <95% purity because of their low tendency to crystallize they are photolytically remarkably stable when only one ortho-CH<sub>3</sub>- group is attached to the aromatic ring. In the presence of two ortho-methyl groups the primarily formed endocyclic silenes rearrange further by the photolytically induced C-H addition to the Si=C double bond under formation of substituted

spirobenzocyclobutenes. Follow-up studies with the primary aim to generalize the observed reactivity pattern and to isolate related species in a pure state are currently underway.

## 2.3.6 Experimental Section

### 2.3.6.1 General Considerations

All experiments were performed under a nitrogen atmosphere using standard Schlenk techniques. Solvents were dried using a column solvent purification system.<sup>18</sup> Commercial KO $t$ Bu (97 %) and acid chlorides CICOR were used as purchased. Et<sub>3</sub>N (99 %) was dried by distillation from solid KOH, commercial anhydrous MeOH was dried with 3Å molecular sieve. <sup>1</sup>H (299.95 MHz), <sup>13</sup>C (75.43 MHz) and <sup>29</sup>Si (59.59 MHz) NMR spectra were recorded on a Varian INOVA 300 spectrometer in C<sub>6</sub>D<sub>6</sub> or CDCl<sub>3</sub> solution and referenced versus TMS using the internal <sup>2</sup>H-lock signal of the solvent. (Me<sub>3</sub>Si)<sub>2</sub>Si<sub>6</sub>Me<sub>8</sub>(SiMe<sub>3</sub>)<sub>2</sub> and (Me<sub>3</sub>Si)<sub>2</sub>Si<sub>6</sub>Me<sub>8</sub>(SiMe<sub>3</sub>)K<sup>19</sup> were synthesized according to published procedures. HRMS spectra were run on a Kratos Profile mass spectrometer. Infrared spectra were obtained on a Bruker Alpha-P Diamond ATR Spectrometer from the solid sample. Melting points were determined using a Buechi 535 apparatus and are uncorrected. Elemental analyses were carried out on a Hanau Vario Elementar EL apparatus. Photolyses were performed by using a 500 W medium pressure mercury lamp (Original HANAU). Sample solutions were photolyzed under an atmosphere of nitrogen in Pyrex Schlenk tubes immersed in cold water to ensure ambient sample temperature and to prevent irradiation with light of wavelengths  $\lambda < 300$  nm. UV absorption spectra were recorded on a Perkin Elmer Lambda 5 spectrometer. Preparative TLC was performed on SIL G-200 UV<sub>254</sub> TLC plates from Macherey-Nagel with heptane (Chromasolv Plus for HPLC, 99%) as the eluent.

### Synthesis of 1-Acyloctamethyl-1,4,4-tris(trimethylsilyl)cyclohexasilanes (1a-f)

A solution of (Me<sub>3</sub>Si)<sub>2</sub>Si<sub>6</sub>Me<sub>8</sub>(SiMe<sub>3</sub>)K in 20 mL of DME was freshly prepared from 3.00 g (5.16 mmol) of (Me<sub>3</sub>Si)<sub>2</sub>Si<sub>6</sub>Me<sub>8</sub>(SiMe<sub>3</sub>)<sub>2</sub> and 0.64 g (5.67 mmol) of KO $t$ Bu and slowly added to a solution of 5.67 mmol of the respective acylchloride in 50 mL diethyl ether at -80°C. Subsequently the mixture was stirred for another 30 min at -80 °C, allowed to warm to room temperature and finally stirred for additional 60 minutes. After aqueous work up with 100 mL of 3 % sulphuric acid the organic layer was separated, dried over Na<sub>2</sub>SO<sub>4</sub> and the solvents were stripped off with a rotary evaporator. Drying in vacuo (0.02 mbar) and crystallization from acetone solution at -30°C afforded the analytically pure products **1a-f** as slightly yellow crystals.

**1a,d**: data consistent with literature<sup>12</sup>

**1b**: isolated yield: 45 %. mp: 123-124 °C. Anal. Found: C, 48.25; H, 9.26 %. Calc.: C, 48.68; H, 9.43 %. <sup>29</sup>Si-NMR (C<sub>6</sub>D<sub>6</sub>, TMS, ppm): -7.82, -8.59, -10.48 (SiMe<sub>3</sub>); -36.84, -38.11 (SiMe<sub>2</sub>); -67.24

(SiC=O); -131.48 (Si(SiMe<sub>3</sub>)<sub>2</sub>). <sup>13</sup>C-NMR (C<sub>6</sub>D<sub>6</sub>, TMS, ppm): 241.27 (C=O); 147.42, 138.05, 131.84, 131.19, 125.92, 124.53 (aryl-C); 19.72, 15.48 (aryl-CH<sub>3</sub>); 3.71, 3.67, 1.77 (Si(CH<sub>3</sub>)<sub>3</sub>); -0.98, -1.10, -2.36, -2.74 (Si(CH<sub>3</sub>)<sub>2</sub>). <sup>1</sup>H-NMR (C<sub>6</sub>D<sub>6</sub>, TMS, ppm): 7.35 (d, 1H, aryl-H); 7.01-6.87 (m, 2H, aryl-H); 2.23, 1.90 (s, 3H each, aryl-CH<sub>3</sub>); 0.48 (s, 6H, Si(CH<sub>3</sub>)<sub>2</sub>); 0.42 (s, 12H Si(CH<sub>3</sub>)<sub>2</sub>); 0.36 (s, 6H Si(CH<sub>3</sub>)<sub>2</sub>); 0.29 (s, 18H, Si(CH<sub>3</sub>)<sub>3</sub>); 0.20 (s, 9H, Si(CH<sub>3</sub>)<sub>3</sub>). IR (neat): ν(C=O) = 1616 (m) cm<sup>-1</sup>. HRMS: calc. for [C<sub>26</sub>H<sub>60</sub>OSi<sub>9</sub>]<sup>+</sup> (M<sup>+</sup>): 640.2568; found: 640.2614. UV-VIS: λ [nm] (ε [L mol<sup>-1</sup> cm<sup>-1</sup>]) = 257 (16500), 410 (210).

**1c:** isolated yield: 40 %. mp: 108-109 °C. Anal. Found: C, 48.89; H, 9.35 %. Calc.: C, 48.68; H, 9.43 %. <sup>29</sup>Si-NMR (CDCl<sub>3</sub>, TMS, ppm): -7.53, -8.72, -10.20 (SiMe<sub>3</sub>); -36.21, -37.69 (SiMe<sub>2</sub>); -66.71 (SiC=O); -131.39 (Si(SiMe<sub>3</sub>)<sub>2</sub>). <sup>13</sup>C-NMR (CDCl<sub>3</sub>, TMS, ppm): 240.46 (C=O); 143.00, 140.33, 134.26, 132.42, 130.48, 125.48 (aryl-C); 21.40, 20.19 (aryl-CH<sub>3</sub>); 3.92, 2.12 (Si(CH<sub>3</sub>)<sub>3</sub>); -0.92, -1.06, -2.20, -2.58 (Si(CH<sub>3</sub>)<sub>2</sub>). <sup>1</sup>H-NMR (C<sub>6</sub>D<sub>6</sub>, TMS, ppm): 7.61, 6.87, 6.68 (s, 1H each, aryl-H); 2.46, 1.97 (s, 3H each, aryl-CH<sub>3</sub>); 0.47 (s, 12H, Si(CH<sub>3</sub>)<sub>2</sub>); 0.44, 0.36 (s, 6H each, Si(CH<sub>3</sub>)<sub>2</sub>); 0.29, 0.28, 0.25 (s, 9H each, Si(CH<sub>3</sub>)<sub>3</sub>). IR (neat): ν(C=O) = 1602 (m) cm<sup>-1</sup>. HRMS: calc. for [C<sub>26</sub>H<sub>60</sub>OSi<sub>9</sub>]<sup>+</sup> (M<sup>+</sup>): 640.2568; found: 640.2574. UV-VIS: λ [nm] (ε [L mol<sup>-1</sup> cm<sup>-1</sup>]) = 263 (42000), 415 (170).

**1e:** isolated yield: 43 %. mp: 167-168 °C. Anal. Found: C, 48.13; H, 9.26 %. Calc.: C, 48.68; H, 9.43 %. <sup>29</sup>Si-NMR (C<sub>6</sub>D<sub>6</sub>, TMS, ppm): -8.22, -8.35, -12.48 (SiMe<sub>3</sub>); -37.56, -38.42 (SiMe<sub>2</sub>); -71.23 (SiC=O); -131.67 (Si(SiMe<sub>3</sub>)<sub>2</sub>). <sup>13</sup>C-NMR (C<sub>6</sub>D<sub>6</sub>, TMS, ppm): 245.95 (C=O); 149.58, 131.29, 128.00 (aryl-C); 19.85 (aryl-CH<sub>3</sub>); 3.68, 3.63, 1.38 (Si(CH<sub>3</sub>)<sub>3</sub>); -0.83, -1.14, -2.01, -2.54 (Si(CH<sub>3</sub>)<sub>2</sub>). <sup>1</sup>H-NMR (C<sub>6</sub>D<sub>6</sub>, TMS, ppm): 6.90 (t, 1H, aryl-H), 6.72 (d, 2H, aryl-H), 2.16 (s, 6H, aryl-CH<sub>3</sub>), 0.55, 0.42, 0.36, 0.35 (s, 6H each, Si(CH<sub>3</sub>)<sub>2</sub>), 0.34, 0.29, 0.05 (s, 9H each, Si(CH<sub>3</sub>)<sub>3</sub>). IR (neat): ν(C=O) = 1613 (m) cm<sup>-1</sup>. HRMS: calc. for [C<sub>26</sub>H<sub>60</sub>OSi<sub>9</sub>]<sup>+</sup> (M<sup>+</sup>): 640.2568; found: 640.2586. UV-VIS: λ [nm] (ε [L mol<sup>-1</sup> cm<sup>-1</sup>]) = 255 (14100), 377 (120), 393 (180), 411 (145).

**1f:** isolated yield: 8 %.<sup>[20]</sup> mp: 168-170 °C. Anal. Found: C, 49.91; H, 9.85 %. Calc.: C, 50.07; H, 9.91 %. <sup>29</sup>Si-NMR (C<sub>6</sub>D<sub>6</sub>, TMS, ppm): -8.14, -8.25, -13.16 (SiMe<sub>3</sub>); -37.02, -37.90 (SiMe<sub>2</sub>); -70.79 (SiC=O); -131.78 (Si(SiMe<sub>3</sub>)<sub>2</sub>). <sup>13</sup>C-NMR (C<sub>6</sub>D<sub>6</sub>, TMS, ppm): 246.25 (C=O); 149.09, 146.19, 142.73, 120.20 (aryl-C); 34.37, 29.73, 26.84, 23.94, 21.08 (aryl-CH(CH<sub>3</sub>)<sub>2</sub>); 3.75, 3.68, 1.51 (Si(CH<sub>3</sub>)<sub>3</sub>); -0.74, -1.09, -2.20, -3.00 (Si(CH<sub>3</sub>)<sub>2</sub>). <sup>1</sup>H-NMR (C<sub>6</sub>D<sub>6</sub>, TMS, ppm): 7.03 (s, 2 H, aryl-H); 2.95 (2H, sept, o-CH(CH<sub>3</sub>)<sub>2</sub>); 2.75 (1H, s, sept, p-CH(CH<sub>3</sub>)<sub>2</sub>); 1.35 (d, 6H, p-CH(CH<sub>3</sub>)<sub>2</sub>); 1.19 (d, 6H, o-CH(CH<sub>3</sub>)<sub>2</sub>); 1.17 (d, 6H, o-CH(CH<sub>3</sub>)<sub>2</sub>); 0.55, 0.43, 0.37, 0.36 (s, 6H each, Si(CH<sub>3</sub>)<sub>2</sub>); 0.59, 0.47 (s, 6H each, Si(CH<sub>3</sub>)<sub>2</sub>); 0.38 (s, 12H Si(CH<sub>3</sub>)<sub>2</sub>); 0.37, 0.31, -0.03 (s, 9H each, Si(CH<sub>3</sub>)<sub>3</sub>). IR (neat): ν(C=O) = 1605 (m) cm<sup>-1</sup>. HRMS: calc. for [C<sub>33</sub>H<sub>74</sub>OSi<sub>9</sub>]<sup>+</sup> (M<sup>+</sup>): 738,3663; found: 738,3680. UV-VIS: λ [nm] (ε [L mol<sup>-1</sup> cm<sup>-1</sup>]) = 250 (17100), 375 (140), 391 (180), 407 (150).

### Photolysis of 1a-c in C<sub>6</sub>D<sub>6</sub>

A solution of 0.10 mmol of acylcyclohexasilane in 0.6 mL of d<sub>6</sub>-benzene in an NMR tube was photolyzed with a 600 W mercury lamp at 25 °C for 30 min. At this time NMR analysis of the resulting yellow solution showed that the starting material had been consumed completely and that the endocyclic silenes had been formed along with minor amounts of by-products of unknown composition. Removal of the volatile components in vacuo afforded yellow oils. Attempts to isolate the products by crystallization diethyl ether, pentane, diisopropyl ether or toluene did not result in the formation of crystalline material.

**3a:**  $^{29}\text{Si}$ -NMR ( $\text{C}_6\text{D}_6$ , TMS, ppm): 48.60 (Si=C); 18.01 (OSiMe<sub>2</sub>); -8.59, -11.24 (SiMe<sub>3</sub>); -33.67, -34.09, -40.38 (SiMe<sub>2</sub>); -130.22 (Si(SiMe<sub>3</sub>)<sub>2</sub>).  $^{13}\text{C}$ -NMR ( $\text{C}_6\text{D}_6$ , TMS, ppm): 200.51 (C=Si); 145.02, 136.13, 130.74, 129.77, 124.71 (aryl-C); 20.13 (aryl-CH<sub>3</sub>); 3.45, 1.61 (Si(CH<sub>3</sub>)<sub>3</sub>); 0.43, 0.09, -0.45, -1.38, -1.42 (Si(CH<sub>3</sub>)<sub>2</sub>).  $^1\text{H}$ -NMR ( $\text{C}_6\text{D}_6$ , TMS, ppm): 7.32 (d, 1H, aryl-H); 7.05-6.90 (m, 3H, aryl-H); 2.44 (s, 3H, aryl-CH<sub>3</sub>); 0,51-0.00 (several overlapping signals, Si(CH<sub>3</sub>)<sub>n</sub>).

**3b:**  $^{29}\text{Si}$ -NMR ( $\text{C}_6\text{D}_6$ , TMS, ppm): 47.38 (Si=C); 17.71 (OSiMe<sub>2</sub>); -8.59, -11.33 (SiMe<sub>3</sub>); -33.61, -34.15, -40.27 (SiMe<sub>2</sub>); -130.13 (Si(SiMe<sub>3</sub>)<sub>2</sub>).  $^{13}\text{C}$ -NMR ( $\text{C}_6\text{D}_6$ , TMS, ppm): 201.26 (C=Si); 145.11, 136.34, 134.53, 129.59, 129.18, 124.30 (aryl-C); 19.94, 16.78 (aryl-CH<sub>3</sub>); 3.45, 1.63 (Si(CH<sub>3</sub>)<sub>3</sub>); 0.14, -0.42, -1.38, -1.56 (Si(CH<sub>3</sub>)<sub>2</sub>).  $^1\text{H}$ -NMR ( $\text{C}_6\text{D}_6$ , TMS, ppm): 7.25 (d, 1H, aryl-H); 6.95-6.85 (m, 2H, aryl-H); 2.37, 2.05 (s, 3H each, aryl-CH<sub>3</sub>); 0,50-0.00 (several overlapping signals, Si(CH<sub>3</sub>)<sub>n</sub>).

**3c:**  $^{29}\text{Si}$ -NMR ( $\text{C}_6\text{D}_6$ , TMS, ppm): 47.38 (Si=C); 17.68 (OSiMe<sub>2</sub>); -8.59, -11.29 (SiMe<sub>3</sub>); -33.72, -34.16, -40.38 (SiMe<sub>2</sub>); -130.18 (Si(SiMe<sub>3</sub>)<sub>2</sub>).  $^{13}\text{C}$ -NMR ( $\text{C}_6\text{D}_6$ , TMS, ppm): 200.97 (C=Si); 142.36, 137.45, 135.96, 130.88, 130.71, 125.27 (aryl-C); 20.83, 20.10 (aryl-CH<sub>3</sub>); 3.44, 1.68 (Si(CH<sub>3</sub>)<sub>3</sub>); 0.50, 0.15, -0.42, -1.37, -1.57 (Si(CH<sub>3</sub>)<sub>2</sub>).  $^1\text{H}$ -NMR ( $\text{C}_6\text{D}_6$ , TMS, ppm): 7.26 (d, 1H, aryl-H); 6.85-6.75 (m, 2H, aryl-H); 2.45, 2.07 (s, 3H each, aryl-CH<sub>3</sub>); 0,53-0.04 (several overlapping signals, Si(CH<sub>3</sub>)<sub>n</sub>).

### Photolysis of **1a** in $\text{C}_6\text{D}_6/\text{MeOH}$

A solution of 0.50 g (0.80 mmol) of **1a** and 3 drops of anhydrous Et<sub>3</sub>N in 5 mL of benzene and 2 mL of methanol was photolyzed with a 600 W mercury lamp through Pyrex glass at 25 °C for 60 min. At this time NMR analysis showed that the starting material had been consumed completely. After removal of the volatile components on a rotary evaporator 20 mL of pentane were added and the resulting solution was filtered over silica gel. Evaporation of pentane and crystallization of the crude product from acetone at -30 °C afforded 0.44 g (84 %) of pure and crystalline **4a**.

**4a:** mp: 123-124 °C. Anal. Found: C, 46.93; H, 9.19 %. Calc.: C, 47.35; H, 9.48 %.  $^{29}\text{Si}$ -NMR ( $\text{CDCl}_3$ , TMS, ppm): 20.71, 18.36 (OSi); -7.77, -8.80, -18.89 (SiMe<sub>3</sub>); -33.47, -39.86, -43.20 (SiMe<sub>2</sub>); -130.37 (Si(SiMe<sub>3</sub>)<sub>2</sub>).  $^{13}\text{C}$ -NMR ( $\text{CDCl}_3$ , TMS, ppm): 143.54, 132.65, 129.87, 126.55, 125.60, 125.32 (aryl-C6); 68.35 (SiCHO); 53.83 (OCH<sub>3</sub>); 19.83 (aryl-CH<sub>3</sub>); 3.77, 3.72, 0.56 (Si(CH<sub>3</sub>)<sub>3</sub>); 1.50, 0.19, 0.10, -0.49, -0.83, -1.48, -2.10, -3.57 (Si(CH<sub>3</sub>)<sub>2</sub>).  $^1\text{H}$ -NMR ( $\text{CDCl}_3$ , TMS, ppm): 7.35 (1H, d, aryl-H); 7.16-6.98 (3H, m, aryl-H); 5.12 (1H, s, SiCHO); 3.28 (3H, s, OCH<sub>3</sub>); 2.31 (3H, s, aryl-CH<sub>3</sub>); 0.47, 0.37, 0.35, 0.30, 0.28, 0.26, 0.11, -0.01 (3H each, 8 s, Si(CH<sub>3</sub>)<sub>2</sub>); 0.28, 0.27, -0.04 (9H each, s, Si(CH<sub>3</sub>)<sub>3</sub>). HRMS: calc. for [C<sub>26</sub>H<sub>6</sub>O<sub>2</sub>Si<sub>9</sub>]<sup>+</sup> (M<sup>+</sup>): 658.2673; found: 658.2659.

### Photolysis of **1d,e** in $\text{C}_6\text{D}_6$

The procedure followed was that used for the photolysis of **1a-c**. After an irradiation time of 30 min  $^1\text{H}$ - and  $^{29}\text{Si}$ -NMR analysis showed the formation of the silenes **3d,e** along with unreacted starting material. A silene:acylsilane ratio of approximately 1:3 in the resulting yellow solutions was estimated by integration of the CH<sub>3</sub> resonances of the aryl-CH<sub>3</sub>- groups in the  $^1\text{H}$  NMR spectrum. After irradiation for another 40 min the solutions contained **1d,e** and **3d,e**, respectively, in a ratio of 1:1.5 along with considerable amounts of further photolysis products as indicated by the appearance of additional NMR signals. Isolation of individual products by crystallization failed.

**3d**:  $^{29}\text{Si}$ -NMR ( $\text{C}_6\text{D}_6$ , TMS, ppm): 41.82 ( $\text{Si}=\text{C}$ ); 13.76 ( $\text{OSiMe}_2$ ); -8.67, -12.07 ( $\text{SiMe}_3$ ); -33.19, -33.57, -40.04 ( $\text{SiMe}_2$ ); -129.33 ( $\text{Si}(\text{SiMe}_3)_2$ ).  $^{13}\text{C}$ -NMR ( $\text{C}_6\text{D}_6$ , TMS, ppm): 196.08 ( $\text{C}=\text{Si}$ ); 136.78, 136.35, 128.26 (aryl- $\text{C}$ ); 21.29, 20.84 (aryl- $\text{CH}_3$ ); 3.42, 1.10, 0.92, 0.13, -1.01, -1.67 ( $\text{Si}(\text{CH}_3)_n$ ).  $^1\text{H}$ -NMR ( $\text{C}_6\text{D}_6$ , TMS, ppm): 6.74 (s, 2H, aryl- $\text{H}$ ); 2.51 (s, 6H, aryl- $\text{CH}_3$ ); 2.06 (s, 3H, aryl- $\text{CH}_3$ ); 0.55-0.00 (several overlapping signals,  $\text{Si}(\text{CH}_3)_n$ ).

**3e**:  $^{29}\text{Si}$ -NMR ( $\text{C}_6\text{D}_6$ , TMS, ppm): 42.13 ( $\text{Si}=\text{C}$ ); 14.13 ( $\text{OSiMe}_2$ ); -8.67, -12.48 ( $\text{SiMe}_3$ ); -33.08, -33.52, -40.07 ( $\text{SiMe}_2$ ); -129.39 ( $\text{Si}(\text{SiMe}_3)_2$ ).  $^{13}\text{C}$ -NMR ( $\text{C}_6\text{D}_6$ , TMS, ppm): 195.54 ( $\text{C}=\text{Si}$ ); 149.58, 136.52, 131.29, 127.46 (aryl- $\text{C}$ ); 21.34 (aryl- $\text{CH}_3$ ); 3.41, 1.03, 0.86, -0.15, -1.05, -1.70 ( $\text{Si}(\text{CH}_3)_n$ ).  $^1\text{H}$ -NMR ( $\text{C}_6\text{D}_6$ , TMS, ppm): 6.91 (m, 1H, aryl- $\text{H}$ ); 6.72 (d, 2H, aryl- $\text{H}$ ); 2.52 (s, 6H, aryl- $\text{CH}_3$ ); 0.54 - -0.02 (several overlapping signals,  $\text{Si}(\text{CH}_3)_n$ ).

### Photolysis of **1f** in $\text{C}_6\text{D}_6$

The procedure followed was that used for the photolysis of **1a** with 15 mg (0.02 mmol) of **1f** in 0.6 mL  $\text{C}_6\text{D}_6$  and an irradiation time of 30 min. Filtration of the reaction solution over silica gel, removal of the volatile components in vacuo and crystallization of the crude product from acetone at  $-30^\circ\text{C}$  afforded 11 mg (75 %) of pure and crystalline **5a**.

**5a**: mp:  $162 - 164^\circ\text{C}$ . Anal. Found: C, 54.21; H, 10.12 %. Calc.: C, 53.58; H, 10.08 %.  $^{29}\text{Si}$ -NMR ( $\text{CDCl}_3$ , TMS, ppm): 10.42 ( $\text{OSiMe}_2$ ); -8.30, -8.73, -15.46 ( $\text{SiMe}_3$ ); -33.46, -36.77, -43.52 ( $\text{SiMe}_2$ ); -131.33 ( $\text{Si}(\text{SiMe}_3)_2$ ).  $^{13}\text{C}$ -NMR ( $\text{CDCl}_3$ , TMS, ppm): 150.50, 149.48, 143.68, 143.06, 122.21, 115.67 (aryl- $\text{C}$ ); 54.06 ( $\text{SiHCO}$ ); 34.95, 28.75, 27.77, 26.43, 26.17, 24.50, 24.29, 23.32 (iPr- $\text{C}$ ); 4.03, 3.80, 0.72 ( $\text{Si}(\text{CH}_3)_3$ ); 5.81, 1.03, 0.20, -0.26, -0.82, -1.59, -1.74, -2.97 ( $\text{Si}(\text{CH}_3)_2$ ).  $^1\text{H}$ -NMR ( $\text{CDCl}_3$ , TMS, ppm): 6.87, 6.69 (1H, s, aryl- $\text{H}$ ); 3.72 (1H, s,  $\text{SiH}$ ); 3.01, 2.82 (1H each, m,  $\text{CH}(\text{CH}_3)_2$ ); 1.38, 1.37, 1.32, 1.29, 1.24, 1.21, 1.18, 1.17 (18 H, s,  $\text{C}(\text{CH}_3)_2$ ); 0.47, 0.46, 0.39, 0.29, 0.27, 0.26, 0.16, 0.14, -0.05, -0.25 (51H, s,  $\text{Si}(\text{CH}_3)$ ). IR (neat):  $\nu(\text{Si-H}) = 2063$  (m)  $\text{cm}^{-1}$ . HRMS: calc. for  $[\text{C}_{33}\text{H}_{74}\text{OSi}_9]^+$  ( $\text{M}^+$ ): 738.3663; found: 738.3708.

### Photolysis of **1d** in $\text{C}_6\text{D}_6/\text{MeOH}$

The procedure followed was that used for the photolysis of **1a**. After an irradiation time of 90 min a mixture of the E- and the Z-isomer of **4b** in a ratio of 1:3 was obtained. After work up as described above separation of the isomers was achieved by repeated preparative TLC over silica gel plates with heptane as the eluent to give 300.0 mg (57 %) of Z-**4b** and 70.0 mg (13 %) of E-**4b**.

Z-**4b**: mp:  $150 - 154^\circ\text{C}$ . Anal. Found: C, 49.23; H, 9.99 %. Calc.: C, 48.91; H, 9.67 %.  $^{29}\text{Si}$ -NMR ( $\text{CDCl}_3$ , TMS, ppm): 31.79, 17.07 ( $\text{OSi}$ ); -8.31, -8.74, -18.15 ( $\text{SiMe}_3$ ); -32.57, -39.82, -42.69 ( $\text{SiMe}_2$ ); -129.24 ( $\text{Si}(\text{SiMe}_3)_2$ ).  $^{13}\text{C}$ -NMR ( $\text{CDCl}_3$ , TMS, ppm): 137.92, 136.76, 135.15, 132.98, 129.87, 128.78 (aryl- $\text{C}$ ), 70.18 ( $\text{SiCHO}$ ), 53.79 ( $\text{OCH}_3$ ); 23.90, 20.81, 20.79 (aryl- $\text{CH}_3$ ); 3.59, 3.56, 0.12 ( $\text{Si}(\text{CH}_3)_3$ ); 0.66, 0.29, 0.04, -0.71, -1.67, -1.68, -1.83, -2.87 ( $\text{Si}(\text{CH}_3)_2$ ).  $^1\text{H}$ -NMR ( $\text{CDCl}_3$ , TMS, ppm): 6.73 (2H, s, aryl- $\text{H}$ ); 5.25 (1H, s,  $\text{OCHSi}$ ); 3.46 (3H, s,  $\text{OCH}_3$ ); 2.32, 2.25, 2.23 (3H each, s, aryl- $\text{CH}_3$ ); 0.45, 0.34, 0.33, 0.21, -0.19 (3H each, s,  $\text{Si}(\text{CH}_3)_2$ ); 0.30 (6H, s,  $\text{Si}(\text{CH}_3)_2$ ); 0.28, -0.18 (9H each, s,  $\text{Si}(\text{CH}_3)_3$ ); 0.26 (12H, s,  $\text{Si}(\text{CH}_3)_3 + \text{Si}(\text{CH}_3)_2$ ). HRMS: calc. for  $[\text{C}_{28}\text{H}_{66}\text{O}_2\text{Si}_9]^+$  ( $\text{M}^+$ ): 671.2751; found: 671.2748.

E-**4b**: mp:  $145 - 147^\circ\text{C}$ . Anal. Found: C, 48.10; H, 10.12 %. Calc.: C, 48.91; H, 9.67 %.  $^{29}\text{Si}$ -NMR ( $\text{CDCl}_3$ , TMS, ppm): 19.96, 17.22 ( $\text{OSi}$ ); -7.60, -9.45, -19.96 ( $\text{SiMe}_3$ ); -31.97, -40.71, -42.74 ( $\text{SiMe}_2$ ); -129.91 ( $\text{Si}(\text{SiMe}_3)_2$ ).  $^{13}\text{C}$ -NMR ( $\text{CDCl}_3$ , TMS, ppm): 138.77, 136.72, 135.24, 132.48,

130.67, 128.75 (aryl-C), 70.73 (SiCHO), 54.30 (OCH<sub>3</sub>); 21.76, 21.62, 20.80 (aryl-CH<sub>3</sub>); 3.76, 3.69, 0.31 (Si(CH<sub>3</sub>)<sub>3</sub>); 0.76, 0.46, -0.63, -1.45, -1.60, -2.26, -3.08 (Si(CH<sub>3</sub>)<sub>2</sub>). <sup>1</sup>H-NMR (CDCl<sub>3</sub>, TMS, ppm): 6.75, 6.71 (1H each, s, aryl-H); 4.90 (1H, s, OCHSi); 3.28 (3H, s, OCH<sub>3</sub>); 2.52, 2.28, 2.22 (3H each, s, aryl-CH<sub>3</sub>); 0.49, 0.34, 0.33, 0.30, 0.28, 0.23, 0.11, -0.17 (3H each, s, Si(CH<sub>3</sub>)<sub>2</sub>); 0.30 (6H, s, Si(CH<sub>3</sub>)<sub>2</sub>); 0.27, 0.25, 0.02 (9H each, s, Si(CH<sub>3</sub>)<sub>3</sub>). HRMS: calc. for [C<sub>28</sub>H<sub>66</sub>O<sub>2</sub>Si<sub>9</sub>]<sup>+</sup> (M<sup>+</sup>): 671.2751; found: 671.2754.

### X-ray Crystallography

For X-ray structure analysis suitable crystals were mounted onto the tip of glass fibres using mineral oil. Data collection was performed on a Bruker Kappa Apex II CCD diffractometer at 100 K using graphite-monochromated Mo K $\alpha$  ( $\lambda = 0.71073\text{\AA}$ ) radiation. The SHELX version 6.1 program package was used for the structure solution and refinement.<sup>21</sup> Absorption corrections were applied using the SADABS program.<sup>22</sup> All non-hydrogen atoms were refined with anisotropic displacement parameters. Hydrogen atoms were included in the refinement at calculated positions using a riding model as implemented in the SHELXTL program. In the solid state structure of **Z-4b** parts of one of the independent molecules were found disordered over two positions and were accordingly implemented in the structural model. The ratios of occupancy refined to 0.57 : 0.43. All non-hydrogen atoms of the disordered parts were refined anisotropically and hydrogen atoms were placed using standard AFIX commands. CCDC-1035781 (**4a**), CCDC-1035782 (**E-4b**), CCDC-1035783 (**Z-4b**) and CCDC-1035780 (**5a**) contain the supplementary crystallographic data for this paper. These data can be obtained free of charge from The Cambridge Crystallographic Data Centre via [www.ccdc.cam.ac.uk/data\\_request/cif](http://www.ccdc.cam.ac.uk/data_request/cif).

### 2.3.7 References

- 1 A. G. Brook, S. C. Nyburg, F. Abdesaken, B. Gutekunst, G. Gutekunst, R. K. Kallury, Y. C. Poon, Y. M. Chang, W. Wong-Ng, *J. Am. Chem. Soc.* 104 (1982) 5667
- 2 N. Wiberg, G. Wagner, G. Müller, J. Reids, *Angew. Chem., Int. Ed. Engl.* 22 (1984) 381
- 3 a) Y. Apeloig, M. Bendikov, M. Yuzevovich, M. Nakash, D. Bravo-Zhivotovskii, D. Blaser, R. Boese, *J. Am. Chem. Soc.* 118 (1996) 12228; b) K. Sakamoto, J. Ogasawara, Y. Kon, T. Sunagawa, C. Kabuto, M. Kira, *Angew. Chem. Int. Ed.* 41 (2002) 1402
- 4 J. Ohshita, Y. Masaoka, S. Masaoka, M. Hasebe, M. Ishikawa, A. Tachibana, T. Yano, T. Yamabe, *Organometallics* 15 (1996) 3136
- 5 a) S. Spirk, F. Belaj, J. H. Albering, R. Pietschnig, *Organometallics* 29 (2010) 2981; b) G. E. Miracle, J. L. Ball, D. R. Powell, R. West, *J. Am. Chem. Soc.* 115 (1993) 11598
- 6 a) N. Tokitoh, A. Shinohara, T. Matsumoto, T. Sasamori, N. Takeda, Y. Furukawa, *Organometallics* 26 (2007) 4048; b) N. Takeda, A. Shinohara, N. Tokitoh, *Organometallics* 21 (2002) 256; c) N. Takeda, A. Shinohara, N. Tokitoh, *Organometallics* 21 (2002) 4024; d) K. Wakita, N. Tokitoh, R. Okazaki, S. Nagase, *Angew. Chem., Int. Ed.* 39 (2000) 634; e) K. Wakita, N. Tokitoh, R. Okazaki, S. Nagase, P. von Schleyer, H. Jiao, *J. Am. Chem. Soc.* 121 (1999) 11336; f) Tokitoh, N. K. Wakita, R. Okazaki, S. Nagase, P. von Schleyer, H. Jiao, *J. Am. Chem. Soc.* 119 (1997) 6951



- 7 a) D. Bravo-Zhivotovskii, R. Dobrovetsky, D. Nemirovsky, V. Molev, M. Bendikov, G. Molev, M. Botoshansky, Y. Apeloig, *Angew. Chem. Int. Ed.* 47 (2008) 4343; b) S. Inoue, M. Ichinohe, A. Sekiguchi, *Angew. Chem. Int. Ed.* 46 (2007) 3346; c) T. Guliashvili, I. El-Sayed, A. Fischer, H. Ottosson, *Angew. Chem. Int. Ed.* 42 (2003) 1640
- 8 a) T. Iwamoto, N. Ohnishi, N. Akasaka, K. Ohno, S. Ishida, *J. Am. Chem. Soc.* 135 (2013) 10606; b) M. Majumdar, V. Huch, I. Bejan, A. Meltzer, D. Scheschkewitz *Angew. Chem. Int. Ed.* 52 (2013) 3516
- 9 For general reviews about silenes, see e.g.: a) H. Ottosson, J. Ohshita in *Science of Synthesis: Knowledge Updates 2011/3* (Ed.: M. Oestreich), Thieme, Stuttgart, (2011), pp. 47-55; b) H. Ottosson, A. M. Eklöf, *Coord. Chem. Rev.* 252 (2008) 1287.; c) H. Ottosson, P. G. Steel, *Chem. Eur. J.* 12 (2006) 1576; d) L. E. Gusel'nikov, *Coord. Chem. Rev.* 244 (2003) 149; e) R. West, *Polyhedron* 21 (2001) 467; f) T. L. Morkin, W. J. Leigh, *Acc. Chem. Res.* 34 (2001) 129; g) T. Müller, W. Ziche, N. Auner in *The Chemistry of Organic Silicon Compounds, Vol. 2* (Eds.: Z. Rappoport, Y. Apeloig), JohnWiley&Sons Ltd., New York, (1998), pp. 857-1062; h) A. G. Brook, M. A. Brook, *Adv. Organomet. Chem.* 39 (1996) 71
- 10 a) M. Kira, S. Ishida, T. Iwamoto, C. Kabuto, *J. Am. Chem. Soc.* 121 (1999) 9722; b) I. Bejan, D. Güclü, S. Inoue, M. Ichinohe, A. Sekiguchi, D. Scheschkewitz, *Angew. Chem. Int. Ed.* 46 (2007) 3349; c) I. Bejan, S. Inoue, M. Ichinohe, A. Sekiguchi, D. Scheschkewitz, *Chem. Eur. J.* 14 (2008) 7119; d) M. Igarashi, M. Ichinohe, A. Sekiguchi, *J. Am. Chem. Soc.* 129 (2007) 12660; e) J. S. Han, T. Sasamori, Y. Mizuhata, N. Tokitoh *Dalton Trans.*, 39 (2010) 9238; f) R. Kinjo, M. Ichinohe, A. Sekiguchi, N. Takagi, M. Sumimoto, S. Nagase, *J. Am. Chem. Soc.* 129 (2007) 7766
- 11 H. Stueger, B. Hasken, M. Haas, M. Rausch, R. Fischer, A. Torvisco, *Organometallics* 33 (2014) 231
- 12 M. Haas, R. Fischer, M. Flock, S. Mueller, M. Rausch, R. Saf, A. Torvisco, H. Stueger, *Organometallics* 33 (2014) 5956
- 13 in the absence of base C-O or Si-O bond cleavage reactions of the initially formed trapping products occur which are catalyzed by acidic by-products of the photolysis reaction: J. M. Duff, A. G. Brook, *Can. J. Chem.* 51 (1973) 2869
- 14 a) K. M. Baines, A. G. Brook, R. R. Ford, P. D. Lickiss, A. K. Saxena, W. J. Chatterton, J. F. Sawyer, B. A. Behnam, *Organometallics* 8 (1989) 693. b) A. G. Brook, H.-J. Wessely, *Organometallics* 4 (1985) 1487
- 15 analytical data are summarized in the experimental section
- 16 Only the major contributions for the disordered SiMe<sub>3</sub> and SiMe<sub>2</sub> groups in the structure of **Z-4b'** are shown
- 17 M. Kaftory, M. Kapon, M. Botoshansky in *The Chemistry of Organic Silicon Compounds, Vol. 2* (Eds.: Z. Rappoport, Y. Apeloig), JohnWiley&Sons Ltd., New York, (1998), pp. 218-219
- 18 A. B. Pangborn, M. A. Giardello, R. H. Grubbs, R. K. Rosen, F. J. Timmers, *Organometallics* 15 (1996) 1518
- 19 R. Fischer, T. Konopa, S. Ully, J. Baumgartner, C. Marschner, *J. Organomet. Chem.* 685 (2003) 79
- 20 after column chromatography over silica gel with a gradient elution mode (heptane, toluene)
- 21 SHELX and SHELXL PC: VERSION 5.03, Bruker AXS, Inc., Madison, WI, (1994)
- 22 SADABS: Area-detection Absorption Correction: Bruker AXS Inc., Madison, WI, (1995)

## 2.4 Stable Silenolates and Brook-Type Silenes with Exocyclic Structures

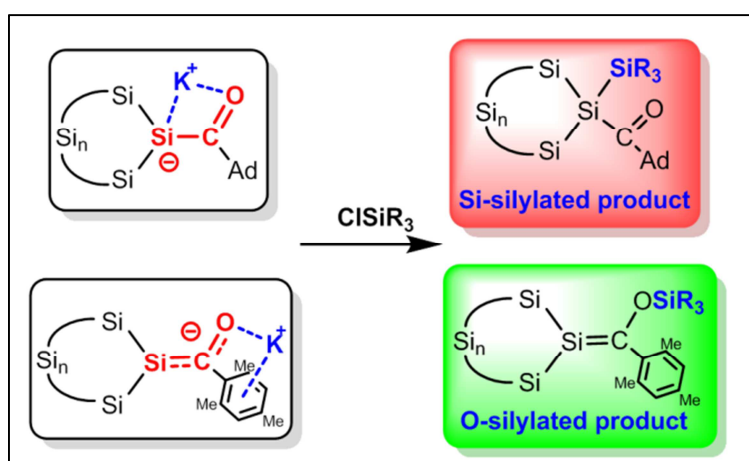
Michael Haas,<sup>[a]</sup> Roland Fischer,<sup>[a]</sup> Michaela Flock,<sup>[a]</sup> Stefan Mueller,<sup>[a]</sup> Martin Rausch,<sup>[a]</sup> Robert Saf,<sup>[b]</sup>  
Ana Torvisco<sup>[a]</sup> and Harald Stueger\*<sup>[a]</sup>

<sup>[a]</sup> Institute of Inorganic Chemistry, Graz University of Technology, Stremayrgasse 9, A-8010 Graz,  
Austria

<sup>[b]</sup> Institute for Chemistry and Technology of Materials, Graz University of Technology,  
Stremayrgasse 9, A-8010 Graz, Austria

published in *Organometallics*, 33 (2014) 5956

graphical abstract:



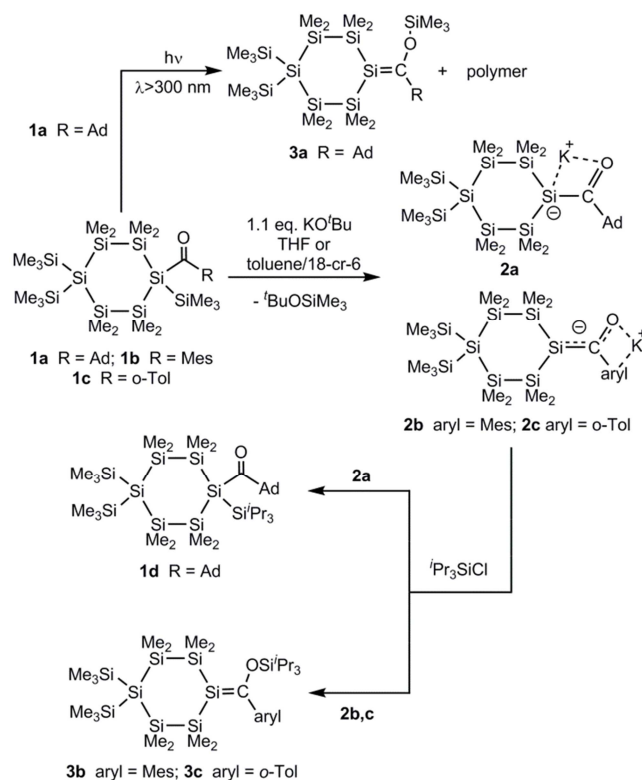
### 2.4.1 Abstract

The first silenolates with exocyclic structures  $[(\text{Me}_3\text{Si})_2\text{Si}(\text{Si}_2\text{Me}_4)_2\text{SiC}(\text{R})\text{O}]^-\text{K}^+$  (**2a**: R = 1-adamantyl; **2b**: mesityl; **2c**: o-tolyl) were synthesized by the reaction of the corresponding acylcyclohexasilanes **1a-c** with  $\text{KO}t\text{Bu}$ . NMR spectroscopy and single-crystal X-ray diffraction analysis suggest that the aryl substituted silenolates **2b,c** exhibit increased character of functionalized silenes as compared to the alkyl substituted derivative **2a** due to the different coordination of the  $\text{K}^+$  counter-ion to the  $\text{SiC}(\text{R})\text{O}$  moiety. **2b,c**, thus, reacted with  $\text{ClSiPr}_3$  to give the exocyclic silenes  $(\text{Me}_3\text{Si})_2\text{Si}(\text{Si}_2\text{Me}_4)_2\text{Si}=\text{C}(\text{OSiPr}_3)\text{R}$  (**3b**: R = Mes; **3c**: o-Tol) while **2a** afforded the Si-silylated acylcyclohexasilane **1d**. The thermally remarkably stable compound **3b** which is the first isolated silene with the  $\text{sp}^2$  silicon atom incorporated into a cyclopolysilane framework, could be fully characterized structurally and spectroscopically.

## 2.4.2 Introduction

There is no doubt about the central role of alkenes and metal enolates  $[(R_2CC(R)O)]M^+$  in organic chemistry which has led to thorough understanding of chemical and physical properties and numerous applications of such compounds. In contrast, much less is known about the analogous silenes ( $R_2Si=CR_2$ ) and silenolates  $[(R_2SiC(R)O)]M^+$  which were long considered unstable and only existent as reactive intermediates.<sup>1,2</sup> The first stable silene ( $Me_3Si)_2Si=C(OSiMe_3)Ad$  has been isolated by Brook in 1981 after the photolysis of the acylpolysilane  $(Me_3Si)_3SiC(Ad)=O$ .<sup>3</sup> Since then a relatively large number of stable silenes with various substitution patterns has been synthesized by several alternative preparative approaches.<sup>1</sup> Studies on metal silenolates are less abundant in the literature and only three isolable species have been prepared and structurally characterized so far by Ottosson et al.<sup>2i</sup> and by the group of Bravo-Zhivotovskii and Apeloig.<sup>2j</sup> Valuable contributions to the field also have been made by Oshita, Ishikawa and co-workers who synthesized and characterized Li silenolates  $\{(Me_3Si)_2SiC(R)O\}Li^+$  ( $R = tBu, 1-Ad, o-Tol, Mes$ ) by NMR spectroscopy and investigated their reactivity.<sup>2b-h</sup>

Most known silenes and silenolates are acyclic molecules. Compounds with the coordinatively unsaturated silicon atom incorporated into a cyclopolysilane ring, in particular, have not yet been isolated although such species are likely to exhibit unusual molecular structures, electronic spectra and reactivity patterns. Recently we found that moderately stable alkyl substituted methylenecyclohexasilanes such as **3a** (Scheme 1) can be generated photochemically as mixtures with unreacted starting material and polymeric by-products and characterized by NMR and UV/Vis spectroscopy.<sup>4</sup>



**Scheme 1.** Synthesis of cyclic silenes and silenolates from acylcyclohexasilanes.

Now we would like to report the synthesis, the spectroscopic characterization and the molecular structures of the first cyclic silenolates **2a-c** and the selective conversion of **2b** to the silene **3b**, which is the first example of an isolated stable exocyclic silene with the  $sp^2$  silicon atom incorporated into a cyclopolysilane framework. Based on structural and NMR data we further provide striking evidence that the different reactivity observed for alkyl (**2a**) and aryl substituted (**2b,c**) silenolates is primarily governed by the different coordination of the  $K^+$  counter-ion to the SiC(R)O moiety.

**2a-c** were obtained with remarkable selectivity by the addition of 1.05 equiv. of KO<sup>t</sup>Bu to the acylcyclohexasilanes **1a-c**<sup>5</sup> either in THF or in toluene solution in the presence of 1.05 equiv. of 18-crown-6 at  $-50$  °C (Scheme 1).<sup>6</sup> The THF solutions, thus obtained, could be used directly for further derivatization. For isolation, **2a-c** were crystallized from toluene/[18]crown-6 at  $-30$  °C to give red crystals of the 1 : 1 [18]crown-6 adducts which, after filtration, can be stored at  $-30$  °C in the absence of air even for prolonged periods of time. The products, however, immediately decomposed to uncharacterized material upon exposure to the atmosphere or the attempted removal of residual solvent and volatile components in vacuo.

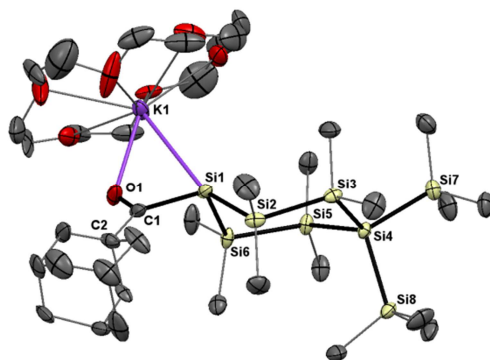


**Figure 1.** ORTEP diagram for compound **2a** (1 : 1 adduct with [18]crown-6). Thermal ellipsoids are depicted at the 50 % probability level. Hydrogen atoms are omitted for clarity

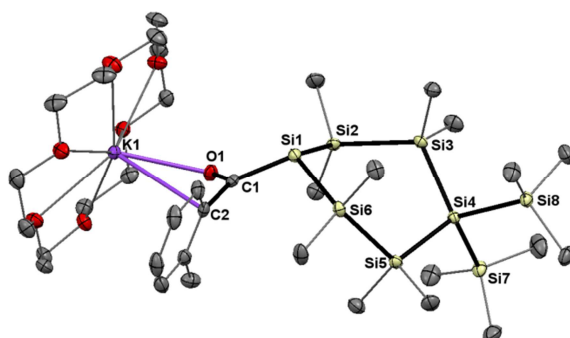


**Figure 2.** ORTEP diagram for compound **2c** (1 : 1 adduct with [18]crown-6). Thermal ellipsoids are depicted at the 50 % probability level. Hydrogen atoms are omitted for clarity.

**2a** and **2c** afforded crystals of sufficient quality for single crystal X-ray crystallography. The molecular structures are depicted in Figures 1 and 2, selected bond lengths and the sum of valence angles around the central Si-C moiety are summarized in Table 1.

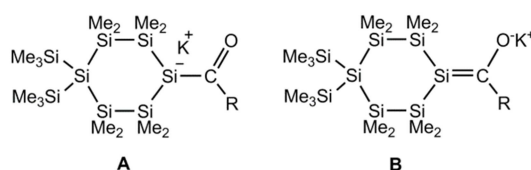
**Table 1.** Selected bond lengths  $d$  [Å] and sum of valence angles  $\Sigma\alpha(\text{Si1})$  and  $\Sigma\alpha(\text{C1})$  [deg] for K-silenolates **2a**, **c**.

	<b>2a</b>	<b>2c</b>
$d$ C(1)-Si(1)	1.966(2)	1.874(2)
$d$ C(1)-O(1)	1.244(2)	1.260(2)
$d$ K(1)-O(1)	2.743(1)	2.701(1)
$d$ K(1)-Si(1)	3.603(2)	4.935(1)
$d$ K(1)-C(2)	4.899(2)	3.257(2)
$\Sigma\alpha(\text{Si1})$	316.7	326.8
$\Sigma\alpha(\text{C1})$	359.9	359.7

Surprisingly the observed molecular structures are strongly influenced by the nature of the R group attached to the carbonyl C atom. **2a** adopts a structure quite close to the one observed for the acyclic

silenolate  $[(\text{Me}_3\text{Si})_2\text{SiC}(t\text{Bu})\text{O}]^-\text{K}^+$  [18]crown-6 (**5**) by Ottosson et al.<sup>2i</sup> with simultaneous coordination of the  $\text{K}^+$  cation to O and Si, a C-Si bond which is even longer than typical Si-C single bonds,<sup>7</sup> a C-O bond length characteristic of C=O double bonds<sup>8</sup> and a markedly pyramidal central Si atom. Based on these structural features Ottosson concluded that **5** is best described as an acyl silyl anion which is certainly also valid for compound **2a** (structure A in Chart 1). In comparison the structure of **2c** is quite different:  $\text{K}^+$  now is coordinated to O and the aromatic ring, the Si-C distance is significantly smaller, the C-O bond is slightly longer and the sum of valence angles  $\Sigma\alpha(\text{Si}1)$  is larger by  $10^\circ$ . These findings are perfectly in line with the results of a recent computational study on the effects of counterion coordination on the structures of silenolates.<sup>9</sup> There it has been pointed out that metal ion coordination to the O atom results in shorter Si-C bonds and a smaller degree of pyramidalization around Si(1) as compared to the naked silenolate due to the increasing influence of the enol structure (structure B in Chart 1) to overall molecular geometry. Thus, aryl substituted silenolates such as **2b,c** apparently exhibit increased character of functionalized silenes and link the properties of Ottosson's keto-form silenolate **5** with the enol-form silenolates  $(\text{R}_3\text{Si})_2\text{Si}=\text{C}(\text{Ad})\text{OLi}$  recently published by Apeloig and Bravo-Zhivotovskii.<sup>2j</sup> This study also relates the relative contribution of the keto- and the enol form to the structure of silenolates mainly to solvation effects.

**Chart 1.** (A) Keto- and (B) enol form of 2a-c.



This picture is supported further by the NMR data obtained for **2a-c**.<sup>6</sup> Again in close agreement with the corresponding data of **5**  $^{29}\text{Si}$  and  $^{13}\text{C}$  NMR chemical shifts of the Si and C atoms of the Si-C bond of  $\delta = -92.0$  and  $272.2$  ppm, respectively, were measured for **2a**·[18]crown-6. For the [18]crown-6 adducts of **2b,c** the  $^{29}\text{Si}$  signals of the central Si atoms are significantly low field shifted to  $\delta = -67.1$  (R = *o*-Tol) and  $\delta = -73.1$  ppm (R = Mes) while only minor shift differences were found for the  $^{13}\text{C}$  resonances. Similar trends were observed earlier by Ishikawa and Oshita for Li-silenolates  $(\text{Me}_3\text{Si})_2\text{SiC}(\text{OLi})\text{R}$  (R = *t*Bu, Ad, *o*-Tol, Mes) and rationalized in terms of increased double bond character of the central Si-C bond in the aryl substituted derivatives<sup>2b</sup> although the measured  $^{29}\text{Si}$  NMR shifts are still in the range typical for silyl anions.<sup>10</sup> In line with this interpretation three  $\text{SiMe}_2$  resonances at 0.6, 0.5,  $-0.45$  ppm are clearly resolved in the  $^{13}\text{C}$  spectrum of the Mes derivative **2b** while in the  $^1\text{H}$  and  $^{29}\text{Si}$  spectra the signals at 0.6 and  $-35.1$  ppm, respectively, arising from the  $\text{SiMe}_2$  groups adjacent to the central silicon atom are significantly broadened. This finding clearly indicates hindered rotation around the central Si-C bond in compound **2b** which suggests enhanced  $\text{sp}^2$  character.

The reactivity of **2a-c** with chlorosilanes also reflects the different coordination of the central silicon atom in the alkyl and the aryl derivatives (compare Scheme 1). While **2a** with an alkyl group attached to the carbonyl C atom smoothly reacted with an equimolar amount of *i*Pr<sub>3</sub>SiCl at 0 °C in THF to give the Si-silylated product **1d** in nearly quantitative yields,<sup>6</sup> the aryl substituted compounds **2b,c** under the same conditions exclusively afforded the O-silylated silenes **3b,c**. This result parallels the chemical behavior of Oshita's and Ishikawa's Li-silenolates and easily can be explained by the structural and NMR spectroscopic data discussed above. Apparently the coordination of K<sup>+</sup> to O (1) and the aromatic ring in **2b,c** effectively withdraws negative charge from Si(1) which makes O(1) to the preferred reaction site for R<sub>3</sub>Si<sup>+</sup> while **2a** with the K<sup>+</sup> cation coordinated simultaneously to O(1) and Si (1) behaves more or less like a typical silyl anion.

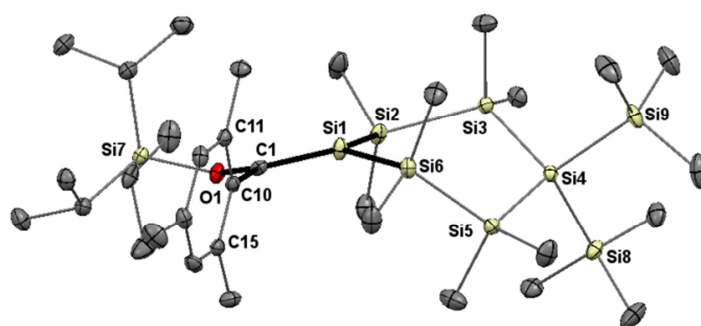
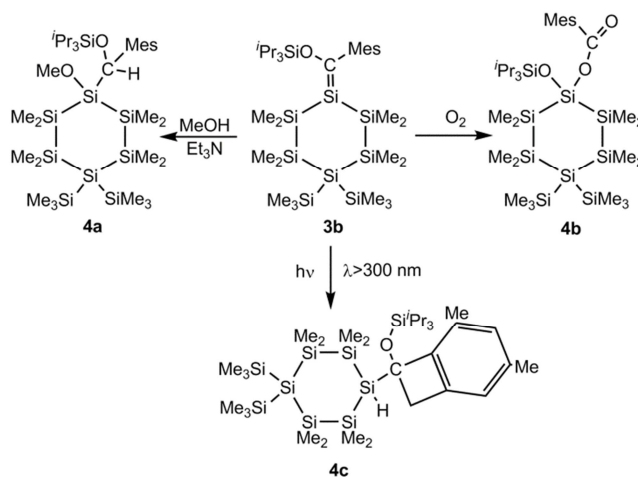


**Figure 3.** ORTEP diagram for compound **3b**. Thermal ellipsoids are depicted at the 50 % probability level. Hydrogen atoms are omitted for clarity. Selected bond lengths [Å] and bond and torsional angles [deg] with estimated standard deviations: Si(1)-C(1) 1.767(2), C(1)-O(1) 1.386(2), Si-Si (mean) 2.345, Si-Si-Si (endo, mean) 110.9,  $\Sigma\alpha$ Si(1) 357.8,  $\Sigma\alpha$ C(1) 359.8, Si(6)-Si(1)-C(1)-C(10) 10.6(2), Si(2)-Si(1)-C(1)-O(1) -0.8, C(11)-C(10)-C(1)-Si(1) 71.9, Si(1)-C(1)-C(10)-C(11) 71.9°, Si(1)-C(1)-C(10)-C(11) -105.9°.

**3b** turned out to be thermally remarkably stable and could be isolated as yellow crystals in 60 % yield by crystallization from diethyl ether and fully characterized structurally and spectroscopically.<sup>6</sup> **3c**, in contrast, was formed already along with considerable amounts of several unidentified by-products and could not be purified by crystallization because it decomposed further even at -70°C possibly due to incomplete steric protection of the Si=C double bond.

Figure 3 shows the molecular structure of **3b** as determined by single crystal X-ray crystallography. The geometry of the central Si-C moiety closely resembles the one observed for Brook's acyclic silene (Me<sub>3</sub>Si)<sub>2</sub>Si=C(OSiMe<sub>3</sub>)Ad (**6**)<sup>3,11</sup> with nearly identical Si=C bond lengths (1.767 vs. 1.762 Å) and an essentially planar C(1) atom ( $\Sigma\alpha$ C(1) = 359.8°). As compared to **6** Si(1) in **3b** is slightly more pyramidalized by 2° while the twist angle around the Si=C bond in **3b** is significantly smaller as shown by the torsion angles Si(6)-Si(1)-C(1)-C(10) and Si(2)-Si(1)-C(1)-O(1) likely as a result of the incorporation of Si(1) into the cyclohexasilane cycle. Otherwise the Si<sub>6</sub> ring in **3b** adopts a twisted

conformation with unexceptional endocyclic Si-Si bond distances and Si-Si-Si bond angles. For steric reasons, finally, the mesityl ring is arranged roughly perpendicular to the adjacent Si=C double bond with a torsion angle Si(1)-C(1)-C(10)-C(11) of 71.9°.



**Scheme 2.** Reactivity of compound **3b**.

NMR spectral data and the reactivity of **3b** (compare Scheme 2) are also typical of a Brook-type silene.  $^{13}\text{C}$  and  $^{29}\text{Si}$  signals characteristic of Si=C were observed at  $\delta(^{29}\text{Si}) = 31.2$  ppm and  $\delta(^{13}\text{C}) = 200.3$  ppm. The  $^1\text{H}$ ,  $^{13}\text{C}$ , and  $^{29}\text{Si}$  NMR spectra, furthermore, display sharp distinct absorptions for each of the four endocyclic SiMe<sub>2</sub> groups present which are magnetically nonequivalent due to the lack of freedom of rotation about the silicon-carbon double bond. Methanol readily adds across the Si=C bond to give the expected product **4a**. When **3b** was treated with dry air for 2 h, the ester **4b** was formed just as observed earlier for acyclic Brook-type silenes.<sup>12</sup> On photolysis of **3b**, finally, the C-H bond of the ortho methyl group of the mesityl substituent added to the silicon-carbon double bond to form the benzocyclobutene **4c**. Older studies reported similar reactions for acyclic mesityl substituted Brook-type silenes.<sup>13</sup> While **4a,c** could be isolated and completely characterized only slightly impure samples of **4b** were obtained due to the lack of crystallization.<sup>14</sup>

Silene **3b** showed an intense absorption band at 364 nm ( $\epsilon = 16500$ ) which is the longest wavelength absorption maximum measured for a Brook-type silene so far. It is considerably red-shifted relative to the corresponding bands in the spectra of the acyclic silene **6** ( $\lambda_{\text{max}} = 340$  nm,  $\epsilon = 7400$ )<sup>3</sup> and the endocyclic silene [-Tip2Si-TipSi=C(Ad)-O-] ( $\lambda_{\text{max}} = 354$  nm).<sup>15</sup> According to time-dependent DFT calculations at the mPW1PW91/6-31+G\*\* level performed for **3b** and **6**<sup>16</sup> these longest wavelength absorption bands are unequivocally assigned to the HOMO-LUMO transition with a smaller excitation energy for **3b** due to slight destabilization of the HOMO and stabilization of the LUMO. Both compounds possess nearly identical HOMOs dominated by the  $\pi$  (Si-C) bond with some admixture of the oxygen lone pair of proper symmetry. The LUMO of **6**, however, primarily is  $\pi^*(\text{Si-C})$  of nature,



while the LUMO of **3b** is localized mainly on the aromatic ring (compare Figure 4). As a result **3b** shows a HOMO-LUMO transition of different origin ( $\pi_{\text{Si=C}} \rightarrow \pi^*_{\text{Si=C}}$  for **6** vs.  $\pi_{\text{Si=C}} \rightarrow \pi^*_{\text{aryl}}$  for **3b**).

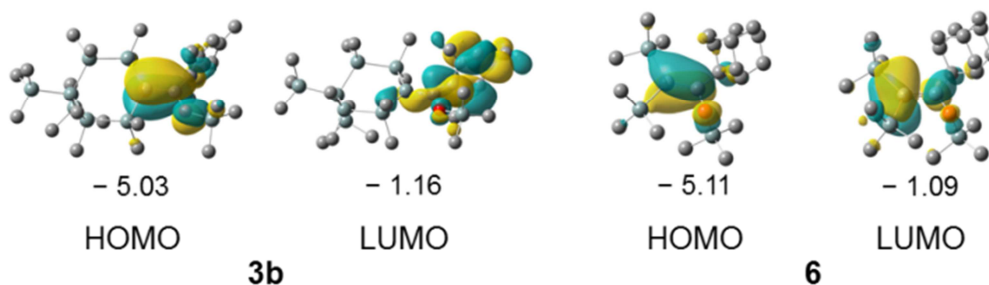


**Figure 4.** Frontier orbitals and orbital energies in eV for model compound of **3b** and **6**.

### 2.4.3 Conclusion

In conclusion, we were able to demonstrate that the stable silenolates **2a-c** and the silene **3b** with the coordinatively unsaturated silicon atom incorporated into cyclohexasilane frameworks are synthetically accessible and can be isolated and structurally characterized spectroscopically and by X-ray crystallography. Furthermore, the disagreeing reactivities of silenolates with alkyl or aryl substituents attached to the carbonyl C atom towards chlorosilanes  $\text{ClSiR}_3$  could be related to the different coordination of the  $\text{K}^+$  counter-ion to the  $\text{SiC(R)O}$  moiety and to the resulting increased enol character of the aryl substituted derivatives. UV absorption spectroscopy and DFT calculations, finally, provide evidence for considerable contributions of the aromatic  $\pi$  system to the UV/vis absorption characteristics of **3b**.

### 2.4.4 Experimental Section

#### 2.4.4.1 General Considerations

All experiments were performed under a nitrogen atmosphere using standard Schlenk techniques. Solvents were dried using a column solvent purification system.<sup>17</sup> Commercial  $\text{KO}t\text{Bu}$  (97 %),  $\text{ClCOMes}$  (99 %),  $\text{ClCOAd}$  (98 %),  $\text{ClCO}o\text{-Tol}$  (99 %),  $i\text{Pr}_3\text{SiCl}$  (97 %) and [18]crown-6 (99 %) were used as purchased.  $\text{Et}_3\text{N}$  (99 %) was dried by distillation from solid  $\text{KOH}$ , commercial anhydrous  $\text{MeOH}$  was dried with  $3\text{\AA}$  molecular sieve.  $^1\text{H}$  (299.95 MHz),  $^{13}\text{C}$  (75.43 MHz) and  $^{29}\text{Si}$  (59.59 MHz) NMR spectra were recorded on a Varian INOVA 300 spectrometer in  $\text{C}_6\text{D}_6$  or  $\text{CDCl}_3$  solution and referenced versus TMS using the internal  $^2\text{H}$ -lock signal of the solvent.  $(\text{Me}_3\text{Si})_2\text{Si}_6\text{Me}_8(\text{SiMe}_3)_2$ ,<sup>18</sup>  $(\text{Me}_3\text{Si})_2\text{Si}_6\text{Me}_8(\text{SiMe}_3)\text{K}^1$  and **1a**<sup>19</sup> were synthesized according to published procedures. HRMS spectra were run on a Kratos Profile mass spectrometer. Infrared spectra were obtained on a Bruker Alpha-P Diamond ATR Spectrometer from the solid sample. Melting points were determined using a

Buechi 535 apparatus and are uncorrected. Elemental analyses were carried out on a Hanau Vario Elementar EL apparatus. Photolyses were performed by using a 500 W medium pressure mercury lamp (Original HANAU). Sample solutions were photolyzed under an atmosphere of nitrogen in Pyrex Schlenk tubes immersed in cold water to ensure ambient sample temperature and to prevent irradiation with light of wavelengths  $\lambda < 300$  nm. UV absorption spectra were recorded on a Perkin Elmer Lambda 5 spectrometer.

### Synthesis of **1b**

A solution of  $(\text{Me}_3\text{Si})_2\text{Si}_6\text{Me}_8(\text{SiMe}_3)\text{K}$  in 20 mL of DME was freshly prepared from 3.00 g (5.16 mmol) of  $(\text{Me}_3\text{Si})_2\text{Si}_6\text{Me}_8(\text{SiMe}_3)_2$  and 0.64 g (5.67 mmol) of KO $t$ Bu and slowly added to a solution of 1.04 g (5.67 mmol) 2,4,6-trimethylbenzoylchloride in 50 mL diethyl ether at  $-80^\circ\text{C}$ . Subsequently the mixture was stirred for another 30 min at  $-80^\circ\text{C}$ , allowed to warm to room temperature and finally stirred for additional 60 minutes. After aqueous work up with 100 mL of 3 % sulfuric acid the organic layer was separated, dried over  $\text{Na}_2\text{SO}_4$  and the solvents were stripped off with a rotary evaporator. Drying in vacuo (0.02 mbar) and crystallization from acetone solution at  $-30^\circ\text{C}$  afforded 3.30 g (98%) of analytically pure **1b** as slightly yellow crystals.

**mp:**  $185^\circ\text{C}$ . **Anal. Found:** C, 49.75; H, 9.33 %. **Calc.:** C, 49.47; H, 9.53 %.  **$^{29}\text{Si-NMR}$**  ( $\text{C}_6\text{D}_6$ , TMS, ppm):  $-8.22, -8.37, -12.46$  ( $\text{SiMe}_3$ );  $-37.61, -38.46$  ( $\text{SiMe}_2$ );  $-71.14$  ( $\text{SiC=O}$ );  $-131.67$  ( $\text{Si}(\text{SiMe}_3)_2$ ).  **$^{13}\text{C-NMR}$**  ( $\text{C}_6\text{D}_6$ , TMS, ppm): 246.17 ( $\text{C=O}$ ); 147.19, 137.41, 131.31, 128.67 (Mes-C); 20.60, 19.86 (Mes- $\text{CH}_3$ ); 3.70, 3.64, 1.45 ( $\text{Si}(\text{CH}_3)_3$ );  $-0.83, -1.12, -1.99, -2.51$  ( $\text{Si}(\text{CH}_3)_2$ ).  **$^1\text{H-NMR}$**  ( $\text{C}_6\text{D}_6$ , TMS, ppm): 6.55 (s, 2 H, Mes-H); 2.17 (6H, s, Mes- $\text{CH}_3$ ); 2.01 (3H, s, Mes- $\text{CH}_3$ ); 0.55, 0.43, 0.37, 0.36 (s, 6H each,  $\text{Si}(\text{CH}_3)_2$ ); 0.34, 0.29, 0.07 (s, 9H each,  $\text{Si}(\text{CH}_3)_3$ ). **IR** (neat):  $\nu(\text{C=O}) = 1608$  (m)  $\text{cm}^{-1}$ . **HRMS:** calc. for  $[\text{C}_{27}\text{H}_{62}\text{OSi}_9]^+$  ( $\text{M}^+$ ): 654.2724; found: 654.2752. **UV-VIS:**  $\lambda$  [nm] ( $\epsilon$  [ $\text{L mol}^{-1} \text{cm}^{-1}$ ]) = 254 (16800), 393 (230).

### Synthesis of **1c**

The procedure followed was that used for **1b** with 3.00 g (5.16 mmol) of  $(\text{Me}_3\text{Si})_2\text{Si}_6\text{Me}_8(\text{SiMe}_3)_2$ , 0.64 g (5.67 mmol) of KO $t$ Bu and 0.88 g (5.67 mmol) 2-methylbenzoylchloride. Yield: 3.00 g (93 %) of analytically pure **1c** as slightly yellow crystals.

**mp:**  $128^\circ\text{C}$ . **Anal. Found:** C, 47.54; H, 9.00 %. **Calc.:** C, 47.85; H, 9.32 %.  **$^{29}\text{Si-NMR}$**  ( $\text{C}_6\text{D}_6$ , TMS, ppm):  $-7.66, -8.66, -10.29$  ( $\text{SiMe}_3$ );  $-36.51, -37.87$  ( $\text{SiMe}_2$ );  $-66.79$  ( $\text{SiC=O}$ );  $-131.42$  ( $\text{Si}(\text{SiMe}_3)_2$ ).  **$^{13}\text{C-NMR}$**  ( $\text{C}_6\text{D}_6$ , TMS, ppm): 239.77 ( $\text{C=O}$ ); 145.43, 134.24, 131.64, 130.10, 129.80, 124.85 (o-Tol-C); 20.09 (o-Tol- $\text{CH}_3$ ); 3.74, 3.71, 1.84 ( $\text{Si}(\text{CH}_3)_3$ );  $-0.89, -1.15, -2.34, -2.67$  ( $\text{Si}(\text{CH}_3)_2$ ).  **$^1\text{H-NMR}$**  ( $\text{C}_6\text{D}_6$ , TMS, ppm): 7.59 - 6.88 (4H, o-Tol-H); 2.40 (3H, o-Tol- $\text{CH}_3$ ); 0.45, 0.41, 0.35, 0.28, 0.27, 0.20 (s, 51H,  $\text{Si}(\text{CH}_3)_2 + \text{Si}(\text{CH}_3)_3$ ). **IR** (neat):  $\nu(\text{C=O}) = 1601$  (m)  $\text{cm}^{-1}$ . **HRMS:** calc. for  $[\text{C}_{25}\text{H}_{58}\text{OSi}_9]^+$  ( $\text{M}^+$ ): 626.2411; found: 626.2453. **UV-VIS:**  $\lambda$  [nm] ( $\epsilon$  [ $\text{L mol}^{-1} \text{cm}^{-1}$ ]) = 254 (18200), 414 (240).

### Synthesis of [18]-crown-6 adduct of **2a**

300 mg (0.447 mmol) of **1a** and 0.124 mg (0.447 mmol) of [18]crown-6 were dissolved in 4 mL of toluene, cooled to  $-50^\circ\text{C}$  and 46.9 mg (0.447 mmol) of KO $t$ Bu were added. After stirring for

additional 30 minutes the mixture was allowed to warm to room temperature and finally stirred for an additional hour. At this time reaction control by  $^{29}\text{Si}$ -NMR showed that the starting material completely had been consumed. For isolation the product was crystallized from toluene at  $-30^\circ\text{C}$  to give 210 mg of the 1 : 1 [18]crown-6 adduct of **2a** as red crystals which after filtration contained variable amounts of residual toluene and  $\text{Me}_3\text{SiOtBu}$  and immediately decomposed to uncharacterized material upon the attempted removal of the volatile components in vacuo.

$^{29}\text{Si}$ -NMR ( $\text{C}_6\text{D}_6$ , TMS, ppm):  $-8.52$  ( $\text{SiMe}_3$ );  $-33.10$ ,  $-35.07$  ( $\text{SiMe}_2$ );  $-92.01$  ( $\text{SiCOAryl}$ );  $-131.30$  ( $\text{Si}(\text{SiMe}_3)_2$ ).  $^{13}\text{C}$ -NMR ( $\text{C}_6\text{D}_6$ , TMS, ppm):  $272.23$  ( $\text{C}=\text{O}$ );  $69.62$  ( $-\text{CH}_2-\text{CH}_2-\text{O}-$ );  $50.59$  ( $\text{Ad}-\text{C}-\text{CO}$ );  $39.70$ ,  $37.65$  ( $\text{Ad}-\text{CH}_2$ );  $29.30$  ( $\text{Ad}-\text{CH}$ );  $4.12$  ( $\text{Si}(\text{CH}_3)_3$ );  $2.77$ ,  $-0.11$  ( $\text{Si}(\text{CH}_3)_2$ ).  $^1\text{H}$ -NMR ( $\text{C}_6\text{D}_6$ , TMS, ppm):  $3.23$  ( $-\text{CH}_2-\text{CH}_2-\text{O}-$ );  $2.3 - 1.5$  ( $\text{Ad}-\text{CH}_2$ ,  $\text{Ad}-\text{CH}$ ; partially superimposed by toluene- $\text{CH}_3$ );  $0.74$ ,  $0.62$  (12H each, s,  $\text{Si}(\text{CH}_3)_2$ );  $0.48$  (18H, s,  $\text{Si}(\text{CH}_3)_3$ ).

### Synthesis of [18]-crown-6 adduct of **2b**

The procedure followed was that used for **2a** with 300 mg (0.458 mmol) of **1b**, 0.127 mg (0.481 mmol) of [18]crown-6 and 53.9 mg (0.481 mmol) of  $\text{KOtBu}$ . Yield: 240 mg of the 1 : 1 [18]crown-6 adduct of **2b** as red crystals which after filtration contained variable amounts of residual toluene and other minor impurities and immediately decomposed to uncharacterized material upon the attempted removal of the volatile components in vacuo.

$^{29}\text{Si}$ -NMR ( $\text{C}_6\text{D}_6$ , TMS, ppm):  $-8.79$  ( $\text{SiMe}_3$ );  $-35.09$  (broad),  $-36.40$  ( $\text{SiMe}_2$ );  $-73.11$  ( $\text{SiC}=\text{O}$ );  $-131.13$  ( $\text{Si}(\text{SiMe}_3)_2$ ).  $^{13}\text{C}$ -NMR ( $\text{C}_6\text{D}_6$ , TMS, ppm):  $264.65$  ( $\text{C}=\text{O}$ );  $152.02$ ,  $133.17$ ,  $131.87$  ( $\text{Mes}-\text{C}$ );  $69.82$  ( $-\text{CH}_2-\text{CH}_2-\text{O}-$ );  $20.85$  ( $\text{Mes}-\text{CH}_3$ );  $20.72$  ( $\text{Mes}-\text{CH}_3$ );  $4.01$  ( $\text{Si}(\text{CH}_3)_3$ );  $0.59$ ,  $0.54$ ,  $-0.47$  ( $\text{Si}(\text{CH}_3)_2$ ).  $^1\text{H}$ -NMR ( $\text{C}_6\text{D}_6$ , TMS, ppm):  $6.78$  (s, 2 H,  $\text{Mes}-\text{H}$ );  $3.12$  ( $-\text{CH}_2-\text{CH}_2-\text{O}-$ );  $2.67$  (6H, s,  $\text{Mes}-\text{CH}_3$ );  $2.16$  (3H, s,  $\text{Mes}-\text{CH}_3$ );  $0.66$ ,  $0.65$  (s, 24H  $\text{Si}(\text{CH}_3)_2$ );  $0.48$  (s, 18H,  $\text{Si}(\text{CH}_3)_3$ ).

### Synthesis of [18]-crown-6 adduct of **2c**

The procedure followed was that used for **2a** with 300 mg (0.478 mmol) of **1c**, 0.139 mg (0.526 mmol) of [18]crown-6 and 59.0 mg (0.526 mmol) of  $\text{KOtBu}$ . Yield: 75 mg of the 1 : 1 [18]crown-6 adduct of **2c** as dark red crystals which after filtration contained variable amounts of residual toluene,  $\text{Me}_3\text{SiOtBu}$  and  $(\text{Me}_3\text{Si})_2\text{O}$  and immediately decomposed to uncharacterized material upon the attempted removal of the volatile components in vacuo.

$^{29}\text{Si}$ -NMR ( $\text{C}_6\text{D}_6$ , TMS, ppm):  $-8.78$  ( $\text{SiMe}_3$ );  $-34.26$ ,  $-36.60$  ( $\text{SiMe}_2$ );  $-66.95$  ( $\text{SiC}=\text{O}$ );  $-131.49$  ( $\text{Si}(\text{SiMe}_3)_2$ ).  $^{13}\text{C}$ -NMR ( $\text{C}_6\text{D}_6$ , TMS, ppm):  $265.07$  ( $\text{C}=\text{O}$ );  $153.68$ ,  $131.04$ ,  $129.99$ ,  $127.04$ ,  $125.67$ ,  $123.82$  ( $o\text{-Tol}-\text{C}$ );  $69.57$  ( $-\text{CH}_2-\text{CH}_2-\text{O}-$ );  $19.81$  ( $o\text{-Tol}-\text{CH}_3$ );  $4.03$  ( $\text{Si}(\text{CH}_3)_3$ );  $0.81$ ,  $-0.53$  ( $\text{Si}(\text{CH}_3)_2$ ).  $^1\text{H}$ -NMR ( $\text{C}_6\text{D}_6$ , TMS, ppm):  $7.65$  (d,  $o\text{-Tol}-\text{H}$ );  $3.05$  ( $-\text{CH}_2-\text{CH}_2-\text{O}-$ );  $2.55$  (3H, s,  $o\text{-Tol}-\text{CH}_3$ );  $0.61$  (s, 12H,  $\text{Si}(\text{CH}_3)_2$ ),  $0.56$  (s, 12H  $\text{Si}(\text{CH}_3)_2$ );  $0.45$  (s, 18H,  $\text{Si}(\text{CH}_3)_3$ ).

### Reaction of **2a** with $i\text{Pr}_3\text{SiCl}$

A solution of **2a** was freshly prepared by stirring a mixture of 46.9 mg (0.447 mmol) of  $\text{KOtBu}$  and 300 mg (0.447 mmol) of **1a** in 5 mL of THF for 1 h at  $-70^\circ\text{C}$ . Now the resulting red solution was warmed to  $0^\circ\text{C}$  and 0.10 g (0.447 mmol) of  $i\text{Pr}_3\text{SiCl}$  were added drop wise. Immediately the solution

turned colorless. After aqueous work up with 100 mL of 3 % sulfuric acid the organic layer was separated, dried over Na<sub>2</sub>SO<sub>4</sub> and the solvents were stripped off with a rotary evaporator. Drying in vacuum (0.001 mbar) and crystallization from acetone solution at –30°C afforded 270 mg (80%) of the analytically pure acylcyclohexasilane **1d** as white crystals.

**mp:** 127 °C. **Anal. Found:** C, 53.92; H, 10.24 %. **Calc.:** C, 54.03; H, 10.40 %. **<sup>29</sup>Si-NMR** (CDCl<sub>3</sub>, TMS, ppm): –7.29, –8.55 (*SiMe*<sub>3</sub>); –33.80, –35.69 (*SiMe*<sub>2</sub>); –69.72 (*SiC=O*); –131.35 (*Si(SiMe*<sub>3</sub>)<sub>2</sub>). **<sup>13</sup>C-NMR** (CDCl<sub>3</sub>, TMS, ppm): 250.91 (*C=O*); 52.00, 37.83, 36.62, 28.10 (*Ad-C*); 20.45 (*CH-(CH*<sub>3</sub>)<sub>2</sub>), 14.76 (*CH-(CH*<sub>3</sub>)<sub>2</sub>); 4.14, 4.08 (*Si(CH*<sub>3</sub>)<sub>3</sub>); 0.45, –0.18, –0.19, –0.49 (*Si(CH*<sub>3</sub>)<sub>2</sub>). **<sup>1</sup>H-NMR** (CDCl<sub>3</sub>, TMS, ppm): 2.05 (3H, b, *Ad-CH*); 1.72 (12H, b, *Ad-CH*<sub>2</sub>); 1.30 (3H, m, *CH-(CH*<sub>3</sub>)<sub>2</sub>); 1.17 (18H, d, *CH-(CH*<sub>3</sub>)<sub>2</sub>); 0.37, 0.34, 0.30, 0.29, (6H each, s, *Si(CH*<sub>3</sub>)<sub>2</sub>); 0.24, 0.23 (9H each, s, *Si(CH*<sub>3</sub>)<sub>3</sub>). **IR** (neat):  $\nu(\text{C=O}) = 1614$  (m) cm<sup>–1</sup>. **HRMS:** calc. for [C<sub>34</sub>H<sub>78</sub>OSi<sub>9</sub>]<sup>+</sup> (M<sup>+</sup>): 754.3976; found: 754.3955.

### Reaction of **2b** with *i*Pr<sub>3</sub>SiCl

162 mg (0.839 mmol) of *i*Pr<sub>3</sub>SiCl were added drop wise at 0 °C to a solution of **2b** in 5 mL of THF freshly prepared from 500 mg (0.763 mmol) of **1b** and 94.0 mg (0.839 mmol) of KO<sup>*t*</sup>Bu according to the procedure described above. Immediately the red solution turned yellow. After removal of the volatile components in vacuo the remaining yellow solid was dissolved in heptane, filtered over dry celite and the solvent was stripped off again. Recrystallization from diethyl ether afforded 330 mg (59%) of the analytically pure silene **3b** as yellow crystals.

**mp:** 85-86 °C (dec.). **Anal. Found:** C, 53.23; H, 10.25 %. **Calc.:** C, 53.58; H, 10.08 %. **<sup>29</sup>Si-NMR** (C<sub>6</sub>D<sub>6</sub>, TMS, ppm): 31.22 (*Si=C*); 13.08 (*iPr*<sub>3</sub>*SiO*); –8.66 (*SiMe*<sub>3</sub>); –35.57, –35.67, –37.35, –37.57 (*SiMe*<sub>2</sub>); –132.05 (*Si(SiMe*<sub>3</sub>)<sub>2</sub>). **<sup>13</sup>C-NMR** (C<sub>6</sub>D<sub>6</sub>, TMS, ppm): 200.31 (*Si=C*); 142.96, 136.94, 136.64, 128.62 (*Mes-C*); 21.27, 20.99 (*Mes-CH*<sub>3</sub>); 18.31 (*CH(CH*<sub>3</sub>)<sub>2</sub>); 13.96 (*CH(CH*<sub>3</sub>)<sub>2</sub>); 3.48 (*Si(CH*<sub>3</sub>)<sub>3</sub>); –1.30, –1.37, –1.80, –3.12 (*Si(CH*<sub>3</sub>)<sub>2</sub>). **<sup>1</sup>H-NMR** (C<sub>6</sub>D<sub>6</sub>, TMS, ppm): 6.73 (s, 2 H, *Mes-H*); 2.54 (6H, s, *Mes-CH*<sub>3</sub>); 2.07 (3H, s, *Mes-CH*<sub>3</sub>); 1.01-0.9 (21 H, b, *CH(CH*<sub>3</sub>)<sub>2</sub>); 0.68, 0.40, 0.29, –0.03 (6H each, s, *Si(CH*<sub>3</sub>)<sub>2</sub>); 0.28 (18H, *Si(CH*<sub>3</sub>)<sub>3</sub>). **IR** (neat):  $\nu(\text{Si=C}) = 1155$  (s) cm<sup>–1</sup>. **HRMS:** calc. for [C<sub>33</sub>H<sub>74</sub>OSi<sub>9</sub>]<sup>+</sup> (M<sup>+</sup>): 738.3663; found: 738.3628. **UV-VIS:**  $\lambda$  [nm] ( $\epsilon$  [L mol<sup>–1</sup> cm<sup>–1</sup>]) = 308 (3100), 364 (16500).

### Reaction of **2c** with *i*Pr<sub>3</sub>SiCl

170 mg (0.876 mmol) of *i*Pr<sub>3</sub>SiCl were added drop wise at 0 °C to a solution of **2c** in 5 mL of THF freshly prepared from 500 mg (0.797 mmol) of **1c** and 94 mg (0.876 mmol) of KO<sup>*t*</sup>Bu according to the procedure described above. Immediately the red solution turned yellow. After removal of the volatile components in vacuo the remaining yellow solid was dissolved in heptane, filtered over dry celite and the solvent was stripped off again. The target silene **3c** was formed along with several unidentified by-products. Purification of the crude material by crystallization was not successful because it decomposed further even at –70°C.

**<sup>29</sup>Si-NMR** (C<sub>6</sub>D<sub>6</sub>, TMS, ppm): 36.65 (*Si=C*); 14.63 (*iPr*<sub>3</sub>*SiO*); –8.67, –8.73 (*SiMe*<sub>3</sub>); –35.21, –35.62, –37.33, –37.57 (*SiMe*<sub>2</sub>); –132.01 (*Si(SiMe*<sub>3</sub>)<sub>2</sub>).

### Reaction of 3b with MeOH

300 mg (0.410 mmol) of **3b** were dissolved in 6 mL THF and added drop wise to a mixture of 2 mL of MeOH with 3 drops of Et<sub>3</sub>N. After removal of the volatile components on a rotary evaporator 5 mL of pentane were added and the resulting solution was filtered over silica gel. Evaporation of pentane followed by crystallization from acetone at -30 °C afforded 190 mg (61%) of analytically pure **4a** as white crystals.

**mp:** 164-165 °C. **Anal. Found:** C, 53.07; H, 9.60 %. **Calc.:** C, 52.91; H, 10.16 %. **<sup>29</sup>Si-NMR** (CDCl<sub>3</sub>, TMS, ppm): 21.54 (*SiOMe*); 14.76 (*iPr<sub>3</sub>SiO*); -6.24, -9.41 (*SiMe<sub>3</sub>*); -33.96, -34.45, -39.16, -41.59 (*SiMe<sub>2</sub>*); -131.73 (*Si(SiMe<sub>3</sub>)<sub>2</sub>*). **<sup>13</sup>C-NMR** (CDCl<sub>3</sub>, TMS, ppm): 138.47, 137.90, 135.42, 132.86, 130.20, 128.75 (*Mes-C*); 70.30 (*SiCHMesOSi*); 54.49 (*OCH<sub>3</sub>*); 22.71, 21.32, 20.80 (*Mes-CH<sub>3</sub>*); 18.27, 17.99 (*CH(CH<sub>3</sub>)<sub>2</sub>*); 12.65 (*CH(CH<sub>3</sub>)<sub>2</sub>*); 4.01, 3.84, (*Si(CH<sub>3</sub>)<sub>3</sub>*); -0.60, -0.66, -1.71, -2.07, -3.54, -4.43, -4.65, -4.88 (*Si(CH<sub>3</sub>)<sub>2</sub>*). **<sup>1</sup>H-NMR** (CDCl<sub>3</sub>, TMS, ppm): 6.76, 6.71 (1H each, s, *Mes-H*); 5.42 (1H, s, *CHMesOSi*); 3.49 (3H, s, *OCH<sub>3</sub>*); 2.42, 2.30, 2.22 (3H each, s, *Mes-CH<sub>3</sub>*); 1.01 (12H, b, *CH(CH<sub>3</sub>)<sub>2</sub> + CH(CH<sub>3</sub>)<sub>2</sub>*); 0.90 (9H, b, *CH(CH<sub>3</sub>)<sub>2</sub> + CH(CH<sub>3</sub>)<sub>2</sub>*); 0.29, 0.28, -0.06, -0.16 (3H each, s, *Si(CH<sub>3</sub>)<sub>2</sub>*); 0.25 (15H, s, *Si(CH<sub>3</sub>)<sub>2</sub> + Si(CH<sub>3</sub>)<sub>3</sub>*); 0.20 (12H s, *Si(CH<sub>3</sub>)<sub>2</sub>*); 0.19 (9H, s, *Si(CH<sub>3</sub>)<sub>3</sub>*). **HRMS:** calc. for [C<sub>32</sub>H<sub>74</sub>O<sub>2</sub>Si<sub>9</sub>]<sup>+</sup> (M<sup>+</sup>): 770.3925; found: 770.3910.

### Reaction of 3b with O<sub>2</sub>

A solution of 300 mg (0.410 mmol) of **3b** in 6 mL of THF was stirred in contact with air at room temperature for 2 h. After removal of the volatile components on a rotary evaporator the product was chromatographed twice on silica gel, eluting with gradient (heptane, toluene), to give 100 mg (32%) of a semi-solid residue of slightly impure **4b**.

**<sup>29</sup>Si-NMR** (CDCl<sub>3</sub>, TMS, ppm): 9.59 (*iPr<sub>3</sub>SiO*); 2.83 (*OSiO*); -7.20, -8.64 (*SiMe<sub>3</sub>*); -35.77, -40.62 (*SiMe<sub>2</sub>*); -132.15 (*Si(SiMe<sub>3</sub>)<sub>2</sub>*). **<sup>13</sup>C-NMR** (CDCl<sub>3</sub>, TMS, ppm): 169.45 (*C=O*); 139.12, 136.30, 130.87, 128.86 (*Mes-C*); 29.70, 21.07 (*Mes-CH<sub>3</sub>*); 18.00 (*Si(CHCH<sub>3</sub>)<sub>3</sub>*); 13.02 (*Si(CHCH<sub>3</sub>)<sub>3</sub>*); 3.74 (*Si(CH<sub>3</sub>)<sub>3</sub>*); -1.18, -1.30, -4.76, -4.84 (*Si(CH<sub>3</sub>)<sub>2</sub>*). **<sup>1</sup>H-NMR** (CDCl<sub>3</sub>, TMS, ppm): 6.83 (s, 2 H, *Mes-H*); 2.41 (s, 6H, *Mes-CH<sub>3</sub>*); 2.27 (s, 3H, *Mes-CH<sub>3</sub>*); 1.05 (18 H, b, *CH(CH<sub>3</sub>)<sub>2</sub> + CH(CH<sub>3</sub>)<sub>2</sub>*); 0.35 (s, 6H, *Si(CH<sub>3</sub>)<sub>2</sub>*); 0.32 (s, 6 H *Si(CH<sub>3</sub>)<sub>2</sub>*); 0.30 (s, 6H, *Si(CH<sub>3</sub>)<sub>2</sub>*); 0.26 (s, 12H, *Si(CH<sub>3</sub>)<sub>2</sub> + Si(CH<sub>3</sub>)<sub>3</sub>*); 0.25 (s, 12 H *Si(CH<sub>3</sub>)<sub>2</sub> + Si(CH<sub>3</sub>)<sub>3</sub>*). **IR** (neat): ν(*C=O*) = 1609 (s) cm<sup>-1</sup>; ν(*Si-O(CO)R*) = 1073, 1034 (s) cm<sup>-1</sup>. **HRMS:** calc. for [C<sub>33</sub>H<sub>74</sub>O<sub>3</sub>Si<sub>9</sub>]<sup>+</sup> (M<sup>+</sup>-CH<sub>3</sub>): 755.3327; found: 755.3225.

### Photolysis of 3b

A solution of 300 mg (0.410 mmol) of **4c** in 5 mL of benzene was photolyzed with a 500 W mercury lamp at 25 °C for 12 h. At this time <sup>1</sup>H- and <sup>29</sup>Si-NMR analysis showed that the starting material completely had been consumed. After removal of the volatile components on a rotary evaporator 5 mL of pentane were added and the resulting solution was filtered over silica gel. Evaporation of pentane followed by crystallization from acetone at -30 °C afforded 175 mg (58 %) of analytically pure **4c** as white crystals.

**mp:** 130-131 °C. **Anal. Found:** C, 53.30; H, 9.65 %. **Calc.:** C, 53.58; H, 10.08 %. **<sup>29</sup>Si-NMR** (CDCl<sub>3</sub>, TMS, ppm): 12.36 (*OSi(iPr)<sub>3</sub>*); -7.45, -8.99 (*SiMe<sub>3</sub>*); -36.45, -36.72, -39.04, -40.75 (*SiMe<sub>2</sub>*); -56.45

(SiH); -131.85 (Si(SiMe<sub>3</sub>)<sub>2</sub>). <sup>13</sup>C-NMR (C<sub>6</sub>D<sub>6</sub>, TMS, ppm): 149.12, 139.43, 138.49, 132.54, 129.64, 121.52 (aryl-C); 76.31 (SiC(Me<sub>3</sub>)OSi); 46.83 (aryl-CH<sub>2</sub>); 21.73 (aryl-CH<sub>3</sub>); 18.38 (CH(CH<sub>3</sub>)<sub>2</sub>); 18.20 (CH(CH<sub>3</sub>)<sub>2</sub>); 17.19 (aryl-CH<sub>3</sub>); 13.56 (CH(CH<sub>3</sub>)<sub>2</sub>); 3.59, 3.47, (Si(CH<sub>3</sub>)<sub>3</sub>); -1.03, -1.12, -1.87, -2.07, -2.76, -4.09, -4.40, -4.67 (Si(CH<sub>3</sub>)<sub>2</sub>). <sup>1</sup>H-NMR (CDCl<sub>3</sub>, TMS, ppm): 6.74 (1H, s, aryl-H); 6.67 (1H, s, aryl-H); 3.90 (1H, s, SiH); 3.37, 3.32, 3.21, 3.16 (2H, CH<sub>a</sub>H<sub>b</sub>); 2.28, 2.24 (3H each, s, aryl-CH<sub>3</sub>); 1.0 -0.9 (21H, b, CH(CH<sub>3</sub>)<sub>2</sub>+CH(CH<sub>3</sub>)<sub>2</sub>); 0.34, 0.27, 0.26, 0.19, 0.18, -0.05, -0.36 (3H each, s, Si(CH<sub>3</sub>)<sub>2</sub>); 0.23 (12H, s, Si(CH<sub>3</sub>)<sub>3</sub>+Si(CH<sub>3</sub>)<sub>2</sub>); 0.20 (9H, s, Si(CH<sub>3</sub>)<sub>3</sub>). IR (neat): ν(Si-H) = 2069 (s) cm<sup>-1</sup>; HRMS: calc. for [C<sub>33</sub>H<sub>74</sub>OSi<sub>9</sub>]<sup>+</sup> (M<sup>+</sup>): 738.3684; found: 738.3663.

#### 2.4.4.2 X-ray Crystallography

For X-ray structure analysis suitable crystals were mounted onto the tip of glass fibres using mineral oil. Data collection was performed on a Bruker Kappa Apex II CCD diffractometer at 100 K using graphite-monochromated Mo K $\alpha$  ( $\lambda = 0.71073\text{\AA}$ ) radiation. Details of the crystal data and structure refinement are provided in Tables S1 – S4. The SHELX version 6.1 program package was used for the structure solution and refinement.<sup>20</sup> Absorption corrections were applied using the SADABS program.<sup>21</sup> All non-hydrogen atoms were refined with anisotropic displacement parameters. Hydrogen atoms were included in the refinement at calculated positions using a riding model as implemented in the SHELXTL program. In the solid state structure of **2a** the adamantyl group as well as the crown ether molecule were found disordered over two positions and were accordingly implemented in the structural model. The ratios of occupancy refined to 0.65:0.35 (adamantyl group) and 0.60:0.40 (crown ether), respectively. All non-hydrogen atoms of the disordered parts were refined anisotropically and hydrogen atoms were placed using standard AFIX commands. Crystallographic data (excluding structure factors) have been deposited with the Cambridge Crystallographic Data Centre as supplementary publications CCDC-1012279 (**1d**), CCDC-1012280 (**2a**), CCDC-1012281 (**2c**), CCDC-1012282 (**3b**), CCDC-1012283 (**4c**). Copies of the data can be obtained free of charge on application to The Director, CCDC, 12 Union Road, Cambridge CB2 1EZ, UK (fax (internat.) +44-1223/336-033; e-mail deposit@ccdc.cam.ac.uk).

#### 2.4.4.3 Computational Methods

All calculations were carried out using the Gaussian09 program package<sup>22</sup> on a computing cluster with blade architecture. For all calculations the mPW1PW91 hybrid functional was used<sup>23</sup> together with the 6-31+G\*\* basis set. After structure optimizations the vibrational frequencies were calculated to ensure minimum structures. The same combination of functional and basis set was used to calculate the excited states via time dependent (TD)-DFT. Compound **3b** was modeled by substituting the OSiPr<sub>3</sub> group by OSiMe<sub>3</sub>.

### 2.4.5 References

<sup>1</sup> For general reviews about silenes, see e.g.: a) H. Ottosson, J. Ohshita, in: M. Oestreich, (Ed.), *Science of Synthesis: Knowledge Updates 2011/3*; Thieme: Stuttgart, (2011), pp 47-55; b) H. Ottosson, A. M. Eklöf, *Coord. Chem. Rev.* 252 (2008) 1287; c) H. Ottosson, P. G. Steel, *Chem.*

*Eur. J.* 12 (2006) 1576; d) Gusel'nikov, L. E. *Coord. Chem. Rev.* 244 (2003) 149; e) West, R. J. *Organomet. Chem.* 2001, 21, 467. f) T. L. Morkin, W. Leigh, *J. Acc. Chem. Res.* 34 (2001) 129; g) T. Müller, W. Ziche, N. Auner, in: Z. Rappoport, Y. Apeloig, (Eds.), *The Chemistry of Organic Silicon Compounds*, Vol. 2, JohnWiley&Sons Ltd., New York, (1998), pp. 1233–1310. h) A. G. Brook, M. A. Brook, *Adv. Organomet. Chem.* 39 (1996) 71

<sup>2</sup> For example a) I. S. Biltueva, D. A. Bravo-Zhivotovskii, I. D. Kalikhman, V. Yu. Vitovskii, S. G. Shevchenko, N. S. Vyazankin, M. G. Voronkov, *J. Organomet. Chem.* 368 (1989) 163; b) J. Ohshita, Y. Masaoka, S. Masaoka, M. Hasebe, M. Ishikawa, A. Tachibana, T. Yano, T. Yamabe, *Organometallics* 15 (1996) 3136; c) Guliashvili, T.; El-Sayed, I.; Fischer, A.; Ottosson, H. *Angew. Chem., Int. Ed.* 2003, 42, 1640; d) R. Dobrovetsky, L. Zborovsky, D. Sheberla, M. Botoshansky, D. Bravo Zhivotovskii, Y. Apeloig, *Angew. Chem., Int. Ed.* 49 (2010) 4084

<sup>3</sup> A. G. Brook, S. C. Nyburg, F. Abdesaken, B. Gutekunst, G. Gutekunst, R. K. Kallury, Y. C. Poon, Y. M. Chang, W. Wong-Ng, *J. Am. Chem. Soc.* 104 (1982) 5667

<sup>4</sup> H. Stueger, B. Hasken, M. Haas, M. Rausch, R. Fischer, A. Torvisco, *Organometallics* 33 (2014) 231

<sup>5</sup> **1b,c** were easily synthesized using a slightly modified procedure which previously had been applied for the preparation of **1a**: ref 3. Experimental details, analytical and structural data are included in the Supporting Information

<sup>6</sup> Experimental details and analytical data for **2a-c**, **1d** and **3b** are given in the Supporting information

<sup>7</sup> M. Kaftory, M. Kapon, M. Botoshansky, In *The Chemistry of Organic Silicon Compounds*, Vol. 2; Z. Rappoport, Y. Apeloig, Eds., Wiley: Chichester, (1998); p. 181.

<sup>8</sup> G. Berthier, J. Serre, In *The Chemistry of the Carbonyl Group*, Vol. 1; Patai, S., Ed., Wiley, London, (1966), p. 1.

<sup>9</sup> A. M. Eklöf, H. Ottosson, *Tetrahedron* 65 (2009) 5521

<sup>10</sup> K. Tamao, A. Kawashi, *Adv. Organomet. Chem.* 38 (1995) 1

<sup>11</sup> S. C. Nyburg, A. G. Brook, F. Abdesaken, G. Guteknust, W. Wong-Ng, *Acta Crystallogr.* 41 (1985) 1632

<sup>12</sup> A. G. Brook, A. Baumegeger. A. J. Lough, *Organometallics* 11 (1992) 3088

<sup>13</sup> a) K. M. Baines, A. G. Brook, R. R. Ford, P. D. Lickiss, A. K. Saxena, W. J. Chatterton, J. F. Sawyer, B. A. Behnam, *Organometallics* 8 (1989) 693; b) A. G. Brook, H.-J. Wessely, *Organometallics* 4 (1985) 1487

<sup>14</sup> Experimental details and analytical data including the molecular structure of **4c** are given in the Supporting information

<sup>15</sup> I. Bejan, D. Güclü, S. Inoue, M. Ichinohe, A. Sekiguchi, D. Scheschkewitz, *Angew. Chem.Int. Ed.* 46 (2007) 3349

<sup>16</sup> For simplification **3b** was modeled by substituting the OSiPr<sub>3</sub> group by OSiMe<sub>3</sub>. Detailed computational results are given in SI

<sup>17</sup> A. B. Pangborn, M. A. Giardello, R. H. Grubbs, R. K. Rosen, F. J. Timmers, *Organometallics* 15 (1996) 1518

<sup>18</sup> R. Fischer, T. Konopa, S. Ully, J. Baumgartner, C. Marschner, *J. Organomet. Chem.* 685 (2003) 79

<sup>19</sup> H. Stueger, B. Hasken, M. Haas, M. Rausch, R. Fischer, A. Torvisco, *Organometallics* 33 (2014) 231

<sup>20</sup> SHELX and SHELXL PC: VERSION 5.03, Bruker AXS, Inc., Madison, WI, (1994)

<sup>21</sup> SADABS: Area-detection Absorption Correction: Bruker AXS Inc., Madison, WI, (1995)

- <sup>22</sup> M. J. Frisch, G. W. Trucks, H. B. Schlegel, G. E. Scuseria, M. A. Robb, J. R. Cheeseman, G. Scalmani, V. Barone, B. Mennucci, G. A. Petersson, H. Nakatsuji, M. Caricato, X. Li, H. P. Hratchian, A. F. Izmaylov, J. Bloino, G. Zheng, J. L. Sonnenberg, M. Hada, M. Ehara, K. Toyota, R. Fukuda, J. Hasegawa, M. Ishida, T. Nakajima, Y. Honda, O. Kitao, H. Nakai, T. Vreven, Jr., J. A. Montgomery, J. E. Peralta, F. Ogliaro, M. Bearpark, J. J. Heyd, E. Brothers, K. N. Kudin, V. N. Staroverov, R. Kobayashi, J. Normand, K. Raghavachari, A. Rendell, J. C. Burant, S. S. Iyengar, J. Tomasi, M. Cossi, N. Rega, J. M. Millam, M. Klene, J. E. Knox, J. B. Cross, V. Bakken, C. Adamo, J. Jaramillo, R. Gomperts, R. E. Stratmann, O. Yazyev, A. J. Austin, R. Cammi, C. Pomelli, J. W. Ochterski, R. L. Martin, K. Morokuma, V. G. Zakrzewski, G. A. Voth, P. Salvador, J. J. Dannenberg, S. Dapprich, A. D. Daniels, O. Farkas, J. B. Foresman, J. V. Ortiz, J. Cioslowski, D. J. Fox, *Gaussian 09, Revision A.1*, Gaussian, Inc., Wallingford CT, (2009)
- <sup>23</sup> C. Adamo, V. Barone, *J. Chem. Phys.* 108 (1998) 664



## 2.5 Stable Germanolates and Germanes with Exocyclic Structures

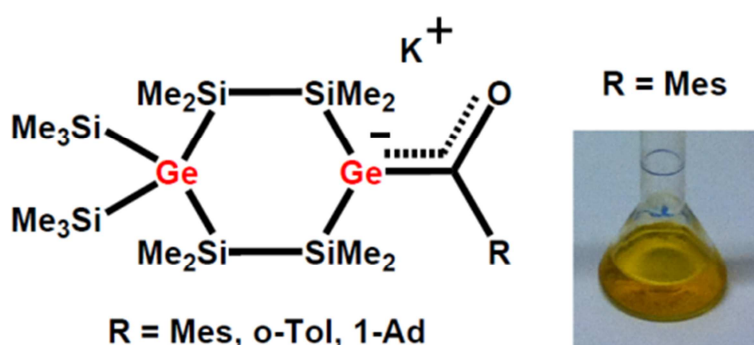
Michael Haas\*,<sup>[a]</sup> Mario Leybold,<sup>[b]</sup> Dominik Schnalzer,<sup>[a]</sup> Ana Torvisco<sup>[a]</sup> and Harald Stueger<sup>[a]</sup>

<sup>[a]</sup> Institute of Inorganic Chemistry, Graz University of Technology, Stremayrgasse 9, A-8010 Graz, Austria

<sup>[b]</sup> Institute of Organic Chemistry, Graz University of Technology, Stremayrgasse 9, A-8010 Graz, Austria

submitted to *Organometallics*

graphical abstract:



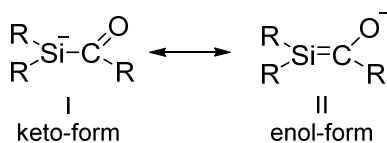
### 2.5.1 Abstract

The first germanolates with exocyclic structures  $[(\text{Me}_3\text{Si})_2\text{Ge}(\text{Si}_2\text{Me}_4)_2\text{GeC}(\text{R})\text{O}]^-\text{K}^+$  (**5a**: R = Mes; **5b**: *o*-Tol; **5c**: 1-Ad) were synthesized by the reaction of the corresponding cyclic acylgermanes with KO*t*Bu. **5a-c** could be isolated by crystallization. The remarkable thermal stability of **5a-c** even at room temperature allowed full characterization by NMR- and UV-Vis spectroscopy and by single crystal X-ray crystallography. Spectroscopic and structural features in combination with DFT quantum mechanical calculations indicated that **5a-c** are best described as acyl germyl anions in solution and in the solid state as well. The reactivity of **5a-c** versus chlorosilanes parallels the one observed for the structurally related silenolates. The aryl substituted compounds **5a,b**, thus, reacted with ClSiMe<sub>3</sub> to give the exocyclic germanes  $(\text{Me}_3\text{Si})_2\text{Ge}(\text{Si}_2\text{Me}_4)_2\text{Ge}=\text{C}(\text{OSiMe}_3)\text{R}$  (**6a**: R = Mes; **6b**: *o*-Tol), while the alkyl substituted species **5c** afforded the Ge-silylated cyclic acylgermane. TDDFT calculations were used to assign the UV-Vis absorption spectra and to gain more insight into the electronic nature of **5a-c** and **6a**.

## 2.5.2 Introduction

While the chemistry of metal enolates is well developed and numerous applications for such compounds exist,<sup>1</sup> much less is known about their heavier congeners  $[(R_2EC(R)O)]M^+$  (E = Si, Ge; M = Li, K), namely silenolates and germenolates. As in the case of enolates, two tautomeric structures of silenolates can be drawn: the keto-form (I) with the negative charge residing predominantly on the silicon atom, while in the enol-form (II) the negative charge is located primarily on the oxygen atom (Chart 1).

**Chart 1.** Keto (I)- and enol (II) form of silenolates.

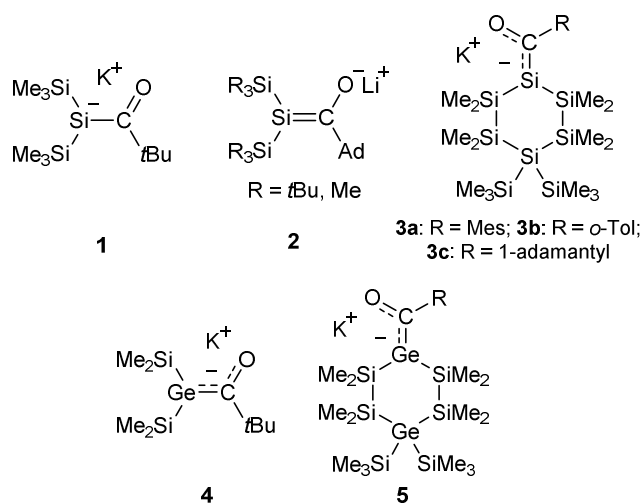


Apeloig *et al.* and later Ohshita, Ishikawa and co-workers synthesized and characterized a series of moderately stable Li-silenolates  $\{(\text{Me}_3\text{Si})_2\text{SiC(R)O}\}\text{Li}^+$  (R = *t*Bu, 1-Ad, *o*-Tol, Mes) by NMR spectroscopy and investigated their reactivity.<sup>2</sup> However, the low thermal stability of these Li-silenolates prevented their structural characterization and their general use as reagents for further derivatization. In 2004 Ottosson *et al.* reported the synthesis and the molecular structure of the K-silenolate **1** (structural formulae of compounds **1** – **5** are depicted in Chart 2), which is totally stable under an inert atmosphere at ambient temperature. According to X-ray crystallography **1** adopts a keto-type structure with a strongly pyramidal central silicon atom and an unusually long Si-C single bond (1.926 Å).<sup>3</sup> More recently Bravo-Zhivotovskii and Apeloig *et al.* reported the synthesis, isolation and X-ray molecular structure of the first enol-form silenolates  $[(\text{RR}'_2\text{Si})_2\text{Si}=\text{C}(\text{OLi})\text{Ad}]$  (R, R' = *t*Bu, Me) (**2**) with remarkably short SiC bonds (1.819 – 1.823 Å) and a planar environment around the central silicon atom.<sup>4</sup> In our laboratories, finally, we successfully isolated a series of cyclic silenolates  $[(\text{Me}_3\text{Si})_2\text{Si}(\text{Si}_2\text{Me}_4)_2\text{SiC(R)O}]^-\text{K}^+$  (**3**) (R = 1-Ad, Mes, *o*-Tol) and investigated their chemical and structural properties.<sup>5</sup>

The keto-enol equilibrium in metal silenolates has also been addressed computationally and it has been found that in non-solvating media the enol-form of the silenolate dominates, while effective solvation of the cation e.g. by crown ethers strongly favors the keto-form.<sup>4</sup> Furthermore, Ottosson *et al.* observed in a related DFT study that coordination of a solvated metal ion to the oxygen atom in type **1** silenolates results in shorter SiC bond lengths, a smaller degree of pyramidalization around Si(1), and lower the charge difference at the carbon and at the silicon atom  $\Delta q(\text{SiC})$  as compared to the naked silenolate.<sup>6</sup>

To the best of our knowledge only two studies with regard to germenolates have been published in the literature by Bravo-Zhivotovskii et al. who reported briefly on the formation of germenolate anions **4** from the reaction of bulky acylgermanes such as  $(\text{Me}_3\text{Si})_3\text{GeC(O)}t\text{Bu}$  with  $\text{Et}_3\text{GeLi}$ .<sup>7</sup> Spectroscopic and structural data of **4**, however, were not given. Otherwise acylgermanes and related species recently attracted considerable attention because of possible applications as photoinitiators or sources for germanium centered radicals.<sup>8</sup> Thus, based on the observation that the cyclic silenolates **3** can be prepared and isolated with remarkable selectivity, we decided to attempt the synthesis of the related germanium based species and to study their chemical and structural properties. In this paper we report on the synthesis, the characterization and the molecular structures of the first isolated germenolates **5a-c** and the conversion of **5a,b** to the corresponding germenes  $(\text{Me}_3\text{Si})_2\text{Ge}(\text{Si}_2\text{Me}_4)_2\text{Ge}=\text{C}(\text{OSiMe}_3)\text{R}$  ( $\text{R} = \text{Mes}, o\text{-Tol}$ ) **6a,b** which represent the first examples of isolated stable germenes with exocyclic structures.

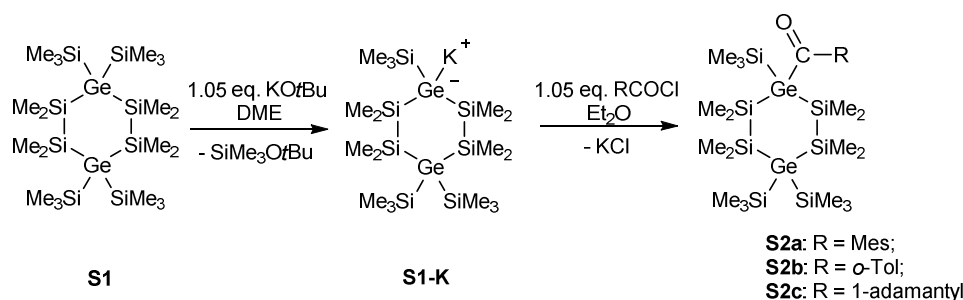
Chart 2.



## 2.5.3 Results and Discussion

### 2.5.3.1 Synthesis of Germenolates

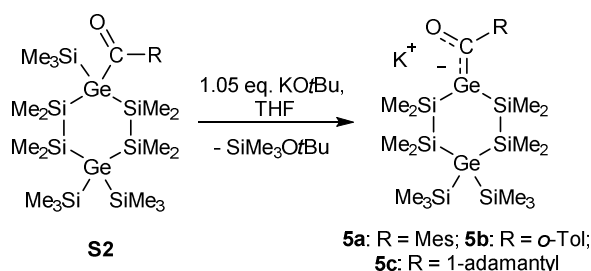
Standard procedures for cyclopolysilane synthesis were employed to prepare the cyclic acylgermanes **S2a-c** according to Scheme 1 following a synthetic protocol already used for the synthesis of the corresponding acylcyclohexasilanes.<sup>9;10</sup>



**Scheme 1.** Synthesis of cyclic acylgermanes **S2a-c**.

The air-stable and crystalline target compounds were obtained in isolated yields of >65 %. Analytical and spectroscopic data which perfectly support the structural assignment are given in the Experimental Section together with experimental details. The molecular structures of **S2a-c** as determined by single-crystal X-ray crystallography are included in the Supporting Information.

The reactivity pattern of **S2a-c** closely resembles the one found for the corresponding cyclic acylsilanes.<sup>4</sup> Thus, upon the addition of 1.05 equiv. of KOtBu to THF solutions of **S2a-c** at  $-70\text{ }^{\circ}\text{C}$  we observed the facile and quantitative formation of the cyclic germenolates **5a-c** (Scheme 2) as indicated by a  $\sim 40$  ppm downfield shift of the C=O  $^{13}\text{C}$  resonance line and by the disappearance of the  $^{13}\text{C}$  and  $^{29}\text{Si}$  NMR signals of one  $\text{Me}_3\text{Si}$  group in the region  $\delta^{29}\text{Si} = 1.09 - 4.47$  ppm and  $\delta^{13}\text{C} = 2.1 - 4.3$  ppm.



**Scheme 2.** Synthesis of cyclic germenolates **5a-c**.

The resulting red solutions can be used directly for further derivatization or can be stored at  $-30\text{ }^{\circ}\text{C}$  in the absence of air even for several months. Upon the attempted removal of the solvents and other volatile components in vacuo, however, the products immediately decomposed to uncharacterized material.

After addition of [18]crown-6 in toluene we were able to grow crystals of the 1 : 1 [18]crown-6 adducts of **5b** and **5c** which were suitable for single crystal X-ray crystallography. The molecular structures are depicted in Figure 1. Table 1 shows selected bond lengths and the sum of valence angles around the central Ge-C moiety together with the corresponding data of the structurally related K-silenolates **3b,c** and calculated values derived from the B3LYP/6-31+G(d,p) optimized structures. As

can be seen from Table 1 excellent agreement between the experimental and the calculated data is observed throughout.

For cyclic silenolates **3** different modes of coordination of the  $K^+$  counter ion for species with an alkyl or an aryl group attached to the carbonyl C-atom recently have been detected.<sup>5</sup> Based on the significantly larger value of  $\Sigma\alpha Si_1$  (326.8 vs. 316.7°), a considerably shortened  $Si_1-C_1$  bond (1.874 vs. 1.966 Å) and a slightly elongated C-O bond (1.260 vs. 1.244 Å) it has been concluded that species with aryl groups at the carbonyl C-atom exhibit increased contributions of the enol-form. In contrast, the germenolates **5b,c** are best described as acyl germanyl anions (keto-form I in chart 1) irrespective of the nature of the R-group at the carbonyl function.

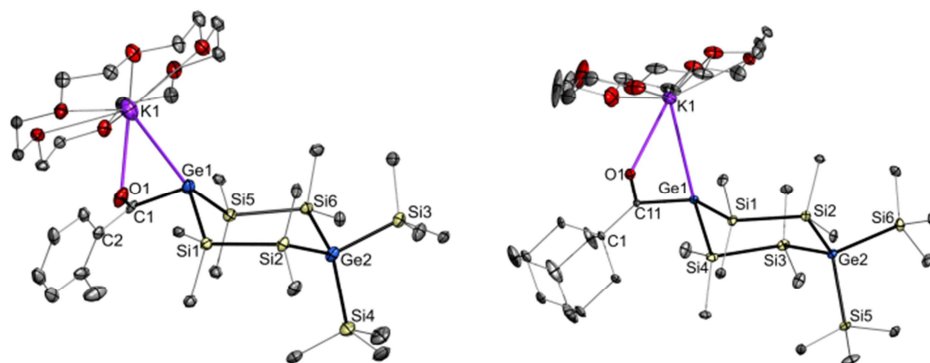


**Figure 1.** ORTEP diagram for compounds **5b** and **5c** (1:1 adducts with [18]crown-6). Thermal ellipsoids are depicted at the 50 % probability level. Hydrogen atoms are omitted for clarity.

**Table 1.** Experimental and B3LYP/6-31+G(d,p) calculated selected bond lengths  $d$  [Å] and sum of valence angles  $\Sigma\alpha(E1)$  [deg] and NPA charges calculated at the PCM B3LYP/6-31+G(d,p) level in THF as a solvent for the K-silenolates **1**, **3b,c** and the K-germenolates **5b,c**.

	<b>3b</b>		<b>3c</b>		<b>5b</b>		<b>5c</b>		<b>1<sup>a</sup></b>	
	exp. <sup>b</sup>	calc.	exp. <sup>b</sup>	calc.	exp.	calc.	exp.	calc.	exp.	calc.
$d C_1-E_1$	1.874(2)	1.924	1.966(2)	1.960	2.007(5)	2.003	2.063(2)	2.025	1.926(3)	1.946
$d C_1-O_1$	1.260(2)	1.250	1.244(2)	1.242	1.236(6)	1.243	1.231(3)	1.238	1.245(3)	1.239
$d K_1-O_1$	2.701(1)	-	2.743(1)	-	2.733(4)	-	2.740(2)	-	2.846(2)	-
$d K_1-E_1$	4.935(1)	-	3.603(2)	-	3.855(6)	-	3.613(9)	-	3.714(1)	-
$d K_1-C_2$	3.257(2)	-	4.899(2)	-	4.582(5)	-	4.926(2)	-	-	-
$\Sigma\alpha E_1$	326.8	321.3	316.7	310.5	304.6	306.1	310.7	310.7	317.8	307.0
$q(E1)$	-	-0.12	-	-0.16	-	-0.19	-	-0.22	-	-0.12

<sup>a</sup> data taken from ref. 3. <sup>b</sup> data taken from ref. 5.

C-O bond lengths observed for **5b,c** are nearly identical ( $\Delta d(C-O) = 0.005$  Å) with numerical values close to the ones measured for the alkyl substituted keto-type silenolates **1** and **3c**. The  $Ge_1-C_1$  bond in **5c** is significantly elongated relative to **5b** (2.063 vs. 2.007 Å) very likely for steric reasons, because both values closely match the C-Ge single bond distances in the acylgermanes **S2b,c** (2.050 and 2.009 Å)<sup>11</sup>. Again in close analogy to **1** and **3c** the  $K^+$  cation coordinates simultaneously to Ge1 and O1 in **5b**

and **5c** as well with the O atom showing a closer contact than the Ge atom.<sup>3</sup> Furthermore, the central Ge-atoms of **5b,c** ( $\Sigma\alpha\text{Ge}_1 = 304.6$  and  $310.7^\circ$ ) are even more pyramidal than the central Si-atoms in the molecular structures of **1** and **3c** ( $\Sigma\alpha\text{Si}_1 = 317.8$  and  $316.7^\circ$ ). The natural population analysis (NPA) charges  $q(E_1)$  calculated at the PCM B3LYP/6-31+G(d,p) level in THF as a solvent, finally, are even larger for Ge<sub>1</sub> of **5b,c** ( $-0.19$  e;  $-0.22$  e) as compared to Si<sub>1</sub> of **1** ( $-0.12$  e)<sup>3</sup> and **3c** ( $-0.16$  e) which possibly at least to a certain extent reflects the higher electronegativity of Ge relative to Si. Alternatively, the larger concentration of electron density on Ge in **5b,c** relative to the silicon analogues might also be attributed to a weaker Ge=C bond due to poorer orbital overlap. The slightly higher negative charge placed on Ge<sub>1</sub> and Si<sub>1</sub> in **5c** and **3c** as compared to **5a,b** and **3a,b**, furthermore, might also be responsible for the observed reactivity differences between alkyl- and aryl substituted germenolates and silenolates versus chlorosilanes R<sub>3</sub>SiCl mentioned below.

NMR data also support the conclusion that the dominant structure of **5a-c** is the keto-form. In close analogy to Ottosson's keto-type silenolate **1** ( $\delta^{13}\text{C}_{\text{C=O}} = 274.1$  ppm) all three compounds exhibit very similar <sup>13</sup>C chemical shifts for the carbonyl C atom between  $\delta = 279.5$  and  $281.9$  ppm.<sup>3</sup> Furthermore, **5a-c** exhibit only two sharp SiMe<sub>2</sub> resonance lines in <sup>29</sup>Si-NMR at  $\delta = -27.9$  -  $-30.4$  ppm which clearly suggests free rotation around the Ge<sub>1</sub>-C<sub>1</sub> bond (compare Figure 2). In case of hindered rotation due to increased Ge=C double bond character at least the signal of the SiMe<sub>2</sub> groups adjacent to Ge(1) is likely to split up into two lines or to show some line broadening. In fact, the germene **6a** actually exhibits two individual <sup>29</sup>Si resonances for the magnetically non-equivalent  $\alpha$ -SiMe<sub>2</sub> groups while in the <sup>1</sup>H and <sup>29</sup>Si spectra of the aryl substituted cyclic silenolate **3a** one of the SiMe<sub>2</sub> signals appears unusually broadened. Similar features are apparent in the NMR spectra of Li-silenolates (Me<sub>3</sub>Si)<sub>2</sub>SiC(OLi)R (R = *t*Bu, Ad, *o*-Tol, Mes) and have been rationalized in terms of increased double bond character of the central Si-C bond in the aryl substituted derivatives.<sup>2e</sup>

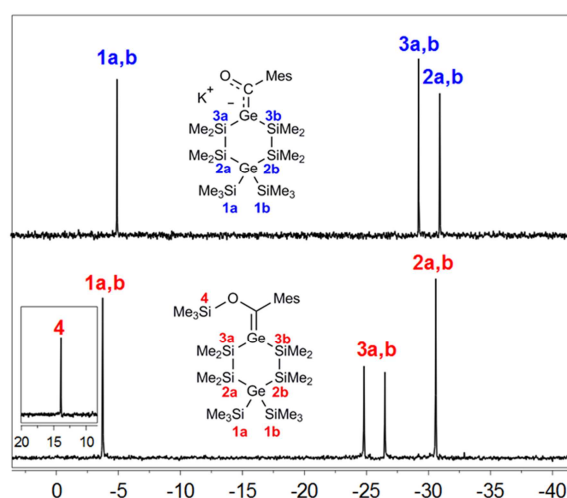


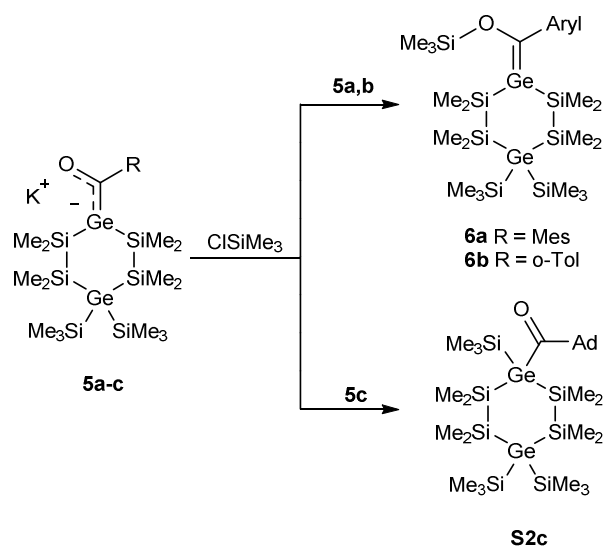
**Figure 2.** INEPT <sup>29</sup>Si NMR spectra of **5a** (top) and **6a** (bottom). The SiMe<sub>2</sub> groups 3a,b exhibit two resonance lines due to hindered rotation around the Ge=C bond.

### 2.5.3.2 Synthesis of Exocyclic Germenes

The reactivity of **5a-c** versus chlorosilanes parallels the one observed earlier for type **1** and **3** alkali metal silenolates.<sup>2e,5</sup> Thus, **5c** with an alkyl group attached to the carbonyl moiety reacted with an equimolar amount of Me<sub>3</sub>SiCl at 0 °C in THF under formation of the acylgermane **S2c**, while the aryl-substituted compounds **5a,b**, under the same conditions, exclusively afforded the O-silylated germenes **6a,b** (compare Scheme 3). After crystallization from diethyl ether, we were able to obtain yellow crystals of pure **6a** in 95 % yield and to characterize the remarkably stable germene structurally and spectroscopically. In contrast to **6a**, which can be stored at -30 °C for several months without any noticeable decomposition, it was not possible to separate pure **6b** from several unidentified by-products because it decomposed rather rapidly, even at -70 °C, possibly due to incomplete steric protection of the Ge=C double bond.

The NMR data of **6a** are consistent with the structural assignment to a Brook-type germene. Spectra and assignment can be found in the Experimental Section and in the Supporting Information. A <sup>13</sup>C signal characteristic of the Ge=C double bond was observed at  $\delta(^{13}\text{C}) = 210.0$  ppm. The <sup>1</sup>H and <sup>13</sup>C spectra, furthermore, display sharp distinct absorptions for each of the four endocyclic SiMe<sub>2</sub> groups. The <sup>29</sup>Si spectrum only shows three SiMe<sub>2</sub> signals, one resonance line each for Si<sub>2</sub> and Si<sub>4</sub> and one superimposed signal for Si<sub>3</sub> and Si<sub>5</sub> (compare Figure 2) which are magnetically non-equivalent due to the lack of freedom of rotation around the germanium-carbon double bond.

The molecular structure of **6a** as determined by single crystal X-ray crystallography is depicted in Figure 3 together with selected bond lengths and bond and torsion angles. The Ge=C distance of 1.84 Å is similar to the values found in other germenes (1.77 - 1.86 Å).<sup>12</sup>



**Scheme 3.** Reaction of **5a-c** with ClSiMe<sub>3</sub>.

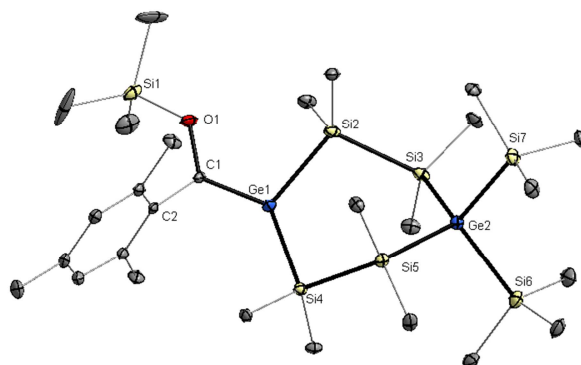


**Figure 3.** ORTEP diagram for compound **6a**. Thermal ellipsoids are depicted at the 50 % probability level. Hydrogen atoms are omitted for clarity. Selected bond lengths [Å] and bond and torsion angles [deg] with estimated standard deviations: Ge(1)-C(1) 1.835(2), C(1)-O(1) 1.388(3),  $\Sigma\alpha_{\text{Ge}(1)}$  351.7,  $\Sigma\alpha_{\text{C}(1)}$  360.0, Si(4)-Ge(1)-C(1)-C(2) -18.11, Si(2)-Ge(1)-C(1)-O(1) 9.96.

As compared to the corresponding cyclic silene  $(\text{Me}_3\text{Si})_2\text{Si}(\text{Si}_2\text{Me}_4)_2\text{Si}=\text{C}(\text{OSi}i\text{Pr}_3)\text{Mes}$  (**7**),<sup>5</sup> the double bond in **6a** is considerably more distorted as indicated by the larger torsion angles Si<sub>4</sub>-Ge<sub>1</sub>-C<sub>1</sub>-C<sub>2</sub> and Si<sub>2</sub>-Ge<sub>1</sub>-C<sub>1</sub>-O<sub>1</sub> and by the larger pyramidalization of Ge<sub>1</sub> ( $\Sigma\alpha_{\text{Ge}_1} = 351.7^\circ$  vs.  $\Sigma\alpha_{\text{Si}_1} = 357.8^\circ$  in **7**). Otherwise the Si<sub>4</sub>Ge<sub>2</sub> ring in **6a** adopts a twisted conformation with unexceptional endocyclic bond distances and angles.



### 2.5.3.3 UV-Vis Absorption Spectra

To gain more insight into the electronic nature of **5a-c** and **6a**, UV-Vis absorption spectra were recorded and the longest wavelength absorption bands were assigned for the conformational minimum structures via TDDFT-PCM calculations at the B3LYP/6-31+G(d,p) level. The obtained experimental and computational data are summarized in Table 2 and show reasonable agreement.

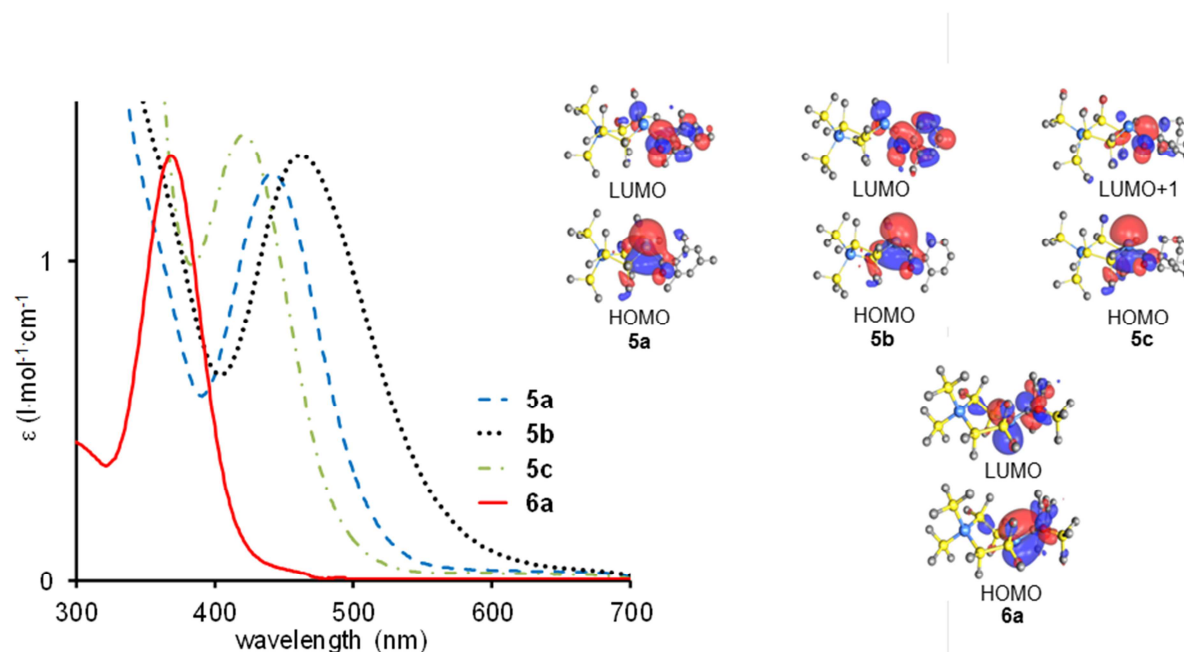


**Figure 4.** UV-Vis absorption spectra of **5a-c** (THF solution;  $c = 5 \cdot 10^{-4}$  M) and **6a** (n-hexane solution;  $c = 1 \cdot 10^{-4}$  M) and frontier orbitals calculated at the TDDFT-PCM B3LYP/6-31+G(d,p) level of theory in THF for **5a-c** and heptane for **6a**.

Figure 4 shows the experimental UV-Vis absorption spectra together with the calculated frontier orbitals. The high intensity absorption band in the UV-Vis spectrum of **6a** centered at 368 nm is easily assigned to a  $\pi \rightarrow \pi^*$  transition within the Ge=C double bond. This band is responsible for the yellow color of **6a** and appears slightly shifted to the red by 4 nm as compared to the corresponding band in the absorption spectrum of the isostructural silene.<sup>5</sup> All three germenolates exhibit an intense absorption maximum between 422-463 nm which is red-shifted in the order **5c**  $\rightarrow$  **5a**  $\rightarrow$  **5b**. According to our calculations at the TDDFT-PCM B3LYP/6-31+G(d,p) level of theory in THF, these bands are unequivocally assigned to the HOMO  $\rightarrow$  LUMO transition for **5a,b** while for **5c** the calculated HOMO  $\rightarrow$  LUMO+1 transition primarily contributes to the observed absorption band. The HOMOs of **5a-c** (Figure 4) mainly correspond to the  $p_z$  orbital of the germanium atom with little variation in shape and energy. Upon excitation, electron density is displaced into the  $\pi^*$  orbital of the carbonyl moiety (LUMO or LUMO+1). In the LUMOs of the aryl substituted species **5a,b** our calculations additionally showed considerable conjugation of the carbonyl and the aromatic  $\pi$  systems which are not possible for the alkyl substituted germenolate **5c**. These conjugational type interactions are even enhanced in the case of **5b** due to the smaller dihedral angle between the C=O group and the

aromatic ring plane. As a consequence the empty orbitals (LUMO or LUMO+1) are stabilized in the order **5c** → **5a** → **5b** which results in smaller excitation energies and in the observed bathochromic shifts of the corresponding absorption bands.

**Table 2.** Experimental and TDDFT-PCM B3LYP/6-31+G(d,p) calculated longest wavelength absorption maxima  $\lambda$  [nm], extinction coefficients  $\epsilon$  [ $\text{L}\cdot\text{mol}^{-1}\cdot\text{cm}^{-1}$ ] resp. oscillator strengths  $f$  for **5a-c** (THF) and **6a** (heptane).

	$\lambda_{\text{max}}$ exp. ( $\epsilon$ )	$\lambda_{\text{max}}$ calc. ( $f$ )	Assignment	
<b>5a</b>	442	426	$p_z \rightarrow \pi^*$	HOMO → LUMO
	(2550)	(0.1341)	(CO/Aryl)	
<b>5b</b>	463	496	$p_z \rightarrow \pi^*$	HOMO → LUMO
	(2660)	(0.1312)	(CO/Aryl)	
<b>5c</b>	422	412	$p_z \rightarrow \pi^*$	HOMO → LUMO+1
	(2790)	(0.0609)	(CO)	
<b>6a</b>	368	401	$\pi \rightarrow \pi^*$	HOMO → LUMO
	(13050)	(0.4387)	(Ge=C)	

## 2.5.4 Conclusion

In summary, we have demonstrated that stable germenolates can be synthesized and isolated by crystallization if the Ge atom is incorporated into a cyclohexasilane ring. In contrast to the behavior of the isostructural silenolates the resulting germenolates **5a-c** almost exclusively exhibit the character of acyl germyl anions with a negatively charged Ge atom, a Ge-C single bond and a C=O double bond irrespective of the nature of the substituent attached to the carbonyl group. This finding allows to conclude that germenolates like most silenolates are structurally dissimilar to enolates. Furthermore, it has been shown that the reaction of the aryl substituted species **5a,b** towards  $\text{ClSiMe}_3$  straightforwardly affords the first isolable Brook-type germene **6a** with an exocyclic structure. UV-Vis absorption spectroscopy measurements, finally, indicated that light absorption and color of **5a-c** can be tuned by the substitution pattern and the geometry of the  $-\text{C}(\text{O})\text{R}$  moiety.

## 2.5.5 Experimental Section

### 2.5.5.1 General Considerations

All experiments were performed under a nitrogen atmosphere using standard Schlenk techniques. Solvents were dried using a column solvent purification system.<sup>13</sup> Commercial KO $t$ Bu (97 %), ClCOMes (99 %), ClCOAd (98 %), ClCO $o$ -Tol (99 %), Me<sub>3</sub>SiCl (97 %) and [18]crown-6 (99 %) were used as purchased. <sup>1</sup>H (299.95 MHz), <sup>13</sup>C (75.43 MHz) and <sup>29</sup>Si (59.59 MHz) NMR spectra were recorded on a Varian INOVA 300 spectrometer and referenced versus TMS using the internal <sup>2</sup>H-lock signal of the solvent. 1,1,4,4-Tetrakis(trimethylsilyl)-2,2,3,3,5,5,6,6-octamethyl-1,4-digermacyclohexasilane (**S1**) was synthesized according to published procedures.<sup>9a</sup> HRMS spectra were run on a Kratos Profile mass spectrometer equipped with a solid probe inlet. Infrared spectra were obtained on a Bruker Alpha-P Diamond ATR Spectrometer from the solid sample. Melting points were determined using a Buechi 535 apparatus and are uncorrected. Elemental analyses were carried out on a Hanau Vario Elementar EL apparatus. UV absorption spectra were recorded on a Perkin Elmer Lambda 5 spectrometer.

### Synthesis of S2a

2.00 g (2.98 mmol) of **S1** and 0.35 g (3.13 mmol) of KO $t$ Bu were dissolved in 20 mL of DME. After stirring for 60 min **S1** was completely consumed as monitored by <sup>29</sup>Si-NMR spectroscopy. This freshly prepared solution was slowly added to a solution of 0.65 g (3.13 mmol) of 2,4,6-trimethylbenzoylchloride in 50 mL of diethyl ether at -80 °C. Subsequently the mixture was stirred for another 30 min at -80 °C, allowed to warm to room temperature and finally stirred for additional 60 minutes. After aqueous work-up with 100 mL of 3 % sulfuric acid, the organic layer was separated, dried over Na<sub>2</sub>SO<sub>4</sub> and the solvents were stripped off with a rotary evaporator. Drying in vacuo (0.02 mbar) and crystallization from acetone solution at -30 °C afforded 1.44 g (1.93 mmol) (72 %) of analytically pure **S2a** as yellow crystals.

mp: 110-112 °C. Anal. Calc. for C<sub>27</sub>H<sub>62</sub>Ge<sub>2</sub>OSi<sub>7</sub>: C, 43.55; H, 8.39. Found: C, 43.69; H, 8.55 %. <sup>29</sup>Si-NMR (C<sub>6</sub>D<sub>6</sub>, TMS, ppm): -1.09, -1.13, -2.70 (SiMe<sub>3</sub>); -28.37, -29.44 (SiMe<sub>2</sub>). <sup>13</sup>C-NMR (C<sub>6</sub>D<sub>6</sub>, TMS, ppm): 243.9 (GeC=O); 147.3, 137.3, 130.7, 128.7 (Mes-C); 20.6, 19.6 (Mes-CH<sub>3</sub>); 4.2, 4.1, 2.1 (Si(CH<sub>3</sub>)<sub>3</sub>); -0.3, -0.6, -1.3, -2.1 (Si(CH<sub>3</sub>)<sub>2</sub>). <sup>1</sup>H-NMR (C<sub>6</sub>D<sub>6</sub>, TMS, ppm): 6.56 (s, 2H, Mes-H); 2.20 (6H, s, ortho-CH<sub>3</sub>); 2.02 (s, 3H, para-CH<sub>3</sub>); 0.59, 0.49, 0.42, 0.40 (s, 6H each, Si(CH<sub>3</sub>)<sub>2</sub>); 0.36, 0.34, 0.12 (s, 9H each, Si(CH<sub>3</sub>)<sub>3</sub>); IR (neat): ν(C=O) = 1635, 1623, 1608 (m) cm<sup>-1</sup>. HRMS: calc. for [C<sub>27</sub>H<sub>62</sub>Ge<sub>2</sub>OSi<sub>7</sub>]<sup>+</sup> (M<sup>+</sup>): 744.1628; found: 744.1638. UV-Vis: λ [nm] (ε [L·mol<sup>-1</sup>·cm<sup>-1</sup>]) = 256 (39580), 365 (259), 382 (295), 400 (280).

### Synthesis of S2b

The same procedure as for **S2a** was followed with 2.00 g (2.98 mmol) of **S1**, 0.35 g (3.13 mmol) of KO $t$ Bu and 0.48 g (3.13 mmol) of 2-methylbenzoylchloride. Yield: 1.38 g (1.94 mmol) (65 %) of analytically pure **S2b** as yellow crystals.

mp: 111-112 °C. Anal. Calc. for C<sub>25</sub>H<sub>58</sub>Ge<sub>2</sub>OSi<sub>7</sub>: C, 41.90; H, 8.16. Found: C, 42.10; H, 8.21 %. <sup>29</sup>Si-NMR (C<sub>6</sub>D<sub>6</sub>, TMS, ppm): -2.92, -3.22, -3.70 (SiMe<sub>3</sub>); -30.05, -30.63 (SiMe<sub>2</sub>). <sup>13</sup>C-NMR (C<sub>6</sub>D<sub>6</sub>, TMS, ppm): 238.4 (GeC=O); 145.3, 133.8, 131.6, 130.4, 130.0, 125.0 (*o*-Tol-C); 20.1 (*o*-Tol-CH<sub>3</sub>); 4.2, 2.5 (Si(CH<sub>3</sub>)<sub>3</sub>); -0.4, -0.5, -1.6, -2.2 (Si(CH<sub>3</sub>)<sub>2</sub>). <sup>1</sup>H-NMR (C<sub>6</sub>D<sub>6</sub>, TMS, ppm): 7.62-6.84 (4H, *o*-Tol-H); 2.42 (s, 3H, *o*-Tol-CH<sub>3</sub>); 0.49, 0.39 (s, 6H each Si(CH<sub>3</sub>)<sub>2</sub>); 0.46 (s, 12H, Si(CH<sub>3</sub>)<sub>2</sub>); 0.31, 0.30, 0.26 (s, 9H each Si(CH<sub>3</sub>)<sub>3</sub>); IR (neat): ν(C=O) = 1619 (m) cm<sup>-1</sup>. HRMS: calc. for [C<sub>25</sub>H<sub>58</sub>Ge<sub>2</sub>OSi<sub>7</sub>]<sup>+</sup> (M<sup>+</sup>): 716.1315; found: 716.1324. UV-Vis: λ [nm] (ε [L·mol<sup>-1</sup>·cm<sup>-1</sup>]) = 247 (15690), 288 (3198), 411 (180).

### Synthesis of S2c

The same procedure as for **S2a** was followed with 2.55 g (3.80 mmol) of **S1**, 0.45 g (3.99 mmol) of KO<sup>*t*</sup>Bu and 0.79 g (3.99 mmol) of 1-adamantoylchloride. Yield: 2.28 g (3.00 mmol) (79 %) of analytically pure **S2c** as colorless crystals.

mp: 145-147 °C. Anal. Calc. for C<sub>28</sub>H<sub>66</sub>Ge<sub>2</sub>OSi<sub>7</sub>: C, 44.21; H, 8.75. Found: C, 44.10; H, 8.90 %. <sup>29</sup>Si-NMR (C<sub>6</sub>D<sub>6</sub>, TMS, ppm): -2.93, -3.76, -4.47 (SiMe<sub>3</sub>); -30.47, -30.64 (SiMe<sub>2</sub>). <sup>13</sup>C-NMR (C<sub>6</sub>D<sub>6</sub>, TMS, ppm): 243.7 (GeC=O); 51.6, 37.2, 36.6, 28.1 (Ad-C); 4.3, 4.2, 3.3 (Si(CH<sub>3</sub>)<sub>3</sub>); -0.1, -0.3, -1.1, -1.4 (Si(CH<sub>3</sub>)<sub>2</sub>). <sup>1</sup>H-NMR (C<sub>6</sub>D<sub>6</sub>, TMS, ppm): 1.89, 1.73, 1.56 (s, 15H, Ad-CH); 0.54, 0.41 (s, 6H each, Si(CH<sub>3</sub>)<sub>2</sub>); 0.44 (s, 12H, Si(CH<sub>3</sub>)<sub>2</sub>); 0.36, 0.34, 0.32 (s, 9H each, Si(CH<sub>3</sub>)<sub>3</sub>); IR (neat): ν(C=O) = 1635 (m) cm<sup>-1</sup>. HRMS: calc. for [C<sub>28</sub>H<sub>66</sub>Ge<sub>2</sub>OSi<sub>7</sub>]<sup>+</sup> (M<sup>+</sup>): 760.1942; found: 760.1904. UV-Vis: λ [nm] (ε [L·mol<sup>-1</sup>·cm<sup>-1</sup>]) = 363 (299).

### Synthesis of 5a

300 mg (0.403 mmol) of **S2a** were dissolved in 4 mL of THF, cooled to -80 °C and 47.5 mg (0.420 mmol) of KO<sup>*t*</sup>Bu were added. After stirring for additional 30 minutes the mixture was allowed to warm to room temperature and finally stirred for an additional hour (the reaction mixture turned dark red). At this time reaction control by NMR spectroscopy showed clean conversion of the starting material to the desired germenolate **5a**, Me<sub>3</sub>SiO<sup>*t*</sup>Bu and Me<sub>3</sub>SiOSiMe<sub>3</sub>. Upon the attempted removal of the volatile components in vacuo **5a** decomposed to uncharacterized degradation products.

<sup>29</sup>Si-NMR (THF/D<sub>2</sub>O, TMS, ppm): -4.36 (SiMe<sub>3</sub>); -28.67, -30.38 (SiMe<sub>2</sub>). <sup>13</sup>C-NMR (THF/D<sub>2</sub>O, TMS, ppm): 281.6 (GeC=O); 152.4, 133.4, 129.9, 127.8 (Mes-C); 20.2, 19.9 (Mes-CH<sub>3</sub>); 4.1 (Si(CH<sub>3</sub>)<sub>3</sub>); 0.1, -0.3 (Si(CH<sub>3</sub>)<sub>2</sub>). <sup>1</sup>H-NMR (THF/D<sub>2</sub>O, TMS, ppm): 6.72 (s, 2H, Mes-*H*); 2.36 (s, 6H, ortho-CH<sub>3</sub>); 2.27 (s, 3H, para-CH<sub>3</sub>), 0.35 (b, 42H, Si(CH<sub>3</sub>)<sub>3</sub> + Si(CH<sub>3</sub>)<sub>2</sub>). UV-Vis: λ [nm] (ε [L·mol<sup>-1</sup>·cm<sup>-1</sup>]) = 442 (2546).

### Synthesis of 5b

The same procedure as for **5a** was followed with 210 mg (0.293 mmol) of **S2b** in 2 mL of THF and 34.5 mg (0.308 mmol) of KO<sup>*t*</sup>Bu.

<sup>29</sup>Si-NMR (THF/D<sub>2</sub>O, TMS, ppm): -4.35 (SiMe<sub>3</sub>); -28.93, -29.65 (SiMe<sub>2</sub>). <sup>13</sup>C-NMR (THF/D<sub>2</sub>O, TMS, ppm): 279.5 (GeC=O); 153.9, 129.8, 128.9, 126.2, 125.8, 124.1 (*o*-Tol-C); 19.2 (Mes-CH<sub>3</sub>); 4.1 (Si(CH<sub>3</sub>)<sub>3</sub>); 0.29, 0.31 (Si(CH<sub>3</sub>)<sub>2</sub>). <sup>1</sup>H-NMR (THF/D<sub>2</sub>O, TMS, ppm): 7.51-7.05 (m, 4H, *o*-Tol-*H*); 2.32 (s, 3H, ortho-CH<sub>3</sub>); 0.34 (s, 42H, Si(CH<sub>3</sub>)<sub>3</sub> + Si(CH<sub>3</sub>)<sub>2</sub>). UV-Vis: λ [nm] (ε [L·mol<sup>-1</sup>·cm<sup>-1</sup>]) = 463 (2664).

### Synthesis of **5c**

The same procedure as for **5a** was followed with 300 mg (0.394 mmol) of **S2c** in 4 mL of THF and 46.5 mg (0.414 mmol) of KO $t$ Bu.

$^{29}\text{Si}$ -NMR (THF/D $_2$ O, TMS, ppm): -4.21 (*SiMe* $_3$ ); -27.90, -29.91 (*SiMe* $_2$ ).  $^{13}\text{C}$ -NMR (THF/D $_2$ O, TMS, ppm): 281.9 (GeC=O); 51.8, 39.2, 37.5, 29.2 (Ad-C); 4.2 (*Si(CH* $_3$ ) $_3$ ); 1.9, 0.0 (*Si(CH* $_3$ ) $_2$ ).  $^1\text{H}$ -NMR (THF/D $_2$ O, TMS, ppm): 0.40, 0.37 (s, 12H each *Si(CH* $_3$ ) $_2$ ); 0.35 (s, 18H, *Si(CH* $_3$ ) $_3$ ); UV-Vis:  $\lambda$  [nm] ( $\epsilon$  [L $\cdot$ mol $^{-1}$  $\cdot$ cm $^{-1}$ ]) = 422 (2790).

### Synthesis of **6a**

46.0 mg (0.423 mmol) of Me $_3$ SiCl were added dropwise at 0 °C to a solution of **5a** in 4 mL of THF freshly prepared from 300 mg (0.403 mmol) of **S2a** and 47.5 mg (0.423 mmol) of KO $t$ Bu according to the procedure described above. Immediately the red solution turned yellow. After removal of the volatile components in vacuo the remaining yellow solid was dissolved in heptane, filtered over dry celite and the solvent was stripped off again. Recrystallization from diethyl ether afforded 285 mg (95 %) of the analytically pure germene **6a** as yellow crystals.

mp: 88-89 °C (dec.). Anal. Calc. for C $_{27}$ H $_{62}$ Ge $_2$ OSi $_7$ : C, 43.55; H, 8.39. Found: C, 43.32; H, 7.94 %.  $^{29}\text{Si}$ -NMR (C $_6$ D $_6$ , TMS, ppm): 13.88 (OSiMe $_3$ ); -3.73 (*SiMe* $_3$ ); -24.81, -26.49, -30.59 (*SiMe* $_2$ ).  $^{13}\text{C}$ -NMR (C $_6$ D $_6$ , TMS, ppm): 210.0 (Ge=C); 143.9, 136.3, 134.7, 128.2 (Mes-C); 21.0, 20.8 (Mes-CH $_3$ ); 3.9 (*Si(CH* $_3$ ) $_3$ ); 0.4, -0.8, -0.85, -1.5, -2.6 (*Si(CH* $_3$ ) $_2$ ).  $^1\text{H}$ -NMR (C $_6$ D $_6$ , TMS, ppm): 6.73 (s, 2H, Mes-*H*); 2.49 (s, 6H, ortho-*CH* $_3$ ); 2.06 (s, 3H, para-*CH* $_3$ ); 0.69, 0.43, 0.09, -0.02 (s, 6H each *Si(CH* $_3$ ) $_2$ ); 0.30 (s, 27H *Si(CH* $_3$ ) $_3$ ); IR (neat):  $\nu$ (Ge=C) = 1134 (m) cm $^{-1}$ . HRMS: calc. for [C $_{27}$ H $_{62}$ Ge $_2$ OSi $_7$ ] $^+$  (M $^+$ ): 744.1628; found: 744.1665. UV-Vis:  $\lambda$  [nm] ( $\epsilon$  [L $\cdot$ mol $^{-1}$  $\cdot$ cm $^{-1}$ ]) = 369 (13054).

### Synthesis of **6b**

The same procedure as for **6a** was followed with 48.0 mg (0.440 mmol) of Me $_3$ SiCl and a solution of **5b** in 4 mL of THF freshly prepared from 300 mg (0.419 mmol) of **S2b** and 49.3 mg (0.440 mmol) of KO $t$ Bu. The target germene **6b** was formed along with several unidentified by-products. Purification of the crude material by crystallization was not successful.

$^{29}\text{Si}$ -NMR (C $_6$ D $_6$ , TMS, ppm): 16.09 (OSiMe $_3$ ); -3.72 (*SiMe* $_3$ ); -25.10, -30.48, -30.54 (*SiMe* $_2$ ).  $^{13}\text{C}$ -NMR (C $_6$ D $_6$ , TMS, ppm): 214.8 (Ge=C).

#### 2.5.5.2 X-ray Crystallography:

For X-ray structure analysis suitable crystals were mounted onto the tip of glass fibers using mineral oil. Data collection was performed on a Bruker Kappa Apex II CCD diffractometer at 100 K using graphite-monochromated Mo K $\alpha$  ( $\lambda$  = 0.71073 Å) radiation. Details of the crystal data and structure refinement are provided in the Supporting Information. The SHELX version 6.1 program package was used for the structure solution and refinement.<sup>14</sup> Absorption corrections were applied using the SADABS program.<sup>15</sup> All non-hydrogen atoms were refined with anisotropic displacement parameters. Hydrogen atoms were included in the refinement at calculated positions using a riding model as implemented in the SHELXTL program. Disorder for compound **5b** and **5c** was handled by modeling

the occupancies of the individual orientations using free variables to refine the respective occupancy of the affected fragments. For **5b**, disordered positions for two silicon atoms with respective CH<sub>3</sub> groups in the main heterocycle were refined using 60/40 split positions. Disorder of the SiMe<sub>3</sub> moiety and a CH<sub>3</sub> groups was refined using split positions, 60/40 and 50/50 respectively. For **5c**, disordered positions for two carbon in the [18]crown-6 moiety were refined using 68/32 split positions. Crystallographic data (excluding structure factors) have been deposited with the Cambridge Crystallographic Data Centre as supplementary publications CCDC-1060653 (**S2a**), CCDC-1060654 (**S2b**), CCDC-1060655 (**S2c**), CCDC-1060656 (**5b**), CCDC-1060657 (**5c**), CCDC-1060658 (**6a**). Copies of the data can be obtained free of charge on application to The Director, CCDC, 12 Union Road, Cambridge CB2 1EZ, UK (fax (internat.) +44-1223/336-033; e-mail deposit@ccdc.cam.ac.uk).

### 2.5.5.3 Computational Methods

All computational studies were executed on a computing cluster with blade architecture using the Gaussian09 software package.<sup>16</sup> In every listed calculation the Becke's three-parameter hybrid functional<sup>17</sup> for exchange and the Lee-Yang-Parr nonlocal correlation functional<sup>18</sup> (B3LYP) together with the 6-31+G(d,p) basis set<sup>19</sup> of Pople and coworkers for all atoms were used. Molecular geometries of the anions **3b,c** and **5a-c** were fully optimized in the gas phase and minimum structures were characterized by harmonic frequency calculations. The vertical excitations of conformational minimum structures were calculated via time-dependent DFT (TDDFT) with the same combination of functional and basis set, additionally using the polarized continuum model (PCM)<sup>20</sup> for solvation effects. Tetrahydrofuran was used as a solvent for the germenolate structures **5a-c**, heptane for germenone **6a**. Test calculations suggested only minimal changes in calculated energies of conformers when other hybrid functionals (i.e. mPW1PW91),<sup>21</sup> larger basis sets (i.e. 6-31+G(2d,p), 6-311+G(d,p) and 6-311++G(d,p))<sup>19</sup> or structures with potassium as the counter ion for the germenolates **5a-c** were employed. Additionally vertical excitation energies could not be further improved when long range corrected hybrid functionals or larger basis sets were applied (i.e. TDDFT-PCM CAM-B3LYP/6-31+G(d,p)//B3LYP/6-31+G(d,p), TDDFT-PCM B3LYP/6-31+G(2d,p)//B3LYP/6-31+G(d,p) and TDDFT-PCM CAM-B3LYP/6-31+G(2d,p)//B3LYP/6-31+G(d,p)).<sup>18-20,22</sup> If not explicitly mentioned, all molecular orbitals were plotted using the Gabedit software package<sup>23</sup> with iso-values of 0.025. Natural population analysis (NPA) charges for the germenolates **5b,c** and the silanolate **3c** were calculated at the PCM B3LYP/6-31+G(d,p) level of theory in THF as a solvent.

## 2.5.6 References

- <sup>1</sup> For general reviews about enolates, see e.g.: a) D. Stolz, U. Kazmaier in *The Chemistry of Metal Enolates, Part 1* (Eds.: Z. Rappoport, J. Zabicky), Wiley, Hoboken, (2009), pp. 355-411. b) P. Veya, C. Floriani, A. Chiessi-Villa, C. Rizzoli, *Organometallics* 13 (1994) 214; c) D. Seebach, *Angew. Chem.* 100 (1988) 1685; *Angew. Chem. Int. Ed. Engl.* 27 (1988) 1624
- <sup>2</sup> a) J. Ohshita, H. Sakurai, S. Masaoka, M. Tamai, A. Kunai, M. Ishikawa, *J. Organomet. Chem.* 633 (2001) 131; b) J. Ohshita, M. Tamai, H. Sakurai, A. Kunai, *Organometallics* 20 (2001) 1065; c) J. Ohshita, H. Sakurai, Y. Tokunaga, A. Kunai, *Organometallics* 18 (1999) 4545; d) J. Ohshita, S. Masaoka, Y. Morimoto, M. Sano, M. Ishikawa, *Organometallics* 16 (1997) 1123; e) J. Ohshita, Y. Masaoka, S. Masaoka, M. Hasebe, M. Ishikawa, A. Tachibana, T. Yano, T. Yamabe, *Organometallics* 15 (1996) 3136; f) J. Ohshita, S. Masaoka, M. Ishikawa, *Organometallics* 15 (1996) 2198; g) J. Ohshita, Y. Masaoka, S. Masaoka, M. Ishikawa, A. Tachibana, T. Yano, T. Yamabe, *J. Organomet. Chem.* 473 (1994) 15; h) D. Bravo-Zhivotovskii, Y. Apeloig, Y. Ovchinnikov, V. Igonin, Y. T. Struchkov, *J. Organomet. Chem.* 446 (1993) 123
- <sup>3</sup> T. Guliashvili, I. El-Sayed, A. Fischer, H. Ottosson, *Angew. Chem. Int. Ed.* 42 (2003) 1640;
- <sup>4</sup> R. Dobrovetsky, L. Zborovsky, D. Sheberla, M. Botoshansky, D. Bravo Zhivotovskii, Y. Apeloig, *Angew. Chem. Int. Ed.* 49 (2010) 4084
- <sup>5</sup> M. Haas, R. Fischer, M. Flock, S. Mueller, M. Rausch, R. Saf, A. Torvisco, H. Stueger, *Organometallics* 33 (2014) 5956
- <sup>6</sup> A. M. Eklöf, H. Ottosson, *Tetrahedron* 65 (2009) 5521
- <sup>7</sup> a) I. S. Biltueva, D. A. Bravo-Zhivotovskii, I. D. Kalikhman, V. Yu. Vitkovskii, S. G. Shevchenko, N. S. Vyazankin, M. G. Voronkov, *J. Organomet. Chem.* 368 (1989) 163; b) I. S. Biltueva, D. A. Bravo-Zhivotovskii, I. D. Kalikhman, N. S. Vyazankin, M. G. Voronkov, *Izv. Akad. Nauk SSSR, Seriya Khimicheskaya* (1988) 1947
- <sup>8</sup> a) D. Neshchadin, A. Rosspeintner, M. Griesser, B. Lang, S. Mosquera-Vazquez, E. Vauthey, V. Gorelik, R. Liska, C. Hametner, B. Ganster, R. Saf, N. Moszner, G. Gescheidt, *J. Am. Chem. Soc.* 135 (2013) 17314; b) V. Y. Lee, A. Sekiguchi, *Organometallic Compounds of Low-Coordinate Si, Ge, Sn and Pb: From Phantom Species to Stable Compounds*; Wiley & Sons Inc., Chichester, (2010). c) J. Lalevée, X. Allonas, J. P. Fouassier, *Chem. Phys. Lett.* 469 (2009) 298; d) B. Ganster, U. K. Fischer, N. Moszner, R. Liska, *Macromolecules* 41 (2008) 2394
- <sup>9</sup> a) J. Hlina, R. Zitz, H. Wagner, F. Stella, J. Baumgartner, C. Marschner, *Inorg. Chim. Acta* 422 (2014) 120; b) R. Fischer, T. Konopa, S. Ully, J. Baumgartner, C. Marschner, *J. Organomet. Chem.* 685 (2003) 79
- <sup>10</sup> H. Stueger, B. Hasken, M. Haas, M. Rausch, R. Fischer, A. Torvisco, *Organometallics* 33 (2014) 231
- <sup>11</sup> for structural data of **S2b,c** see Supporting Information
- <sup>12</sup> a) V. Y. Lee, A. Sekiguchi, *Organometallics* 23 (2004) 2822; b) N. Tokitoh, R. Okazaki, in Z. Rappoport, (Ed.), *The Chemistry of Organic Germanium, Tin and Lead Compounds*, Vol. 2, Part 1, Wiley, Chichester, (2002), 855-870. c) K. M. Baines, W. G. Stibbs, *Coord. Chem. Rev.* 145 (1995) 157
- <sup>13</sup> A. B. Pangborn, M. A. Giardello, R. H. Grubbs, R. K. Rosen, F. J. Timmers, *Organometallics* 15 (1996) 1518
- <sup>14</sup> SHELX and SHELXL PC: VERSION 5.03, Bruker AXS, Inc., Madison, WI, (1994)
- <sup>15</sup> SADABS: Area-detection Absorption Correction: Bruker AXS Inc., Madison, WI, (1995)
- <sup>16</sup> M. J. Frisch, G. W. Trucks, H. B. Schlegel, G. E. Scuseria, M. A. Robb, J. R. Cheeseman, G. Scalmani, V. Barone, B. Mennucci, G. A. Petersson, H. Nakatsuji, M. Caricato, X. Li, H. P.

- Hratchian, A. F. Izmaylov, J. Bloino, G. Zheng, J. L. Sonnenberg, M. Hada, M. Ehara, K. Toyota, R. Fukuda, J. Hasegawa, M. Ishida, T. Nakajima, Y. Honda, O. Kitao, H. Nakai, T. Vreven, Jr., J. A. Montgomery, J. E. Peralta, F. Ogliaro, M. Bearpark, J. J. Heyd, E. Brothers, K. N. Kudin, V. N. Staroverov, R. Kobayashi, J. Normand, K. Raghavachari, A. Rendell, J. C. Burant, S. S. Iyengar, J. Tomasi, M. Cossi, N. Rega, J. M. Millam, M. Klene, J. E. Knox, J. B. Cross, V. Bakken, C. Adamo, J. Jaramillo, R. Gomperts, R. E. Stratmann, O. Yazyev, A. J. Austin, R. Cammi, C. Pomelli, J. W. Ochterski, R. L. Martin, K. Morokuma, V. G. Zakrzewski, G. A. Voth, P. Salvador, J. J. Dannenberg, S. Dapprich, A. D. Daniels, O. Farkas, J. B. Foresman, J. V. Ortiz, J. Cioslowski, D. J. Fox, *Gaussian 09, Revision D.01*, Gaussian, Inc., Wallingford CT, **2013**
- <sup>17</sup> A. J. Becke, *Chem. Phys.* 98 (**1993**) 1372
- <sup>18</sup> C. Lee, W. Yang, R. Parr, *Phys. Rev. B* 37 (**1988**) 785;
- <sup>19</sup> a) P. C. Hariharan, J. A. Pople, *Theor. Chim. Acta* 28 (**1973**) 213; b) W. J. Hehre, R. Ditchfield, J. A. Pople, *J. Chem. Phys.* **1972**, 56, 2257-2261. c) Ditchfield, R.; Hehre, W. J.; Pople, J. A. *J. Chem. Phys.* 54 (**1971**) 724
- <sup>20</sup> J. Tomasi, B. Mennucci, R. Cammi, *Chem. Rev.* 105 (**2005**) 2999
- <sup>21</sup> C. Adamo, V. Barone, *J. Chem. Phys.* 108 (**1998**) 664
- <sup>22</sup> T. Yanai, D. Tew, N. Handy, *Chem. Phys. Lett.* 393 (**2004**) 51
- <sup>23</sup> J. Allouche *Comput. Chem.* 32 (**2011**) 174



## 2.6 Synthesis and Characterization of the First Relatively Stable Dianionic Germanolates

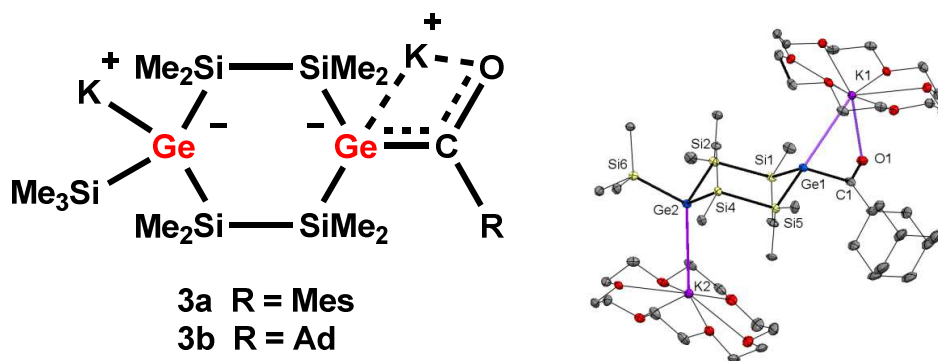
Michael Haas\*,<sup>[a]</sup> Mario Leypold,<sup>[b]</sup> Dominik Schnalzer,<sup>[a]</sup> Ana Torvisco<sup>[a]</sup> and Harald Stueger<sup>[a]</sup>

<sup>[a]</sup> Institute of Inorganic Chemistry, Graz University of Technology, Stremayrgasse 9, A-8010 Graz, Austria

<sup>[b]</sup> Institute of Organic Chemistry, Graz University of Technology, Stremayrgasse 9, A-8010 Graz, Austria

submitted to *Phosphorus, Sulfur Silicon Relat. Elem.*

graphical abstract:



### 2.6.1 Abstract

The previously unknown dianionic species **3a,b** with exocyclic structures were synthesized by the reaction of the corresponding cyclic acylgermanes with 2.1 equiv. of KO<sup>*t*</sup>Bu. The structural properties of the resulting products were analyzed by a combination of NMR and UV-Vis absorption spectroscopy, single X-ray crystallography and DFT quantum chemical calculations and it has been found that **2a-c** and **3b,c** are best described by the keto-form (resonance structure I) in solution and in the solid state as well. The reactivity of **2a-c** and **3b,c** towards a variety of selected electrophiles was also examined.

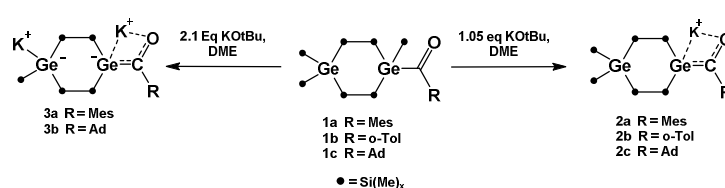
## 2.6.2 Introduction

Enolates and silenolates are widely employed in organic and in inorganic chemistry as well.<sup>1,2</sup> However, to the best of our knowledge only a few studies concerning relatively stable germenolates have been published in literature thus far. Bravo-Zhivotovskii *et al.* reported briefly on the formation of the germenolate anion  $(\text{Me}_3\text{Si})_2\text{GeC}(\text{OLi})^t\text{Bu}$ . Spectroscopic and structural data of the resulting product, however, were not given.<sup>3</sup> As we have shown earlier, it is possible to synthesize and to characterize cyclic silenolates with remarkable stability and to react them with various electrophiles.<sup>4</sup> Based on this work, we recently succeeded in isolating and fully characterizing the structurally related germenolates **2a-c** and to convert them to the corresponding germenes.<sup>5</sup> Herein, we would like to present a related study focused on the dianionic species **3a,b**.

## 2.6.3 Results and Discussion

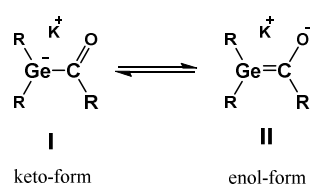
### 2.6.3.1 Cyclic Germenolates

The cyclic acylgermanes **1a-c** reacted cleanly with 1.05 eq. of  $\text{KO}^t\text{Bu}$  to give the corresponding cyclic germenolates **2a-c**. With 2.1 eq. of  $\text{KO}^t\text{Bu}$  the dianionic species **3a,b** were obtained.



**Scheme 1** Synthesis of germenolates **2a-c** and **3a,b**

For **2a-c** and **3a,b** two tautomeric structures can be drawn: one with the negative charge residing predominately on the germanium atom (I), while in the other one (II) it is located on the oxygen atom.



For cyclic silenolates significantly, different modes of coordination of the  $\text{K}^+$  counter-ion for species with an alkyl or an aryl group attached to the carbonyl C-atom have been detected and it has been concluded that species with aryl groups at the carbonyl C-atom exhibit increased contributions of the enol form.<sup>4</sup> In contrast, **2a-c** did not show similar substituent dependencies and are best described as acyl germyl anions (resonance structure I).<sup>5</sup> Apparently the same is true for the dianionic species **3**. Single crystal X-ray crystallography showed closely related coordination of the  $\text{K}^+$  counter-ion to the  $\text{GeC}(\text{R})\text{O}$  moiety in the solid state structures of **2b,c** and **3b** with simultaneous coordination of the  $\text{K}^+$  cation to Ge(1) and O(1) (compare Figures 1 and 2 and Table 1). Nearly identical C(1)-O(1) and

Ge(1)-C(1) bond distances were measured for **2b,c** and **3b**. Furthermore, numerical values of  $d(\text{C}-\text{O})$  appear in a typical range for  $\text{C}=\text{O}$  double bonds, while the  $\text{Ge}(1)-\text{C}(1)$  bond lengths closely match the  $\text{C}-\text{Ge}$  single bond distances in the acylgermanes **1b,c**.<sup>5</sup>

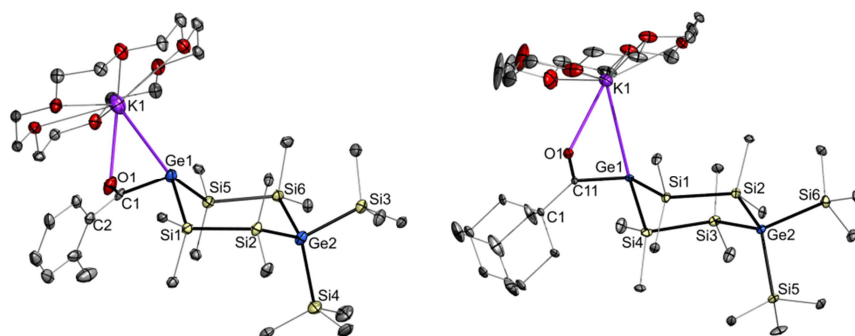


**Figure 1** ORTEP diagram for **2b** (right) and **2c** (left) (1:1 adduct with [18]crown-6)

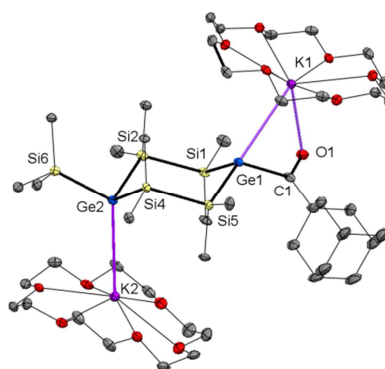


**Figure 2** ORTEP diagram for **3b** (1:2 adduct with [18]crown-6)

**Table 1** Selected experimental and B3LYP/6-31+G(d,p) calculated bond lengths  $d[\text{\AA}]$ , sum of valence angles  $\Sigma\alpha_{\text{Ge}(1)}$  and NPA charges  $q(\text{Ge}_i)$  for the K-germenolates **2b,c** and **3b**.

	<b>2b</b>		<b>2c</b>		<b>3b</b>	
	exp.	calc.	exp.	calc.	exp.	calc.
$d \text{ C}_1-\text{Ge}_1$	2.007(5)	2.003	2.063(2)	2.025	2.055(3)	2.009
$d \text{ C}_1-\text{O}_1$	1.236(6)	1.243	1.231(3)	1.238	1.252(4)	1.244
$d \text{ K}_1-\text{O}_1$	2.733(4)	-	2.740(18)	-	2.758(8)	-
$d \text{ K}_1-\text{Ge}_1$	3.855(6)	-	3.613(9)	-	3.423(2)	-
$d \text{ K}_1-\text{C}_2$	4.582	-	4.926	-	-	-
$\Sigma\alpha_{\text{E}_1}$	304.6	306.1	310.7	310.7	314.02	318.3
$q(\text{Ge}_i)$	-	-0.19	-	-0.22	-	-0.25

NMR data also support the conclusion that the dominant structure of **3a,b** is the keto-form (compare Table 2). <sup>13</sup>C-NMR chemical shifts were observed at  $\delta = 282.45$  and  $281.87$  ppm, respectively, which are typical for  $sp^2$  hybridization and close to the ones measured for **2a-c**.<sup>5</sup> Furthermore, **2a-c** and **3a,b** exhibit only two sharp SiMe<sub>2</sub> resonance lines in <sup>29</sup>Si-NMR between  $\delta = -26.36 - -28.96$  ppm which clearly suggests free rotation around the Ge<sub>1</sub>-C<sub>1</sub> bond. In case of hindered rotation due to increased Ge=C double bond character, the signal of the -SiMe<sub>2</sub> groups adjacent to Ge(1) is likely to split up into two lines or at least to show some line broadening.

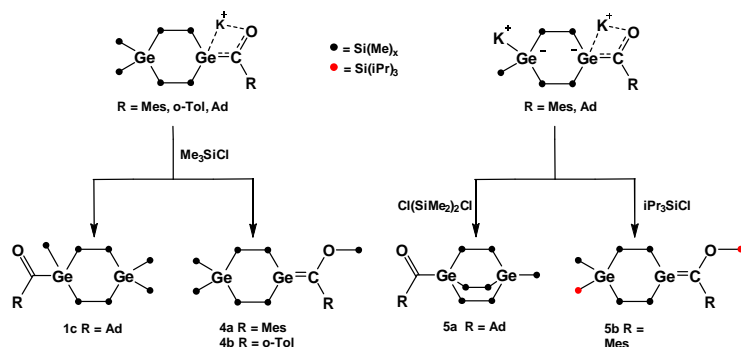
**Table 2** Selected <sup>13</sup>C- and <sup>29</sup>Si-NMR chemical shifts for the acylgermanes **1** and germenolates **2,3**

	<b>1</b> (ppm) <sup>a</sup>		<b>2</b> (ppm) <sup>b</sup>		<b>3</b> (ppm) <sup>b</sup>	
	Mes	Ad	Mes	Ad	Mes	Ad
$\delta^{13}\text{C}$ (C=O)	243.85	243.73	281.60	281.87	282.45	282.78
	-1.09	-2.93				
$\delta^{29}\text{Si}$ (SiMe <sub>3</sub> )	-1.13	-3.76	-4.36	-4.21	-0.49	-0.62
	-2.70	-4.47				
$\delta^{29}\text{Si}$ (SiMe <sub>2</sub> )	-28.37	-30.47	-28.67	-27.90	-27.37	-26.34
	-29.44	-30.64	-30.38	-29.91	-28.96	-28.75

$\delta$  values relative to ext. TMS; <sup>a</sup> in C<sub>6</sub>D<sub>6</sub> at 22 °C, <sup>b</sup> in THF/D<sub>2</sub>O at 22 °C

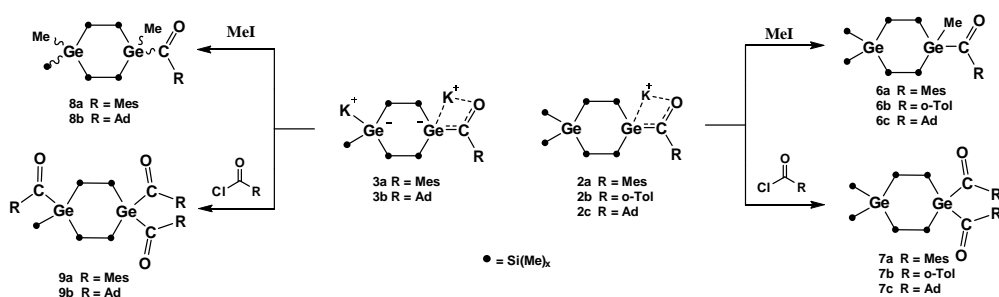
### 2.6.3.2 Reactivity towards Electrophiles

As shown in Scheme 2 the K-germenolates **2a-c** and **3a,b** reacted with chlorosilanes to give either germenenes or acylgermanes depending on the nature of the R-group attached to the carbonyl C atom. With aromatic R-groups the germenenes **4a,b** and **5b** were obtained while aliphatic R-groups gave rise to the formation of the acylgermanes **1c** and **5a**. Natural population analysis (NPA) charges calculated at the PCM B3LYP/6-31+G(d,p) level of theory in THF as a solvent (compare Table 1), showed a slightly higher negative charge placed on the central Ge(1) atom in **2c** (-0.22 e) as compared to **2b** (-0.19 e). This could be responsible for the observed different reactivities between alkyl- and aryl-substituted K-germenolates versus chlorosilanes.



**Scheme 2** Reactivities of germenolates **2a-c** and **3a,b** towards chlorosilanes

With carbon centered electrophiles such as alkyl halides or acid chlorides **2a-c** exclusively reacted under carbon-germanium bond formation (compare Scheme 3). Apparently only the oxophilic silicon based electrophiles lead to the formation of germenes in certain cases.



**Scheme 3** Reactivities of germenolates **2a-c** and **3a,b** towards selected carbon centered electrophiles

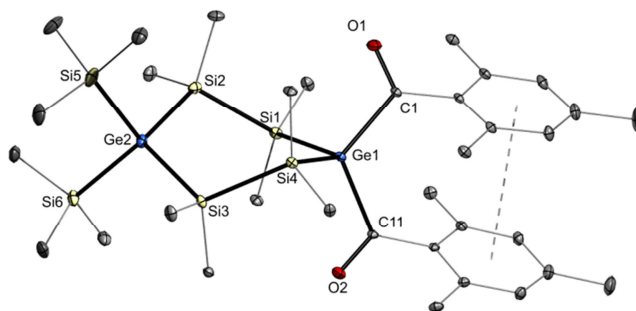


**Figure 3** ORTEP diagram for **7a**. Selected bond lengths (Å) and bond and torsion angles (deg) with estimated standard deviations: Ge-Si (mean) 2.396, Si-Si (mean) 2.3425, C-O (mean) 1.221, Ge(1)-C<sub>acyl</sub> (mean) 2.037, Si(1)-Ge(1)-Si(4) 111.023 (10), Si(6)-Ge(2)-Si(2) 111.356 (12), Si(6)-Ge(2)-Si(3) 107.757 (13), Si(2)-Ge(2)-Si(3) 111.360 (11), Si(2)-Ge(2)-Si(5) 108.492 (12), Si(2)-Si(1)-Ge(1) 111.020 (13), Si(1)-Si(2)-Ge(2) 111.703 (13), Si(4)-Si(3)-Ge(2) 113.462 (13), Si(3)-Si(4)-Ge(1) 112.820 (13)

**7a**, which represents the first silylated geminal bisacylgermane, crystallizes in the monoclinic space group  $P2_1/n$ . The cyclohexasilane ring adopts a twisted boat conformation. The average Ge(1)-Si bond distance is 2.396 Å, while the average Si-Ge bond distance of the germanium atom attached to the carbonyl moiety is slightly elongated by 0.024 Å. In addition, the mesityl rings align parallel to each

other exhibiting a  $\pi$ - $\pi$  stacking interaction with a distance between the ring planes of 3.46 Å and an offset of 1.54 Å. These values fall within the expected ranges for these interactions and are a well described phenomenon in aromatic systems.<sup>6,7</sup>

## 2.6.4 References

- <sup>1</sup> For general reviews about enolates, see e.g.: a) D. Stolz, U. Kazmaier in *The Chemistry of Metal Enolates, Part 1* (Eds.: Z. Rappoport, J. Zabicky), Wiley, Hoboken, (2009), pp. 355-411. b) P. Veya, C. Floriani, A. Chiessi-Villa, C. Rizzoli, *Organometallics* 13 (1994) 214; c) D. Seebach, *Angew. Chem.* 100 (1988) 1685; *Angew. Chem. Int. Ed. Engl.* 27 (1988) 1624
- <sup>2</sup> For example: a) R. Dobrovetsky, L. Zborovsky, D. Sheberla, M. Botoshansky, D. Bravo-Zhivotovskii, Y. Apeloig, *Angew. Chem. Int. Ed.* 49 (2010) 4084; b) T. Guliashvili, I. El-Sayed, A. Fischer, H. Ottosson, *Angew. Chem. Int. Ed.* 42 (2003) 1640; c) J. Ohshita, S. Masaoka, Y. Masaoka, H. Hasebe, M. Ishikawa, A. Tachibana, T. Yano, T. Yamabe, *Organometallics* 15 (1996) 3136; d) D. Bravo-Zhivotovskii, Y. Apeloig, Y. Ovchinnikov, V. Igonin, Y. T. Struchkov, *J. Organomet. Chem.* 446 (1993) 123
- <sup>3</sup> a) I. S. Biltueva, D. A. Bravo-Zhivotovskii, I. D. Kalikhman, V. Yu. Vitkovskii, S. G. Shevchenko, N. S. Vyazankin, M. G. Voronkov, *J. Organomet. Chem.* 368 (1989) 163; b) I. S. Biltueva, D. A. Bravo-Zhivotovskii, I. D. Kalikhman, N. S. Vyazankin, M. G. Voronkov, *Izv. Akad. Nauk SSSR, Seriya Khimicheskaya* (1988) 1947
- <sup>4</sup> H. Stueger, B. Hasken, M. Haas, M. Rausch, R. Fischer, A. Torvisco, *Organometallics* 33 (2014) 231
- <sup>5</sup> M. Haas, M. Leybold, D. Schnalzer, A. Torvisco, H. Stueger, *Organometallics* (2015) submitted
- <sup>6</sup> E. A. Meyer, R. K. Castellano, F. Diederich, *Angew. Chem. Int. Ed.* 42 (2003) 1210
- <sup>7</sup> C. A. Hunter, J. K. M. Sanders, *J. Am. Chem. Soc.* 112 (1990) 5525

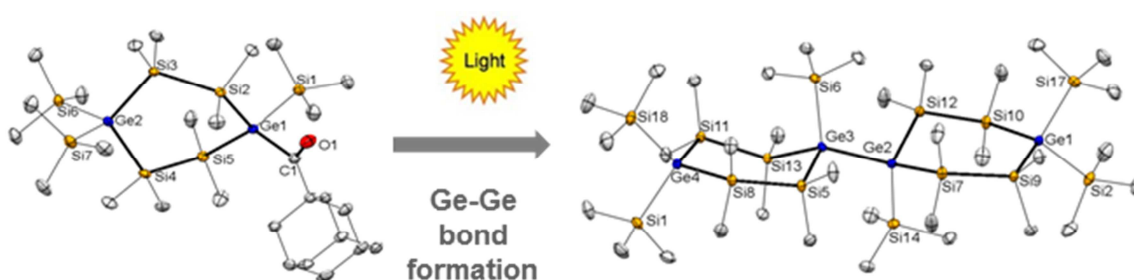
## 2.7 Photochemical Reactivity of Cyclic Acylgermanes

Dominik Schnalzer,<sup>[a]</sup> Michael Haas\*,<sup>[a]</sup> Ana Torvisco<sup>[a]</sup> and Harald Stueger<sup>[a]</sup>

<sup>[a]</sup> Institute of Inorganic Chemistry, Graz University of Technology, Stremayrgasse 9, A-8010 Graz, Austria

submitted to *Phosphorus, Sulfur Silicon Relat. Elem.*

graphical abstract:



### 2.7.1 Abstract

After irradiation with light ( $\lambda > 360$  nm) the newly synthesized cyclic acylgermanes **3a-c** afforded the Ge-Ge coupling product **5** with remarkable selectivity, which can be explained by the enhanced stability of the cyclic germyl radical **4**. The previously unknown compound **5** was isolated and fully characterized spectroscopically and by single crystal X-ray crystallography.

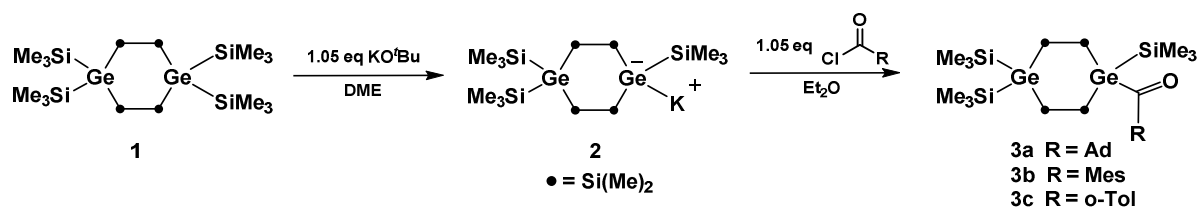
## 2.7.2 Introduction

The photoreactivity of acylgermanes is significantly different from that of acylsilanes due to the fact that acylgermanes do not undergo Brook-type rearrangement reactions.<sup>1</sup> Instead, upon irradiation, acylgermanes predominantly react via Norrish type I cleavage of the germanium-carbon bond.<sup>2,3,4</sup> Recently acylgermanes attracted considerable attention because of possible applications as photoinitiators or sources for germanium centered radicals. In the case of acyclic acylgermanes, however, photolysis affords complex product mixtures caused by follow-up reactions of the initially formed germyl radicals.<sup>5</sup> In our laboratories it has been discovered just recently that acylpolysilanes with cyclic structures exhibit different photochemical reactivity patterns as compared to their open-chained analogues.<sup>6</sup> Based on this observation, we decided to attempt the synthesis of structurally related germanium based species and to study their chemical and structural properties. In this paper we describe the outcome of a recent photolysis study employing the cyclic acylgermasilanes **3a–c** and the isolation and characterization of the photoproduct **5** which was formed with unexpected selectivity.

## 2.7.3 Results and Discussion

### 2.7.3.1 Cyclic Acylgermanes

In previous studies it has been reported that the 1,4-Digermacyclohexasilane **1** reacts with 1.05 equivalents of KO<sup>t</sup>Bu to give the acyl germanide **2** which cleanly afforded the air stable and crystalline cyclic acylgermanes **3a–c** upon treatment with equimolar amounts of acid chlorides ClCOR (R= Mes, o-Tol and 1-Ad) (Scheme 1).<sup>7,8</sup>



**Scheme 1** Synthesis of cyclic acylgermanes **3a–c**

**Table 1** <sup>13</sup>C- and <sup>29</sup>Si-NMR Shifts for compounds **1**, **3a–c** and **5**

	<b>2</b> <sup>a</sup>	<b>3a</b> <sup>b</sup>	<b>3b</b> <sup>b</sup>	<b>3c</b> <sup>b</sup>	<b>5</b> <sup>b</sup>
$\delta^{13}\text{C}$ (C=O)	-	243.73	243.85	238.42	-
$\delta^{29}\text{Si}$ (SiMe <sub>3</sub> )	-0.86	-2.93	-1.09	-2.92	-2.20
	-4.21	-3.76	-1.13	-3.22	-3.08
$\delta^{29}\text{Si}$ (SiMe <sub>2</sub> )	-4.46	-4.47	-2.70	-3.70	-4.46
	-29.16	-30.47	-28.37	-30.05	-27.42
	-29.90	-30.64	-29.44	-30.63	-28.82

$\delta$  values relative to ext. TMS; <sup>a</sup> in C<sub>6</sub>D<sub>6</sub> at 22 °C, <sup>b</sup> in THF/D<sub>2</sub>O at 22 °C



The obtained acylgermanes were isolated and fully characterized spectroscopically and by single crystal X-ray crystallography. NMR data obtained for **3a-c** (compare Table 1) were fully consistent with the proposed structures. The molecular structures of **3a-c** are depicted in Figure 1 together with selected bond lengths and angles. **3a-c** crystallize in the monoclinic space groups P2(1)/n and P2(1)/c, respectively. Ge-Si bond lengths between 2.37 – 2.42 Å were measured with slightly larger values at the Ge atom attached to the bulky carbonyl moiety. The average Ge-Si bond distance of 2.40 Å agrees well with Ge-Si single bond lengths found in related compounds.<sup>9</sup> Carbonyl C=O bond distances are also unexceptional,<sup>10</sup> while the silicon carbonyl group bond lengths of 2.01 – 2.05 Å are considerably elongated relative to the length of typical Ge-C(sp<sup>3</sup>) bonds<sup>11</sup> just as observed earlier for the Si-CO distances of acyl silanes.<sup>12</sup> For steric reasons the *o*-Tol derivative **3c** exhibits a significantly smaller dihedral angle  $\gamma$  between the C=O group and the aromatic ring plane as compared to the mesityl compound **3b** which allows increased conjugational type interactions between the C=O and the aromatic  $\pi$ -systems.

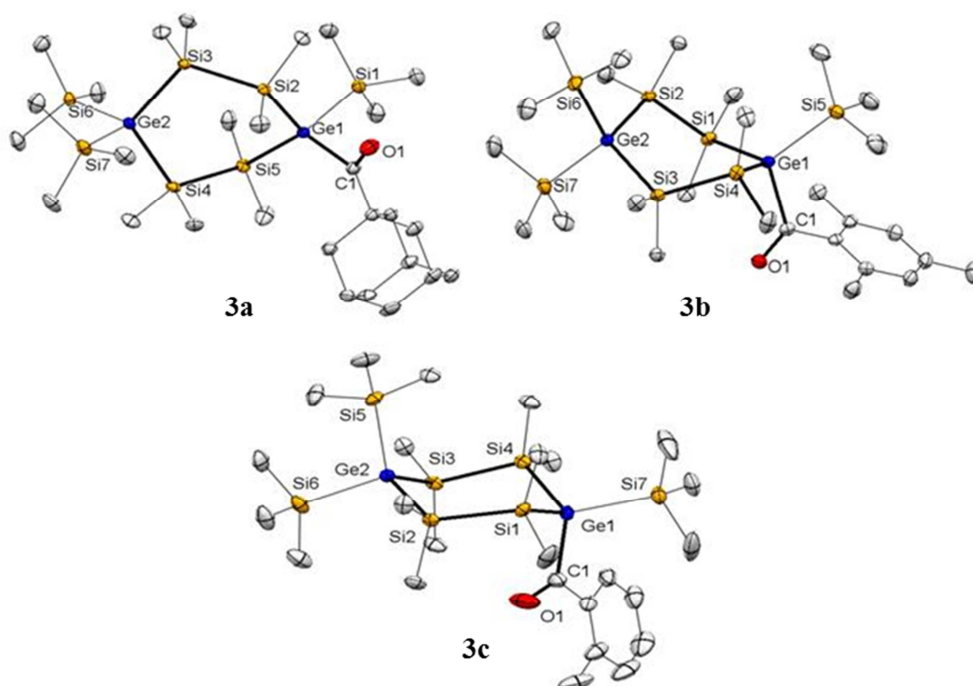
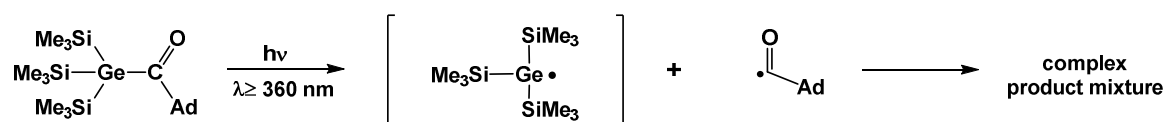


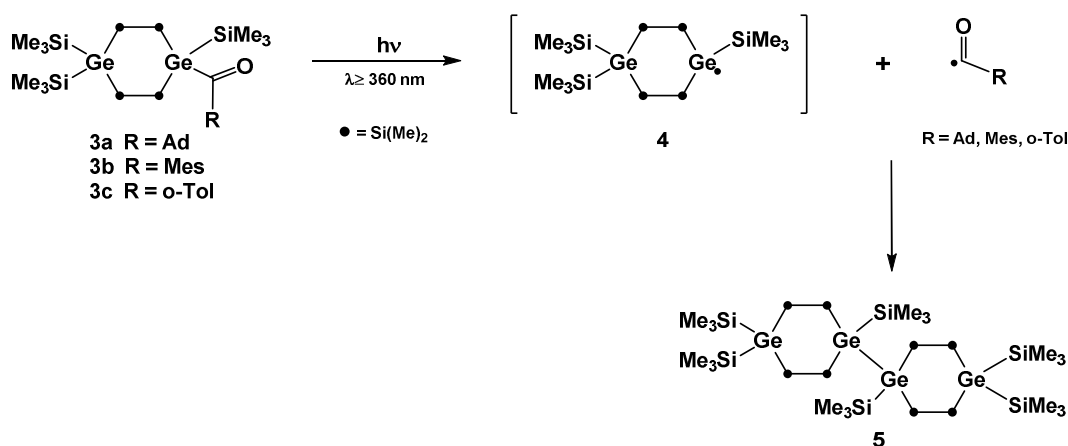
**Figure 1** ORTEP diagrams for compounds **3a-c**. Thermal ellipsoids are depicted at the 50 % probability level. Hydrogen atoms are omitted for clarity. Selected bond lengths [Å] and torsion angles  $\gamma$  [deg] with estimated standard deviations: **3a**: dGe(1)-C(1) 2.050(1), dC(1)-O(1) 1.210(2), dGe(1)-Si(2) 2.403(1), dGe(1)-Si(5) 2.403(1), dGe(2)-Si(3) 2.389(1), dGe(2)-Si(4) 2.384(1). **3b**: dGe(1)-C(1) 2.044(2), dC(1)-O(1) 1.217(2), dGe(1)-Si(1) 2.415(1), dGe(1)-Si(4) 2.422(1), dGe(2)-Si(2) 2.374(1), dGe(2)-Si(3) 2.380(1),  $\gamma$ O(1)-C(1)-C(2)-C(7) -64.7(2). **3c**: dGe(1)-C(1) 2.009(5), dC(1)-O(1) 1.215(7), dGe(1)-Si(1) 2.400(1), dGe(1)-Si(4) 2.415(1), dGe(2)-Si(2) 2.386(1), dGe(2)-Si(3) 2.387(1),  $\gamma$ O(1)-C(1)-C(2)-C(7) -22.8(8).

### 2.7.3.2 Photochemical Reactivity

As already mentioned, acylgermanes undergo homolytic cleavage of the Ge-C bond via a Norrish type I reaction when irradiated with  $\lambda > 300$  nm light. Furthermore, Brook *et al.* showed that the photolysis of tris(trimethylsilyl)acylgermanes affords a complex product mixture due to extensive follow-up reactions of the initially formed highly reactive germyl radicals (Scheme 2).<sup>13</sup> Now we have found that in the case of the cyclic acylgermanes **3a-c** photolysis with light of wavelength  $\lambda > 360$  nm leads to the formation of the Ge-Ge coupling product **5** with remarkable selectivity due to the enhanced stability of the cyclic germyl radical **4** (Scheme 3).

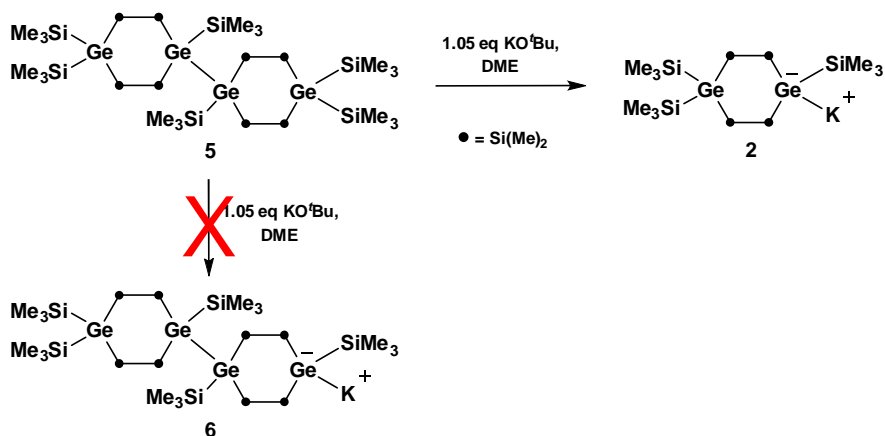


**Scheme 2** Photochemical reactivity of tris(trimethylsilyl)acylgermanes



**Scheme 3** Photochemical reactivity of cyclic acylgermanes **3a-c**.

Interestingly, the formation of the Ge-Ge bond could not be observed if substituents bulkier than Me<sub>3</sub>Si are linked to the Ge atom bearing the carbonyl group. Thus, photolysis of acylgermane precursors with iPr<sub>3</sub>Si- or tBuMe<sub>2</sub>Si groups at Ge(1) under identical conditions only afforded undefined product mixtures. Apparently, in this case the bulky  $\alpha$ -SiR<sub>3</sub> group prevents effective recombination of the photolytically generated germyl radical. Finally, treatment of **5** with KO<sup>t</sup>Bu with the intention to generate the germanide anion **6** exclusively lead to Ge-Ge bond cleavage instead of Ge-Si bond cleavage under formation of the potassium germanide **2** (Scheme 4).



**Scheme 4** Reaction of **5** with 1,05 eq. KO $t$ Bu

The previously unknown compound **5** could be isolated straightforwardly from the crude photolysis mixture by crystallization from acetone solution in 65 % yield. NMR data of **5** are included in Table 1, the molecular structure of **5** as determined by single crystal X-ray crystallography is depicted in Figure 2 along with selected bond distances.

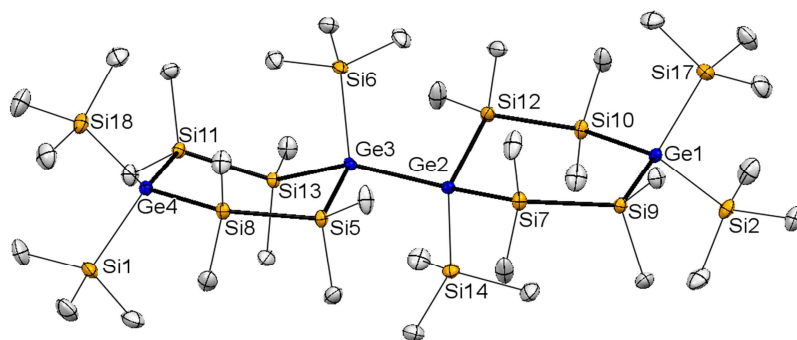


**Figure 2** ORTEP diagram for compound **5**. Thermal ellipsoids are depicted at the 50 % probability level. Hydrogen atoms are omitted for clarity. Selected bond lengths [Å] with estimated standard deviations: dGe(2)-Ge(3) 2.498(1), dGe(1)-Si(9) 2.398(1), dGe(1)-Si(10) 2.398(1), dGe(2)-Si(7) 2.392(1), dGe(2)-Si(12) 2.396(1), dGe(3)-Si(5) 2.407(1), dGe(3)-Si(13) 2.401(1), dGe(4)-Si(8) 2.404(1), dGe(4)-Si(11) 2.400(1).

**5** crystallizes in the triclinic space group P-1. Both rings adopt slightly twisted chair conformations and are linked in equatorial positions. Bond lengths and angles are unexceptional, the length of the central Ge-Ge bond measured at 2.498 Å and the mean bond distance of the endocyclic Si-Ge bonds of 2.40 Å exhibit typical values for singly bonded germasilanes.<sup>9,11</sup>

### 2.7.3.3 UV-Vis Spectroscopy

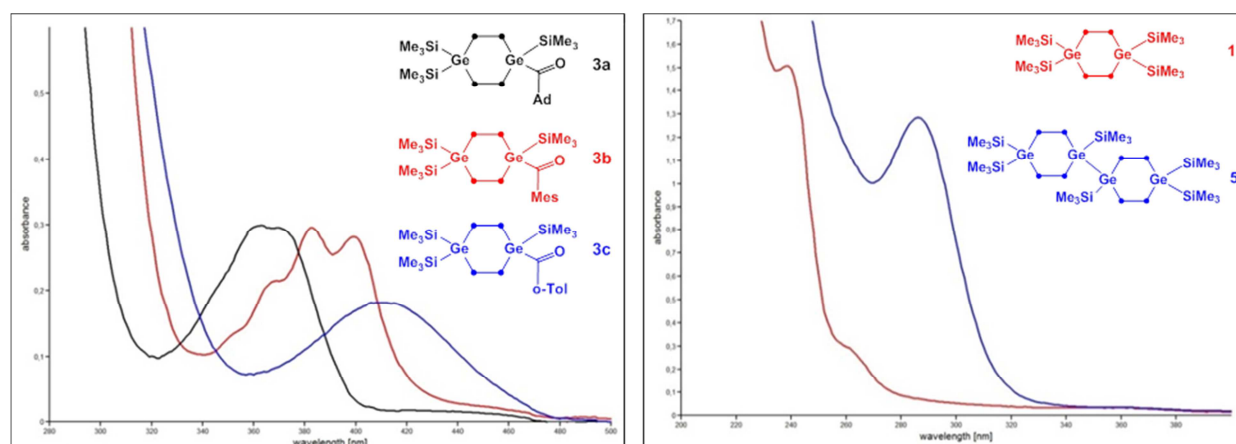


**Figure 3** UV-Vis absorption spectra of **3a-c** (left) and **1** and **5** (right) (n-hexane solution,  $c = 1 \cdot 10^{-3} \text{M}$  (**3a-c**),  $c = 5 \cdot 10^{-5}$  (**1,5**))

**Table 2** Absorption maxima  $\lambda_{\text{max}}$  and extinction coefficients  $\epsilon$  of **1**, **3a-c** and **5** (n-hexane solution)

	$\lambda_{\text{max}}$ [nm] ( $\epsilon$ [ $\text{L} \cdot \text{mol}^{-1} \cdot \text{cm}^{-1}$ ])	Assignment
<b>1</b>	240 (30160)	$\sigma \rightarrow \sigma^*$
<b>3a</b>	363 (299)	$n(\text{CO}) \rightarrow \pi^*(\text{CO})$
<b>3b</b>	400 (280), 382 (295), 365 (259), 350 (132)	$n(\text{CO}) \rightarrow \pi^*(\text{aryl})$
<b>3c</b>	410 (183)	$n(\text{CO}) \rightarrow \pi^*(\text{aryl})$
<b>5</b>	286 (25720)	$\sigma \rightarrow \sigma^*$

UV-Vis absorption spectra were recorded in order to estimate the extent of conjugational-type interactions within **3a-c** and **5**. The experimental spectra are depicted in Figure 3, absorption maxima and intensities are summarized in Table 3 along with a qualitative assignment of the absorption bands. All acylgermanes exhibit long-wavelength, low-intensity absorption bands between 360–410 nm due to  $n-\pi^*$  type excitations which are red-shifted in the order **3a**→**3b**→**3c**. The bathochromic shift of **3b,c** as compared to **3a** is caused by  $\pi-\pi$  conjugation of the carbonyl group with the aromatic ring. Due to the smaller torsion angle between the plane of the aromatic ring and the C=O group in **3c** the  $n-\pi^*$  absorption band is further shifted bathochromically relative to **3b**. The absorption spectrum of **3b**

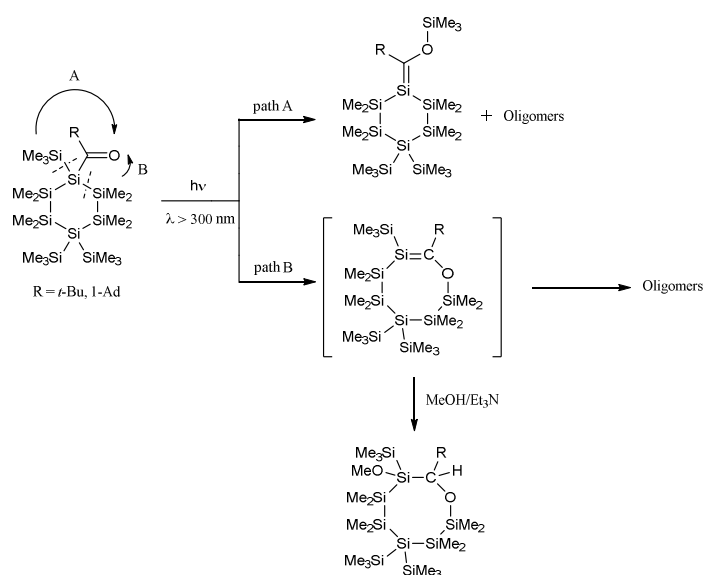
exhibits considerable fine structure consisting of three main bands which is not unusual and parallels the behavior of structurally related acylsilanes.<sup>12</sup> **1** and **5** exhibit intense absorption maxima in the near UV arising from  $\sigma$ - $\sigma^*$  transitions within the extended Si-Si-Ge skeleton. As in the case of cyclopolysilanes<sup>14</sup> we observed a bathochromic shift for **5** as compared to **1** caused by the larger  $\sigma$ -conjugated system.

## 2.7.4 References

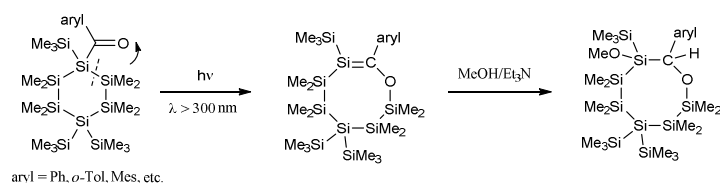
- <sup>1</sup> A. G. Brook, *Acc. Chem. Res.*, **7** (1974)77
- <sup>2</sup> K. Mochida, K. Ichikawa, S. Okui, Y. Sakaguchi, H. Hayashi, *Chem. Lett.*, **14** (1985) 1433
- <sup>3</sup> M. B. Taraban, V. I. Maryasova, T. V. Leshina, L. I. Rybin, D. V. Gendin, N.S. Vyazankin, *J. Organomet. Chem.*, **326** (1987) 347
- <sup>4</sup> S. Kiyooka, M. Hamada, H. Matsue, M. Hamada, R. Fujiyama, *J. Org. Chem.*, **55** (1990) 5562
- <sup>5</sup> a) D. Neshchadin, A. Rosspointner, M. Griesser, B. Lang, S. Mosquera-Vazquez, E. Vauthey, V. Gorelik, R. Liska, C. Hametner, B. Ganster, R. Saf, N. Moszner, G. Gescheidt, *J. Am. Chem. Soc.* **135** (2013) 17314; b) V. Y. Lee, A. Sekiguchi, *Organometallic Compounds of Low-Coordinate Si, Ge, Sn and Pb: From Phantom Species to Stable Compounds*; Wiley & Sons Inc., Chichester, (2010). c) J. Lalevée, X. Allonas, J. P. Fouassier, *Chem. Phys. Lett.* **469** (2009) 298; d) B. Ganster, U. K. Fischer, N. Moszner, R. Liska, *Macromolecules* **41** (2008) 2394
- <sup>6</sup> a) H. Stueger, B. Hasken, M. Haas, M. Rausch, R. Fischer, A. Torvisco, *Organometallics* **33** (2014) 231; b) M. Haas, R. Fischer, L. Schuh, R. Saf, A. Torvisco, H. Stueger, *Eur. J. Inorg. Chem.* (2015) 997
- <sup>7</sup> J. Hlina, R. Zitz, H. Wagner, F. Stella, J. Baumgartner, C. Marschner, *Inorg. Chim. Acta* **442** (2014)120.
- <sup>8</sup> M. Haas, M. Leypold, D. Schnalzer, A. Torvisco, H. Stueger, *Organometallics* (2015) submitted for publication.
- <sup>9</sup> K. V. Zaitsev, E. K. Lermontova, A. V. Churakov, V. A. Tafeenko, B. N. Tarasevich, O. K. Poleshchuk, A. V. Kharcheva, T. V. Magdesieva, O. M. Nikitin, G. S. Zaitseva, S. S. Karlov., *Organometallics* **34** (2015) 2765
- <sup>10</sup> C=O distances are close to the ones observed found in simple organic ketones, carboxylic acids and esters: a) R. J. Berry, R. J. Waltman, J. Pacansky, A. T. Hagler, *J. Phys. Chem.* **99** (1995) 10511; b) J. A. Kanters, J. Kroon, A. F. Peerdeman, J. C. Schoone, *Tetrahedron* **23** (1967) 4027
- <sup>11</sup> M. L. Amadorge, C. S. Weinert, *Chem. Rev.* **108** (2008) 4253
- <sup>12</sup> P. C. Bulman Page, M. J. McKenzie, S. S. Klair, S. Rosenthal, In *The Chemistry of Organic Silicon Compounds, Vol. 2*; Z. Rappoport, Y. Apeloig, Eds., Wiley: Chichester, (1998); p 1605.
- <sup>13</sup> A. G. Brook, F. Abdesaken H. Söllradl, *J. Organomet. Chem.*, **299** (1986) 9
- <sup>14</sup> a) V. V. Semenov, *Russ. Chem. Rev.* **80** (2011) 313; b) R. D. Miller, J. Michl, *Chem. Rev.* **89** (1989) 1359

### 3. Conclusion and Outlook

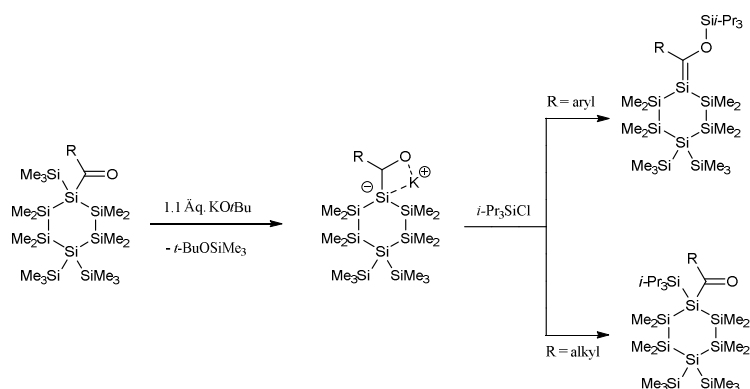
In summary, we have found that acylcyclohexasilanes undergo photochemically induced Brook type rearrangement. The outcome of the reaction is significantly influenced by the nature of the substituent group attached to the carbonyl C atom. Thus, the photolysis of alkyl substituted substrates afforded photolytically labile mixtures of six- and eight membered cyclopolysilanes with exo- and endocyclic Si=C double bonds formed by two competing reaction mechanisms. The exocyclic product was stable enough to allow detection by NMR and UV absorption spectroscopy while the less stable endocyclic product could only be observed in form of its methanol adduct.



Under the same conditions, aryl substituted acylcyclohexasilanes exclusively undergo ring scission adjacent to the Si-C=O group followed by 1,3-Si→O migration of the resulting terminal SiMe<sub>2</sub> group to give the ring enlarged product with an endocyclic Si=C bond. The resulting endocyclic silenes could be isolated in > 95% purity and were stable enough to allow detection by NMR and UV absorption spectroscopy.

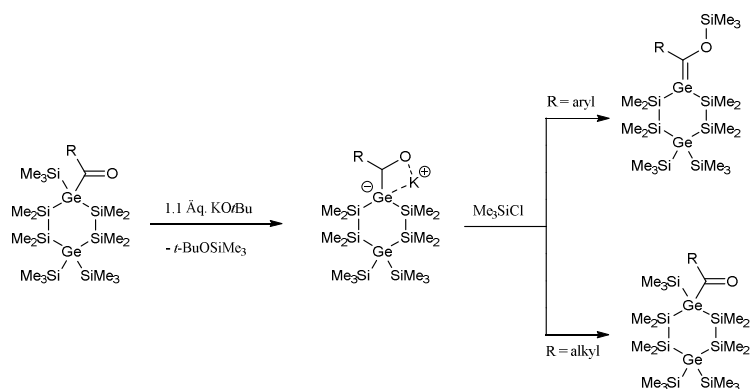


Furthermore, we were able to demonstrate that acylcyclohexasilanes react with KO*t*Bu by the formation of stable silenolates. Subsequently, we observed different reactivities of silenolates with alkyl or aryl substituents attached to the carbonyl C atom. Only aryl substituted silenolates reacted with chlorosilanes under formation of a stable exocyclic silene, while alkyl substituted silenolates gave the corresponding acylcyclohexasilane. Additionally we were able to show that the observed reactivity differences are related to the mode of coordination of the K<sup>+</sup> counter-ion to the SiC(R)O moiety and to the resulting increased enol character of the aryl substituted derivatives.



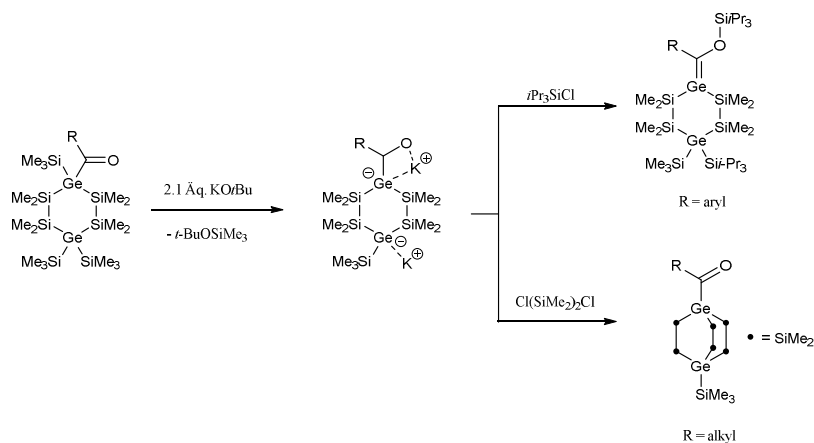
#### Synthesis of cyclic silenes and silenolates from acylcyclohexasilanes

Moreover, we have established that stable germenolates can be synthesized and isolated if the germanium atom is incorporated into a cyclohexasilane ring. In contrast to the behavior of the isostructural silenolates, the resulting germenolates almost exclusively exhibit the character of acyl germyl anions with a negatively charged Ge atom, a Ge-C single bond and a C=O double bond irrespective of the nature of the substituent attached to the carbonyl group. This finding allowed us to conclude that germenolates, like alkyl substituted silenolates, are structurally dissimilar to enolates. In addition, it has been shown that the reaction of the aryl substituted species towards ClSiMe<sub>3</sub> straightforwardly affords the first isolable Brook-type germene with an exocyclic structure.



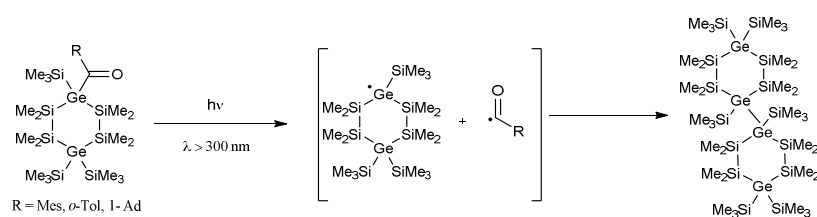
#### Synthesis of cyclic germenes and germenolates from cyclic acylgermanes

In a follow-up study, we additionally synthesized previously unknown dianionic 1,4-digermacyclohexasilanes by the reaction of the corresponding cyclic acylgermanes with 2.1 equiv. of KO<sup>t</sup>Bu. The structural properties of the resulting products were analyzed by a combination of NMR and UV-Vis absorption spectroscopy, single X-ray crystallography and DFT quantum chemical calculations. The reactivity of these dianionic species towards a variety of selected electrophiles was also examined and the same reactivity as for the germenolates was observed.



#### Synthesis and reactivity of dianionic 1,4-digermacyclohexasilanes towards chlorosilanes

Finally we discovered that the photochemistry of acylgermanes is significantly different from that of acylsilanes due to the fact that acylgermanes do not undergo Brook-type rearrangement reactions. Upon irradiation of cyclic acylgermanes homolytic cleavage of the Ge-C bond *via* a Norrish type I reaction occurs. Subsequently the initially formed highly reactive germyl radicals recombine under formation of germanium-germanium bonds. The resulting coupling product is formed with remarkable selectivity and could be isolated and fully characterized.

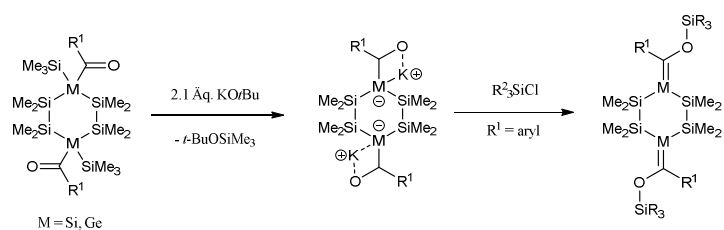


#### Photochemical reactivity of cyclic acylgermanes



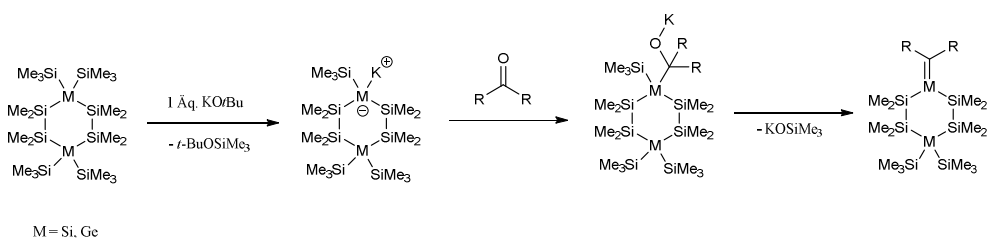
The main targets of this work have been accomplished by the isolation and characterization of endo- and exocyclic silenes and exocyclic germenes. According to spectroscopic data and time-dependent DFT calculations we finally can state that our cyclic silenes and germenes show only minor conjugation between the delocalized  $\sigma$ -electrons along the silicon backbone and our exo- or endocyclic double bonds.

The results obtained in the course of this thesis, finally, provide an excellent basis for future investigations. 1,4-bisacylcyclohexasilanes and the corresponding germanium compounds, for instance, could be valuable starting materials for the synthesis of hitherto unknown bissilenes and -germenes using synthetic protocols developed in this work.



Possible synthesis of bissilenes and -germenes

Alternatively the Sila-Peterson alkenation reaction of 1-potassiumcyclohexasilanes with carbonyl compounds might be a feasible way to synthesize hitherto unknown stable and donor-free cyclic silenes and germenes as we have shown that cyclic silenolates as well as -germenolates exhibit increased stability as compared to their acyclic counterparts.



Possible Sila-Peterson alkenation of cyclic substrates

## 4. Lebenslauf:

### Persönliche Daten

---

Name: Haas Michael  
Geboren am: 06.10.1986  
Geburtsort: Graz  
Staatsbürgerschaft: Österreich  
Familienstand: ledig  
Religion: römisch / katholisch

### Schulbildung

---

1993 – 1997 Volksschule Augraben, Semriach  
1997 – 2005 BG Gymnasium Rein, Rein  
Mai 2005 Reifeprüfung mit gutem Erfolg

### Studium

---

2006-2010 Bachelorstudium der Chemie  
2010-2012 Masterstudium Technische Chemie  
Nov. 2011 – Nov. 2012 Diplomarbeit "Elektrochemische Untersuchungen zur magnesiuminduzierten Si-Übergangsmetall Bindungsknüpfung" am Institut für Anorganische Chemie  
07. Dez. 2012 Diplomprüfung  
Jan. 2013 – Dez. 2015 Doktorstudium der technischen Wissenschaften an der Technischen Universität Graz  
Dissertation „Cyclic Silenes and Germenes“ am Institut für Anorganische Chemie